Copyright Warning & Restrictions

The copyright law of the United States (Title 17, United States Code) governs the making of photocopies or other reproductions of copyrighted material.

Under certain conditions specified in the law, libraries and archives are authorized to furnish a photocopy or other reproduction. One of these specified conditions is that the photocopy or reproduction is not to be "used for any purpose other than private study, scholarship, or research." If a, user makes a request for, or later uses, a photocopy or reproduction for purposes in excess of "fair use" that user may be liable for copyright infringement,

This institution reserves the right to refuse to accept a copying order if, in its judgment, fulfillment of the order would involve violation of copyright law.

Please Note: The author retains the copyright while the New Jersey Institute of Technology reserves the right to distribute this thesis or dissertation

Printing note: If you do not wish to print this page, then select "Pages from: first page # to: last page #" on the print dialog screen

ABSTRACT

UTILIZATION OF MUNICIPAL SOLID WASTE INCINERATOR FLY ASH IN CEMENT MORTARS

by
Manaskorn Rachakornkij

Disposal of municipal solid waste has become a major problem in many countries around the world. With the benefits of substantial weight and volume reduction and potential energy recovery, incineration has become a promising municipal solid waste (MSW) management option. Despite the fact that incineration reduces volume and mass of the wastes by as much as 80%, there are still residues to be properly managed. This research is aimed at evaluating the potential of different types of MSWI fly ash from an incineration facility to be used in cement mortars by using existing standard test methods for cement and coal fly ash.

Two types of MSWI fly ash samples: chemically treated and untreated fly ashes, were used. The treated fly ash was used to replace fine aggregates while the finer untreated fly ash was used to directly replace cement in mortars. Fractionation by air classification was introduced to separate the raw untreated fly ash into fine and coarse fractions to improve usability. MSWI fly ash, in its raw and fractionated forms, has been characterized with a view to utilizing the material to replace part of portland cement in mortars. Characterization involved chemical and physical analyses, observation under Environmental Scanning Electron Microscope (ESEM), and X-ray fluorescence (XRF) and X-ray Diffraction (XRD) analyses.

Results showed that both raw and fractionated fly ashes significantly enhanced compressive strengths of mortar specimens. Attempts were also made to specify the

sources of the additional strength by microstructural examination as well as XRD analyses of the hydration products of MSWI fly ash-cement mortar pastes. A new chemical phase was identified exclusively in the MSWI fly ash-cement paste. High absorption capacity of the fly ashes and the formation of $C_3A.CaCl_2.10H_2O$ were responsible for the superior strength properties. Toxicity Characteristic Leaching Procedure (TCLP) tests were performed on these specimens to assess the likelihood of heavy metals being released into the environment. The benefits of using MSWI fly ash in mortar are twofold; namely, the cost savings stemming from reduction in the cement used, and the ecological advantage of ensuring a final destination for the ash.

UTILIZATION OF MUNICIPAL SOLID WASTE INCINERATOR FLY ASH IN CEMENT MORTARS

by
Manaskorn Rachakornkij

A Dissertation
Submitted to the Faculty of
New Jersey Institute of Technology
In Partial Fulfillment of the Requirements for the Degree of
Doctor of Philosophy in Civil Engineering

Department of Civil and Environmental Engineering

January 2000

APPROVAL PAGE

UTILIZATION OF MUNICIPAL SOLID WASTE INCINERATOR FLY ASH IN CEMENT MORTARS

Manaskorn Rachakornkij

Dr. Methi Wecharatana, Thesis Advisor — Date
Professor of Civil and Environmental Engineering, NJIT

Dr. John Liskowitz, Committee Member — Date
Professor of Civil and Environmental Engineering, NJIT

Prof. William Librizzi, Committee Member — Date
Director of Hazardous Substance Management Research Center

Dr. Dorairaja Raghu, Committee Member — Date
Professor of Civil and Environmental Engineering, NJIT

Dr. Namunu Meegoda, Committee Member — Date
Associate Professor of Civil and Environmental Engineering, NJIT

BIOGRAPHICAL SKETCH

Author: Manaskorn Rachakornkij

Degree: Doctor of Philosophy in Civil Engineering

Date: January 2000

Undergraduate and Graduate Education:

- Doctor of Philosophy in Civil Engineering,
  New Jersey Institute of Technology, Newark, New Jersey, 2000
- Master of Science in Environmental Engineering,
  University of Michigan, Ann Arbor, Michigan, 1991
- Bachelor of Engineering in Sanitary Engineering,
  Chulalongkorn University, Bangkok, Thailand, 1988

Major: Civil Engineering

Presentations and Publications:

Methi Wecharatana, Walairat Bumrongjaroen, and Manaskorn Rachakornkij. 1998. "Characteristics of Processed Fly Ash for Concrete." *Proceedings of the Sixth CANMET/ ACI International Conference on Fly Ash, Silica Fume, Slag, and Natural Pozzolans in Concrete*, Bangkok, Thailand, May 31-June 5.

Audrey D. Levine and Manaskorn Rachakornkij. 1994. "Effects of Chemicals on Microorganisms." *Water Environment Research*, Vol.66, No.4.

Thongchai Panswad, B. Mahamontri, N. Rutwet, M. Rachakornkij, and S. Vongpanit. 1992. "Wastewater Management in a Detergent Factory." *Proceedings of International Conference on Industrial Waste Minimization '92*, Taipei, Taiwan, R.O.C., June 2-4.

TABLE OF CONTENTS

Manaskorn Rachakornkij, Weerawat Taechasoontarovat, and Sangson Kittichaikulkit. 1988. *Chemical Treatment of Lead-Containing Wastewater*. Undergraduate Senior Project, Department of Environmental Engineering, Faculty of Engineering, Chulalongkorn University, Thailand.

This Dissertation is dedicated to
my parents and my family for their constant inspiration

ACKNOWLEDGMENT

I would like to express my sincerest gratitude to my advisor, Professor Methi Wecharatana, for his support, guidance, and insightful comments, throughout this research.

Special thanks to Dr. Dorairaja Raghu, Professor of Civil and Environmental Engineering, Dr. Namunu Meegoda, Associate Professor of Civil and Environmental Engineering, Professor William Librizzi, Director of the Technical Outreach Services for Communities Program, the Hazardous Substance Research Center, and Dr. John Liskowitz, Distinguished Professor (Emeritus) of Civil and Environmental Engineering, for serving as members of the committee and for their invaluable inputs.

I am very grateful to Chulalongkorn University for initial funding of the research, to Dr. Anna-Lisa Gotschlich of the Gotschlich Foundation, to Professor Edward Dauenheimer and Professor Hsin-Neng Hsieh of the Department of Civil and Environmental Engineering, and to Dr. Ronald Kane of the Graduate Studies for additional funding. Much appreciation also goes to Ms. Laurie Cooper and Mr. Marty Suchane of American Ref-fuel, Inc. for their assistance with the samples

I do appreciate the timely help and suggestions from Mr. Allyn Luke, Assistant to the Chairman for Concrete and Structure Laboratory, Dr. Sudhi Mukherajee, Mr. Chandrakant Patel, and Mr. Clint Brockway of Department of Civil and Environmental Engineering.

Special thanks should go to Dr. Walairat Bumrongjaroen, Mr. Wiwat Kamolpornwijit, Mr. Pusit Lertwattanaruk, Miss Wonsiri Punurai for their great assistance in everything, and to all Thai students at NJIT for their friendship.

Most particularly, I would also like to thank my parents and my wife's family for their tremendous supports along the way. However, by far the biggest thanks must go to my beloved wife, Penwipa Rachakornkij, for her assistance in keeping me focused and on-track while writing this dissertation. Without her love, encouragement, and incessant support, I would never have been able to achieve so much. I am so blessed to share my life with her.

TABLE OF CONTENTS
(Continued)

Chapter **Page**

TABLE OF CONTENTS
(Continued)

Chapter **Page**

TABLE OF CONTENTS
(Continued)

Chapter **Page**

TABLE OF CONTENTS
(Continued)

Chapter **Page**

TABLE OF CONTENTS
(Continued)

Chapter **Page**

LIST OF TABLES

LIST OF TABLES
(Continued)

LIST OF TABLES
(Continued)

Table **Page**

LIST OF TABLES
(Continued)

Table **Page**

LIST OF FIGURES

LIST OF FIGURES
(Continued)

LIST OF FIGURES
(Continued)

Figure **Page**

LIST OF FIGURES
(Continued)

Figure **Page**

LIST OF FIGURES
(Continued)

Figure **Page**

LIST OF SYMBOLS AND ABBREVIATIONS

APC	Air Pollution Control
APC residue	Solid residue retrieved from Air Pollution Control systems, such as acid gas scrubbers.
ASTM	American Society for Testing of Materials
C_2S	$2CaO.SiO_2$, dicalcium silicate also forms calcium silicate hydrate gel (C-S-H) although at much lower rate.
C_3A	$3CaO.Al_2O_3$, tricalcium aluminate is another important component of cement although it is present at lower quantity (10%). It forms ettringite $[C_3A.3CaSO_4.32H_2O]$ when supply of gypsum $[CaSO_4]$ is ample.
C_3S	$3CaO.SiO_2$, tricalcium silicate is the primary cement component (60%) that forms calcium silicate hydrate gel [C-S-H] during hydration.
CH	Calcium hydroxide $[Ca(OH)_2]$, a product of cement hydration. It also participates in pozzolanic reactions to produce additional compressive strength at later age.
C-S-H	Calcium silicate hydrate, amorphous or semi-crystalline of varying stoichiometries
$d_{10\%}$, $d_{50\%}$, $d_{90\%}$	Percentile points (microns) show the given percent of the volume (or weight assuming that the specific for all particles is the same) that is smaller than the indicated size.
$d_{50\%}$	Median particle size in which 50% of the sample volume is smaller than.
EDX	Energy Dispersive X-ray Spectrometer
ESEM	Environmental Scanning Electron Microscope
ESP	Electrostatic precipitator, a particulate removal unit as a part of a APC system
FF	Fabric Filter, a particulate removal unit as a part of an APC system

LIST OF SYMBOLS AND ABBREVIATIONS
(Continued)

Fly Ash	A generic descriptor for all types of finely divided ash carried over from incinerator and sorbent material collected in APC systems. However, due to the very different chemical and physical properties of the different residue streams generated in an incineration facility, it is more prudent and much more accurate to use specific terms to avoid any potential confusion. Typically, the residue is best described by the type of unit where the residue has been collected.
LOI	Loss on ignition (%) is defined by ASTM C311 as the weight fraction of material that is lost by heating the oven-dried sample at 750°C. It is used to indicate the degree of burnout in the operation of incinerator.
MSW	Municipal Solid Waste
MSWI	Municipal Solid Waste Incineration
NJIT 1 Fly Ash	The fly ash was sampled earlier in the research. It is virtually treated NJIT 2 fly ash. It was sampled from a fly ash treatment unit that utilizes proprietary phosphoric acid solution to stabilize heavy metals in the ash.
NJIT 2 Fly Ash	This fly ash was sampled from electrostatic precipitators (ESPs) downstream from acid gas scrubbers, as parts of the APC system of the facility.
psi	Pound per square inch (lb/in^2, 1 $lb/in^2 = 6.895x10^{-3}$ MPa)
TCLP	Toxicity Characteristic Leaching Procedure as described in U.S. EPA SW-846 Method 1311.
w/(c+fa)	Water-to-binder ratio, the weight ratio of water to cement and fly ash
w/c	Water-to-cement ratio
XRD	X-ray Diffraction Spectrometer
XRF	X-ray Fluorescence Spectroscopy

CHAPTER 1

INTRODUCTION

1.1 Statement of the Problems

Disposal of municipal solid waste (MSW) has become a major problem in many countries around the world. Many problems arise owing to the fact that existing landfills are rapidly being filled as a result of the ever-increasing volume of wastes and because of rising costs associated with landfill operation and possible groundwater contamination by landfill leachates. Disposal alternatives to landfill are desperately needed. Obviously, there is a significant economic incentive to reduce the volume of the incoming waste streams. While reduction, reuse, and recycling (3-R) practices should be exercised with highest priority as the means for reducing waste, there is still a significant volume of waste to be disposed. Therefore, with the benefits of substantial weight and volume reduction and potential energy recovery, incineration has become a promising municipal solid waste management option.

Incineration can reduce solid waste volume by 75-90% and weight by 65-80%. Further, design and operation of an incineration facility is subject to stringent rules and regulations mandated by the government to protect human health and the environment. Construction cost of incineration facilities can be very high; however, once they are operational, the costs tend to be stable. Most of the modern incinerators now are equipped with energy-recovery systems, especially in WTE (Waste-To-Energy) facilities, which capture the heat released during combustion and convert it to electricity. Such

systems can help reduce some of the operational cost as well as generate revenue to partially offset the costs of the incinerators.

The greatest challenge facing the incineration industry nowadays lies, however, in public acceptance. Highly publicized environmental disasters resulting from improper past disposal practices or mismanagement have intensified public awareness and, frequently, induced general skepticism toward incineration. In spite of the fact that incineration of municipal solid waste reduces its volume and mass by as much as 80%, it still leaves a residue of ash and inert materials that have to be properly handled. There are two types of ashes: fly ash accounting for 5-25% by weight consists of small particles that are removed by air pollution control (APC) devices; bottom ash, 75-95% by weight, is the material that remains in the bottom of the combustion chamber. Incinerator ash handling practice in the past consisted of combining the two ashes and disposing them in a sanitary landfill along with other solid wastes. Recent studies show that incineration destroys bulky matrix in the solid waste that retards the distribution of heavy metals, thus making them more available and mobile (Carotti and Smith, 1974; Greenberg et al., 1978; Clapp et al., 1989; Lee and Huffman, 1989; Fernández et al., 1992; Goldin et al., 1992; Ham et al., 1992; Buchholz and Landsberger, 1993; Wu et al., 1994; Brereton, 1996; Chandler et al., 1997; Chiang et al., 1997; Saxena and Jotshi, 1997). Thanks also to the acidic condition caused by biodegradation of solid wastes in co-disposal landfills, the bound metals become mobile and leachable. Moreover, incineration has been known as a source of polychlorinated dibenzo-p-dioxins (PCDDs) and polychlorinated dibenzofurans (PCDFs), which are carcinogenic (Travis and Hattermer-Frey, 1989; Konduri and Altwicker, 1994; Chandler et al., 1997). Consequently, a pretreatment to detoxify the

municipal solid waste incinerator (MSWI) fly ash may be necessary to guarantee safe ultimate disposal or utilization. There are many state-of-the-art technologies which could be used to achieve this objective, including solidification/stabilization (S/S) by adding agents to prevent hazardous materials from leaching out (Simpson and Charlesworth, 1989; Cheng and Bishop, 1992a&b; Glasser, 1992; McKinley et al., 1992; Reddy et al., 1994; Reardon et al., 1995; Albino et al., 1996; Brereton, 1996; Chandler, 1997), stabilization through thermal vitrification (Jakob and Kuhn, 1995; Brereton, 1996; Hjelmar, 1996), and leaching process to remove the heavy metals from the ash (Legiec et al., 1989; Gong and Kirk, 1994; Buchholz and Landsberger, 1995; Lin and His, 1995). These technologies have shown promises as the means to convert combustion residues of wastes from production and consumption into products that would relieve environmental stresses and, perhaps, provide new economic development opportunities.

While bottom ash is usually safe for disposal, common practice is to mix bottom ash and APC residues together and to dispose as a combined ash (Brereton, 1996; Hjelmar, 1996). Residues are subject to testing by the Toxicity Characteristic Leaching Procedure (TCLP) provided in the US EPA Test Methods for Evaluating Solid Waste, Physical/Chemical Methods (SW-846) Method 1311 prior to disposal. Residues that fail to meet the TCLP limits found in 40CFR 266 Appendix VII are subject to management as a hazardous waste or special waste, depending on state requirements. In practice, operations at most municipal solid waste incinerators have been tailored to produce residues that rarely fail the TCLP, so non-compliance is a rare event. The most frequent disposal option practiced is disposal in landfills that receive only MSWI residues, or monofills.

Utilization of MSWI residues has been limited to applications involving bottom ash since metal-rich fly ash may require some treatments before it can be safely utilized. Various researchers have studied the use of fly ash in place of cement, as has been done with coal fly ash. Nonetheless, as the results so far have been contradictory due to the heterogeneous and complex nature of fly ash (Hamernik and Frantz, 1991a and 1991b; Mangialardi et al., 1998), more research work is essential to assess whether this option is environmentally as well as economically viable. Other promising application of MSWI fly ash being explored is as a partial replacement for cement in concrete. Coal fly ash has been successfully utilized in construction works throughout the world as a means to achieve more economical product, better workability, lower permeability, better strength properties, and better chemical resistance (Plowman, 1984; Langley et al., 1989; Jaturapitakkul, 1993; Berry et al., 1994; Bilodeau et al., 1994; Oluokun, 1994).

Unlike coal fly ash, few studies have been conducted on utilization of MSWI fly ash as a cement replacement. Most of the research works so far (Hamernik and Frantz, 1991a and 1991b) have been concentrated on using the fly ash as-is. It was found that MSWI fly ash exhibited some pozzolanic behavior similar to that of coal fly ash. As in the case of coal fly ash, fineness of the material affects both pozzolanic activity and workability of concrete (Mangialardi et al., 1998). The use of MSWI fly ash in fractionated forms, thus, comes naturally to mind as the next step towards the attempt to fully realize its potential.

In order to thoroughly understand the complex nature of MSWI fly ash, one needs to obtain information that includes basic physical and chemical characteristics, bulk chemical composition, mineralogy, morphology and elemental surface analysis, particle

size distribution, and mechanical properties. Lastly, before MSWI fly ash utilization can be materialized, its impact on the environment needs to be evaluated.

1.2 Scope of Investigation

The scope of investigation of this study can be divided into three main parts as follow.

1. Ash Acquisition. Upon conducting this research, we have explored the utilization of MSWI fly ash from a resource recovery facility in New Jersey. This WTE facility handles 2,505 tons of MSW and produces approximately 70 tons of fly ash daily.

Figure 1.1 Municipal Solid Waste Incineration Plant Diagram

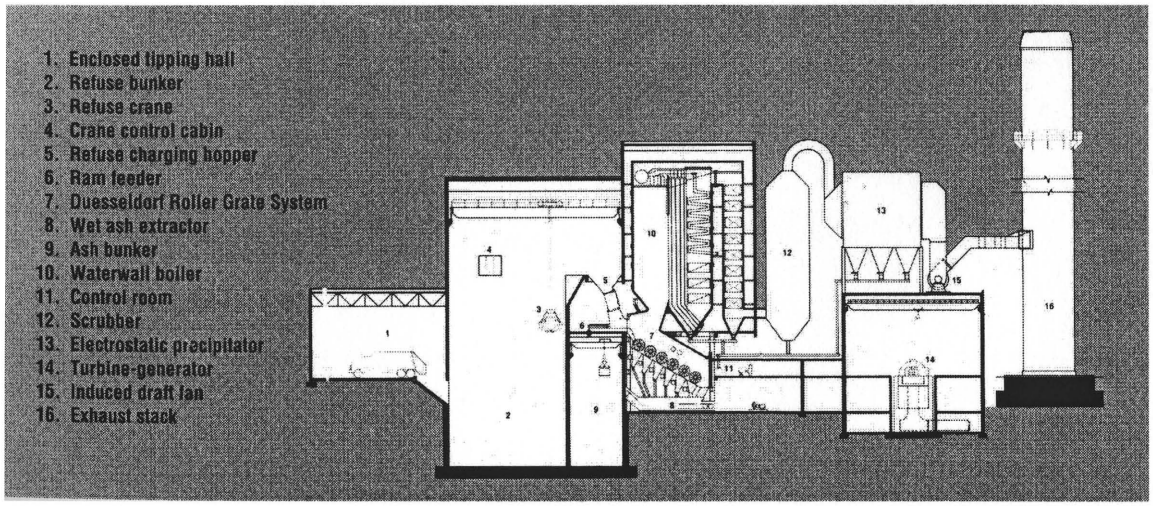

As seen in Figure 1.1, MSW is deposited daily in a refuse bunker (2) waiting to be lifted by a crane (3). The waste is then introduced to the combustion chamber through a charging hopper (5). Upon entering the chamber, the waste is allowed to dry on a Düsseldorf rolling grate system (7) which consists of a series of drums placed at a downward slope of around 30 percent (Saxena and Jotshi, 1997). Each drum rests

separately over individual steel compartments for the purpose of zoning the input of underfire air and the siftings discharge. The radiant heat emitted from the hot furnace walls and burning waste causes a temperature profile across the depth of the grate. The waste moves through different heating zones; drying, pyrolysis, combustion, and burnout zones as illustrated in Figure 1.2 (Chandler et al., 1997).

Figure 1.2 Temperature Zones on Typical Grating System

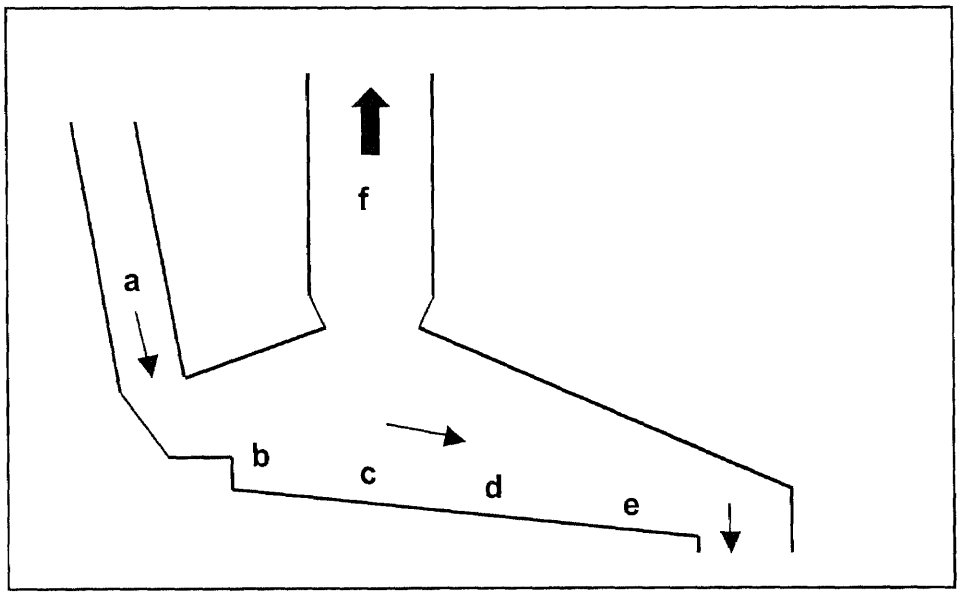

The charged waste is first exposed to mild heat (50°C) in the hopper (a) where the moisture is driven off into the flue gas stream (f). Further heating in the drying zone (b) increases the temperature to about 100°C. As the waste moves further, the temperature increases to approximately 500° C and pyrolysis starts (c). At this temperature, most organic compounds start to disintegrate. The decomposition products are volatile or semi-volatile organic compounds, carbon element, and tar. The volatile species are oxidized in the gas phase, releasing a lot of heat in the process while carbon element and tar are

burned as they move along the grate. In the combustion zone (d) where the temperature goes beyond 500°C, the waste combusts. The maximum temperature in the fuel bed is found at the transition zone between combustion zone (d) and burnout zone (e). The burned out waste (also called bottom ash or slag) tumbles down the grate and is collected in a quench tank (8) before being dewatered and conveyed to a bottom ash storage bunker (9).

The volatile gases enter the flue gas stream that passes through waterwall boiler (10) at temperature above 850°C. More oxygen is supplied to ensure complete oxidation and conversion of the organic gases to carbon dioxide and water. The heat produced in this stage is captured by the boiler to generate steam that, in turns, is used to produce electricity (14). Flue gas stream along with entrained fly ash from the boiler is sprayed with lime in the dry scrubbers (12) to remove acid gases and stabilize metals. Most of the fly ash particulates that contain metal condensates are then captured in the subsequent electrostatic precipitators (ESP) (13) before releasing the gas consisting mostly of steam into the atmosphere through the exhaust stack (16).

For the particular resource recovery facility, the fly ash produced is transported to the proprietary ash treatment unit on-site that utilizes phosphoric acid to further stabilize heavy metals in the fly ash. Before being transported to a final disposal destination in a monofill, the stabilized fly ash is combined with bottom ash. This is to provide residual buffer and chemicals necessary to stabilize the bottom ash.

The fly ashes used in this study were acquired in two separate batches from different points in the process. The first batch, dubbed NJIT 1, was sampled from the proprietary fly ash treatment unit. The second batch, NJIT 2, was taken directly from the

ESP units which is downstream from lime-injected acid gas scrubbers. Each batch was further sampled so as to ensure that good representative samples were obtained for all of the tests.

2. Potential Utilization. Each fly ash sample was put through a battery of tests that include physical and chemical characterizations. Particle sizes (by means of sieving and particle size analyzer), moisture content, loss-on-ignition (LOI), specific gravity, absorption capacity, and pH were determined for the fly ashes. NJIT 1 fly ash, with its large particle sizes, was tested if it was suitable for use as an aggregate replacement. NJIT 2 fly ash of which particle size distribution is close to that of cement was a candidate for use as a cement replacement. An air classifier was introduced as a means to separate fine particles and coarse particles from the pre-sieved raw NJIT 2 fly ash.

To study the contribution of MSWI fly ashes to the compressive strength development of MSWI fly ash-cement mortars, the fractionated portions as well as the raw NJIT 2 fly ashes were used to replace cement by 15%, 25%, and 35% in mortar mixes. The influence of the ratio of the amount of water at mixing to the amount of cement and fly ash (water-to-binder ratio) was also studied by varying the ratio from 0.45 to 0.55. Preliminary test results show that all of the fly ash fractions provided enhancement to 28-day compressive strength, ranging from 138% to 153% of that of the control mortars when used to replace 15% of cement at the water-to-binder ratio of 0.45. However, as the replacement percentage went beyond 15%, the compressive strengths of the MSWI fly ash mortar specimens decreased.

Since it is known that salts, particularly chlorides, produced undesirable effects in concrete and reinforced concrete, simple washing of MSWI fly ash was introduced.

Washing of MSWI fly ash was found to effectively remove most of salts, such as sodium chloride, that may be deleterious to steel in reinforced concrete. It was doubtful if washing might also remove components that could be responsible for superior compressive strengths. Compressive strength test was therefore conducted using the washed fly ash.

Since the compressive strength test merely supplied the information on the overall result of the effects of the MSWI fly ash on the strength. The question remained as to what really contributed to the additional strength. It needed to be further explored in the microscopic level. Progress of hydration of MSWI fly ash-cement pastes at different replacement levels was examined through the use of X-ray diffraction spectroscopy (XRD). Results reveal that, aside from replacing the amount of calcium silicates (C_3S and C_2S), reactive ingredients necessary for hardening of cement, MSWI fly ashes may, in fact, aid in the process. Environmental scanning electron microscopy (ESEM) equipped with energy dispersive X-ray spectrometry (EDX) was employed to provide further inspection of microstructures of the pastes and their surface elemental compositions.

3. Environmental Concerns. Bulk chemical analysis results showed that the MSWI fly ashes had high concentrations of cadmium (Cd), chromium (Cr), lead (Pb), and antimony (Sb) which are toxic heavy metals according to the Toxicity Characteristic criteria (40CFR 261.24). Therefore, the MSWI fly ash-cement solidified mortar specimens were assessed for their potential to leach toxic metals above the levels of concern. Details of all the investigations mentioned above are elaborated in this dissertation.

CHAPTER 2

LITERATURE SURVEY

2.1 MSWI Fly Ash and Regulations

In the United States, municipal solid waste (MSW) is regulated at the federal level by the Resource Conservation and Recovery Act (RCRA) of 1976, as amended by the Solid Waste Disposal Act of 1980, and the Hazardous and Solid Waste Amendment (HSWA) of 1984. Additionally, the Comprehensive Environmental Response, Compensation and Liability Act (CERCLA) of 1980 was enacted in response to the numerous environmental catastrophes resulting from improper waste disposal practices of the past. The purpose of these laws is to assure the reliable management of hazardous and toxic waste disposal operations and dumpsite cleanup.

In late 1995, the U.S. EPA issued the new Clean Air Act rules regulating MSW incinerators (Eighmy and Kosson, 1996). The new maximum achievable control technology (MACT) rules, which impose strict limits on metals and dioxins for new and existing facilities, impacted about 121 waste-to-energy (WTE) facilities and nine combustors. The Act requires that all retrofits be completed by the year 2000.

As a normal practice, bottom ash and air pollution control (APC) residues are mixed together and disposed of as combined ash in a monofill that only receives municipal solid waste incinerator (MSWI) residues. Prior to disposal, residues are subject to testing by the Toxicity Characteristic Leaching Procedure (TCLP, SW-846 Method 1311). Residues that pass the TCLP are subject to management as non-hazardous solid

waste according to subtitle D of RCRA, while those that fail are subject to management as a hazardous waste or special waste, depending on state requirements.

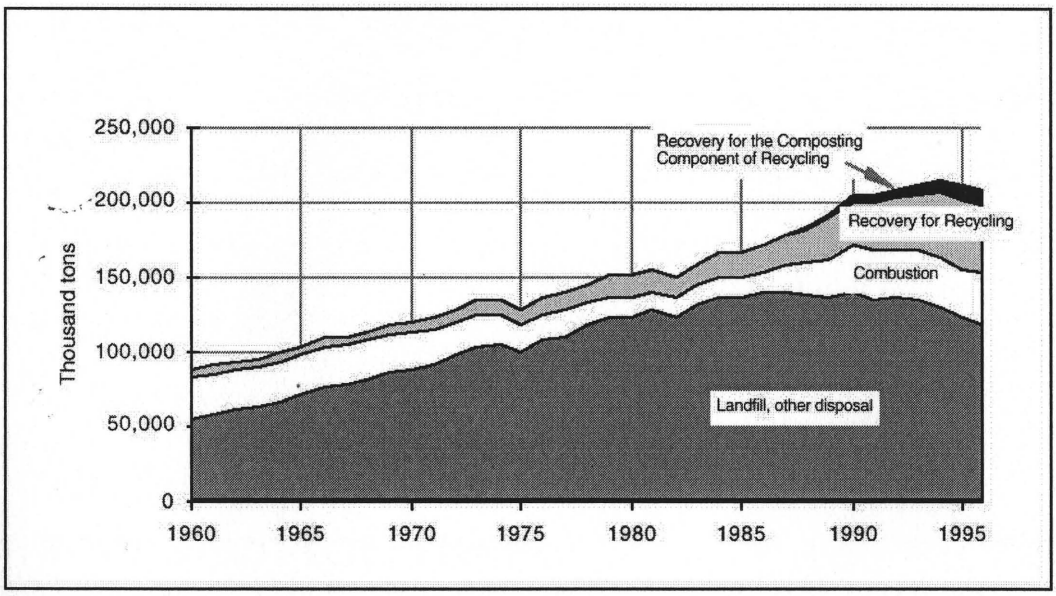

Figure 2.1 Municipal Solid Waste Management, 1960-1996

As seen in Figure 2.1, according to the U.S. EPA (1998), municipal solid waste generation had grown relatively steadily from 88 million tons in 1960 to 214 million tons in 1994. However, after peaking in 1994, MSW generation in 1995 and 1996 experienced a decline (both in product and non-product waste categories). In 1996, MSW generation was less than 210 million tons, reflecting a trend in source reduction. Landfill disposal typically consisted of open dumping, often accompanied with open burning of the waste to reduce its volume. From 1960s to early 1970, a large percentage of MSW was burned, with little recovery for recycling. Through the mid-1980s, incineration declined considerably and landfills became difficult to site, while waste generation continued to increase. Materials recovery was not at all vigorously carried out, resulting in dramatic

burden on the nation's landfills. As Figure 2.1 graphically shows, discards of MSW to landfill or other disposal apparently peaked in the 1986-1987 period, then they began to decline as materials recovery and combustion increased. Recovery of products and yard trimmings increased steadily, while combustion had stayed relatively constant at 5 to 17 percent of total MSW generation. Consequently, MSW discards to landfills continued to decrease in 1990's. Landfilling accounted for 116.2 million tons of MSW in 1996. As a percent of total MSW generation, landfilling has consistently decreased—from 83.2 percent of generation in 1986 to 55.4 percent in 1996.

2.2 Origin of MSWI Fly Ash

Whereas the primary purpose of burning coal is to produce energy, this aspect is of only secondary importance where incineration of municipal solid wastes is concerned. The main goal is rather to reduce their volume because of great difficulties involving MSW handling and disposal. Incineration reduces volume of waste by approximately 80% and allows for recovery of much of the energy bound in the waste. However, the incineration process is not a final waste treatment stage. In fact, the high temperature in the incinerator helps to release heavy metals as well as produce harmful compounds, such as dioxins, from MSW. Metals with low vapor pressures are collected in bottom ash. As described by Cahill and Newland (1982), a volatilization-condensation mechanism involves entrapment of volatile metals in flue gas stream and later deposition of these metals on fly ash particles in subsequent APC devices, thereby increasing their concentrations by several folds. To avoid landfilling and problems associated with handling of these potentially hazardous materials, many researchers are investigating the

possibility of utilizing MSWI ashes (Ali and Chang, 1994; Hamernik and Frantz, 1991a&b; and Mangialardi et al., 1998).

Bottom ash, which normally passes the TCLP test, has been used as an aggregate substitute in road construction applications as well as an aggregate substitute in asphalt pavement. Investigations on engineering properties by Goh and Tay (1993) indicated that MSWI fly ash has the necessary properties for use in geotechnical applications. They successfully used the fly ash as an admixture to stabilize soft marine clay and to enhance the behavior of cement and lime treated soils. Addition of MSWI fly ash to clay samples showed improved undrained shear strength, higher permeability, and lower compression properties. The potential utilization of the material was also realized as a source of fill material, with low compacted density and high strength. Few researchers have also studied the utilization of MSWI ashes in portland cement concrete, as has commonly been done with coal fly ash (Hamernik and Frantz, 1991a&b and Mangialardi et al., 1998). The benefits of using MSWI fly ash in mortar are twofold; namely, the cost savings stemming from reduction in the amount of cement used, and the ecological advantage of ensuring a final destination for the ash. Nevertheless, up to this point, the results have been inconsistent and thus inconclusive at best.

Historically, the term "fly ash" has been used to describe all types of finely sized ash and sorbent material collected in APC systems. However, due to the very different physical and chemical properties of the different residue streams, it is more precise to identify the ash based on type of unit that the ash was collected in, such as electrostatic precipitator (ESP) ash.

Although the APC technology is the single most important factor influencing characteristics of the APC residues, several other factors also play a role. Other influences are type of incinerator, operating condition, and feed composition. There are two main types of incinerators; mass-burn and refuse-derived fuel (RDF) incinerators (Brereton, 1996). A mass-burn incinerator burns wastes as delivered with only minimal pretreatment although removal of oversized material is critical. The other type of incinerator, an RDF, burns pellets containing only combustible materials processed from raw refuse. This can alleviate the problem of heterogeneity of feed stream to provide material composition that is more consistent for smoother operation. Obviously, the feed composition has a great influence on the properties of fly ashes. The net effect of RDF systems on ash quality is a reduction in the quantity of ash produced per ton of waste incinerated since most of the non-combustibles are removed in the process. Moreover, removal of ferrous and other materials from the feed stream changes the composition of the ashes.

Typical ranges of the amounts of residues produced from the major APC processes at mass-burn systems are given in Table 2.1. Since there is usually no upstream removal of fly ash, it can make up a substantial proportion of the collected residues in particulate collection unit, such as an electrostatic precipitator (ESP) or a fabric filter (FF), downstream from acid gas scrubbers. Based on the US EPA report (1998), 36.1 million tons of MSW (17.2%) was incinerated, which generated approximately 0.72 to 1.81 million tons of dry APC residues.

Table 2.1 Typical Amounts of Residues Produced per ton of Feed Waste

Type	Amount (kg/ton)	Amount (Million tons)
Bottom ash	250-420	8.23-13.82
Fly ash	10-30	0.36-1.08
Acid gas scrubbing residues		
- Dry process[1]	20-50	0.72-1.81
- Semidry process[1]	15-40	0.54-1.44
- Wet process[2]	1-3	0.04-0.11

Note: 1. Including 10-30 kg/ton fly ash.
2. Dry weight of sludge from wastewater treatment
With data from Hjelmar (1996) and US EPA (1998)

2.3 Chemical and Mineralogical Compositions of MSWI Fly Ashes

Major elements with concentration of more than 10,000 mg/kg (>1.0%) are O, Cl, Ca, Si, Mg, Fe, Al, K, Na, Zn, S, and Pb. Oxygen is probably the most abundant element in fly ash since it is present as oxides of several of the other major, minor, and trace elements, especially Si, Ca, Mg, Fe, Al, Na, K, S, and C. Chlorine is in the chloride forms, which are both products of condensation on fly ash particles, and, to the larger extent, reaction product of flue gas control in dry and semi-dry scrubbers, $CaCl_2$. Calcium is present both as one of the major matrix constituents of the fly ash particles and as part of the major reaction product in dry and semi-dry scrubbers. Pb and Zn, which are also present as major constituents in fly ash, particularly Pb, pose a serious concern in relation to disposal and utilization of MSWI fly ash.

Minor elements with concentrations of between 1,000 and 10,000 mg/kg (0.1-1.0%) in MSWI fly ash are Ti, Mn, Ba, Sn, and Cu. Inorganic carbon is also present in the form of carbonates and soot or char carried over from the furnace. Hg, Cd, Sb, Cr, Sr,

Ni, As, V, Ag, Co, Mo, and Se are present in trace amounts with concentrations of lower than 1,000 mg/kg (<0.1%).

The mineralogical characteristics of MSWI fly ashes play a crucial role in determining their application and leaching behavior, thus a thorough understanding of the mineralogy of the ashes is necessary for the development of an environmentally sustainable fly ash management strategy. Ubbriaco (1996) found that the major mineralogical constituents determined by X-ray diffraction (XRD) were KCl (sylvite), NaCl (halite), $CaSO_4$ (anhydrite), $CaCO_3$ (calcite), and α-SiO_2. Minor constituents were $Ca(OH)_2$ (portlandite), CaO (lime), α-Fe_2O_3, silicates, and calcium aluminate. Others have found $CaCl_2$, CaClOH, $PbSO_4$, $PbCl_2$, $ZnSO_4$, γ-$CaSO_4$, $PbTi_3O_7$, $Na_{21}MgCl_3(SO_4)_{10}$, $K_2Ca(SO_4)_2.H_2O$ (McKinley et al., 1992; Eighmy et al., 1993&1995; Hjelmar, 1992; Kirby et al., 1993&1994). Mangialardi et al. (1998) also found Ca_2SiO_4, Ca_3SiO_3, and $NaAlSi_3O_8$ (albite) in their ESP fly ash.

Leman, Walder, and Schwyn (1995) studied the management of waste batteries in Switzerland as a significant source of heavy metals. They concluded that although batteries of different kinds were mercury-free and 50-55% of them were collected separately, the rest of the batteries still contributed considerable amount of heavy metals, especially, Cd, Cu, Mn, Ni, and Zn, in the waste incineration process. They therefore recommended a promotion of battery recycle program through informational campaigns as well as a total battery collection and recycling. In a study conducted by Sawell et al. (1993), MSW samples were spiked with lead acid batteries and cadmium-bearing plastic stabilizers to verify if they were a potential sources of lead and cadmium in the fly ash. Their results showed that an increase of batteries in the input stream did not result in an

increase in soluble lead in the fly ash although it did result in a lead increase in the bottom ash. They, however, found that there was an increase in soluble cadmium in the fly ash in the cadmium-spiked sample. Their results indicate that the combustible fraction of the input stream contribute to leachable metals in the fly ash.

Metals enter the combustion waste stream in a variety of chemical forms. These include pure metals, oxides, halides, and other inorganic and organometallic species. Temperature, chloride content of the waste, and thermodynamics of the metals dictate metal distribution (Brereton, 1996). Cahill and Newland (1982) theorized that metals with higher boiling points than typically found in a combustion chamber would serve as nucleation particles. Thus, aluminum, silicon, and manganese would form the core of the fly ash particles (Ontiveros et al., 1989). Fernández et al. (1992) proposed three different relative stability criteria for a heavy metal compound present in an MSW incinerator, depending on the thermodynamic stability of its oxide being greater than, equal to, or lower than its chloride. If the oxide is more stable than the chloride, the element is transported mechanically and is found in the matrix of the fly ash particles giving them alkalinity. The element of which oxide and chloride present similar stabilities is transported by both mechanical and volatilization-condensation mechanisms. If the oxide is less stable than the chloride, the heavy metal chloride is transported principally by volatilization-condensation. It then deposits on the surface of the fly ash particles, forming highly soluble compounds. Increase in both chloride content of waste and combustion temperature causes the formation of volatile heavy metal compounds, hence increasing metal partitioning to the fly ash particles and the flue gas (Chiang et al, 1997).

2.4 Particle Size Distribution and Morphology of MSWI Fly Ash

In general, particle size distribution of MSWI fly ash depends upon where in the process the fly ash was taken from. Waste feed composition, incinerator type, operating conditions, and type of APC devices also have great influences on the size distribution. Dry and semi-dry process residues generally contain a higher proportion of fine materials than fly ash without acid-gas cleaning residues. Fabric filters (FF) are more efficient at removing submicron size particles than ESPs; therefore, the proportion of fine materials in fabric filter residues will be higher than that in residues collected in ESPs (Chandler et al., 1997). Chandler et al. (1997) reported that the particle size distribution of ESP residues determined optically is in the range of 40 to larger than 200 microns. The FF residues, however, have a distribution that falls between 10 to 40 microns in diameter.

McKinley et al. (1992) used sieves to separate MSWI fly ash from an ESP from a mass-burn incinerator into size classes ranging from 45 to 600 microns. Inductively-coupled plasma (ICP) analysis results indicated very little variation in chemical compositions between relatively coarse sizes and very fine sizes. Having used a scanning electron microscope (SEM) to confirm their finding, they discovered that the fly ash particles tended to form large agglomerates. Stuart and Kosson (1994) encountered the same problem and suspected that static charge removal system was inadequate on the smaller screens. Electrostatic charges may have caused the agglomeration or prevented particles from getting through the screen fibers of the mesh.

Researchers, including Ontiveros et al. (1989), Buchholz and Landsberger (1993), and Richers and Birnbaum (1998), investigated variation of elemental distribution in MSWI fly ash and semi-dry APC residues as a function of particle size. It was found that

more volatile elements such as cadmium, chromium, and lead were enriched substantially in smaller particles of fly ash, whereas the opposite was true for matrix elements, such as aluminum, iron, manganese, and potassium. The enrichment may be due to condensation of volatile metals on the surface of the smaller particles that possess larger surface area to volume ratios than bigger particles.

A wide variety of highly crystalline structures were observed. Unlike coal fly ash, which exists predominantly as spherical particles, municipal fly ash contains planar, cylindrical, and sintered agglomerations of particles as well as spherical particles. However, the spherical particles do not predominate. The most dominant feature in the micrographs was the occurrence of crystals residing on the fly ash particles. This can be explained by the volatilization-condensation theory. Most of the crystals are salts of volatile metals that deposited on the surface of the fly ash particles. Sodium chloride (NaCl), in the form of cubic crystals, was abundant in the study done by Hinshaw (1994). He postulated that the salt might originate from newspaper feed material. Calcium sulfate ($CaSO_4$) was also found in the particles from spray-dry scrubber unit.

Particle size distribution is analyzed by utilizing the phenomenon of light scattering from particles. Typically, the sizes of liquidborne particle can be categorized into three regimes. Each regime uses different equation to calculate the particle size. Rayleigh theory is applied to measure the scattered light intensity at 90° when particles present in a fluid are significantly smaller than the wavelength of light with which they are illuminated. The second regime where particle sizes are of the same order of magnitude as the wavelength can be analyzed using Mie theory. To minimize refractive index effects, the near forward scattered light intensity is measured. When particles are

larger than the wavelength, most of the scattered light is in the forward direction, and diffraction occurs.

Leeds+Northrup Microtrac particle analyzer utilizes all three regimes to measure the particle size in a double optical bench model. The small particle analyzer bench is a field-scanning device in which two optical light beams are used. Laser beam is projected through a stream of particle. The scattered light from particles is collected by photo detectors located at 90° to measure particles in the Rayleigh regime (0.12 to 0.35 microns) and in the near forward direction to measure those from 0.35 to 40 microns. Microtrac software then analyzes the information and determines the size distribution of the sample. The second optical bench implements diffraction pattern analysis. Parallel monochromatic light incident onto a field of opaque, mono-sized, spherical particles is diffracted through specific angles, depending on the size. The light is then focused as a rotationally symmetrical pattern in the focal plane (Allen and Davies, 1987).

The advantage of this technique is that it can measure particles in the range from 0.1 to 1000 microns. The amount of sample used in particle analysis is very small comparing to that required by sieve analysis and other methods. The de-agglomeration procedure is applied in order to obtain the true size of each particle.

X-ray element mapping can be accomplished by energy dispersive and wavelength dispersive techniques. The energy dispersive X-ray spectrometers (EDX or EDS) identify the characteristic X-rays produced by electron bombardment in the microprobe with energy specific detectors. Wavelength dispersive spectrometers (WDS) employ diffraction by crystals to separate X-rays from different elements prior to their striking a detector. The EDX is useful for rapid qualitative analysis where interferences

from X-rays with overlapping energies are minimal whereas the WDS is preferred for quantitative analysis. Nevertheless, the results obtained are considered semi-quantitative because of small size, variability, and possibly hollow nature of the fly ash particles (Plüss and Ferrell, Jr., 1991). Element ratios should approximate those actually occurring in the particles, however.

Sandell et al. (1996) used a scanning electron microscope (SEM) and an EDX to examine lead-bearing fly ash particles from an ESP in a mass-burn facility. They reported that two major types of lead forms were predominant. These are lead-rich inclusions found inside of particles and lead in low concentrations in chloride-rich crystals found on the surfaces. Apparently, the volatilization-condensation theory may not apply in this case. They suggested that the initial form of lead in the input stream must be considered, rather than the transport mechanisms based on elemental boiling points.

2.5 Particle Size Fractionation

The behavior of fly ashes can be modulated by several procedures: a) chemical treatments, which produce a modification of chemical surface composition and texture; b) physical treatments, such as air separation, sieving, modifying fineness and particle size distribution; c) thermal treatments, such as slow or rapid cooling, producing changes in the vitreous/crystalline ratio; and d) mechanical treatments, such as grinding, where the fineness and morphology of particles are altered (Payá et al., 1996).

As in the case of coal fly ash, the fineness of the material affects both pozzolanic activity and the workability of the ensuing concrete (Mangialardi et al., 1998). Ukita et al. (1989) employed air separation technique to classify coal fly ashes into three particle size

classes: 5, 10, and 20 microns. Results showed that utilization of air-classified fly ash reduced water requirement, improved workability, as well as enhanced strength and water tightness in concrete. He further concluded that the increase in the percentage of finer particles (<20 microns) incorporated in concrete mixes improved the strength. Jaturapittakul (1993) studied the influence of incorporating classified coal fly ashes from various sources to replace cement in concrete. The coal fly ashes were air-classified into size fractions ranging from 5 to 150 microns. His results showed that concrete specimens that incorporated finer fractions exhibited higher strength than those with coarser ones. The strength of specimens mixed with 15% of 5-micron fly ash surpassed that of control specimen at an early age of 14 days. He suggested that there was an optimal degree of cement replacement over which strength started to decrease. This is in disagreement with Ukita's conclusion.

Ranganath et al. (1995) suggested that combined parameters of fineness and soluble silica content be used to evaluate the potential contribution of fly ash since the mechanisms and the rate of formation of calcium silicate gel are both physical and chemical. At early ages, fineness of fly ash helps increase the strength via micro-filling and cement dispersion effect while, at later ages, the soluble silica content of the fly ash or its pozzolanicity becomes more significant.

Despite all the potential benefits, large-scale separation of the particles prior to utilization may not likely be commercially viable due to mass dominance of the smallest particles and problems encountered separating the fractions (Buchholz and Landsberger, 1993).

2.6 MSWI Fly Ash as a Cementitious Material

Berry et al. (1994) proposed two possible cementing mechanisms that might influence mechanical properties and permeability of solidified products: a) Enhanced reaction of the portland cement component, with the consequent production of larger quantities of hydration products, exceeding the usual stoichiometric proportions; and b) Formation of additional cementing constituents through chemical reactions involving fly ash.

Many companies producing portland cement concrete already use coal fly ash very successfully as a cement replacement in their mix design. The advantages of using coal fly ash in portland cement concrete includes a more economical product, better workability of the mix, better strength properties, better chemical resistance (sulfate resistance and aggregate-alkali resistance), and lower permeability. However, unlike coal fly ash, few studies have been carried out so as to explore the feasibility of using MSWI fly ash as a cement replacement for cement. Ali and Chang (1994) reported that MSWI fly ash may exhibit some pozzolanic behavior but did not show any self-cementitious properties.

MSWI fly ash when incorporated in cement mixes may help produce products with satisfactory compressive strength, but it has been found that the cementitious matrices contain toxic heavy metals and prevent them from being exposed to the environment as well (Simpson and Charlesworth, 1989; Goumans et al., 1991; Glasser, 1992; McKinley et al., 1992; Rashid and Frantz, 1992; Ali and Chang, 1994; Yang and Chen, 1994; Rebeiz and Mielich, 1995; Albino et al., 1996; Hjelmar, 1996; Webster and Loehr, 1996; Chandler et al., 1997; Mangialardi et al., 1998). Typically, one of the options generally suggested as a means to reduce the solubility of trace metals contained

in MSWI fly ash, is solidification/stabilization (S/S). Both terms are commonly used interchangeably and the processes are usually combined although their meanings are distinctly different. Solidification refers to the techniques that encapsulate the waste in a monolithic solid of high structural integrity. It does not necessarily involve a chemical reaction. Migration of contaminants is thus limited by smaller surface area exposed to the environment. Stabilization, on the other hand, refers to the techniques that reduce the hazard potential of a waste by converting contaminants into their least soluble, mobile or toxic forms. The physical nature and handling characteristics of the waste may not be changed by the techniques (Chandler et al., 1997).

Glasser (1992) distinguishes two types of the immobilization of heavy metals in cement pastes: physical and chemical immobilization. Physical immobilization is normally associated with the microporosity of the calcium silicate hydrate (C-S-H) phase and, consequently, adsorption of ions and particles on this newly formed phase. Chemical immobilization, on the other hand, takes place as a result of formation and precipitation in the pastes of compounds of low solubility products, most of which are hydroxides of heavy metals due to high pH. Nonetheless, other products of hydration of cementitious compounds also play an important role in immobilization of heavy metals. These are hydroaluminates and calcium hydrosulfoaluminates in portland cement pastes.

It was demonstrated by McKinley et al. (1992) that MSWI fly ash could be successfully stabilized in a 1:1 mixture of fly ash and portland cement which met all environmental requirements. Leachate concentrations of Cd and Pb from both intact specimens and crushed specimens were found to be much lower than those from as-received fly ash. This indicates that the immobilization of Cd and Pb in the fly

ash/cement mixture is primarily chemical in nature. A possible explanation for the chemical immobilization is the formation of insoluble silicates and hydroxides in the highly alkaline environment of the cement. One disadvantage of stabilization process is the large increase in mass of the final disposal product.

Wilson and Akers (1970) reported loss on ignition (LOI) values for MSWI fly ash ranging from 0.35 to 14.45%, compared with the acceptable level of less than 6% as required by ASTM C618. In other words, about 13% of the materials within MSWI fly ash is not burnt during the combustion process. That is, the incinerator fly ash generally contains a high content of carbonaceous materials. Various authors noted that that a coal fly ash having LOI greater than 6% reduced entrained air content in concrete which also reduced durability and workability. Yang and Chen (1994) showed that the pore structure of MSWI fly ash provides good surface sites for physical adsorption and chemisorption of polycyclic aromatic hydrocarbons (PAHs). It was speculated that carbonaceous materials in the fly ash might have adsorption/absorption effects on heavy metals. If that were true, it would explain why portland cement alone can satisfactorily stabilize heavy metals of concern in MSWI fly ash.

Hamernik and Frantz (1991a) conducted batteries of tests to determine the physical and chemical properties of several MSWI fly ashes. They found that RDF fly ashes had potential use as a pozzolan in concrete according to Class C pozzolan requirements (ASTM C618) except for fineness and loss on ignition (LOI). Mass-burn fly ash did not meet several of the chemical requirements, however. Both types of fly ashes had cement pozzolanic activity indexes comparable to that of coal fly ash. In a subsequent study, Hamernik and Frantz (1991b) found that at up to 30 percent cement

replacement levels in concrete mixes, specimens containing the RDF fly ashes produced better strengths than or comparable to those containing only cement. However, the same was not true for the specimens incorporating mass-burn fly ash that produced significantly lower strengths. As the cement replacement percentage increased, the concrete compressive strength decreased for all of the fly ashes. Yang and Chen (1994) also found that MSWI fly ash enhanced the unconfined compressive strength of solidified specimens while maintaining TCLP limit compliance. The reason for this may be due to the great capacity of water adsorption of MSWI fly ash during mixing, resulting in lower water-to-cementitious material ratio, and thus greater compressive strengths.

The main hydration products of mixture of MSWI fly ash and lime-natural pozzolan were ettringite and chloroaluminate hydrate. The formation of these two products was induced by sulfate and chloride contained in the MSWI fly ash. These reacted with reactive constituents of the pozzolan and calcium hydroxide, creating a cementitious matrix from the solidified mixture (Ubbriaco, 1996).

2.7 Hydration of Cement-MSWI Fly Ash Pastes

Many coal combustion residues are cementitious since they react and harden when mixed with water. That is, they are composed of a number of compounds that undergo hydration reactions in the presence of water and form hydrated products. While the chemical reactions describing hydration of cement and coal fly ash-cement compounds have been well studied, apparently more research is needed to describe hydration of MSWI fly ash-cement mixtures.

Hydration of tricalcium silicates (C_3S) and dicalcium silicates (C_2S), which are key components in cement, produces calcium silicate hydrate and calcium hydroxide ($Ca(OH)_2$). The formula for calcium silicate hydrate ($C_3S_2H_3$) or C-S-H gel is only approximate since the composition of this compound varies over a wide range. This poorly crystalline material is responsible for strength in concrete. The equation describing hydration of these two compounds are as follow.

$$2C_3S + 6H \rightarrow C_3S_2H_3 + 3CH$$

$$2C_2S + 4H \rightarrow C_3S_2H_3 + CH \ ,$$

where C : CaO, S : SiO_2, H : H_2O, and CH : $Ca(OH)_2$.

These reactions usually remain incomplete, with grains of unhydrated cement present. Due to the non-stoichiometric nature of C-S-H, the exact amount of $Ca(OH)_2$ produced is always uncertain (Berry et al., 1994). Direct XRD examination of hydrate phases is also difficult since most of them are non-crystalline and non-stoichiometric. Nevertheless, the relative formation of $Ca(OH)_2$ and the relative disappearance of C_3S should indicate any major differences in the stoichiometry and nature of hydration between MSWI fly ash-cement and cement pastes as can be seen in studies done by Berry et al. (1994), Xu and Sarkar (1991, 1994).

Hydration of coal fly ash is believed to begin with the breaking down of its glass phases to release alumina and silica at a high pH of about 13.3 or higher in the presence of lime. High pH can be achieved by adding NaOH in the fly ash; however, that may reduce the solubility of $Ca(OH)_2$ due to common ion effect. If this is the case, then

substitution of sodium for calcium in C-S-H may occur. It is also well known that alkalis in cement increase the early strength at the expense of the later age strength. (Xu and Sarkar, 1991).

The hydration kinetics can be better understood when the relative intensities of C_3S and/or C_2S consumed and $Ca(OH)_2$ produced in hydration process are plotted as a function of hydration time. At very early ages up to one day, hydration process of a pure cement paste shows significant decreases in C_3S and C_2S contents and at the same time a sudden rise in $Ca(OH)_2$ content. A fly ash-cement paste follows the similar trend, although to a lesser degree. As hydration progresses, the amount of $Ca(OH)_2$ increases up to 7 to 28 days. After 28 days, $Ca(OH)_2$ content begins to decrease because of the conversion of $Ca(OH)_2$ to C-S-H gel or the calcium exchange mechanism. This effect is more conspicuous in the fly ash-cement paste where it leads to a considerable decrease in $Ca(OH)_2$ due to pozzolanicity of fly ash (Xu and Sarkar, 1991; Berry et al., 1994).

It is known that the pozzolanic reaction of fly ash in concrete is significant after a couple of weeks. Until this period, fly ash particles behave more or less as an inert material which only serve as precipitation nucleus for C-S-H gel and $Ca(OH)_2$ from the hydration process. Moreover, fly ash particles considerably disperse the cement grains, thus allowing more available sites for reactions (Berry et al., 1994). The surfaces of nucleating fly ash particles provide sites for $Ca(OH)_2$, C-S-H, and other hydration products to precipitate, thereby leading to a more homogeneous distribution of hydration products (Xu and Sarkar, 1994). Berry et al. (1994) proposed that aspects of the hydration of fly ash-cement systems resulted from the interplay of hydrolysis, ion exchange, and precipitation processes. The essential components for these processes were water, alkalis,

and calcium ions that reacted together with the aluminosilicate glass constituents of fly ash through the medium of pore fluids.

Pozzolanic reactions involve depolymerization of the glass matrix of the fly ash particles initiated or catalyzed by alkali ions at high pH. At the early stages, most of the hydrolyzed products remain attached to the matrix. As more bonds are hydrolyzed, low molecular weight polymer fragments and oligomers will cause the increase in aluminate, silicate, and aluminosilicate oligomers and monomers to enter the pore fluid. $Ca(OH)_2$ is consumed by the reactions that result in precipitation of various calcium silicates, aluminates, and aluminosilicates. Silica and alumina from fly ash react with alkalis produced during cement hydration to form cementitious compounds as shown below (Plowman, 1984).

$$SiO_2 + 2Na^+ \text{ (or } 2K^+) + 2OH^- \rightarrow Na_2\,(K_2)\,SiO_3H_2O$$

$$Ca^{2+} + SiO_2 + H_2O \rightarrow xCaO.ySiO_2.zH_2O$$

$$Ca^{2+} + Al_2O_3 + H_2O \rightarrow xCaO.yAl_2O_3.zH_2O$$

$$Ca^{2+} + SiO_2/Al_2O_3 + H_2O \rightarrow xCaO.yAl_2O_3.zSiO_2.wH_2O$$

$$Ca^{2+} + SO_4^{2-} + Al_2O_3 + H_2O \rightarrow xCaO.yAl_2O_3.zCaSO_4.wH_2O$$

Due to the fact that specific standard method for evaluating MSWI fly ash for application in concrete is non-existent, ASTM methods for concrete materials represent a good starting point for evaluating MSWI fly ash. An example is ASTM C618 which was designed to address issues regarding the specifications for coal fly ash and natural pozzolans for use as an admixture in portland cement concrete. Nonetheless, the

similarities and differences between MSWI fly ash and conventional concrete materials must be acknowledged.

According to the American Society for Testing Materials (ASTM C618), based on its properties, MSWI fly ash may be defined as a pozzolan, a siliceous or siliceous aluminous material, which in itself possesses little cementitious properties, but its finely divided form chemically reacts with calcium hydroxide and in the presence of moisture at normal temperature to form cementitious compounds. Pozzolanic reaction of MSWI fly ash depends on the amount of stabilizer (cement or lime), sufficient moisture, reaction environment (temperature and humidity), fineness of MSWI fly ash, carbon content, and reaction time (Poran and Abtchi-Ali, 1989).

2.8 Leaching of Heavy Metals from MSWI Fly Ash-Cement Products

Unlike organic molecules, which can be destroyed under good combustion conditions, the mass of most metals remains constant in the residue while their concentrations can increase up to tenfold. The transformation induced by the heat alters the chemical matrix of the waste, rendering it more mobile or more stable. The improvement of APC techniques developed to meet more stringent standards in recent years capture most volatile heavy metals in the fly ash. These metals are preferentially deposited on the surface of the ash particles, making them more leachable. (Buchholz and Landsberger, 1995).

In general, a leaching test involves putting a solid material in contact with a leachant to determine which components will dissolve and create a leachate. A variety of test variables, such as sample preparation, leachant composition, method of contact,

liquid-to-solid ratio (L/S), system control (e.g., pH and temperature), leachate separation, and time can be applied depending on objectives. Leaching tests are typically used to provide information about the concentration or the release of constituents from a waste material under reference test conditions, or under conditions that more closely approximate the actual site.

Leaching tests can be separated into two broad categories on the basis of whether or not the leachant is renewed (Chandler et al., 1997). Extraction tests include all tests in which a specific quantity of leachant is contacted with a specific quantity of waste for a certain length of time, without leachant renewal. Dynamic tests include all tests in which the leachant is continuously or intermittently renewed to maintain a driving force for leaching that is solution-controlled.

The underlying assumption in an extraction test is that an equilibrium condition is achieved by the end of the extraction test. There are four types of extraction tests; namely, agitated extraction tests (e.g., TCLP), non-agitated extraction tests, sequential chemical extraction tests, and concentration buildup tests. Dynamic tests, on the other hand, provide information about the kinetics of solid phase dissolution and contaminant flux. Dynamic tests include serial batch tests, flow-around tests, and flow-through tests.

Toxicity Characteristic Leaching Procedure (TCLP)

To determine if a waste is considered hazardous by the Toxicity Characteristic criteria (40CFR 261.24), the waste is subjected to the TCLP (US EPA SW-846 Method 1311), which consists of four major steps. First, particle size of the waste is reduced to smaller than 9.5 mm, if necessary. Then, the appropriate extraction fluid to be used with an L/S

of 20 is determined based upon the alkalinity of the waste. The extraction vessel is rotated at 30 rpm for 18 hours. The final steps involve leachate separation, sample preparation, and analysis. At present, there are only eight metals addressed in the TCLP limits; namely, silver (Ag), arsenic (As), barium (Ba), cadmium (Cd), chromium (Cr), mercury (Hg), lead (Pb), and selenium (Se). This results in an incomplete assessment of environmental impact. However, if a total analysis of the waste demonstrates that concentrations of individual analytes do not exceed the Health-Based Limit for Exclusion of Waste-Derived Residues, found in 40CFR 266 Appendix VII, the TCLP for that analytes need not be run.

Currently, bottom ash and APC residues are mixed together at most MSW incineration facility and disposed of as combined ash. Residues are subject to testing by TCLP prior to disposal. Residues that pass the TCLP are subject to management as a non-hazardous solid waste, while residues that fail the TCLP are subject to management as a hazardous waste or special waste, depending on state requirements. In practice, operations at most MSW incineration facilities have been well adjusted such that failure to pass the TCLP is a rare event. Testing frequency varies considerably from state to state, typically ranging from testing of weekly to quarterly composite samples.

The method was designed primarily to simulate the conditions that occur in a municipal solid waste landfill by using dilute acetic acid, which is the product of anaerobic biodegradation. However, controversy arises due to its application as a means to evaluate MSWI ashes (Egemen and Yurteri, 1996). As a normal practice, at least in the US, both bottom and fly ashes are combined and disposed of in a monofill which does not accept MSW. Apparently, there is no imbedded source of acetic acid that TCLP was

designed to model. Buchholz and Landsberger (1995) reported that the introduction of an acid source in the TCLP greatly overestimated the leaching potential of a monofill. Disposal of bottom ash or combined ash posed no problem from a regulatory standpoint. The serious flaw in the TCLP test was its failure to differentiate between the different chemical environments found in a conventional MSW landfill and an ash monofill.

The applicability of TCLP is also in question since the pH of the resulting leachate is the single greatest factor governing the concentration of metals in solution, not the concentration of the element in the ash (Buchholz and Landsberger, 1993). During single batch extractions, leaching of the alkalinity in concrete leads to high leachate pH values. Most metal complexes at these high pH values are relatively insoluble. As a result, most of the stabilized products are most likely to pass the TCLP. It is very likely, though, that over time, the alkalinity of the concrete may be leached to the extent that the pH drops to levels at which metal complexes are more soluble. This may result in leaching of metals at undesirable concentrations. Obviously, the test does not address the effect of long-term leaching. The TCLP is, therefore, deemed a worst-case estimate of the possible total long-term constituent release from a monofill, but it ignores the slow release rate.

Sequential Chemical Extraction

Sequential extraction procedure is a tool to aid in assessing potential short- and long-term leaching hazards posed by mono- and co-disposal of MSWI ashes. A sequential chemical extraction test is composed of a battery of non-agitated extraction tests. It involves performing sequential elutions of aliquots of a sample with different leachants, which are

increasingly more aggressive in terms of chemical attack toward the residue. The extraction procedure was originally derived by Tessier et al. (1979) to identify the association of trace contaminants with particular chemical phases in sediments. It has been shown, however, that resorption and re-precipitation reactions can dramatically alter the mass fractions that are obtained in the different extractions. Therefore, it appears that the emphasis on interpretation of the sequential chemical extraction data has shifted away from the associated chemical phases toward association with different leaching conditions within an MSW landfill over time.

The fraction order and solvent fluids for sequential batch extraction schemes vary slightly depending on the particular goals of the experiment (Buchholz and Landsberger, 1995). Extraction fluids are chosen to maximize chemical selectivity and minimize interferences. Typically, the order is as shown in Table 2.2 (Chandler et al., 1997).

Table 2.2 Interpretation of the Sequential Chemical Extraction Procedure

Fraction	Interpretation
A	Immediately available
B	Potentially available for leaching under acidic conditions
C	Potentially available for leaching under severe reducing conditions
D	Unavailable for leaching under normal leaching conditions
E	Unavailable for leaching

Note: From Chandler et al. (1997)

Serial Extraction

A serial batch test is usually performed using a granular or crushed sample which is mixed with leachant at a given L/S for a specified period of time. The leachate is then separated from the solids and replaced with fresh leachant until the desired number of leaching periods or cumulative L/S have been achieved.

There has been concern about the alkalinity of ash that might decrease over time as a result of constant leaching by rainwater. Buchholz and Landsberger (1995) found that the buffering capacity of MSWI ashes, especially fly ash, maintained an alkaline leachate. They performed batch extractions of MSWI fly ashes using H_2SO_4 acidified water of pH 4 as an extraction fluid. The pH range of the batch extraction leachates did not change in spite of a cumulative liquid-to-solid ratio (L/S) of 220. They postulated further that an ash monofill of 10 m in depth with a specific gravity of 3.0 would need to receive 6,600 meter of rain to reach an L/S ratio of 220. Therefore, 6,600 years of acid rain and snow in an area with an average annual precipitation of 1 m would have no effect on the pH of an ash monofill. Based on these findings, the fear that the alkalinity of MSWI fly ash would be neutralized by acid rain in a monofill is entirely exaggerated. The clean leachates encountered in the field suggest that the long-term behavior of ash monofill is static.

The use of MSWI fly ash as an ingredient in a portland cement concrete or concrete products offers a great potential market for the utilization of MSWI fly ash as a cost-effective alternative to current disposal practices. Due to the fact that the use of MSWI fly ash as a construction material is a relatively new concept, there are no commercial standards, such as ASTM for evaluating an MSWI fly ash for use in portland

cement concrete or as an aggregate. An evaluation of MSWI fly ash requires a thorough understanding of its effects on hydration of the portland cement concrete besides its strength and durability properties.

A considerable amount of information concerning variability and properties of coal combustion by-products is readily available. The ASTM, ACI, and other standard test methods have been developed so as to evaluate coal fly ash and predict its effects in portland cement concrete. Nonetheless, this type of information on MSWI fly ash is not yet available. The ASTM methods for concrete materials represent a good starting point for evaluating MSWI fly ash. However, the similarities and differences between MSWI fly ash and conventional concrete materials must be acknowledged.

This research is aimed at evaluating the potential of different types of MSWI fly ash from an incineration facility to be used in cement mortars by using existing standard test methods for cement and coal fly ash. The chemical and physical properties of the raw fly ashes as well as processed fly ashes were also carefully tested. Microscopic examination coupled with X-ray analysis was performed on all MSWI fly-cement pastes in order to understand more clearly how the inclusion of MSWI fly ash would affect hardening of cement. To complete the evaluation process, the impact of the MSWI fly ash-cement products on the environment according to the regulatory procedure, TCLP, was also carried out. Until there are specific standards designed for the evaluation of MSWI fly ash in concrete application, this research work should be able to provide some insights into the potential of utilization of MSWI fly ash.

CHAPTER 3

OBJECTIVES

The lack of available landfill sites and the increasing costs of operating landfills has resulted in a move to reduce the volume of municipal solid waste (MSW) disposed of in landfills. Incineration of MSW as a method of volume reduction has been receiving widespread attention. The incineration technology has been improved over the years under strictest regulations and proved environmentally friendly. Despite the benefit from volume reduction of as much as 80%, there is still a sizable amount of fly ash and bottom ash to be carefully handled. The usual practice, at least in the US, is to combine the ash with bottom ash and dispose of in a monofill. Bottom ash having lower heavy metal concentrations has been gaining popularity for use in road construction. Nevertheless, the use of fly ash, which is enriched with heavy metals, has been very limited, if not inexistent.

Fly ash produced from the combustion of coal has gained popularity for its application in concrete as a partial replacement for cement. If the fly ash created from burning MSW is similar to coal fly ash, it could also be used in the same manner, thereby resulting in fewer disposal problems. Additionally, the utilization of MSWI fly ash could reduce consumption of cement and, possibly, improve the properties of concrete. Above all, its economic value would be unimaginable.

This research summarizes the results of the experimental programs that carefully examined the physical and chemical properties of different streams of MSWI fly ash generated from a mass-burn resource recovery facility. Attempt has been made to find

ways to utilize MSWI fly ash in cement mortars. Then, in order to ensure safe utilization, solidified products of MSWI were assessed for their impact on the environment by means of a regulatory leaching procedure, TCLP.

3.1 Chemical and Physical Characterization of MSWI Fly Ashes

In order to evaluate the effect of MSWI fly ashes on their performance as a cement replacement and an aggregate substitute in mortar, chemical and physical characteristics of the MSWI fly ash samples must be thoroughly examined. The ashes were put through a battery of tests that includes gradation analysis, moisture content and loss on ignition test, specific gravity determination, fineness determination, and pH measurement.

The size of coal fly ash has been proved to greatly affect the performance of fly ash-cement concrete. To address this issue in MSWI fly ash, particle size distributions of the MSWI fly ash and its fractionated portions were performed. Bulk chemical compositions and mineralogical compositions were also determined.

3.2 Fractionation of MSWI Fly Ashes

Since addition of fine coal fly ash has been proven beneficial to concrete performance (Ukita et al., 1989; Jaturapitakkul, 1993), attempt was made to examine if this would apply to MSWI fly ash. An air classifier was employed to separate fine particles from coarse particles. Operating parameters of the air classifier; namely, rotor speed, fan speed, and run time were varied in several combinations to produce fine and coarse particles. Criteria were set for the determination of optimal operating condition based upon the highest yield and the particle size.

3.3 Morphology and Elemental Surface Analyses of MSWI Fly Ashes

The fact that MSWI fly ash is a product of the combustion of MSW whereas the coal fly ash is a product of the combustion of coal implies that morphology of particles, aside from the chemical and physical properties, of both types of fly ash should be different. Therefore, MSWI fly ash may not behave in the same manner as coal fly ash in concrete. To understand the differences, an electron scanning electron microscope (ESEM) equipped with an energy dispersive X-ray spectrometer (EDX) was employed to examine the microstructures as well as to determine the elemental compositions of the surface of the fly ash particles .

3.4 Effect of MSWI Fly Ash on Hydration of Fly Ash-Cement Pastes

Since MSWI fly ash is not a self-cementing material, it needs to be mixed with cementitious materials, in this case, cement, to produce solidified product. It may enhance or hinder the hydration process. Therefore, its role in hydration process, which is the reaction responsible for setting and hardening in cement, must be investigated. Raw and fine fly ashes were used to make fly ash-cement pastes at different levels of replacement. Hydration at different stages of the pastes was monitored using an X-ray diffraction (XRD) spectrometer and an electron scanning electron microscope (ESEM) equipped with an energy dispersive X-ray spectrometer (EDX).

3.5 Utilization of MSWI Fly Ashes in Cement Mortars

Due to the fact that its gradation is close to those required by ASTM C330/331 specifications for lightweight fine aggregates for structures and masonry units, NJIT 1 fly

ash was used to directly replace fine aggregate, i.e. sand, in cement mortars that were mixed at the water-to-binder ratios of 0.45, 0.50, and 0.55.

To study the contribution of MSWI fly ashes to the compressive strength development of MSWI fly ash-cement mortars, the fractionated portions as well as the raw NJIT 2 fly ashes were used to replace cement by 15%, 25%, and 35% in mortar mixes. The influence of the ratio of the amount of water at mixing to the amount of cement and fly ash (water-to-binder ratio) was also studied by varying the ratio from 0.45 to 0.55.

3.6 Leachate Characteristics of the MSWI Fly Ash Products

In the field of stabilization of inorganic solid wastes, the use of cement-based processes is widely applied. Stabilization of heavy metal laden MSW can be done by mixing it with coal fly ash and ordinary portland cement. MSWI fly ash is also known for its high concentrations of heavy metals that could leach out and contaminate groundwater. The cementitious matrices in the fly ash-cement may be able to bind these metals and prevent them from leaching out. The US EPA Toxicity Characteristic Leaching Procedure (TCLP) was chosen to perform on the MSWI fly ash-cement solidified specimens to address this issue since even though the products may perform well, they may never be realized in the real-world applications if they are proved to cause adverse impact to the human health and the environment.

CHAPTER 4

MATERIALS AND EXPERIMENTAL METHODS

4.1 Experimental Program

Two types of MSWI fly ash were acquired from a resource recovery facility in New Jersey which serves the population of 850,000. Three mass-burn incineration units employed have a total capacity of 2,505 tons per day and produce about 70 MW of electricity. The incineration facility is equipped with three electrostatic precipitators (ESPs) and three spray-dry scrubber systems producing approximately 70 tons of fly ash and air pollution control (APC) system residues per day. The first type of fly ash, dubbed NJIT 1, was collected from a proprietary ash treatment unit that treats fly ash collected from the ESPs downstream from the dry scrubbers with complex phosphoric acid mixture to ensure regulatory compliance. The second type, NJIT 2, was collected directly from the ESPs upstream without any treatment. After sampling, both of the fly ashes were sealed and stored in PVC-lined steel drums in a cool dry place to prevent carbonation and any increase in its moisture content.

As-received NJIT 1 and 2 fly ashes were characterized with a view to utilizing the materials to replace part of the portland cement normally used for making concrete. Characterization involved chemical and physical analyses, observation under environmental scanning electron microscope (ESEM), unconfined compressive strength test, and X-ray diffraction analysis. Hydration of fly ash-cement pastes at different periods of progression was also studied in details by means of ESEM observation and XRD analysis.

MSWI fly ash usually contains high concentrations of hazardous metals, such as Pb, Cd, and As. However, these metals could be bound in cementitious matrices and thus preventing them from leaching. Toxic Characteristic Leaching Procedure (TCLP) was performed on solidified specimens to assess whether the materials are likely to release heavy metals into the environment and to ensure that the concentrations of these metals in the leachates would meet the regulatory limits.

4.2 Materials

Materials used in this study include two types of MSWI fly ash, type I ordinary portland cement, river sand, and water.

MSWI Fly Ashes Two types of sampled MSWI fly ash from a resource recovery facility in New Jersey.

1. **NJIT 1 Fly Ash**. Sampled from an ash treatment unit, NJIT 1 was, in fact, NJIT 2 fly ash treated with proprietary phosphoric acid to reduce heavy metal mobility for a safe disposal in a monofill. The ash was used as received to explore its application as a fine aggregate replacement detailed in Section 4.3.9.
2. **NJIT 2 Fly Ash.** A batch of finely-divided particles was taken from the ESPs before it entered the ash treatment unit. NJIT 2 fly ash was then separated into two portions using an air classifier. The following types of fly ash were used to replace cement in the experiments described in Sections 4.3.10, 4.3.11, and 4.3.12. Pastes containing raw NJIT 2 fly ash, its processed portions, and cement were made for the

examination on hydration reactions as well as microstructures as described in Sections 4.3.7 and 4.3.8.

2.1. **Raw**. NJIT 2 was used without any modification.

2.2. **Fine**. After an 850-micron sieve to remove large debris and charred particles, NJIT 2 fly ash was fed into the air classifier running at an optimal operating condition determined in the experiment. Fractionated fly ash taken from the fine particle reservoir was then called "Fine".

2.3. **Coarse**. This is the fractionated fly ash taken from the coarse particle reservoir of the classifier.

2.4. **Washed Fine**. Fine fly ash was stirred briskly in water in a heavy-duty blender to remove its soluble contents. Supernatant was removed and replaced with fresh water intermittently. After one hour, the washed ash was dried in an oven over night. Details are given in Section 4.3.12.

NJIT 1, Raw, coarse, and fine portions of NJIT 2 fly ash were used in the mixes at varied degrees of cement replacement and water-to-binder ratios.

Cement Standard ASTM Type I portland cement was used throughout the study.

River Sand Sand passing an ASTM Standard sieve No.4 (4.75-mm openings) was used for all mixes.

Water All mixes incorporated tap water at normal room temperature.

Care was taken to ensure that representative samples used in all of the experiments were obtained.

4.3 Test Programs

4.3.1 Basic Physical and Chemical Properties of MSWI Fly Ash

4.3.1.1 Sieve Analysis: The standard test procedure (ASTM C136) is recommended for materials of which the sizes are larger than the No. 200 sieve (75 microns). As-received samples were first dried to a constant weight at 110 °C. Approximately 500 g of the dried sample was put on the top sieve of a stack consisting of sieves nested in order of decreasing sizes: numbers 4, 8, 10, 20, 50, 100, 200, and 325. Sieve shaker was let to run for at least 30 minutes, or until no more than 1 weight % of sample retained on any individual sieve passed that sieve during 1 minute of continuous hand sieving as described in ASTM C136. Upon completion, the sieves were weighed and the weights were recorded.

4.3.1.2 Fineness: As the sieve analysis result would later show, a significant portion of MSWI fly ash particles in NJIT 2 (more than 30% by weight) was smaller than 45 microns. Additionally, microscopic examination revealed that very fine fly ash particles tended to form clusters, thus rendering the sieve analysis result unrealistic. Since NJIT 2 fly ash would be used to replace cement, the procedure described in ASTM C430 was adopted to determine fineness of raw and processed MSWI fly ashes, so the results could be compared with those of cement and coal fly ash.

1 g of NJIT 2 fly ash was sieved through a 45-micron standard ASTM sieve (No. 325) with an aid from running deionized (DI) water, as recommended by ASTM C430 for the determination of fineness of hydraulic cement. The sieve was then dried in an oven at 110°C for four hours. The Fineness was reported as the weight percentage of particles passing the sieve.

4.3.1.3 Moisture Content and Loss on Ignition: Since fly ashes and cement contain some porosity, water can be absorbed into the body of the particles. Water can be retained on the surface of the particle as a film of moisture. Moisture content affects the water-to-binder ratio of concrete; therefore, it needs to be determined and kept within acceptable limits. The moisture content of a sample can be determined, as described in ASTM C311, by first drying the sample to a constant weight at 110°C in ceramic crucibles. The weight loss is assumed to be due to evaporation of absorbed water.

The loss on ignition (LOI) is defined by ASTM C311 as the weight fraction (expressed as percentage) of material that is lost by heating the oven-dried sample at 750°C. In other words, LOI is used to determine the amount of mass that could be driven off at moderate temperatures. This would include organic constituents (including carbonaceous compounds), highly volatile metals, and waters of hydration. LOI can be used as an important indicator of the degree of burnout in fly ash or the combustion efficiency. The crucibles containing the residues used in the moisture content determination were placed in a muffler furnace that was preheated to 750°C. The residues were ignited to obtain constant weight. The crucibles were let to cool down in a

dessicator and weighed on an analytical balance. The LOI values used in this research were determined by averaging the mass difference of duplicates.

4.3.1.4 Bulk Specific Gravity: Bulk specific gravity is defined as the ratio of the weight of a given volume of a sample, including pores, to the weight of an equal volume of water. Specific gravity provides an indication of the minerals, voids in the particles and existence of non-combusted materials. The procedure involves using a pycnometer in accordance with ASTM C128 although isopropyl alcohol was used in place of water to ensure that all the grains were wetted by the liquid and that hydration of the sample was minimized.

The bulk specific gravity values of the MSWI fly ash and cement samples were determined by putting 0.5 g of oven-dried samples into a 25-ml pycnometer. Then, isopropyl alcohol was carefully added while making sure that there were no air bubbles adhering to the grains, or the inner surface of the pycnometer. The bulk specific gravity can be calculated using the following equation:

$$Sg = \frac{(w_2 - w_1)\ \ Sg_{al}}{(w_2 - w_1) - (w_3 - w_4)},$$

where w_1 = weight of pycnometer

w_2 = weight of pycnometer + dry sample

w_3 = weight of pycnometer + dry sample + alcohol

w_4 = weight of pycnometer + alcohol

Sg_{al} = specific gravity of isopropyl alcohol

The specific gravity of isopropyl alcohol can be calculated from its density divided by the water density at test temperature. Finally, the calculated bulk specific

gravity values for each sample were adjusted and reported for standard test temperature at 25°C.

4.3.1.5 pH and Conductivity: U.S. EPA SW-846 Method 9045C was used as a guideline for measuring pH of the samples as follows. To 5 g of a fly ash sample in a 150-ml beaker, add 100 ml of DI water, cover, and continuously stir the suspension for 5 minutes. Let the fly ash particle suspension stand for about 15 minutes to allow most of the suspended particles to settle out from the suspension. The aqueous phase was then used for pH and conductivity measurements. The measurements were carried out using a pH-conductivity meter, Fisher Scientific Accumet pH Meter 50, which was carefully calibrated using buffer solutions of pH 7 and 10 from Fisher Scientific and a standard solution for conductivity (1409 μmho/cm) from Labchem, Inc.

4.3.1.6 Absorption Capacity: Absorption capacity of MSWI fly ash samples may be used as an indication of how much the ashes would take up water in the mixes. Oven-dried samples were weighed in ceramic or plastic cups which were then placed in a plastic tray with a cover that let moist air flow through, but not water droplets. The tray was put in the concrete specimen curing room. Automatic humidity control system was able to maintain the relative humidity of 100% by intermittently spraying air and water mixture. The samples were allowed to stay in the room for 24 hours since it is assumed that the surface of the fly ash particles would be saturated with moisture. Then, the cups were weighed and their new weight recorded. Absorption capacity was reported as a difference in percent of the weight of the moist sample over the dry sample.

(a) (b)

Figure 4.1 Absorption Capacity Experiment Setup

Figure 4.1 shows how the cups were placed inside the tray (a) and how the tray was put in the curing room (b).

4.3.2 Bulk Chemical Composition of MSWI Fly Ashes

Total quantification of MSWI fly ash requires, for example, neutron activation, X-ray fluorescence spectrometry (XRF), and total digestion followed by spectrophotometric analysis, such as atomic absorption spectrometry (AA) or inductively-coupled plasma – atomic emission spectroscopy (ICP-AES). In this research work, analysis results were obtained for MSWI fly ashes from different techniques; namely, XRF and microwave digestion with nitric acid, HNO_3, (Method 3051) followed by quantification using Inductively-Coupled Plasma Spectroscopy-Atomic Emission Spectroscopy (ICP-AES, Method 6010A), except for mercury which requires Method 7471, according to the U.S. EPA Test Methods for Evaluating Solid Waste: Physical/Chemical Methods (SW-846).

In spite of the fact that HNO_3 digestion is unable to totally destroy the siliceous structures of the fly ash and yield the total quantification, the results from this method are

acceptable. The difference between this method and the total digestion of MSWI fly ash with, hydrofluoric acid, HF, (SW-846 Method 3052 and APHA Standard Method 30301) is probably minor for this particular type of fly ash in which the trace elements are primarily associated with calcium rather than silicates. Moreover, analysis results for silica, chromium, and other trace metals may also be inaccurate due to volatilization and loss caused by the highly oxidative nature of the HF medium. The most important reason, however, why we opted for the HNO_3 digestion rather than the HF is due to the extremely corrosive and toxic nature of HF that requires special handling as well as major modification of the existing instruments.

It should be noted, though, that ICP-AES was used exclusively for the analyses of raw MSWI fly ash samples. The results from the ICP-AES method done by an outside lab were used to compare with those from the XRF done in NJIT laboratory.

X-ray Fluorescence Spectroscopy (XRF) is a very sensitive qualitative and quantitative analytical technique. The advantages of this method lie in its applicability to many types of solid (powders, polished specimens, fused specimens) and its quick analysis. It does not require tedious sample digestion although it does require sample preparation. Since the X-ray only penetrates up to millimeters from surface of a sample, care must be taken to make sure that the sample is finely ground and that it is a good representative of the material of interest.

Samples were first ground in a ceramic mortar to obtain a homogeneous size of below 45 microns. Then, each sample was placed in a plastic cup, covered with Mylar film, and inserted into sample cup. After the samples were loaded on a sample feeder tray, a command was issued to start the measurement. Each sample would take 30

minutes for the instrument to detect characteristic X-rays of elements emitted from the sample in helium environment. The results were then analyzed using Philips SemiQ software. Analysis results of MSWI fly ash samples show great agreement between those obtained from the XRF method and those obtained by the ICP-AES method. Therefore, the bulk chemical compositions of all samples determined by the XRF were reported in this study. Figure 4.2 shows the Philips XRF instrument used in this study.

Figure 4.2 Philips X-ray Fluorescence Spectrometer Model 2400

4.3.3 Mineralogy of MSWI Fly Ash

Philips PW 3040 MPD X-ray Diffractometer with $Cu_{K\alpha}$ radiation (λ = 1.5418 °A), as shown in Figure 4.3, was used to perform the mineralogical analyses for as-received, fractionated, and washed fine fly ash samples as well as cement samples. Samples were analyzed with the following operating conditions: 40 kV accelerating voltage, 45 mA current, 10° to 70° 2θ scanning range, 0.02 step width, and 10-second step increments.

Sample preparation was carried out by grinding the samples in a ceramic mortar for 10 minutes until they became homogeneous with grain size of below 45 microns. The preparation step is very important since large particles can cause problems such as microabsorption and extinction (Chandler et al., 1997). They can also interfere with the underlying assumption of random orientation. Then, the ground powders were backfilled into aluminum specimen holders.

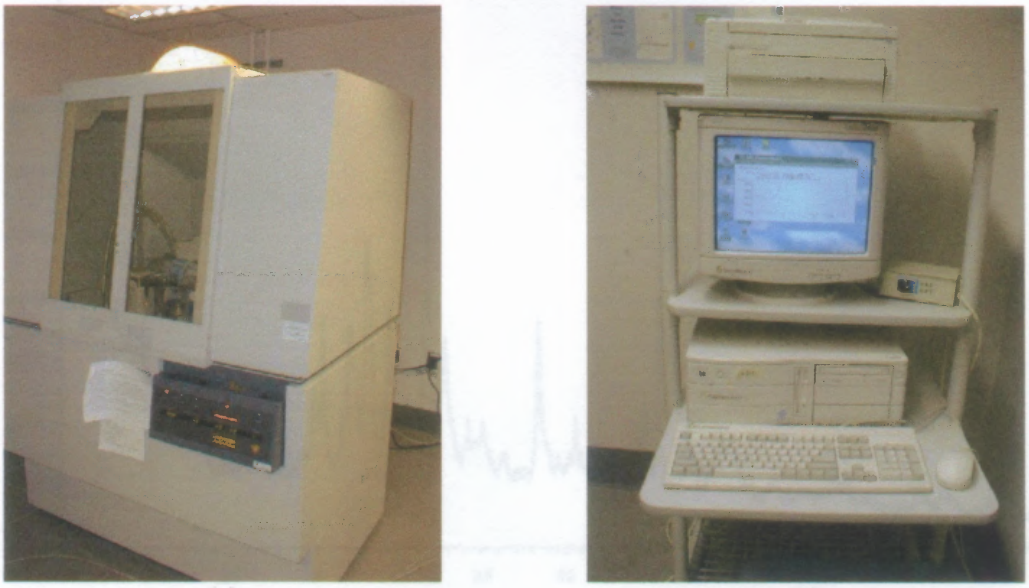

(a) (b)

Figure 4.3 (a) Philips X-ray Diffraction Spectrometer Model 3040 and (b) a Computer Running Philips PCD 4.0b Analysis Software

Possible phases of the resulting scan were identified using Powder Diffraction File, PDF-1, an internal database from International Centre for Diffraction Data (ICDD). Philips PCD 4.0b software produced a list of most likely candidate crystalline phases according to how well a scanned pattern of a given compound matched their reference patterns in the database. The amorphous or glassy phase, however, is defined as a hump, which is the area under the base line of the peaks and above the background curve. The

number of candidate phases in the list was further narrowed down through the use of restriction criteria of the software which were based on group (e.g., cement, inorganic, organic, etc.) and/or possible elements and subgroup (e.g., hydroxides, carbonates, etc). The list of elements obtained in the bulk chemical analysis by the XRF was used for that purpose. A sample of a resulting diffraction pattern is provided in Figure 4.4.

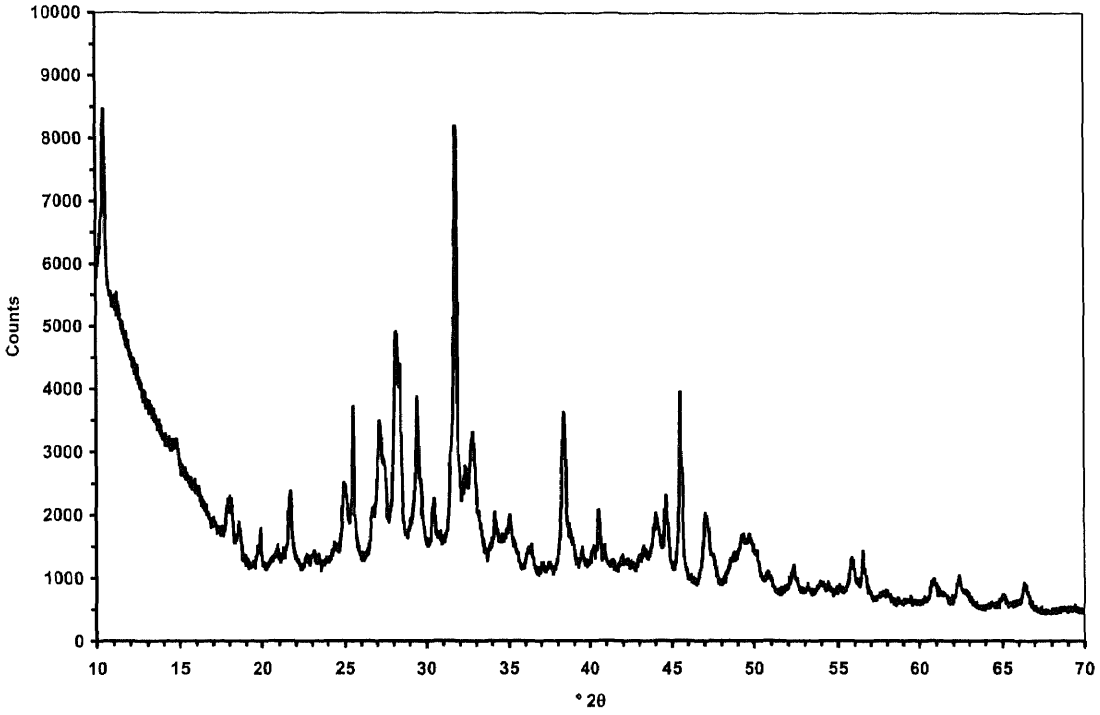

Figure 4.3 Example of Diffraction Pattern Obtained from Philips X-ray Diffraction Spectrometer Model 3040

4.3.4 Fractionation of MSWI Fly Ash

Due to its very high moisture content and the tendency to cluster together, the raw NJIT 1 was not amenable to fractionation. Moreover, oven-dried NJIT 1 fly ash still needed crushing to further reduce its particle size. Its particle sizes were more compatible with an application as a fine aggregate replacement that will be discussed in Section 4.3.9. Therefore, size fractionation using an air classifier was performed solely on NJIT 2 fly

ash because of its more compatible characteristics. Progressive Industry's lab-scale air classifier was used for this purpose.

(a) (b)

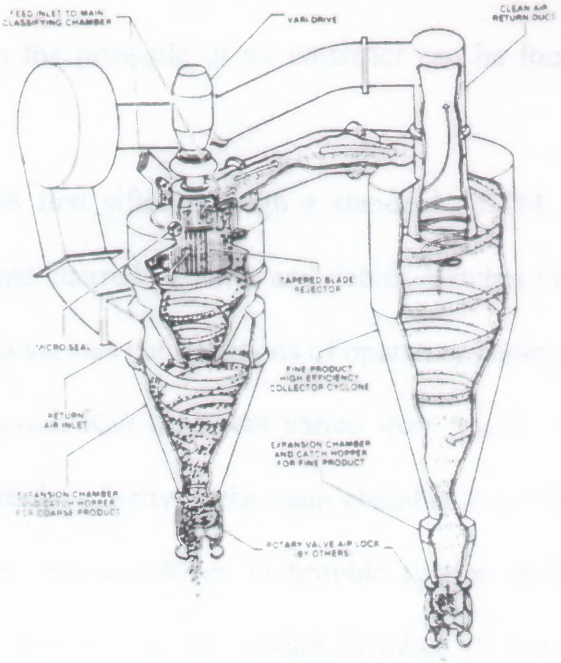

(c)

Figure 4.4 Lab-Scale Air Classifier Unit and Control Module. (a) Air Classifier Unit, (b) Control Module, and (c) Diagram Showing How Separation Occurs Inside the Unit

The classifier consists of two vertical cylindrical bodies, a vacuum cleaner, and a control module as shown in Figure 4.4. Feed is put in the feed hopper on top of the main cylinder and is introduced into the main chamber by means of a rotating gate. Particles exit two off-center ports and get entrained in the tangential airflow provided by the spinning rotor blades. Depending upon the induced particle velocity, larger particles would spiral downward and toward the wall by gravity and centrifugal force. They are later collected in the reservoir at the bottom of the chamber. Finer particles would still be entrained in the air flow and move radially toward the center. The vacuum cleaner provides suction from the second chamber that would induce the upward motion of the air and the entrained fine particles. Upon entering the second chamber, the air velocity reduces and fine particles move tangentially down toward the receiving reservoir. More detailed discussions on the principle of air classifier can be found elsewhere (Rhodes, 1990).

The fly ash was first sifted through a standard ASTM sieve with 850-micron openings to remove large charred particles and debris. Batches of 500 g of the sifted fly ash were then subject to various combinations of operating parameters; namely, run time, rotor speed, and fan speed. Run time was varied from 15, 20, and 30 minutes. Rotor speed that provides particle velocity in the main chamber was varied from 3000 to 6000 rpm. A vacuum cleaner was employed to provide suction in the second chamber to induce updraft of fine particles into the second chamber. Its fan speed was varied from 50, 75, and 100%. Initially, the criteria were set for an optimal operating condition that would result in the highest yield of fly ash with an average particle size ($d_{50\%}$) of less than

20 microns. It should be noted here that the yield is defined as the weight ratio of fine fly ash recovered in the fine particle reservoir to the raw fly ash feed.

The 20-micron size criterion was based on studies conducted by Ukita (1989) and Jaturapitakkul (1993) who found significant increase in strength when fine coal fly ash (<20 microns) was incorporated in concrete mixes. Furthermore, as will be seen in Section 5.5, sub 20-micron fly ash contributes as much as 40% in raw NJIT 2 fly ash. An attempt to separate this fraction would be worthwhile.

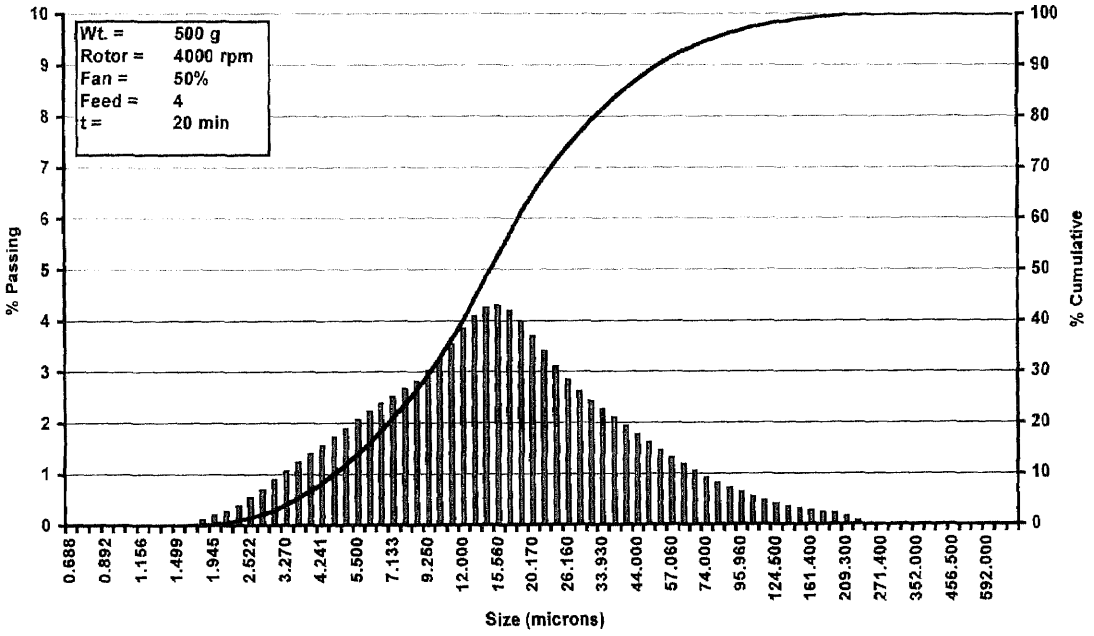

Figure 4.5 Particle Size Distribution of Fine Particles Fractionated at Stated Conditions

Before the first run of each day, the classifier was turned on without feed input for 15 minutes. Then, rubber mallet was used to tap on its sides for several minutes to remove fly ash particles stuck on the wall from previous runs. For each run, the operational parameters were set and the classifier was turned on for the specified amount of time. It was let to rest for 20 minutes between each run to let heat dissipate from rotor

bearings. Moist paper towel was also wrapped around bearing housing to help absorb the heat.

Particles taken from both fine and coarse particle reservoirs at the end of each run were analyzed for particle size distributions by a particle size analyzer. Sample of the result from one of the runs is shown in Figure 4.5.

4.3.5 Particle Size Analyses of MSWI Fly Ash

All fly ash samples were subject to particle size analysis by Leeds+Northrup Microtrac Particle Size Analyzer model SR150 (Figure 4.6) that measures particle sizes ranging from 0.75 to 704.00 microns. The refractive index of 1.81 was chosen for MSWI fly ash and cement particles. This is based on a recommendation from the manufacturer for particles with high concentrations of siliceous compounds. Fluid refractive index was also set at 1.33 for water.

Figure 4.6 Leeds+Northrup Microtrac Particle Size Analyzer Model SR150

Sample preparation was done by stirring 0.20 g of MSWI fly ash sample vigorously in 60 ml of de-ionized (DI) water. The mixture was made into an aqueous solution with an aid from 10 ml of non-ionic dispersing agent, Titron X (10%). Isopropyl alcohol (99%) was used instead of DI water for cement to prevent hydration. The solution was then fed into a recirculation reservoir which supplied a steady stream of solution into the analyzer. The amount of sample required for optimum measurement was calculated by a dedicated computer. Particles were counted based on percent volume. The computer finally gave an average value of a series of three measurements at the end of each run. The procedure was repeated over the course of 10 minutes, or until the results became consistent with one another. Particle size analysis result of raw NJIT 2 of is given as an example in Figure 4.7.

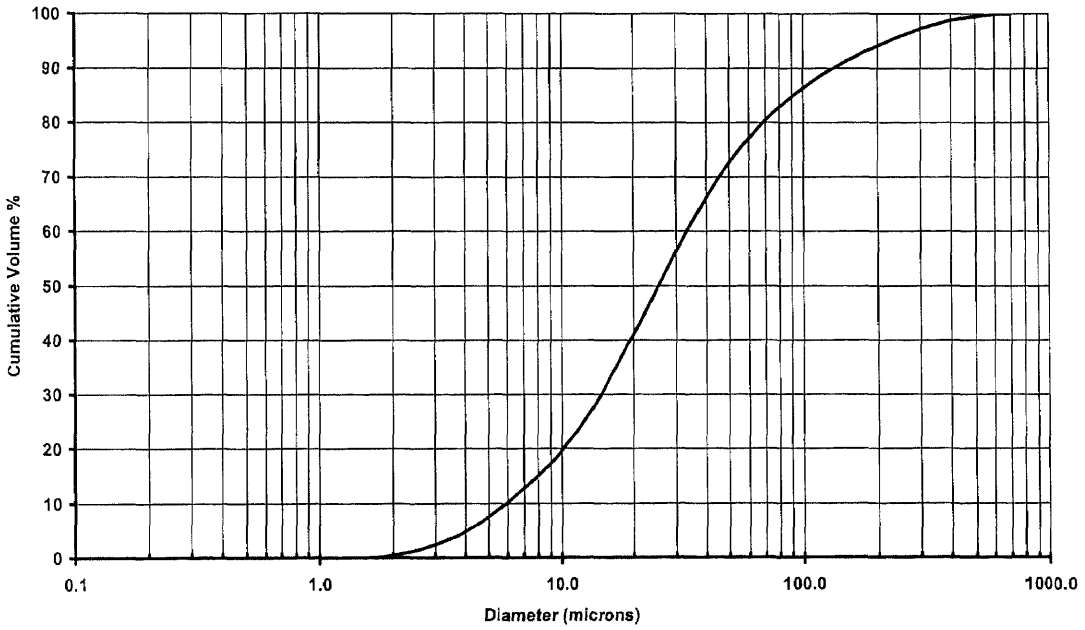

Figure 4.7 Particle Size Distribution of Raw NJIT 2 Fly Ash Sample

4.3.6 Morphology and Elemental Surface Analyses of MSWI Fly Ashes

Generally, X-ray element mapping can be accomplished by energy dispersive and wavelength dispersive techniques. The energy dispersive X-ray spectrometers (EDX or EDS) identify the characteristic X-rays produced by electron bombardment in the microprobe with energy specific detectors. Wavelength dispersive spectrometers (WDS) employ diffraction by crystals to separate X-rays from different elements prior to their striking a detector. The EDX is useful for rapid qualitative analysis where interferences from X-rays with overlapping energies are minimal whereas the WDS is preferred for quantitative analysis.

The fixed beam operating procedure and the EDX detector system were employed to determine the composition at a selected number of points. X-ray intensities were converted to elemental abundance by a theoretical procedure normally referred to as the standardless approach. It utilizes theoretical interaction coefficients to account for atomic number effects, matrix absorption, and fluorescence on the X-ray intensity/elemental abundance relationship (Plüss and Ferrell, Jr., 1991). The results are considered semi-quantitative due to the small size and variability of the fly ash particles. Nevertheless, the element ratios should approximate those actually occurring in the particles. The inability of the EDX system to detect water and elements with atomic numbers lower than sodium poses a potential trouble for the analysis, however.

Philips Environmental Scanning Electron Microscope model 2020 equipped with Kevex energy dispersive X-ray (EDX) detector model Sigma 3, shown here in Figure 4.8, was employed to obtain micrographs of the fly ash samples as well as those of the fly ash-cement pastes. Elemental compositions of surface of the specimens were determined

semi-quantitatively when the EDX detector captured scattered characteristic X-rays from the viewed surface. Kevex SDP and Quasar software calculated the elemental compositions from the captured spectra while Micromap software produced maps of the elements of interest. Several micrographs of each sample with different magnifications and locations were taken to ensure that each sample was well represented. A sample of micrograph of NJIT 1 fly ash particle taken with the ESEM is shown in Figure 4.9.

Figure 4.8 Environmental Scanning Electron Microscope Model 2020

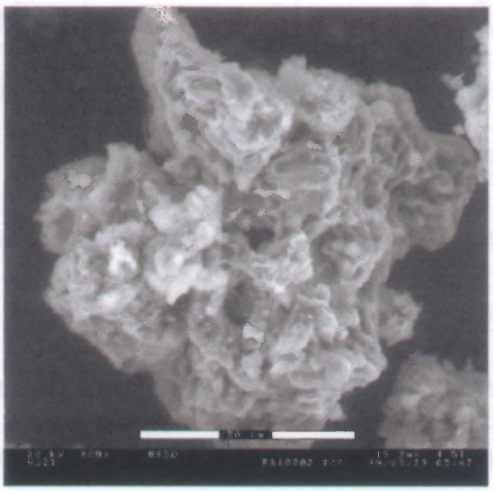

Figure 4.9 Electron Micrograph of NJIT 1 Fly Ash Particle

4.3.7 Investigation on Hydration and Pozzolanic Reactions in MSWI Fly Ash-Cement Pastes by X-ray Diffraction

The objectives of this experiment are to study the hydration process and pozzolanic reaction of MSWI fly ash-cement pastes through XRD analysis. Raw (RW) and fine (CY) NJIT 2 fly ashes were mixed with cement and water at different percent replacements, 15, 35, 50, and 100%, while maintaining the water-to-binder ratio of 0.50. The mixtures were cured in five airtight plastic bags marked with the numbers representing the test ages of 1, 3, 7, 14, 28, and 40 days at 20 °C. This is to minimize the influence of carbonation that would change the chemical and morphological properties of the pastes. At the time of testing, hydration process was stopped by grinding a portion of the content in acetone for 5 minutes. The other portion was saved for microstructure analysis by the ESEM. The soaked sample was then dried in an oven at 60°C for at least 4 hours and ground in a ceramic mortar for 10 minutes to obtain a homogeneous size of approximately 45 microns. The ground sample was then backfilled into a specimen holder for XRD analysis. Care must be taken to make sure that surface of the sample is free from ridges or holes. The operating parameters for the XRD analyses were as described in 4.3.3.

It was found later that the paste containing pure fine fly ash did not solidify after several days of curing. In spite of the fact that fine fly ash is not a self-cementitious material, it may possess a pozzolanic property if ample supply of $Ca(OH)_2$ is provided. Therefore, a sample consisting of CaO (35%) and fine fly ash (65%) was prepared to address this assumption. Also, a sample consisting mainly of cement and water (control) was prepared as a comparison. Aside from phase identification of the samples, intensities of key phases; namely, $Ca(OH)_2$ and C_3S were also determined using the Philips APD 4.0b software for further examination.

4.3.8 Examination on MSWI Fly Ash-Cement Paste Microstructures

Hardened cement paste is produced by hydration reactions that start as soon as dry portland cement is in contact with water. Microstructure of hardened paste is controlled by various parameters: particle size distribution, composition of cement, morphology of individual hydration products, and age of the paste (Ahmed and Struble, 1995). The microstructure, in turn, determines mechanical properties, such as strength. Therefore, examination on MSWI fly ash-cement paste microstructures would provide better understanding on the mechanisms involving strength.

In MSWI fly ash-cement systems, more complex microstructures consisting of those of cement hydration products, fly ash hydration products, and, possibly, reaction products between cement and fly ash are to be expected.

The portions saved from the XRD analyses were subject to microstructure examination by the ESEM right after they were taken out of the airtight plastic bags. A small piece (10mm x 10 mm x 2 mm) was grabbed from the center of each sample and placed on a 13-mm aluminum stub with an aid from conductive carbon paint. The specimen was then examined under high magnifications. Surface elemental analysis was also preformed on the specimen using the EDX. Kevex Quasar software analyzed the obtained spectrum and reported the elemental composition while Kevex Micromap software created intensity maps of elements of interest based on acquired image and spectrum.

Microscopic examination of non-hardened paste was done by first freezing the paste in liquid nitrogen for five minutes. Then, a piece of sample prepared as stated above

was placed on a copper stub that was placed on a cold stage attachment inside the ESEM. A temperature regulator helped maintain temperature to below freezing.

4.3.9 MSWI Fly Ash as Fine Aggregate

Gradation analysis performed on raw NJIT 1 fly ash shows that its particle size distribution is close to those required by ASTM C33 and ASTM C330/331. Therefore, raw NJIT 1 fly ash was used to directly replace sand in mortar mixes for water-to-cement ratios (w/c) of 0.45, 0.50, and 0.55 as shown in Table 4.1.

Table 4.1 Mix Proportions of NJIT 1 Fly Ash Mortars

Mix No.	Mix Proportions						
	w/(c+fa)	%fa	Cement (kg)	Fly ash (kg)	NJIT 1 (kg)	Water (kg)	Wt. (kg)
E45	0.45	0	0.948	0.000	2.606	0.426	3.980
E50	0.50	0	0.922	0.000	2.536	0.461	3.920
E55	0.55	0	0.898	0.000	2.471	0.494	3.863

4.3.10 Effect of Fractionated MSWI Fly Ash on Strength Development of Mortars

Direct replacement of ASTM type I cement by MSWI fly ash was a criterion employed in the mix designs. Cement in the mixes was replaced by raw NJIT 2 MSWI fly ash (RW) and its fractionated fine (CY) and coarse (CC) portions by 15%, 25%, and 35%. Sample identification is of the form, AB1xx, where AB represents the type of fly ash (RW, CY, or CC), and xx, the replacement percentage. For instance, RW125 is the mortar series which was prepared by replacing 25% of cement by raw NJIT 2 fly ash.

Design of the mixes was based on weight ratios of ingredients to binder compounds; namely, cement and fly ash (c+fa). Binder is defined as a compound that is self-cementitious, such as cement, or a compound that is not, but may aid in hardening of mortars. The ratio used is based on the ASTM C109 which uses the ratio of 1.00:2.75:0.50 as the weight ratio between cement:sand:water. The amount of each ingredient required to make enough mortar mix to fill a twelve-cube mold was calculated as shown in Appendix B. A control mix (C50) was prepared from cement, sand, and water. The amounts of fly ash in the fly ash-cement mixes were then determined based on the percent of direct weight replacements. The mix design calculations are given in Table 4.2.

Table 4.2 Mix Proportions of Fly Ash Mortars for w/(c+fa) = 0.50

Ingredient	Processed Fly Ash (by weight)			
	0	**15%**	**25%**	**35%**
Cement	1.00	0.85	0.75	0.65
Fly Ash	-	0.15	0.25	0.35
Sand	2.75	2.75	2.75	2.75
Water	0.50	0.50	0.50	0.50
w/(c+fa)	0.50	0.50	0.50	0.50

A heavy-duty bread-dough type mixer was used to blend the pre-weighed ingredients at room temperature. Well-mixed pastes were then cast into steel molds which hold twelve mortar cubes in each mold. The mortar cubes were let to rest for 24 hours in a concrete curing room that maintained 100% relative humidity. After demolded, they were stored on shelves in the curing room until further testing. Since the mortar cubes were subsequently subject to Toxic Characteristic Leaching Procedure (TCLP) to ensure that they would be environmentally safe, the cubes were not submerged in

saturated lime solution. This was to prevent heavy metals from leaching out from the mortar cubes in to the solution, thereby underestimating the actual leachate concentrations.

Unconfined compressive strength tests were performed on the 2"x2"x2" mortar cubes at the age of 3, 7, 14, and 28 days according to ASTM C109 using an MTS closed-loop servo hydraulic material resting machine Model 810 as depicted in Figure 4.10. The strength development of fly ash mortars at different replacement percentages will be compared with the controlled mix. Each data point was taken from an average of at least three readings from three specimens.

(a) (b)

Figure 4.10 Compressive Strength Test Setup

4.3.11 Effect of Water-to-Binder Ratio (w/(c+fa)) on the Strength of Mortars

Three water-to-binder ratios were used in this study: 0.45, 0.50, and 0.55. The amount of each ingredient was calculated as previously described for a given w/(c+fa). Compressive strength results of the MSWI fly ash-cement mortars with the water-to-binder ratio of 0.50 prepared in the previous section were used. Additional compressive strength tests were done on mortars with the water-to-binder ratios of 0.45 and 0.55 prepared as shown in detailed calculations in Appendix B. Mix proportions for the additional mortar series are given in Table 4.3.

An example of sample identification is CY215. The first two letters represent the type of fly ash as discussed earlier. The next one-digit number, 1, 2, and 3, identifies the water-to-binder ratio as being 0.50, 0.45, and 0.55, respectively. The last two numbers show the percentage of cement replaced by the fly ashes. Therefore, the above example would indicate a series of mortar specimens with 15% cement replacement and the water-to-binder ratio (w/(c+fa)) of 0.45 while CC335 would indicate mortar specimens with 35% replacement at the water-to-binder ratio of 0.55. Figure 4.11 shows how mortars were prepared, cured, and tested.

Table 4.3 Mix Proportions of Fly Ash Mortars for w/(c+fa) = 0.45 and 0.55

Ingredient	Processed Fly Ash (by weight)					
	w/(c+fa) = 0.45			w/(c+fa) = 0.55		
	0	15%	25%	0	15%	25%
Cement	1.00	0.85	0.75	1.00	0.85	0.75
Fly Ash	-	0.15	0.25	-	0.15	0.25
Sand	2.75	2.75	2.75	2.75	2.75	2.75
Water	0.45	0.45	0.45	0.55	0.55	0.55
w/(c+fa)	0.45	0.45	0.45	0.55	0.55	0.55

A summary of calculated weights of mix ingredients of all of the mix series is shown in Table 4.4.

Table 4.4 Summary of Mix Ingredients

Mix No.	Mix Ingredients						
	w/(c+fa)	%fa	Cement (kg)	Fly ash (kg)	Sand (kg)	Water (kg)	Wt. (kg)
C45	0.45	0	0.948	0.000	2.606	0.426	3.980
C50	0.50	0	0.922	0.000	2.536	0.461	3.920
C55	0.55	0	0.898	0.000	2.471	0.494	3.863
RW215	0.45	15	0.805	0.142	2.606	0.426	3.980
RW115	0.50	15	0.784	0.138	2.536	0.461	3.920
RW315	0.55	15	0.764	0.135	2.471	0.494	3.863
RW225	0.45	25	0.711	0.237	2.606	0.426	3.980
RW125	0.50	25	0.692	0.231	2.536	0.461	3.920
RW325	0.55	25	0.674	0.225	2.471	0.494	3.863
RW235	0.45	35	0.616	0.332	2.606	0.426	3.980
RW135	0.50	35	0.600	0.323	2.536	0.461	3.920
RW335	0.55	35	0.584	0.314	2.471	0.494	3.863
CY215	0.45	15	0.805	0.142	2.606	0.426	3.980
CY115	0.50	15	0.784	0.138	2.536	0.461	3.920
CY315	0.55	15	0.764	0.135	2.471	0.494	3.863
CY225	0.45	25	0.711	0.237	2.606	0.426	3.980
CY125	0.50	25	0.692	0.231	2.536	0.461	3.920
CY325	0.55	25	0.674	0.225	2.471	0.494	3.863
CY235	0.45	35	0.616	0.332	2.606	0.426	3.980
CY135	0.50	35	0.600	0.323	2.536	0.461	3.920
CY335	0.55	35	0.584	0.314	2.471	0.494	3.863

Table 4.4 Summary of Mix Ingredients (Continued)

Mix No.	Mix Ingredients						
	w/(c+fa)	%fa	Cement (kg)	Fly ash (kg)	Sand (kg)	Water (kg)	Wt. (kg)
CC215	0.45	15	0.805	0.142	2.606	0.426	3.980
CC115	0.50	15	0.784	0.138	2.536	0.461	3.920
CC315	0.55	15	0.764	0.135	2.471	0.494	3.863
CC225	0.45	25	0.711	0.237	2.606	0.426	3.980
CC125	0.50	25	0.692	0.231	2.536	0.461	3.920
CC325	0.55	25	0.674	0.225	2.471	0.494	3.863
CC235	0.45	35	0.616	0.332	2.606	0.426	3.980
CC135	0.50	35	0.600	0.323	2.536	0.461	3.920
CC335	0.55	35	0.584	0.314	2.471	0.494	3.863

(a)

(b)

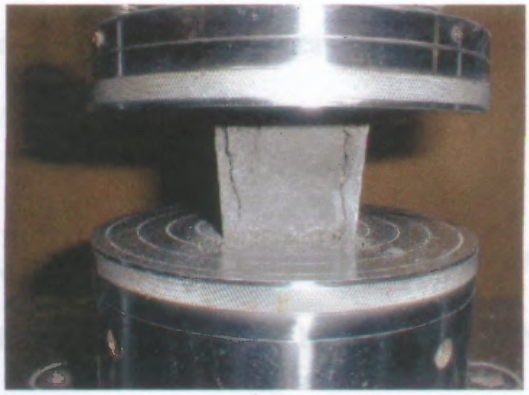

(c)

(d)

Figure 4.11 Preparation and Testing of MSWI Fly Ash Mortar Specimens (a) Molded Mortar Specimens, (b) Demolded Mortars on Shelf Waiting to be Tested, (c) Compressive Strength Testing, (d) Tested Specimens

4.3.12 Effect of MSWI Fly Ash Washing on Strength of Mortars

MSWI fly ash has been known for its high quantity of soluble salts, such as sodium chloride (NaCl) and calcium chloride ($CaCl_2$) which are products of acid gas treatment in an APC device. High salt content in concrete is detrimental. For example, chlorides in abundance cause retardation in concrete and steel corrosion in reinforced concrete. Therefore, removal of these salts seems to be a necessary step in improving the quality of MSWI fly ash to be utilized. Mortars incorporating the washed fly ash were prepared for the compressive strength test in order to evaluate the effect of washing on the strength.

Preparation of washed fine fly ash involves stirring fine fly ash stock vigorously in tap water in a bread-dough type mixer. The mixer was let to run for 8 minutes and rest for 2 minutes. Supernatant was then removed and replaced with fresh water. The process was repeated for one hour. Care must be taken in order to avoid loss of fine particles during removal of supernatant. After the end of one hour, the damp fly ash was heated in an oven at 110°C for one day or until fully dried. At this point, the fly ash formed cake which needed to be crushed by hand to make it in powder form.

Mortars incorporating 15% washed fine fly ash (CW115) were prepared and tested in the same manner as those incorporating 15% fly ash at the water-to-binder ratio of 0.50.

4.3.13 Leachate Characteristics of MSWI Fly Ash-Cement Products

High concentrations of heavy metals in MSWI fly ash have caused concerns regarding possible contamination to the environment. Thus, before the applications of MSWI fly

ash-cement products are to be fully materialized, they need to be tested if their applications are safe to human health and the environment.

The regulatory TCLP (Toxicity Characteristic Leaching Procedure) according to U.S. EPA Test Methods for Evaluating Solid Waste, Physical/Chemical Methods (SW-846) Method 1311 was provided by an outside laboratory to determine if raw NJIT1 fly ash, raw NJIT 2 fly ash, all fractionated portions of the fly ashes, and matured (28-day) fly ash-cement mortars were considered hazardous by the TC criteria.

The TCLP consists of four major steps (40 CFR Part 261.24). First, the waste is subjected to particle size reduction (<9.5 mm) if necessary. Then the appropriate extraction fluid to be used is determined based on the alkalinity of the waste. Then the extraction is added to the sample and rotated at 30 rpm for 18 hours. The extract is then digested by HNO_3 according to method 3051 and analyzed for metals by ICP-AES, method 6010A. Mercury analyses are conducted by the manual cold vapor techniques specified by method 7471. The results were then compared against TCLP limits found in 40CFR 266 Appendix VII which lists concentration limits for eight regulated metals: silver (Ag), arsenic (As), barium (Ba), cadmium (Cd), chromium (Cr), mercury (Hg), lead (Pb), and selenium (Se).

CHAPTER 5

RESULTS AND DISCUSSIONS

5.1 Basic Physical and Chemical Properties of MSWI Fly Ash

5.1.1 Sieve Analysis

Sieve analyses of raw NJIT 1 MSWI fly ash samples were conducted as described in ASTM C136-89, Standard Method for Sieve Analysis of Fine and Coarse Aggregates. The analysis result in Figure 5.1 shows that the particle size gradation of the fly ash almost satisfied the ASTM C330-89 and C331-89 limits for lightweight fine aggregates for structures and masonry units, but it failed the ASTM C33-89 limits for concrete sand. Generally, the ash had too many fines and too few coarse particles to satisfy the ASTM C330/331 completely. However, the ash would be explored for use as an aggregate replacement in the subsequent section.

Visual examination of the particles from the raw NJIT 2 fly ash indicated that black charred particles were present mostly in the larger fractions. However, most of the fly ash was much finer than the raw NJIT 1 fly ash as shown in Figure 5.2. The graph implies that more than 60% of the ash is finer than 100 microns. This result only gives a raw estimate of its particle size distribution since the sizes of sieves employed cover a wide range of particle sizes; from 45 microns to 4.75 mm. As it was found later that the fly ash particles tend to form agglomerates, the ash was, therefore, subjected to wet sieving and particle size analysis by laser diffraction as will be discussed in the following sections.

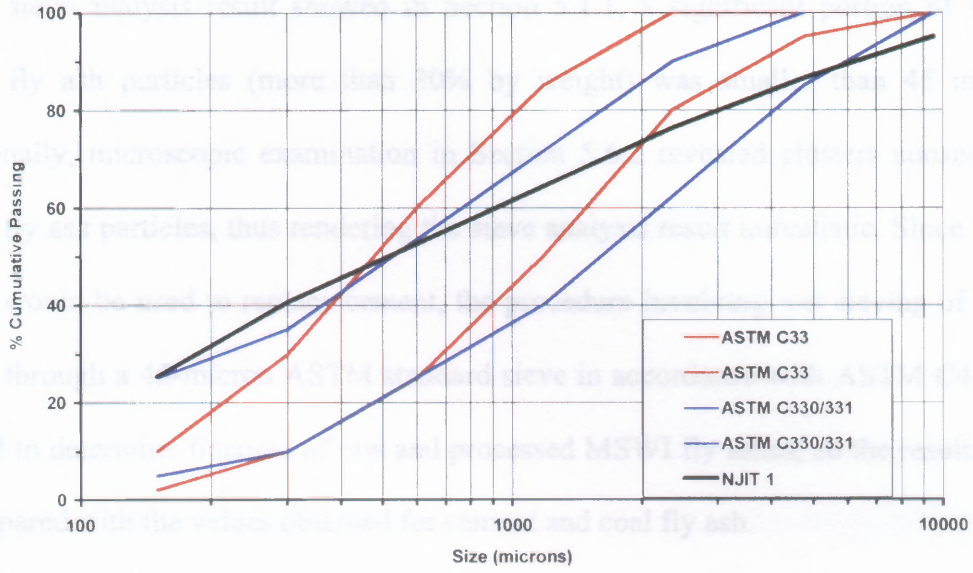

Figure 5.1 Grain Size Distribution of Raw NJIT 1 Fly Ash by Sieve Analysis

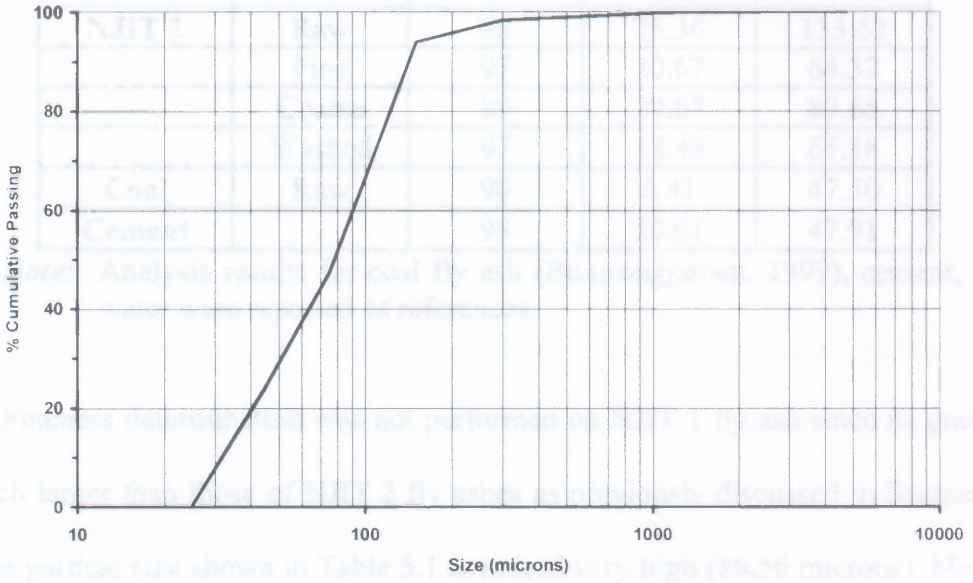

Figure 5.2 Grain Size Distribution of Raw NJIT 2 Fly Ash by Sieve Analysis

5.1.2 Fineness

As the sieve analysis result showed in Section 5.1.1, a significant portion of NJIT 2 MSWI fly ash particles (more than 30% by weight) was smaller than 45 microns. Additionally, microscopic examination in Section 5.6.2 revealed clusters consisting of minute fly ash particles, thus rendering the sieve analysis result unrealistic. Since NJIT 2 fly ash would be used to replace cement, the procedure involving wet sieving of fly ash sample through a 45-micron ASTM standard sieve in accordance with ASTM C430 was adopted to determine fineness of raw and processed MSWI fly ashes, so the results could be compared with the values obtained for cement and coal fly ash.

Table 5.1 Fineness and Particle Sizes of MSWI Fly Ashes

Sample	Condition	Fineness %	$d_{50\%}$ microns	$d_{90\%}$ microns
NJIT 1	Raw	-	86.56	408.48
NJIT 2	Raw	88	25.36	133.62
	Fine	97	20.67	64.37
	Coarse	89	29.67	89.65
	Washed	97	18.48	65.88
Coal	Raw	90	6.41	47.50
Cement	-	99	20.61	47.91

Note: Analysis results for coal fly ash (Bumrongjaroen, 1999), cement, and DI water were reported as references.

Fineness determination was not performed on NJIT 1 fly ash since its grain sizes are much larger than those of NJIT 2 fly ashes as previously discussed in Section 5.1.1. Its mean particle size shown in Table 5.1 is indeed very high (86.56 microns). Moreover, its intentional application was as an aggregate replacement; therefore, sieve analysis would be more proper means of determining its fineness.

It can be seen in Table 5.1 that the sub-45-micron fly ash particles accounted for 88% in raw, 89% in coarse, and 97% in fine and washed fine NJIT 2 fly ashes. Raw and coarse fly ashes have comparable fineness values to that of coal fly ash (90%) while those of fine and washed fly ashes are comparable to that of cement (99%).

Table 5.1 also shows mean particle sizes ($d_{50\%}$) and particle sizes at 90-percentile ($d_{90\%}$) determined by a particle size analyzer discussed in Section 5.5 for comparison. It can be seen that fine NJIT 2 fly ash and cement have comparable fineness values and $d_{50\%}$ values. In fact, particle size analysis results in Section 5.5 show that both have similar particle size distributions. The reference coal fly ash also has comparable fineness value to those of raw and coarse fly ashes although its $d_{50\%}$ and $d_{90\%}$ values are significantly lower than those of the MSWI fly ashes. This may be due to the fact that MSWI fly ash particles formed agglomerates that disintegrated by water pressure during wet sieving. The very fine particles were then able to pass through the sieve, yielding high fineness values.

5.1.3 Moisture Content and Loss on Ignition

Moisture content is an important parameter with respect to utilization and disposal of MSWI fly ash. It affects the maximum density obtained by compaction in the field and thus the internal stability and stiffness. In portland cement concrete design, moisture contents of each ingredient are essential as an input into the design calculations. Moreover, moisture contents of the ingredients need to be controlled so as to ensure same quality of the resulting mixes.

Table 5.2 shows that the moisture content (21.96%) and the LOI value (17.94%) of NJIT 1 raw fly ash were indeed very high. This is because the ash was mixed and treated with a proprietary phosphate solution in a separate ash treatment unit, thus producing hydrated compounds in the process. The whole intention of this process is to immobilize heavy metals in the ash and to significantly reduce its potential leachability during disposal; consequently, metal concentrations in the treated ash would be less than the TCLP regulatory thresholds.

Table 5.2 Moisture Content and Loss on Ignition Analysis Results for MSWI Fly Ashes

Sample	Condition	Moisture Content (%)	LOI (%)
NJIT 1	Raw	21.96	17.94
NJIT 2	Raw	2.83	12.94
	Fine	2.86	12.63
	Coarse	2.51	13.67
	Washed	1.12	19.56
Coal	Raw	0.23	2.05
Cement	-	0.67	1.12

Note: Analysis results for coal fly ash and cement were reported as a reference.

The moisture contents of the raw NJIT 2 fly ash (2.83%) and its fractionated portions, fine (2.86%) and coarse (2.51%), are quite comparable although the moisture content of fine fly ash is somewhat higher than those of raw and coarse NJIT 2 fly ashes. This may be due to higher surface area of smaller particles that could absorb moisture from the air. Low moisture content for washed fine fly ash reflects the moisture driven off when it was dried in an oven at 110°C after washing. The values for NJIT 2 fly ashes are significantly low compared with that of the raw NJIT 1 fly ash (21.96%) and are

within the limits of 3% required by ASTM C618-89 for Class C and F pozzolans. Mineralogical examination of NJIT 2 fly ashes in Section 5.3 reveals high concentration of calcium chloride, which is a hygroscopic compound. This is probably the reason why their moisture content values are much higher than those of coal fly ash (0.23%) and cement (0.67).

All types of MSWI fly ash, including washed fine NJIT 2 fly ash, possess LOI values that are significantly higher than the 6% limit by ASTM C618-89 and thus do not satisfy the requirement. This may be due in part to the presence of unburned carbon or charred particles in the fly ashes.

Washing of fine NJIT 2 fly ash caused metals and their salts on the surface of the particles and water to form hydrated compounds. Heating at lower temperature of 110°C during the moisture content analysis only caused little surface moisture to evaporate since the washed fly ash was pre-dried once before in an oven at the same temperature. However, high heat at 750°C drove off most of the water that was chemically bound as reflected by high LOI value.

LOI also indicates the amount of unburned carbon or charred particles in the fly ash sample, as was the case with NJIT 1 fly ash. LOI value of greater than 6% in coal fly ash was found to reduce entrained air content in concrete, which in turn reduced durability and workability (Hamernik and Franz, 1991a).

Although the use of LOI values is an acceptable surrogate parameter for measuring "burnout" in bottom ash and cement, the interpretation is not accurate when used in context with APC residues. Since the temperature in the flue gases exiting the boiler are much lower than 750°C, any flue gas reaction products which deposited on

particle surfaces will be volatilized during intense heating. Additionally, a portion of the weight loss from APC residues treated with lime is attributable to the loss of water of hydration from the excess lime [$Ca(OH)_2$] and dehydration of calcium chloride [$CaCl_2.2H_2O$]. Caution should be exercised when attempting to compare LOI data from different facilities since stoichiometric ratio of lime addition varies from facility to facility. Therefore, if the difference in excess lime content varies, the amount of hydration water also varies (Chandler et al, 1997).

5.1.4 Bulk Specific Gravity

Specific gravity is defined as the ratio of weight of a given volume of a sample to the weight of an equal volume of water. Apparent specific gravity or absolute specific gravity measures only the volume occupies by solid. Bulk Specific gravity, on the other hand, takes into account the effective volume that fly ash particles would occupy in concrete including their internal pores. It thus is more realistic means to provide an indication of the minerals, voids in the particles and existence of non-combusted materials.

As Table 5.3 shows, the bulk specific gravity values of all of the fly ashes, ranging from 2.09 for coarse to 2.36 for washed fine fly ash, are much lower than those of cement (3.15) and coal fly ashes (2.50). The fine fraction has slightly higher specific gravity. The washed fine fly ash having more fine particles also has higher specific gravity than the fine fly ash. This is in agreement with previous investigation by Jaturapitakkul (1993) who concluded that the finer the fly ash became, the higher its specific gravity would be. As for NJIT 1 fly ash, charred particles or unburned carbon is responsible for its low specific gravity.

Table 5.3 Physical Characteristics of MSWI Fly Ashes

Sample	Condition	Sg @ 25°C	pH	Conductivity mmho/cm	Absorption %
NJIT 1	Raw	2.14	11.4	17.8	142.0
NJIT 2	Raw	2.26	11.8	25.7	170.0
	Fine	2.33	11.7	25.8	131.0
	Coarse	2.09	11.7	24.4	148.0
	Washed	2.36	11.6	11.1	164.0
Coal	Raw	2.50	11.3	0.021	12.0
Cement	-	3.15	11.5	4.53	72.0
DI Water	-	1.00	7.2	0.001	-

Note: Analysis results for coal fly ash (Jaturapitakkul, 1993), cement, and DI water were reported as references.

5.1.5 pH and Conductivity

It can be seen in Table 5.3 that the pH of 11.8 of raw NJIT 2 fly ash was the highest. Normally, fly ash carried over from the boiler contains high concentrations of alkaline materials, such as oxides and carbonates of calcium, sodium, and potassium that contribute to high pH values. Additional alkaline materials are added to the fly ash in acid gas scrubbers that use lime. As a result, high pH values observed in fly ash taken from or downstream from APC devices are typical due to the presence of excess lime. The pH values of all MSWI fly ash samples are comparable to those of coal fly ash and cement since all of these materials have high alkali content [CaO] as will be discussed in Section 5.2. Though not quite obvious, the pH value of the washed fine NJIT 2 fly ash (11.6) was the lowest among NJIT 2 fly ashes, which range from 11.6 to 11.8. The reason for this may be due to the fact that some of the soluble alkaline salts were removed from the ash by washing. However, Gong and Kirk (1994) showed that simple washing in an industrial operation cannot be used to effectively reduce alkalinity of MSWI fly ash since the buffering effect of fly ash is attributed to the acid consumption of solid compounds, not

to water-soluble alkali metals. The same reason may be used to explain the lower pH value of NJIT 1 fly ash (11.4). As previously described, the ash was treated with phosphoric acid solution which might have neutralized and washed out some alkaline salts.

Conductivity of a solution is a measure of the ability of the solution to conduct a current via movement of ions. As ion concentration increases, more current can be conveyed, thus resulting in high conductivity. High conductivity values, ranging from 11.1 for washed fly ash to 25.8 for fine fly ash, were observed for all of the MSWI fly ashes. NJIT 2 fly ash and its fractionated parts have higher conductivities than coal fly ash, and cement (0.021, and 4.53 mmho/cm). That is, the NJIT 2 fly ashes have more soluble compounds that dissociate, once in contact with water, to give more ions. This is more obvious in the case of the washed NJIT 2 fly ash. Its conductivity (11.1 mmoh/cm) is significantly lower than those of the raw and fractionated NJIT 2 fly ashes since most of its soluble compounds were removed during washing. Again, washing of soluble compounds in NJIT 1 fly ash is responsible for its low conductivity of 17.8 mmoh/cm.

The pH and conductivity of fly ash is an indication of how its leachate would behave in the real environment as well as in the leaching test, such as TCLP. Normally, high pH and high soluble alkali compounds in MSWI fly ash, which contribute to high alkalinity, would make it pass the regulatory TCLP test. This is because most regulated metals (silver (Ag), arsenic (As), barium (Ba), cadmium (Cd), chromium (Cr), mercury (Hg), lead (Pb), and selenium (Se)) remain insoluble at high pH. However, as the alkalinity is leached due to environmental exposure, such as rain, these metals may once again become available.

5.1.6 Absorption Capacity

Absorption capacity of MSWI fly ash sample is defined as the ability of an oven-dried fly ash to absorb moisture in a 100% relative humidity environment. The value is a ratio of additional weight of water that fly ash particles absorbed to its original weight. Absorption capacity value may be used as an indication of how much the fly ash would take up water in the mix. A test procedure was designed to measure this quantity as discussed in Section 4.3.1.6.

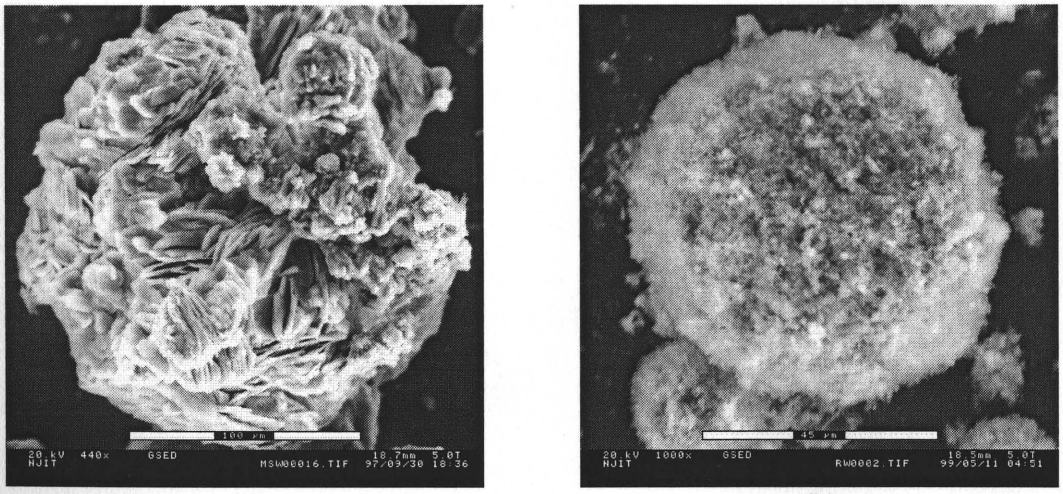

(a) (b)

Figure 5.3 Micrographs of NJIT 1 and 2 Fly Ash Particles Showing Rough Surfaces: (a) NJIT1 Fly Ash Particle, (b) NJIT 2 Fly Ash Particle

The absorption capacity values of all fly ash samples as listed in Table 5.3 are at least twice as much as that of cement (72%), with the absorption capacity of raw NJIT 2 fly ash being the highest (170%). Coal fly ash has the lowest value of 12%. This results in lower water requirement in a mix in which cement is replaced by coal fly ash (Jaturapitakkul, 1993). Microscopic investigation in Section 5.6 reveals that the fly ash particles have high degree of surface roughness as shown in Figure 5.3. The high surface

area of the particles provides sites for absorption. Additional absorption sites are provided by high surface area of charred particles found in raw and coarse NJIT 2 fly ashes. The same is also true for the raw NJIT 1 fly ash (142%).

The inclusion of spongy charred particle is responsible for higher absorption capacity value of raw (170%) and coarse (148%) NJIT 2 fly ashes than that of fine fly ash (131%). Thanks to pre-sieving of raw NJIT 2 fly ash prior to fractionation, coarse fly ash has fewer char particles as reflected by its significantly lower absorption value. However, washing of fine fly ash appeared to increase the absorption capacity (164%) by as much as 25%. This may be due to the fact that rigorously washing of fine fly ash accelerated hydration of compounds on fly ash particles to produce hydrated compounds, as will be discussed in Section 5.3. These newly formed compounds showed high affinity for water after the ash had been dried.

It is a known fact that water is an inevitable component in hydration of cement. Theoretically, minimum water-to-binder (or water-to-cement) ratio that is enough to fully hydrate cement components was estimated to be 0.42 (Mindess and Young, 1981). Although complete hydration is not essential to attain a high ultimate strength, residual unhydrated cement can remain indefinitely in the paste if the supply of water is not ample. Once the water-to-binder ratio is increased, the additional water occupies space that later turns into capillary pores when it evaporates. These newly created pores negatively affect the compressive strength property of concrete. Therefore, the ability of MSWI fly ash to absorb water may reduce the effective water-to-binder ratio, thus providing better compressive strength. Available water might still be enough for

hydration of cement since a portion of cement was replaced by fly ash. Reduction in porosity may thus be responsible for high early strength.

5.2 Bulk Chemical Compositions of MSWI Fly Ashes

Elemental distribution in MSWI fly ash plays a very important role in its chemical behavior. Chemical makeup of MSWI fly ash plays an important role in the physical and mineralogical characteristics as well. Relative partitioning of elements onto fly ash is dependent upon chemical composition of MSW feed, volatility of the element, type of incinerator, operation of the combustion system, and type of APC system.

Chemical compositions of MSWI fly ash can be used to predict the behavior of the fly ash in the environment as well as in its applications. For instance, high chloride content in the ash would have an adverse effect on reinforced steel in concrete. It also reflects the ability of soluble chloride salts of metal to be leached into the environment.

5.2.1 Bulk Chemical Compositions of Raw MSWI Fly Ashes

Table 5.4 summarizes the chemical compositions of the raw MSWI fly ashes as well as coal fly ash and cement for comparison. All of the elemental compositions determined by the XRF are reported in their respective oxide forms. Most of the elements may actually appear in their oxides in the fly ash because of the highly oxidative environment in the incinerator. Moreover, the oxide forms have been used as a reporting format among academia, industries, and people in the field of cement and concrete technology.

Typically, limestone or calcium hydroxide is injected into the high temperature zone of the incinerator where the temperature causes the material to calcine to produce

lime [CaO]. The lime then combines with HCl, SO_2, or HF in the flue gas stream to produce various salts. The salt particulates are then removed in a particulate control device, such as ESP or FF. That is probably the reason why the sampled MSWI fly ashes, such as NJIT 2 fly ash, were enriched with CaO (40.46%) and SO_3 (8.01%). Also present in high concentration (more than 13.41%) was Cl, which is believed to come from combustion of plastic and newspaper in the waste stream (Hinshaw, 1994). TCLP metals, particularly Ba, Cd, Cr, and Pb, were present in trace quantity.

Table 5.4 Chemical Compositions of Raw MSWI Fly Ashes, Coal Fly Ash, and Type I Cement

Oxide	NJIT 1	NJIT 2	Coal	Cement
Al_2O_3	5.87	3.66	27.97	4.14
BaO	0.09	0.00	0.21	0.02
CaO	**36.67**	**40.46**	**5.99**	**64.30**
CdO	0.01	0.02	0.00	0.00
Cr_2O_3	0.06	0.03	0.05	0.00
CuO	0.09	0.09	0.04	0.00
Fe_2O_3	**1.32**	**0.53**	**10.89**	**2.24**
K_2O	2.28	2.27	1.28	1.25
MgO	1.15	0.68	1.03	3.16
MnO_2	0.05	0.01	0.05	0.06
Na_2O	3.14	5.50	0.63	0.22
NiO	0.01	0.01	0.03	0.00
PbO	0.37	0.32	0.03	0.00
Sb_2O_3	0.04	0.11	0.00	0.00
SiO_2	**7.32**	**4.65**	**46.78**	**17.26**
SrO	0.00	0.04	0.44	0.29
TiO_2	1.74	0.88	0.85	0.23
ZnO	0.96	1.05	0.02	0.01
SO_3	**6.80**	**8.01**	**1.58**	**5.43**
P_2O_5	0.69	0.37	0.06	0.16
Cl	**13.41**	**17.98**	**0.00**	**0.01**
LOI	**17.49**	**12.94**	**2.05**	**1.12**
SUM	99.56	99.61	99.98	99.90

According to ASTM C618-89, the Standard Specifications for Fly Ash and Raw or Calcined Natural Pozzolan for Use as a Mineral Admixture in Portland Cement Concrete, the high-calcium class C fly ash should have the total content of SiO_2+Fe_2O_3+Al_2O_3 of at least 50%, while class F requires at least 70%. Clearly, both NJIT 1 (14.51%) and NJIT 2 (8.84%) fly ashes do not satisfy both criteria while coal fly ash (63.66%) satisfies the limit for Class C fly ash. Neither of the MSWI fly ashes, 6.80% for NJIT 1 and 8.01% for NJIT 2, meets the SO_3 limit (maximum of 5%), nor the LOI limit (maximum of 6%), 17.49% and 12.94%, respectively.

In comparison to NJIT 2 fly ash, NJIT 1 fly ash, which is a product of the treatment of APC residue (NJIT 2 fly ash) by proprietary phosphoric acid washing, has low concentration of soluble constituents, such as CaO (36.67% vs. 40.46%). Other constituents are Na_2O (3.14% vs. 5.50%), Cl (13.41% vs. 17.98%), SO_3 (6.80% vs. 8.01%), and CdO (0.01% vs. 0.02%). The constituents may be in their salt forms: NaCl, $CaCl_2$, $CaSO_4$, and $CdCl_2$. During treatment, these soluble compounds found in surface layer of the fly ash particles were leached out, thus leaving kernel of the particles intact. This helps increase the concentrations of Al_2O_3 (5.87% vs. 3.66%), Fe_2O_3 (1.32% vs. 0.53%), and SiO_2 (7.32% vs. 4.65%) which were found to form cores of the fly ash particles (Cheng and Bishop, 1992).

Table 5.5 Bulk Chemical Compositions of MSWI Fly Ashes from Various Sources

	NJIT 1 MB	NJIT 2 MB	BA MB [1]	FA MB [1]	APC MB [1]	FA + APC MB [1]	FA MB [2]	FA MB [3]	FA MB [4]	FA RDF [4]	FA Coal
Ag_2O	-	-	-	-	-	-	-	33-64	-	-	-
Al_2O_3	58664	36600	98228	-	49000	104000	79000-150000	20200-210000	137400	153400	279700
As_2O_3	-	-	7-53	1-3	119	22	-	99-302	-	-	-
BaO	929	-	558-2010	33-89	357	837	2088-3249	782-1451	-	-	200
CaO	366715	404600	70000-126000	70000-140000	406000	168000	84000-108000	118000-393000	266200	237300	59900
CdO	130	159	2-29	114-343	160	35	217-263	91-359	-	-	-
Cl	134072	179800	1000-3000	30000-50000	170000	28000		50000-209000	-	-	-
CoO	-	-	-	-	-	-	-	6-47	-	-	-
Cr_2O_3	629	250	292-1462	15-146	278	585	570-614	137-1264	-	-	500
CuO	881	870	1500-3130	376-1252	626	2128	651-976	-	-	-	400
Fe_2O_3	13218	5260	109000	-	8864	96000	13550-19200	3720-30310	32400	27600	108900
HgO	-	-	0.5-1	1-22	10	3	-	21-226	-	-	-
K_2O	22845	22700	8432-24100	24100-48200	19300	15700	12210-18671	-	19700	5600	12800
MgO	11494	6790	16584-49752	16584-49752	-	-	23380-26370	-	24400	18700	10300
MnO_2	504	145	1741	-	665	3323	1440-2105	285-1583	716	661	500
MoO_2	-	-	5-30	20-60	-	-	-	-	-	-	-
Na_2O	31346	55000	26960		26960	28308	21703-28850	20490-38150	25900	21400	6300
NiO	86	69	-	-	-	-	89-225	-	-	-	300
PbO	3651	3170	1616-3232	4309-8618	3340	1077	5957-6011	-	-	-	300
Sb_2O_3	374	1060	36-239	180-560	1317	300	-	740-1993	-	-	-
SeO	-	-	-	-	-	-	-	2-13	-	-	-
SiO_2	73158	46500	-	-	-	-	-	21396-363732	267100	320700	467800
SrO	-	412	-	-	-	-	-	710	300	400	4400
TiO_2	17373	8760	-	-	-	-	-	4170-41035	24900	26200	8500
V_2O_5	60	-	-	-	-	-	-	16-145	-	-	-

Table 5.5 Bulk Chemical Compositions of MSWI Fly Ashes from Various Sources (Continued)

	NJIT 1 MB	NJIT 2 MB	BA MB [1]	FA MB [1]	APC MB [1]	FA + APC MB [1]	FA MB [2]	FA MB [3]	FA MB [4]	FA RDF [4]	FA Coal
ZnO	9568	10500	2489-4979	12447-24894	21160	7593	-	10816-22654	-	-	200
LOI	17.94	12.94	-	-	-	-	-	-	4.90	13.40	2.05
SO_4	-	-	12000-30000	-	-	-	-	-	-	-	-
SO_3	67980	80100	-	-	-	-	-	-	107300	30000	15800
P_2O_5	6924	3730	-	-	-	-	-	-	13900	10600	600

Table 5.6 Selected Chemical Compositions of MSWI Fly Ashes from Various Sources

Type	%CaO	% SiO_2	%Al_2O_3	%Fe_2O_3	%K_2O	%MgO	%Na_2O	%SO_3	%Cl
NJIT 1 - Raw	36.7	7.3	5.9	1.3	2.3	1.2	3.1	6.8	13.4
NJIT 2 - Raw	40.5	4.7	3.7	0.5	2.3	0.7	5.5	8.0	18.0
NJIT 2 - Fine	40.2	4.5	3.4	0.5	2.6	0.7	4.5	8.0	19.1
Cement Type I	64.3	17.3	4.1	2.2	1.3	3.2	0.2	5.4	0.0
Coal fly ash	6.0	46.8	28.0	10.9	1.3	1.0	0.6	1.6	-
Fly ash + APC [1]	16.8	-	10.4	9.6	1.6	-	2.83	-	2.8
Fly ash [2]	8.4-10.8	-	7.9-15.0	1.4-1.9	1.2-18.7	2.3-2.6	2.2-2.9	-	-
Fly ash [3]	11.8-39.3	2.1-36.4	2.0-21.0	0.4-3.0	-	-	2.1-3.8	-	5.0-20.9
Fly ash [4]	26.6	26.7	13.7	3.2	2.0	2.4	2.6	10.7	-
Fly ash RDF [4]	23.7	32.1	15.3	2.8	0.6	1.9	2.1	3.0	-

Note: from (1) Kosson et al. (1996); (2) Ontiveros et al. (1989); (3) Buchholz et al. (1993); (4) Triano (1992)
BA: bottom ash; FA: fly ash; APC; air pollution control residues; all MSWI fly ashes were sampled from mass-burn incinerators; except for the one marked with RDF: refuse-derived fuel incinerator. "-" means not reported.

Table 5.5 shows ranges of chemical compositions of fly ash from various sources. Data for bottom ash and cement are also provided as a reference. Traditionally, much emphasis has been placed on metals; therefore, metal analyses are widely available for all kinds of MSWI fly ash. Less interest has been directed at understanding the role of the major constituents, especially soluble salts. They may indeed be the most important and problematic constituents, both in terms of environmental risk, residue management and utilization.

Oxygen is one of the most prevalent elements in all fly ashes. It is present as oxides of several of the other major, minor, and trace elements, such as calcium, silicon, aluminum, iron, sodium, magnesium, potassium, sulfur, and carbon.

Calcium is present both as one of the major matrix constituents of the particulate fly ash carried over from the boiler and as part of the major reaction product as well as residual CaO or $Ca(OH)_2$ in APC devices. The amount of calcium as well as those of other constituents is dependable upon location in the process where the fly ash was sampled. Fly ash taken from a particulate control device, such as ESP or FF, upstream from a scrubber shows lower concentration. As shown in Table 5.5, 40.6% or 406,000 mg/kg of the APC residue from a Mass-burn system is calcium which is on par with those of NJIT 1 and 2 fly ashes (36.7 and 40.5%) while those of other fly ashes are present in much lower concentrations. Undoubtedly, the concentrations of chloride and other oxides are also consistently similar for the NJIT 1 and 2 fly ashes and the APC residue.

Chloride from solid wastes is present as a major condensation product on fly ash particles, such as NaCl and $CdCl_2$. Additionally large amount of chloride in the form of $CaCl_2$ comes from reactions in acid gas scrubbers, which utilize lime injection. This is the

reason why the chloride content of APC residue is, thus, several times higher than that of fly ash without scrubber residue.

It is important to note that calcium and chloride are the only major elements that are more abundant in APC residues than in fly ash captured prior to entering APC system alone. The content of very soluble calcium chloride is responsible for many of the difficulties involved in the management and utilization of these residues. Not only does the very high concentration of calcium chloride in the leachate pose a risk to drinking water, but it may help increase the solubility of other contaminants, such as heavy metals, as well.

Most of the volatile metals e.g., cadmium, lead, and zinc, are found in higher concentrations in fly ash and APC residue than in bottom ash. This is because metals with high volatility in gas stream condensate and deposit on fly ash particles in downstream APC or particulate removal units while less volatile metals, such as aluminum and iron, mostly remain in the bottom ash. The rest of aluminum and iron that are entrapped in the gas stream form kernel of the fly ash particles in subsequent APC system (Cheng and Bishop, 1992).

As for coal fly ash, the only major constituents present in concentrations of higher than 10,000 mg/kg (1%) are aluminum, calcium, iron, silicon, potassium, and magnesium. Volatile metals are present only in trace quantities.

Table 5.6 also summarizes the concentrations of key components in cement. It can be seen that the compositions vary widely from incinerator to incinerator, even of the same technology, i.e., mass-burn systems. Composition of fly ash is dependent upon feed composition, incineration technology, operating conditions, and APC technology. That is,

given that incineration is done at the same facility, chemical compositions of different batches of fly ash can vary, still. The waste feed composition fluctuates on a seasonal or even a daily basis. Therefore, commercial utilization of MSWI fly ash may require processes that monitor the compositions in each and every batch of the fly ash and blend the ash with other ingredients to make its composition consistent and in compliance with relevant quality standards. Certainly, that calls for more research necessary to identify the optimal compositions of the MSWI fly ash that would give the best performance and durability as well as endure environmental safety for applications. For example, it will be revealed in the next section that washing is a necessary step toward utilization of MSWI fly ash. Reduction in soluble salts by washing guarantees safety for reinforced steel while high compressive strength can still be achieved.

5.2.2 Bulk Chemical Compositions of Fractionated MSWI Fly Ashes

The chemical compositions of raw and fractionated NJIT 2 fly ashes are shown in Table 5.7. Information on washed fine fly ash will be discussed in the following section.

Table 5.7 Chemical Compositions of Fractionated and Washed NJIT 2 Fly Ashes

Oxide	Raw	Fine	Coarse	Washed
Al_2O_3	3.66	3.40	3.18	5.07
BaO	0.00	0.02	0.02	0.03
CaO	40.46	40.18	43.09	45.47
CdO	0.02	0.02	0.02	0.04
Cr_2O_3	0.03	0.03	0.03	0.05
CuO	0.09	0.09	0.07	0.17
Fe_2O_3	0.53	0.54	0.73	0.93
K_2O	2.27	2.62	1.85	0.98
MgO	0.68	0.73	0.73	1.11
MnO_2	0.01	0.02	0.02	0.03

Table 5.7 Chemical Compositions of Fractionated and Washed NJIT 2 Fly Ashes (Continued)

Oxide	Raw	Fine	Coarse	Washed
Na_2O	5.50	4.46	3.75	0.65
NiO	0.01	0.01	0.01	0.01
PbO	0.32	0.37	0.32	0.55
Sb_2O_3	0.11	0.12	0.08	0.21
SiO_2	4.65	4.54	4.19	6.84
SrO	0.04	0.04	0.04	0.03
TiO_2	0.88	0.93	0.90	1.48
ZnO	1.05	1.28	0.93	2.20
SO_3	8.01	8.04	7.16	8.26
P_2O_5	0.37	0.39	0.32	0.60
Cl	17.98	19.06	18.46	5.17
LOI	12.94	12.63	13.67	19.56
SUM	99.61	99.52	99.57	99.44

Air classification of raw NJIT 2 fly ash yielded fine and coarse fractions as discussed earlier in Sections 4.2 and 4.3.4. Al, Ca, K, Na, Si, Zn, Cl, and SO_3 are present as major compositions (more than 1% or 10,000 ppm) in raw, fine, and coarse fly ashes. As was the case for raw NJIT 2 fly ash (8.84%), the amount of oxides of cementitious components (SiO_2+Fe_2O_3+Al_2O_3) required by ASTM C618-89 for Class C (50%) and F (70%) are not met by both fine (8.48%) and coarse (8.10%) fly ashes. Inherently, both failed the SO_3 (< 5%) and the LOI (< 6%) limits. Moreover, high concentrations of soluble salt components: Na (3.75-4.46%), K (1.85-2.62%), and Cl (18.46-19.06%) indicate potential problem of corrosion to steel reinforcement in concrete. Soluble in organic salt of Zn may retard the setting and hardening of concrete (Mindess and Young, 1981). However, high Ca and Si contents may be indicative of pozzolanicity of the fly ashes. Hydration of Ca in the fly ashes may produce $Ca(OH)_2$ which will participate in

pozzolanic reactions along with amorphous Si to form strength-providing calcium silicate hydrate [C-S-H]. Armed with only the compositional information, we were yet to know for fact that these fly ashes would have high pozzolanicity since the forms of Ca and Si were unknown. Only has the information on mineralogy and behaviors of the fly ashes in cement paste been known before we could realize their potential for pozzolanic use. Sections 5.3, 5.7, and 5.13 will address this issue.

It is apparent that there is no significant difference in the compositional data of raw and fractionated fly ashes. This may be because, as will be seen in Section 5.5, fractionation did not drastically alter particle size distributions. However, their chemical forms in different types of fly ash and their behaviors in cement paste may not be as similar. Discussions will be brought further in Section 5.8.

5.2.3 Bulk Chemical Compositions of Washed MSWI Fly Ash

Fine NJIT 2 fly ash was washed in a heavy-duty bread-dough type blender for 1 hour. Supernatant of the mixture was replaced every ten minutes. After one hour, the remaining particles were dried in an oven at 110°C overnight. The result is the washed fly ash used in the strength development test later in this chapter. Table 5.7 shows the compositional data of the washed fly ash.

Washing reduced Na by as much as 85% and Cl by as much as 73%. They were very likely to be in the form of NaCl that was readily soluble upon contact with water. Other less soluble species, such as Al (5.07%), Fe (0.93%), and Zn (2.20%), seemed to increase in concentrations because of the dilution effect caused by removal of the soluble species.

Chloride ions have the special ability to destroy the passive oxide film of steel even at high alkalinities. The amount of chlorides required to initiate corrosion depends on the pH of the pore solution in contact with the steel. Only small quantities (0.6 to 1.2 kg Cl^-/m^3) may be needed to offset the basicity of portland cement (Mindess and Young, 1981). Washing may, thus, be an essential chloride removal process for the MSWI fly ash before utilization in concrete in order to minimize corrosion of steel in reinforced concrete. Removal of sodium can also be beneficial since the high available alkali can react with reactive silica in aggregate and causes expansion. This alkali-aggregate reaction causes extensive map cracking or surface cracking in concrete structures (Mindess and Young, 1981).

5.3 Mineralogy of MSWI Fly Ash

5.3.1 Mineralogy of Raw MSWI Fly Ash

Information on bulk chemical compositions only gives a rough idea as to how much each element is in the fly ash. What compounds those elements constitute are indeed important for the prediction of chemical reactions that will occur in cement.

XRD examination of NJIT 1 raw fly ash reveals, as shown in Figure 5.4, that the main components of the crystalline phases were NaCl (halite), CaO (lime), $CaCO_3$ (calcite), $Ca_2Al(OH)_7.3H_2O$ (calcium aluminum oxide), $Ca_2Al(OH)_6Cl.2H_2O$ (calcium aluminum hydroxide), $CaSO_4.2H_2O$ (gypsum), $CaSO_4$ (anhydrite), CaClOH (calcium chloride hydroxide), $CaCl_2.Ca(OH)_2.H_2O$ (calcium chloride hydroxide hydrate), and KCl (sylvite). This is consistent with the bulk chemical analysis result in Section 5.2.1 that shows high concentrations of Al, Ca, Cl, K, and Na.

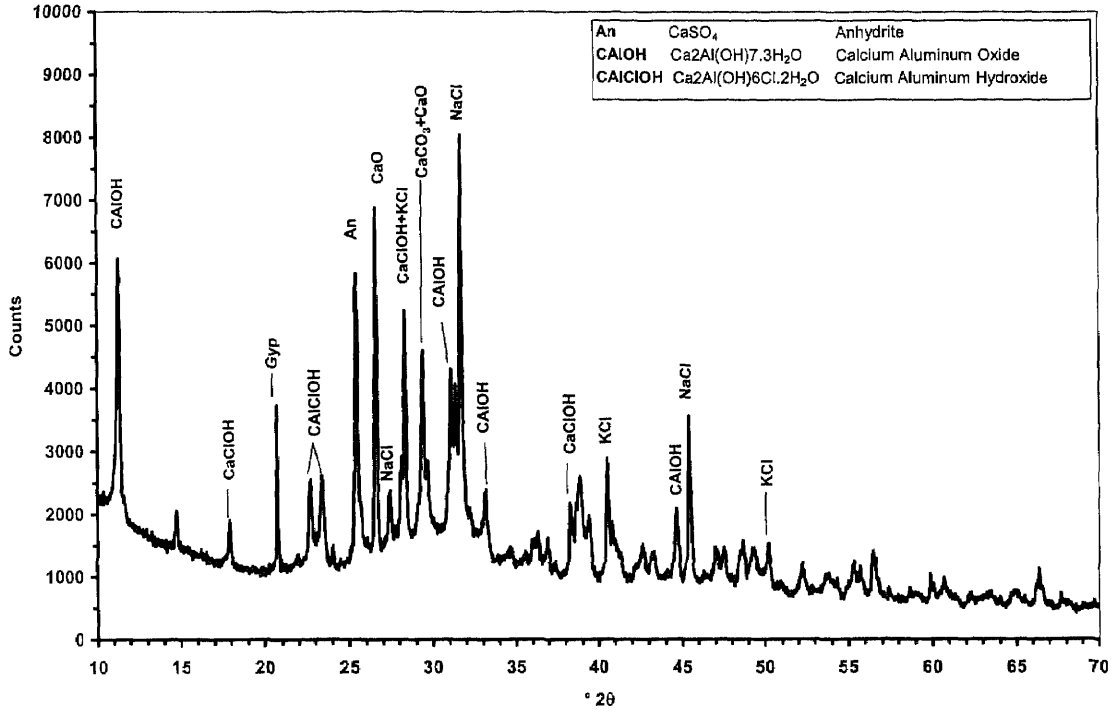

Figure 5.4 XRD Spectrum of Raw NJIT 1 MSWI Fly Ash

The identity of other phases is very difficult to establish because the patterns are characterized by a large number of small, overlapping peaks and the sample contains high quantities of poorly crystalline or amorphous materials.

It is important to note, however, that there are no strong peaks of phases containing phosphorus although NJIT 1 is virtually the APC residue treated with proprietary phosphoric acid compound. As discussed earlier, the solution used in the treatment may wash out some soluble compounds and at the same time may form amorphous phases that are not detectable by the XRD.

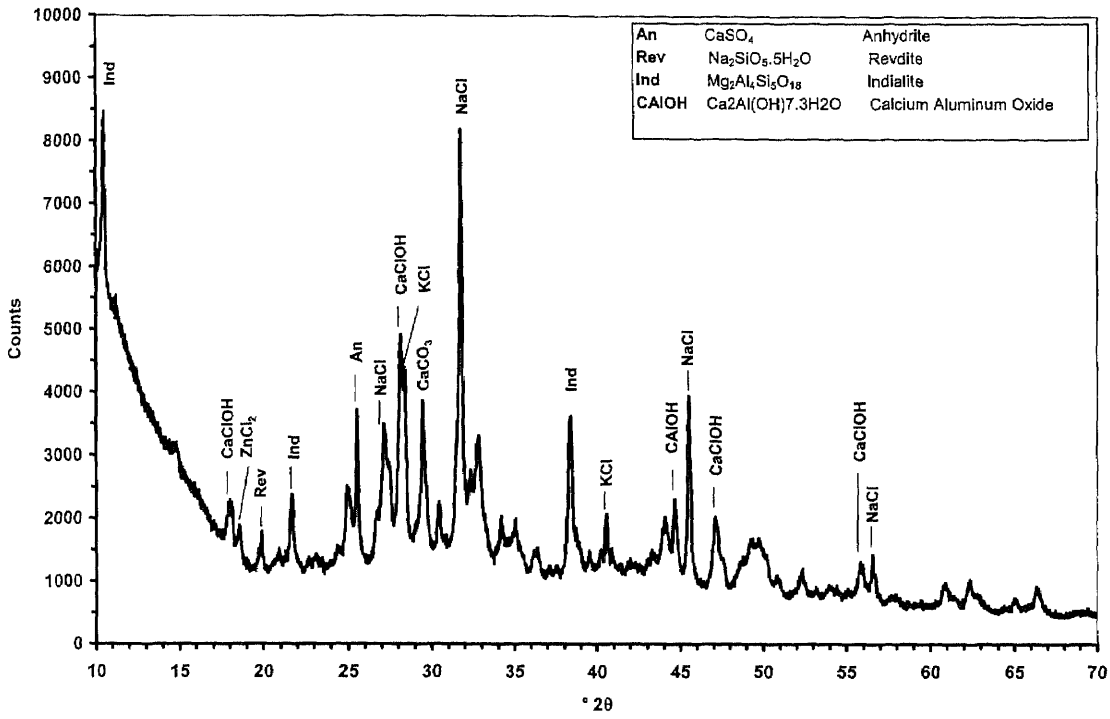

Figure 5.5 XRD Spectrum of Raw NJIT 2 MSWI Fly Ash

Figure 5.5 shows the XRD diffractogram of as-received MSWI fly ash from ESPs downstream from dry scrubbers of the facility (NJIT 2). Major identified phases are CaClOH, $CaCl_2.Ca(OH)_2.H_2O$, $CaCO_3$, $CaSO_4$, KCl, NaCl, $Mg_2Al_4Si_5O_{18}$ (indialite), $Na_2SiO_6.5H_2O$ (revdite), and $ZnCl_2$. Most of the phases appeared in the analysis of the raw NJIT 1 fly ash. This should not cause a surprise since NJIT 1 fly ash is actually NJIT 2 fly ash treated with a phosphoric acid solution.

Calcium chlorides, CaClOH and $CaCl_2.Ca(OH)_2.H_2O$ have similar characteristic peaks. Their presence in both fly ashes was due to reactions in acid gas scrubbers where lime [$Ca(OH)_2$)] was injected into the gas stream to neutralize acid gas [HCl]. The presence of calcium chloride in concrete can be both detrimental and beneficial. Addition of more than 2% of calcium chloride by weight would accelerate concrete setting while

the amount of less than 1% would retard the setting (Lea, 1971). Other effects of calcium chloride regarding compressive strength on MSWI fly ash-cement mortars will be discussed in Section 5.10.

Other calcium salt, $CaCO_3$ occurred as a result of carbonation of CaO or $Ca(OH)_2$ while $CaSO_4$ (anhydrite) was a product of neutralization of H_2SO_4 in the flue gas stream. It is apparent that anhydrite in NJIT 2 fly ash was hydrated during the ash treatment. High peak of gypsum [$CaSO_4.H_2O$] detected in NJIT 1 fly ash confirms this transformation. Dissociation of gypsum in solution during concrete mixing can give off sulfate ions that will form a calcium sulfoaluminate hydrate compound, ettringite. Ettringite is known to contribute to early strength. Its high ability to absorb water can also cause expansion of concrete (Mangialardi et al., 1998).

Obviously, NaCl had a strong presence in all of the fly ash samples. This is consistent with a study done by Hinshaw (1994) who found high NaCl content in MSWI fly ash samples. One reasonable explanation is that NaCl is a highly structured phase with definite crystalline structure that can readily be identified by the XRD. Other less structured phases may appear with lower peak intensities. Other explanation involves preferred orientation of the crystalline structures which made it highly detectable. Another alkali salt, KCl, was also detected, though at lower amount. Chlorides from these salts are detrimental to steel used in reinforced concrete. As far as durability is concerned, ACI Committee 201 recommends that not more than 0.15% chloride ion from all sources should be tolerated in reinforced concrete and not more than 0.10% if it is to be exposed to chlorides in service (Mindess and Young, 1981).

Another chloride salt, $ZnCl_2$, undetected in NJIT 1 fly ash due to leaching may have retarding effect on cement hydration. This is probably due to the formation of protective coating of hydrous zinc hydroxide on the surface of anhydrous compound (Lea, 1971).

Silicate salts of sodium and magnesium, $Mg_2Al_4Si_5O_{18}$ and $Na_2SiO_6.5H_2O$, were also found solely in untreated NJIT 2 fly ash. It is not yet clear what their roles on the strength of MSWI fly ash-cement mixture is. They were not detected in both NJIT 1 and washed fine fly ash, probably due to leaching during treatment. As we will later observe in the compressive strength experiments, their absence did not produce any significant effect. Therefore, it may be safe to assume that their roles on strength properties are inconsequential.

Metal speciation in waste incinerator is a complex process that involves the availability of oxygen and chloride, the affinity of the target metals, and the incineration temperature. The presence of chloride will enhance the formation of metal chlorides that are smaller in particle size and higher in volatility, compared with the corresponding oxides (Chiang et al., 1997). However, other elements may actually appear in other forms, such as chloride, depending on concentrations of the associated species, i.e., Cl.

5.3.2 Mineralogy of Fractionated MSWI Fly Ash

Separation of NJIT 2 fly ash by means of air classification produced two streams of fractionated fly ash: fine and coarse. Particle size distributions of fine and coarse fly ashes obtained in Section 5.5.1 show mean particle sizes ($d_{50\%}$) of 20.67 and 29.67 microns, respectively. That of raw NJIT fly ash was measured at 25.36 microns.

As discussed earlier, mineralogy of fly ash can greatly influence its behavior and thus its application in concrete. Processing of fly ash by fractionation may yield a portion of fly ash with chemical compounds that enhance properties of concrete. As shown in Figure 5.6, phases identified in the diffractograms of raw, fine, and coarse fly ashes are quite different. XRD analyses of the fractionated fly ashes reveal different phases in fine and coarse fly ash fractions. Fine fly ash contained the following phases that were not present in coarse fly ash: $Mg_2Al_4Si_5O_{18}$, $Ca_2Al(OH)_7.3H_2O$, $Na_2SiO_6.5H_2O$, and $ZnCl_2$. Apparently, those phases found mostly and exclusively in fine fly ash seemed to partition onto finer particles. When relative peak height was used to compare the amount of phases, CaClOH, $CaCl_2.Ca(OH)_2.H_2O$, and KCl were found in smaller quantities while NaCl was found in larger quantity in fine fly ash than in coarse fly ash.

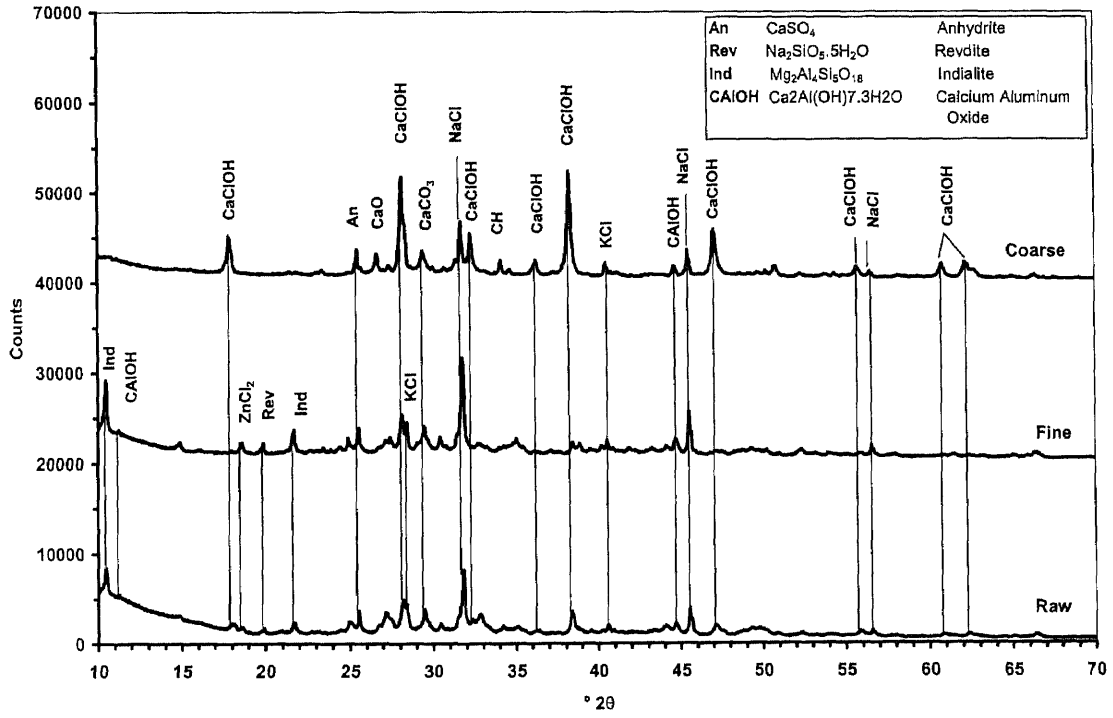

Figure 5.6 XRD Spectrum of Fractionated NJIT 2 MSWI Fly Ash

As discussed earlier, calcium chloride may help improve compressive strength properties of concrete. The effect of significantly high amount of CaClOH and $CaCl_2.Ca(OH)_2.H_2O$ as indicated by high peaks in coarse fly ash will be discussed in Section 5.10.

5.3.3 Mineralogy of Washed MSWI Fly Ash

The XRD pattern of washed NJIT 2 fly ash bears a striking similarity to that of raw NJIT 1 fly ash. Calcium hydrated salts found in NJIT 1, $Ca_2Al(OH)_7.3H_2O$ and $Ca_2Al(OH)_6Cl.2H_2O$, were also present in washed fly ash. Another calcium salt, hydrocalumite, $Ca_4Al_2O_6Cl_2.10H_2O$ or $C_3A.CaCl_2.10H_2O$ (where C=CaO and $A=Al_2O_3$), was exclusively present in washed fine fly ash. Formation of hydrocalumite was also detected in MSWI fly ash-cement pastes discussed in Section 5.7. Compressive strength experiment in Section 5.10 shows that it contributed to compressive strength of MSWI fly ash-cement mortars.

As seen in Figures 5.7 (a) and (b), washing of fine NJIT 2 fly ash removed most of NaCl and $Mg_2Al_4Si_5O_{18}$. At the same time, it produced hydrated compounds, $Ca(OH)_2$, calcium aluminum oxide [$Ca_2Al(OH)_7.3H_2O$], calcium aluminum hydroxide [$Ca_2Al(OH)_6.2H_2O$], hydrocalumite [$C_3A.CaCl_2.10H_2O$], calcium chloride hydroxide [CaClOH], and calcium chloride hydroxide hydrate [$CaCl_2.Ca(OH)_2.H_2O$]. The noticeable increase in anhydrite [$CaSO_4$] may be the result of dehydration of gypsum [$Ca(SO_4)_2.2H_2O$] attained while the washed fly ash was being dried in the oven. The presence of anhydrite may cause the phenomenon where cement stiffens prematurely, or false setting (Lea, 1971).

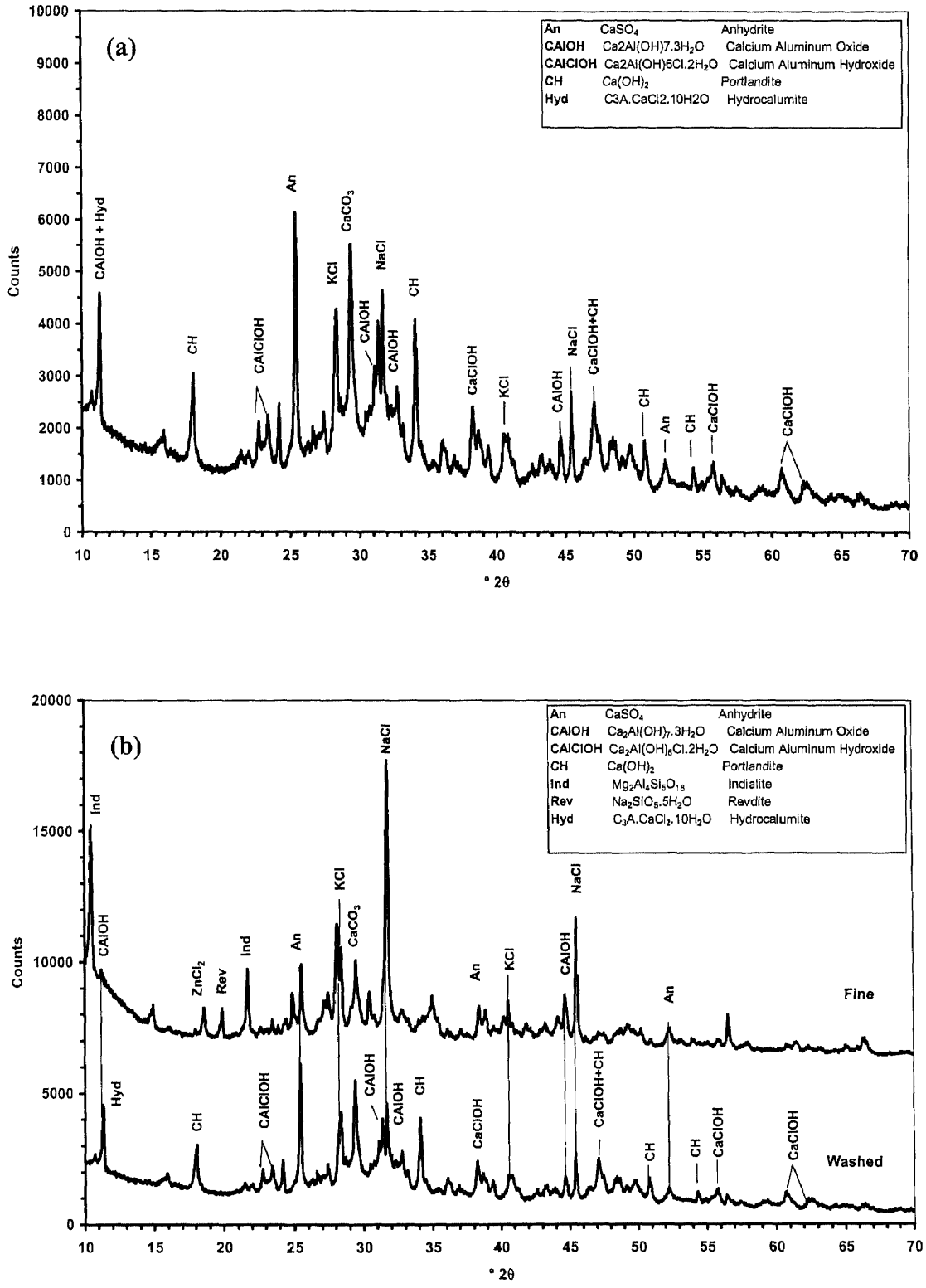

Figure 5.7 (a) XRD Spectrum of Washed Fine NJIT 2 Fly Ash and (b) as a Comparison to The Spectrum of Fine Fly Ash

$Ca(OH)_2$ was exclusively present in the washed fly ash. It is also a product of hydration of cement which was used to indicate the degree of hydration as well as the pozzolanic reactions in Section 5.7.

In addition to various forms of calcium sulfate, many other salts, such as NaCl and $CaCl_2$, can affect the setting of cement. Some salts retard the setting, such as $ZnCl_2$, while others, such as $CaCl_2$, accelerate. Quantity of salts also has influence on the setting. For instance, when present in small quantity of less than 1%, calcium chloride sometimes retards the setting of portland cement, the addition of larger quantity produces an acceleration. Crystallization of salts, such as NaCl, can cause damage to concrete through the development of crystal growth pressure. Chloride ions themselves have the special ability to destroy the passive oxide film of steel even at high alkalinity. Small amount of chlorides can offset the basicity of portland cement and therefore initiate corrosion. Presence of alkali metals in concrete mixes also pose a great threat to stability of concrete structures via alkali-aggregate reaction (AAR). Highly alkaline solution in the pores of concrete helps increase the solubility of reactive silica in aggregates and forms alkali-silica gel that weakens the integrity of the aggregates. The ability of the newly formed gel to incorporate water causes volume expansion. The resulting stress will crack the weakened aggregates and the surrounding cement paste, thereby leading to structural failure.

Experiments on compressive strength of MSWI fly ash-cement mortars in Sections 5.10 and 5.12 revealed significant improvement in the strength performance of MSWI fly ash mortars over control. High amount of hydrated calcium chlorides, CaClOH and $CaCl_2.Ca(OH)_2.H_2O$ in the fly ashes were responsible for the superior strength.

However, aside from the strength performance and durability of MSWI-fly ash mortar still needs to be investigated.

Soluble salts in the MSWI fly ash samples, such as NaCl, KCl, and $CaCl_2$, can create a potentially significant environmental and engineering problem in the utilization or disposal of the ash. Ions from these salts may leach into groundwater near disposal sites, creating serious contamination. These ions will also promote corrosion where ash is utilized as a building material. Hence, processing of MSWI fly (by washing) should rid us of these problems and, at the same time, may enable us to have a new source for construction material.

The presence of alkali and earth alkali salts, such as NaCl and $CaCl_2$, contributes to high alkalinity in leachate. During single batch extractions, such as the TCLP, leaching of the alkalinity present in fly ash-cement products leads to high leachate pH values. At these high pH values, metal complexes, e.g., hydroxides, are relatively insoluble (Webster and Loehr, 1996). In other words, the pH values of the resulting leachates govern their metal concentrations rather then the concentrations of metals in the ash. This could lead to underestimation of potential hazards to human and the environment. Discussions on leaching of MSWI fly ash-cement product will be provided in details in Section 5.14.

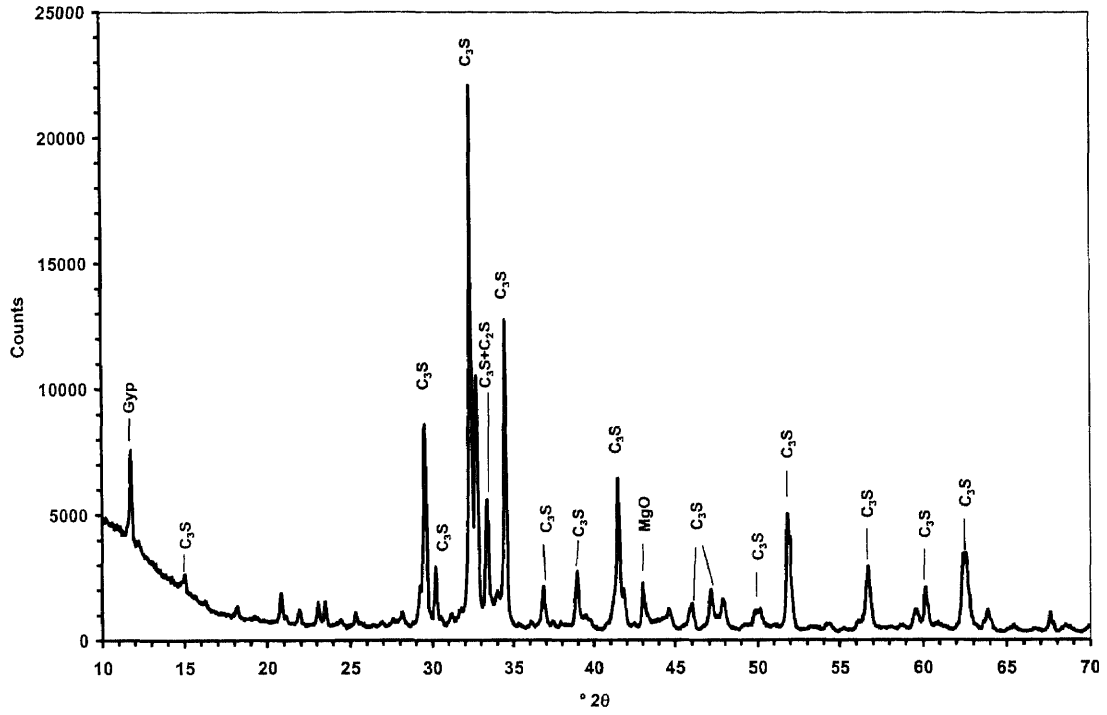

Figure 5.8 XRD Spectrum of Portland Type I Cement

Figure 5.8 shows the diffraction pattern of portland cement Type I used in this research. The spectrum was dominated by distinct peaks of tricalcium silicate, C_3S, the most important cement component. It is the principal reaction involving C_3S during hydration of cement that produces calcium silicate hydrate [C-S-H]. Another significant phase is gypsum [$CaSO_4.2H_2O$] that also forms a strength-providing phase, ettringite. Periclase [MgO] was also present in very small quantity. The presence of its crystal in clinker has been found to lead to long-term unsoundness in resultant cement. This is due to the expansion that accompanies its slow hydration. Small content of up to 2% in cement does not appear to have a significant effect although high content of more than 4% requires rapid cooling of clinker to offset the adverse effect (Lea, 1971).

5.4 Fractionation of MSWI Fly Ash

As in the case of coal fly ash, the fineness of the material affects both pozzolanic activity and the workability of the ensuing concrete (Mangialardi et al., 1998). Ukita et al. (1989) employed air separation technique to classify coal fly ashes into three particle size classes: 5, 10, and 20 microns. Results showed that utilization of air-classified fly ash reduced water requirement, improved workability, as well as enhanced strength and water tightness in concrete. Jaturapittakul (1993) studied the influence of incorporating classified coal fly ashes from various sources to replace cement in concrete. The coal fly ashes were air-classified into size fractions ranging from 5 to 150 microns. His results showed that concrete specimens that incorporated finer fractions exhibited higher strength than those with coarser ones. He suggested that there was an optimal degree of cement replacement over which strength started to decrease. Fractionation of MSWI fly ash by air classifier was then employed to determine if the findings could be applicable to MSWI fly ash.

Criteria were set for the determination of an optimal operating condition that would result in the highest yield of fly ash with a median particle size ($d_{50\%}$) of less than 20 microns. It should be noted here that the yield is defined as the weight ratio of fine fly ash recovered in the fine particle reservoir to the raw fly ash feed.

The 20-micron size criterion was based on studies conducted by Ukita (1989) and Jaturapitakkul (1993) who found significant increase in strength when fine coal fly ash (<20 microns) was incorporated in concrete mixes. Furthermore, as will be seen in Section 5.5, sub 20-micron fly ash contributes as much as 40% in raw NJIT 2 fly ash. An attempt to separate this fraction would be worthwhile.

Humidity greatly affects yield and efficiency of the classifier since moist particles tend to agglomerate and attach themselves to surface of the air classifying equipment. This is due to the fact that NJIT 2 fly ash has high content of calcium chloride, which is a hygroscopic compound (Chandler et al., 1997). Since the laboratory environment was not controlled, experiment runs had to be conducted on days that relative humidity was not high. It was found that relative humidity of below 60% gave better results. For example, for the same operating condition (rotor speed, 3000 rpm; fan speed, 100%; run time 20 minutes), on the day that the relative humidity was 70%, the yield was only 30% while it was 70% on a dryer day.

A fly ash stock was first prepared by sifting raw NJIT 2 Fly ash through an 850-micron (No. 20) sieve to remove large debris as well as large charred particles. Batches of 500 g of the fly ash stock were then subject to various combinations of operating parameters; namely, run time, rotor speed, and fan speed. The result of each combination is an average of three runs. Results for each varied parameter are given in Tables 5.7 and 5.8.

Table 5.8 Particle Size Analysis Results of Fine Fly ash Fractionated at Varied Fan speeds

Time (min)	Rotor (rpm)	Fan (%)	Yield	$d_{50\%}$ (microns)
20	4000	50	5%	14.67
20	4000	75	14%	16.58
20	4000	100	31%	18.65

As shown in Table 5.7, the fan speed that gave the highest yield is 100%. Median diameter of the resulting fine fly ash is 18.65 microns, thereby meeting the criteria stated

above. Therefore, the full fan speed (100%) was used in all other runs where run time and rotor speed were varied.

Table 5.9 Particle Size Analysis Results of Fine Fly ash Fractionated at Varied Run Times and Rotor Speeds

Fan (%)	Rotor (rpm)	Time (min)	Yield	$d_{50\%}$ (microns)
100	3000	15	82%	23.45
100	3000	20	70%	17.77
100	3000	30	55%	15.21
100	4000	15	37%	18.65
100	4000	20	31%	15.45
100	4000	30	27%	12.68
100	5000	15	35%	18.09
100	5000	20	27%	16.04
100	5000	30	22%	14.98
100	6000	15	23%	12.41
100	6000	20	20%	12.20
100	6000	30	20%	10.30

The results in Table 5.8 clearly show that an increase in run time at a given rotor speed resulted in finer fractionated fly ash, although at lower yield. The same is also true for the rotor speed when run time was kept constant.

For better comparison, the data in Table 5.9 were used to prepare the following graphs in Figures 5.9 and 5.10.

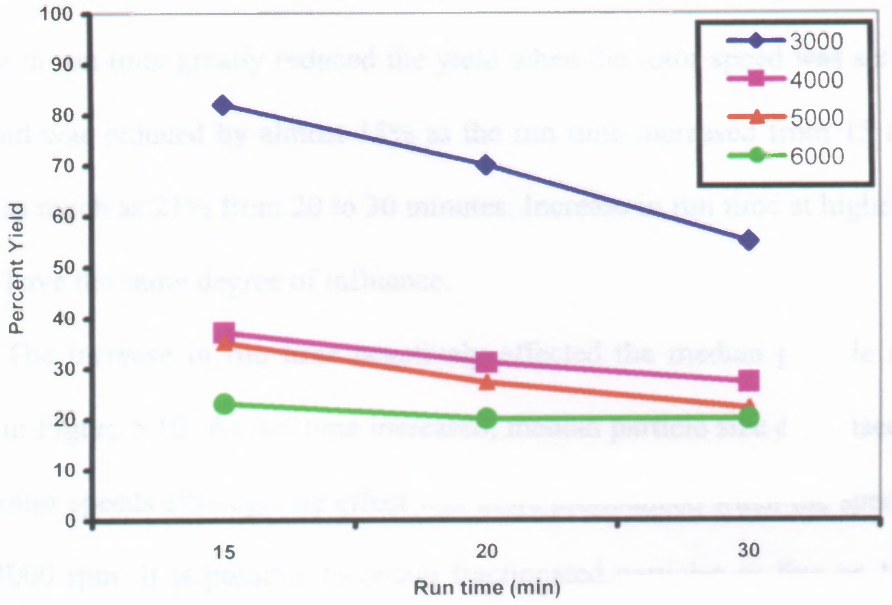

Figure 5.9 Percent Yield of Fine Fly Ash at Different Run Time

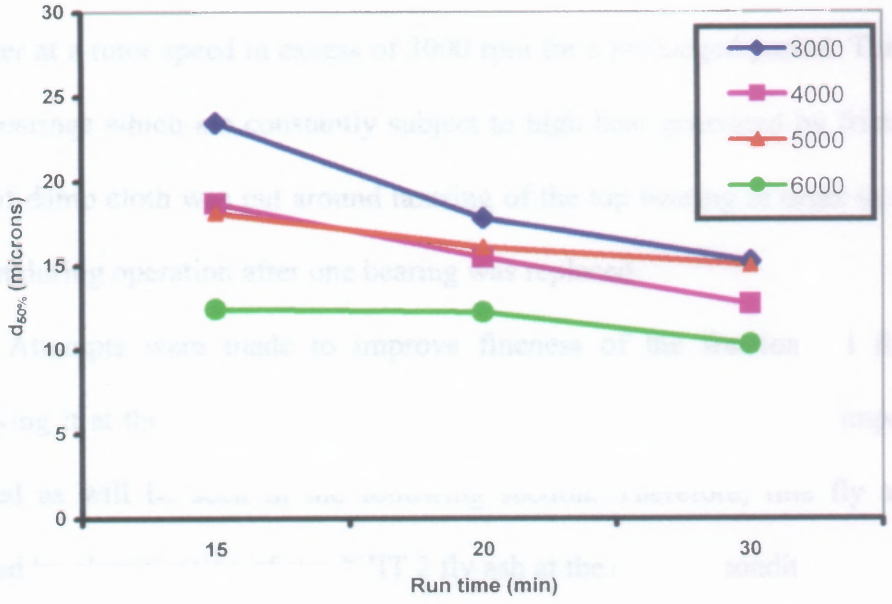

Figure 5.10 Median Particle Size of Fine Fly Ash at Different Run Time

The effect of run time on the yield is illustrated in Figure 5.9. Apparently, increase in run time greatly reduced the yield when the rotor speed was set at 3000 rpm. The yield was reduced by almost 15% as the run time increased from 15 to 20 minutes and by as much as 21% from 20 to 30 minutes. Increase in run time at higher rotor speeds did not have the same degree of influence.

The increase in run time negatively affected the median particle size ($d_{50\%}$) as shown in Figure 5.10. As run time increased, median particle size decreased. This is true for all rotor speeds although the effect was more pronounced when the speed setting was set at 3000 rpm. It is possible to obtain fractionated particles as fine as 10 microns by operating the classifier at 6000 rpm, although at the expense of yield.

From the results, the optimal operational parameters were as follow: run time, 20 minutes; fan speed, 100%; and rotor speed, 3000 rpm. The choice of rotor speed was influenced by the manufacturer's recommendation that discourages operation of the classifier at a rotor speed in excess of 3000 rpm for a prolonged period. This is to protect rotor bearings which are constantly subject to high heat generated by friction. In fact, a piece of damp cloth was put around housing of the top bearing in order to help dissipate the heat during operation after one bearing was replaced.

Attempts were made to improve fineness of the fractionated fly ash by re-classifying it at the optimal operating conditions. However, very little improvement was obtained as will be seen in the following section. Therefore, fine fly ash stock was prepared by classification of raw NJIT 2 fly ash at the optimal condition.

Fractionation of MSWI fly ash by an air classifier should be considered as an alternative to other fractionation methods, such as sieving. It can give a fine particle yield

of more than 70% for particles smaller than 20 microns, which satisfy the criteria. However, better separation of the fly ash into specific class sizes, such as 5-, 10, and 15-microns, using a larger classifier that has fewer limitations must be explored along with an economic study before the method can be fully commercialized.

5.5 Particle Size Analyses of MSWI Fly Ashes

The most dramatic change in incinerator technology over the past decade has been related to the APC systems. Improvements in emission controls currently capture more undesirable potential airborne contaminants in the fly ash, APC residues, and liquid waste streams than did earlier generations of APC systems. Inevitably, that leaves facility managers with burdensome waste to deal with.

As previously discussed, characteristics and properties of particulate matters from an MSW incinerator are dependent upon the location where they are sampled. For example, fly ash captured upstream from a lime-injection dry scrubber is sure to have different chemical makeup than the one captured downstream. Type of APC devices, such as FF or ESP, also has a great influence since FFs are more efficient at removing submicron particles than ESPs. Other factors include waste feed composition, incinerator type, and operating conditions (Chandler et al, 1997).

5.5.1 Particle Size Analyses of Raw MSWI Fly Ashes

Particle size analysis results of raw NJIT 1 and 2 fly ashes by means of a laser diffraction particle size analyzer are shown graphically in Figure 5.11. It is evident that particle size distribution curve of NJIT 1 fly ash is much more to the right of those of NJIT 2 fly ash

and cement. That is, as listed in Table 5.10, NJIT 1 fly ash is the coarsest of all, with a median particle size ($d_{50\%}$) of 86.56 microns compared with 25.36 microns for NJIT 2 and 20.61 microns for cement. The 90-percentile size ($d_{90\%}$) of NJIT 1 fly ash is 408.50 microns while those of NJIT 2 fly ash and cement are 133.62 and 47.91 microns, respectively.

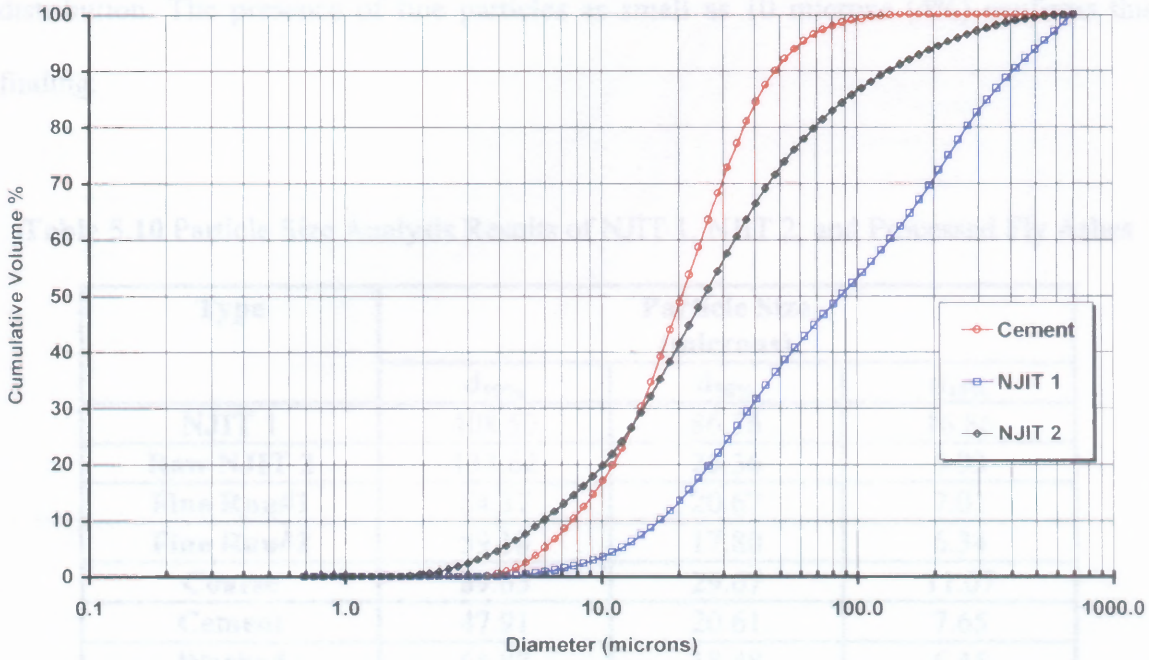

Figure 5.11 Cumulative Particle Size Distributions of Raw MSWI Fly Ashes

It is very imperative to note that there is maximum size limitation of 704 microns to the particle size distribution analysis result using the particle size analyzer as shown in Figure 5.11. That is, it does not take into account particles that are larger than 704 microns despite their presence in the sample. Sieve analysis result in Section 5.1 showed that approximately 55% of NJIT 1 fly ash particles fell below 700-micron size range while almost 100% of the particles determined by the particle size analyzer fell below

that size range. Therefore, comparison between the two methods is not valid for the stated reason.

Microscopic examination of NJIT 1 fly ash in Section 5.6.1 reveals that the ash consists mainly of clusters of fine particles as large as 200 microns in size and large charred platelets. The use of dispersant and rigorous water recirculation employed in the particle size analyzer helped break up particle agglomerates, thus yielding a finer size distribution. The presence of fine particles as small as 10 microns (4%) confirms this finding.

Table 5.10 Particle Size Analysis Results of NJIT 1, NJIT 2, and Processed Fly Ashes

Type	Particle Size (microns)		
	$d_{90\%}$	$d_{50\%}$	$d_{10\%}$
NJIT 1	408.50	86.56	16.86
Raw NJIT 2	133.62	25.36	5.93
Fine Run#1	64.37	20.67	7.01
Fine Run#2	59.18	17.80	6.34
Coarse	89.65	29.67	11.07
Cement	47.91	20.61	7.65
Washed	65.88	18.48	6.45
Coal Fly Ash	47.65	11.00	1.95

5.5.2 Particle Size Analyses of Fractionated MSWI fly ash

Figure 5.12 shows the particle size distribution curves of raw NJIT 2 fly ash and fractionated fly ashes in comparison to those of coal fly ash and cement. The distribution curve of coal fly ash is much to the left toward finer sizes which means that coal fly ash is much finer than raw NJIT fly ash, its fractionated parts, and cement. The median

particle size ($d_{50\%}$) of coal fly ash is about 11 micron while those of NJIT 2 fly ashes and cement are more than 20 microns.

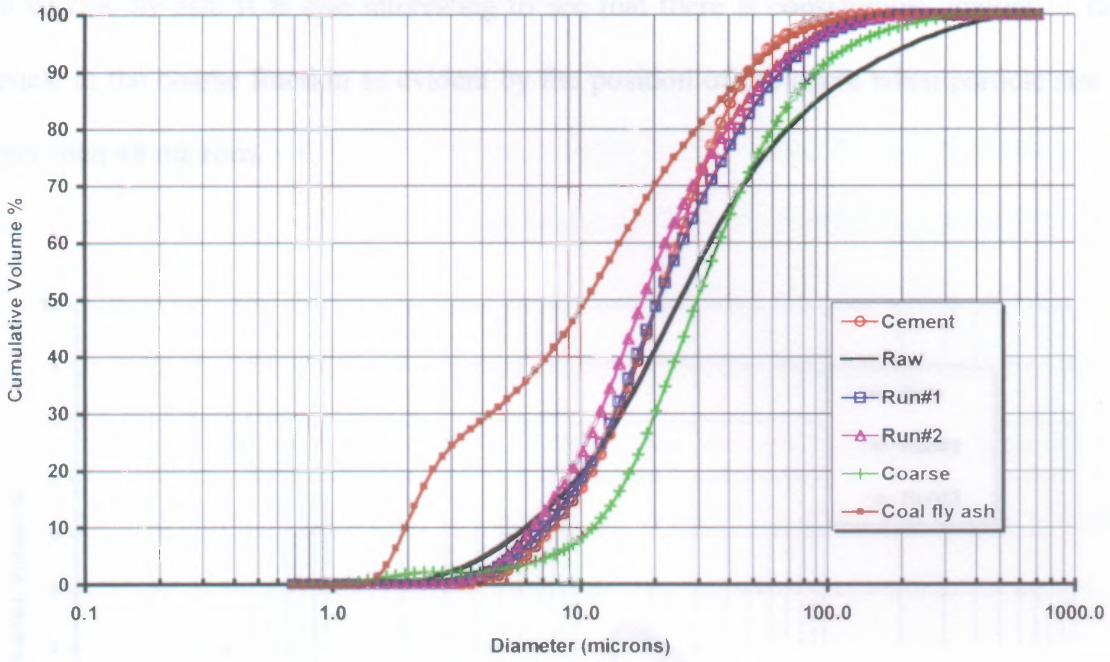

Figure 5.12 Cumulative Particle Size Distributions of Fractionated MSWI Fly Ashes

Fractionation of raw NJIT 2 fly ash at the optimal operating condition discussed earlier resulted in the fine fly ash stock. A sample from the fine fly ash stock was analyzed to produce the particle size distribution curve marked "Run#1". Clearly, the fine fly ash is finer than the raw feed as depicted by the shifting of the curve to the left. Table 5.10, which lists particle sizes measured by the particle size analyzer at different percentiles; 90%, 50%, and 10%, shows more improvement in $d_{90\%}$ than in $d_{50\%}$ of fine fly ash over raw fly ash. This is also evident in the distribution curve in Figure 5.12 which shows very small shift to the left for particles smaller than 15 microns as opposed to the bigger shift for larger particles. The particle size distribution of fine fly ash

resembles that of cement although 90% of cement particles ($d_{90\%}$) are smaller than those of fine fly ash (47.91 vs. 64.37 microns). Fly ash taken from the coarse particle reservoir of the classifier, dubbed "coarse fly ash", shows a distribution curve that is to the right of that of raw fly ash. It is also interesting to see that there is considerable amount of fine particle in the coarse fraction as evident by the position of the curve when particle size is larger than 48 microns.

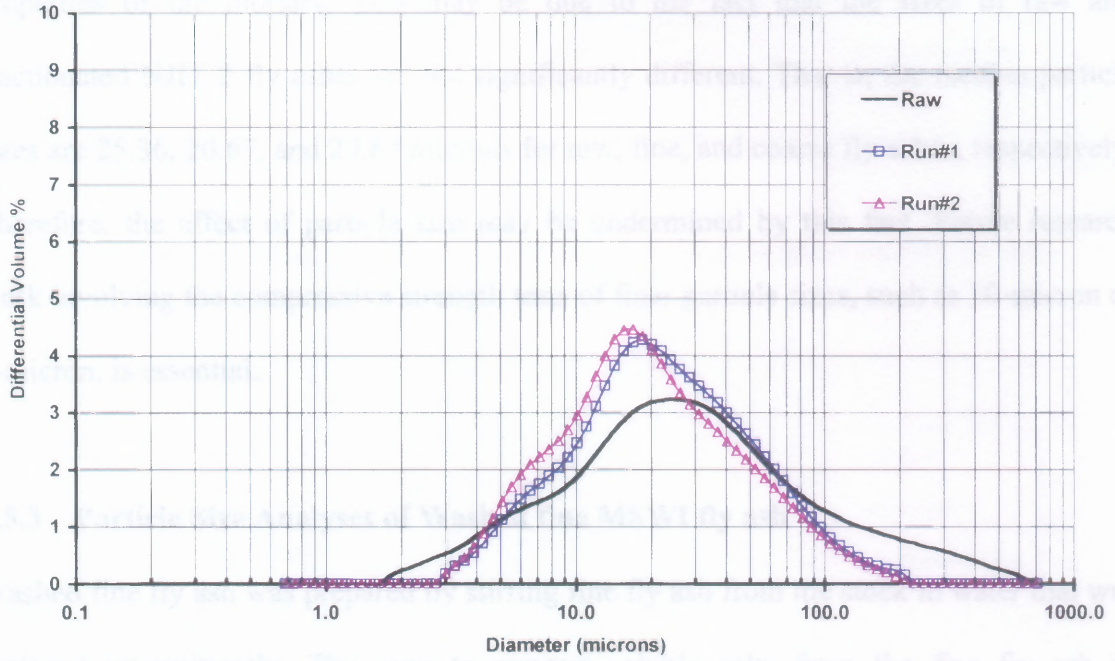

Figure 5.13 Differential Particle Size Distributions of Fractionated MSWI Fly Ashes

Re-fractionation of fine fly ash resulted in somewhat finer particles shown by the curve marked "Run#2" in Figures 5.12 and 5.13. Differential size distributions of Run#1 and Run#2 in Figure 5.13 noticeably shifted to the left of the raw fly ash curve toward finer sizes. The peaks representing the median sizes also shifted toward finer sizes, from 25 microns for raw to 16 microns for fine fractions. It can be seen that the distributions of

Run#1 and Run#2 are comparable. Little improvement of re-fractionation is evident in Table 5.10. The median particle size ($d_{50\%}$) was reduced from 20.67 to 17.80 microns. This was not considered a good incentive to employ re-fractionation to improve fineness of the fine fly ash stock for such little improvement.

The compressive strength test results in Sections 5.10 and 5.11 will later show that the effect of fine particle size is not significant in MSWI fly ash-cement mortars. The effects of water absorption and chemical reactions have more influence on the strength properties of the mortars. This may be due to the fact that the sizes of raw and fractionated NJIT 2 fly ashes are not significantly different. That is, the median particle sizes are 25.36, 20.67, and 29.67 microns for raw, fine, and coarse fly ashes, respectively. Therefore, the effect of particle size may be undermined by this fact. Future research work involving the compressive strength tests of finer particle sizes, such as 10-micron or 5-micron, is essential.

5.5.3 Particle Size Analyses of Washed fine MSWI fly ash

Washed fine fly ash was prepared by stirring fine fly ash from the stock in water that was replaced intermittently. This was to remove soluble salts from the fine fly ash in preparation for the compressive strength experiment in Section 5.12.

Care was taken when decanting supernatant from the mixing bowl so that loss in fine particles was minimized. Figures 5.14 and 5.15 show that particle size distribution of washed fine fly ash is identical to that of fine fly ash. Particle size data listed in Table 5.10 also support this finding.

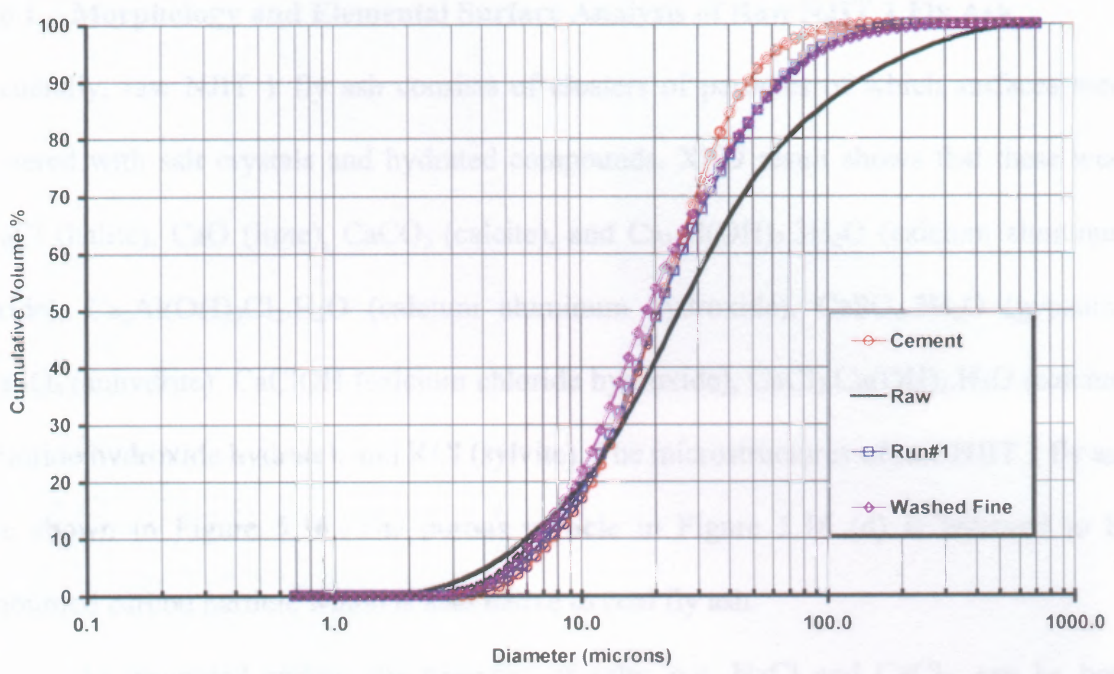

Figure 5.14 Cumulative Particle Size Distribution of Washed MSWI Fly Ash

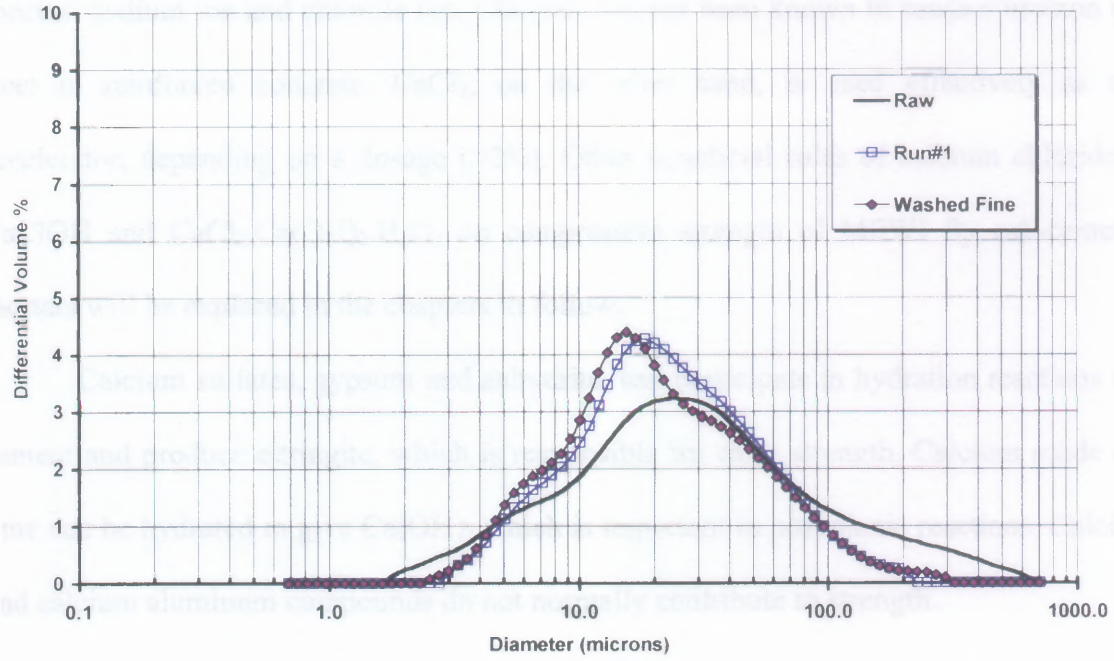

Figure 5.15 Differential Particle Size Distribution of Washed MSWI Fly Ash

5.6 Morphology and Elemental Surface Analysis of MSWI Fly Ashes

5.6.1 Morphology and Elemental Surface Analysis of Raw NJIT 1 Fly Ash

Generally, raw NJIT 1 fly ash consists of clusters of particles of which surfaces were covered with salt crystals and hydrated compounds. XRD result shows that these were NaCl (halite), CaO (lime), $CaCO_3$ (calcite), and $Ca_2Al(OH)_7.3H_2O$ (calcium aluminum oxide), $Ca_2Al(OH)_6Cl_2.H_2O$ (calcium aluminum hydroxide), $CaSO_4.2H_2O$ (gypsum), $CaSO_4$ (anhydrite), CaClOH (calcium chloride hydroxide), $CaCl_2.Ca(OH)_2.H_2O$ (calcium chloride hydroxide hydrate), and KCl (sylvite). The microstructures of raw NJIT 1 fly ash are shown in Figure 5.16. The porous particle in Figure 5.16 (d) is believed to be unburned carbon particle which is also native to coal fly ash.

As discussed earlier, the presence of salts, e.g. NaCl and $CaCl_2$, can be both beneficial and detrimental. NaCl dissociates once in contact with water to give ionic species: sodium ion and chloride ion. Chloride ion has been known to cause corrosion of steel in reinforced concrete. $CaCl_2$, on the other hand, is used effectively as an accelerator, depending on a dosage (>2%). Other beneficial roles of calcium chlorides, CaClOH and $CaCl_2.Ca(OH)_2.H_2O$, on compressive strength of MSWI fly ash-cement mortars will be explored in the chapters to follow.

Calcium sulfates, gypsum and anhydrite, can participate in hydration reactions of cement and produce ettringite, which is responsible for early strength. Calcium oxide or lime can be hydrated to give $Ca(OH)_2$ which is important in pozzolanic reactions. Calcite and calcium aluminum compounds do not normally contribute to strength.

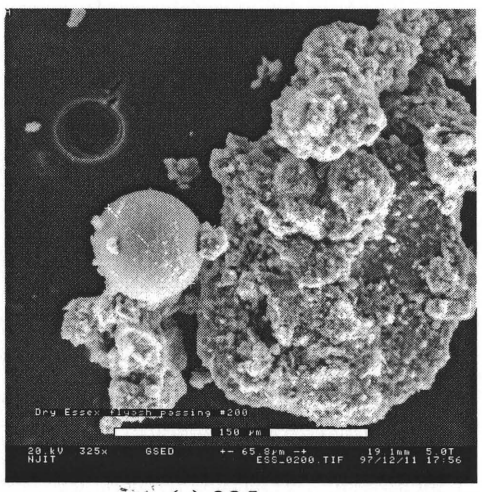

(a) 325x

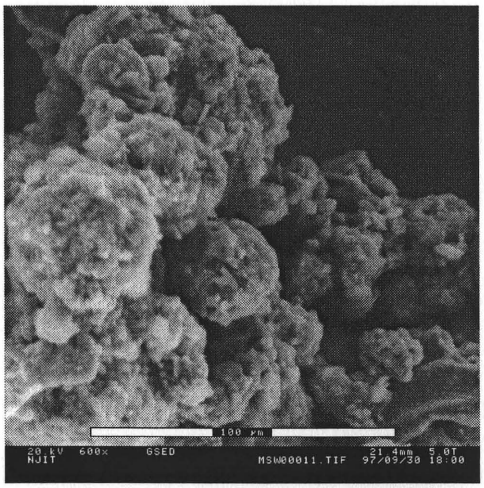

(b) 600x

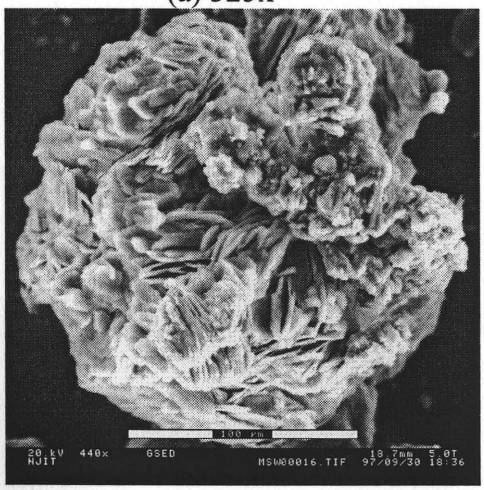

(c) 440x

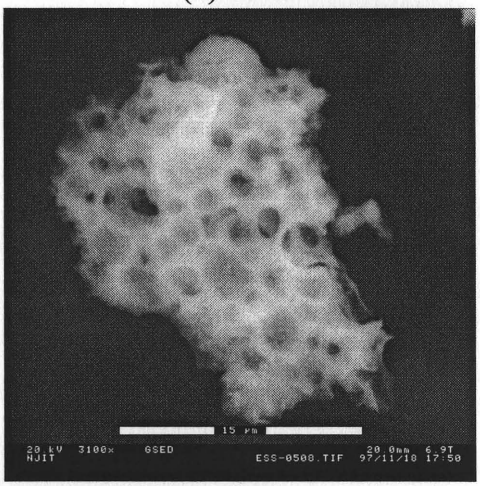

(d) 3100x

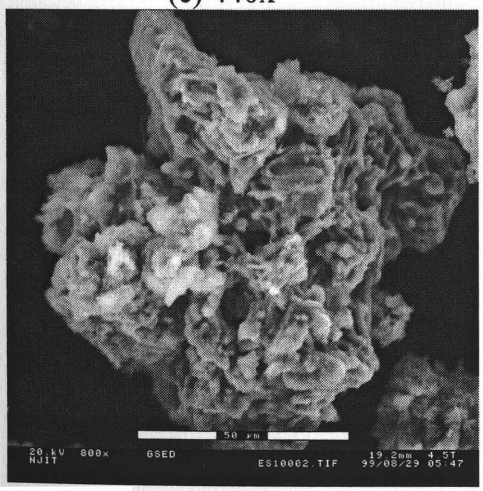

(e) 800x

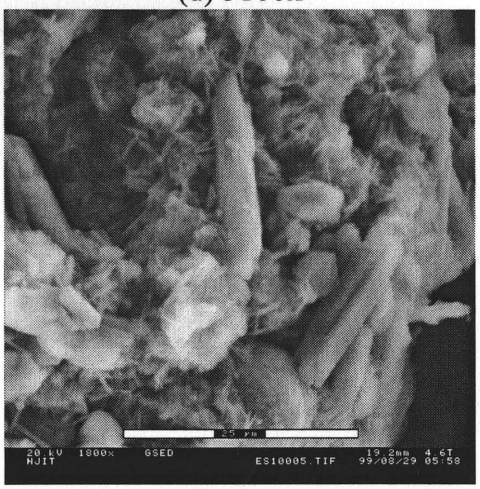

(f) 1800x

Figure 5.16 Micrographs of Raw NJIT 1 Fly Ash

Figure 5.16 (a) shows a rare glass sphere, which is a major microstructure in coal fly ash, along with large particle with rough surfaces. Generally, particles of NJIT fly ash are rather large with the size of more than 100 microns. Observation at higher magnification (600x) in Figure 5.16 (b) reveals that the large object is, in fact, clusters consisting of smaller particles attached together. A larger particle with approximately 200 microns in diameter is shown in Figure 5.16 (c). The surface of the particle appears to be covered with crystals.

In order to obtain information on what elements constitute the object of interest, an EDX (Energy dispersive X-ray spectrometer) was employed. The EDX detects characteristic X-rays of each elements emitted from the surface of the object that has been bombarded with high-energy electrons from the ESEM. The acquired spectrum is compared with the internal database and the X-ray intensities are converted to weight percent. The results are considered semi-quantitative due to the small size and variability of the fly ash particles. Nevertheless, the element ratios should approximate those actually occurring on the surface of the particles.

Table 5.11 gives the EDX results of the surface of the objects in Figures 5.16 (e) and (f). It should be noted that the results are provided in both weight percent (Wt%) as well as atomic percent (At%) which is the normalized ratio of weight percent of a particular element to its atomic weight.

The object in Figure 5.16 (e) having similar microstructural features to that in Figure 5.16 (c) was found to have high concentrations of Ca, Cl, and S, as shown in Table 5.11. These may be CaClOH or $CaCl_2.Ca(OH)_2.H_2O$ and $CaSO_4.xH_2O$. Surface elemental analysis of the rod-shape objects in Figure 5.16 (f) shows that Ca, Cl, S, Al,

and Na are major elements. Possible phases according to the XRD analysis results and the surface elemental composition are NaCl, CaClOH, $CaCl_2.Ca(OH)_2.H_2O$, $CaSO_4.xH_2O$, $Ca_2Al(OH)_7.3H_2O$, and $Ca_2Al(OH)_6Cl_2.H_2O$.

Table 5.11 Semi-quantitative Surface Compositions of Objects in Selected Acquired Images in Figure 5.16

Element.	(e)		(f)	
	Wt%	At%	Wt%	At%
O	44.10	66.98	22.49	48.59
Na	0.00	0.00	1.63	2.47
Mg	0.59	0.59	0.54	0.77
Al	2.81	2.53	5.13	6.57
Si	1.97	1.71	1.21	1.49
P	0.48	0.38	0.80	0.89
S	6.58	4.99	4.06	4.38
Cl	7.77	5.33	5.53	5.39
K	1.16	0.72	0.91	0.80
Ca	21.44	13.00	19.40	16.73
Ti	1.55	0.78	1.14	0.82
Cr	0.52	0.24	0.95	0.63
Mn	0.33	0.15	1.07	0.67
Fe	0.63	0.28	1.56	0.97
Cu	1.65	0.63	3.06	1.67
Zn	1.36	0.51	2.98	1.57
As	0.00	0.00	0.00	0.00
Cd	0.33	0.07	1.80	0.55
Sn	0.45	0.09	1.28	0.37
Sb	3.63	0.72	5.01	1.42
Pb	2.65	0.30	19.45	3.25
Total	100.00	100.00	100.00	100.00

Other phases of major elements present on the surface of the objects in either images, i.e., Si, K, Ti, Mn, Fe, Cu, Cd, Sn, Sb, and Pb were not detected in the XRD analysis. This is due to the preferred orientation of phases that influences detection of the

XRD. Another possible explanation is that these phases may not be in crystalline forms, thereby reducing its detectability.

5.6.2 Morphology and Elemental Surface Analysis of Raw NJIT 2 Fly Ash

Scanning electron micrographs of the raw fly ash particles in Figures 5.17 (a) and (b) show spherical particles at lower magnifications at 300x and 800x, respectively. However, at higher magnification of 1000x shown in Figure 5.17 (c), it is evident that most spherical particles are, in fact, porous structured agglomerates and not single particles. Average size by visual estimation is approximately 30 to 40 microns with the presence of sub 20-micron particles. Large charred particles with size in excess of 100 microns are also present in the ash as shown in Figure 5.18. These fibrous particles are the result of cellulose products, such as paper, which were not completely consumed within the incinerator (Stuart and Kosson, 1994).

Upon closer inspection in Figure 5.17 (c), it was found that the larger agglomerates actually consist of particulates of very small size (0.1 to 1.0 microns). Acid gas reaction products, excess sprayed lime as well as particulate interaction within particulate removal system may be major mechanisms in the formation of these encrusted lime agglomerates within the APC devices.

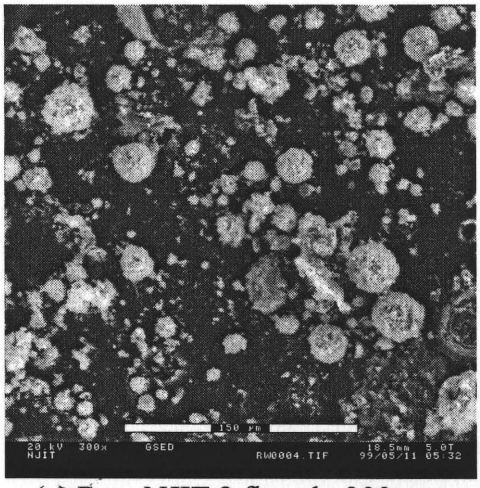

(a) Raw NJIT 2 fly ash, 300x

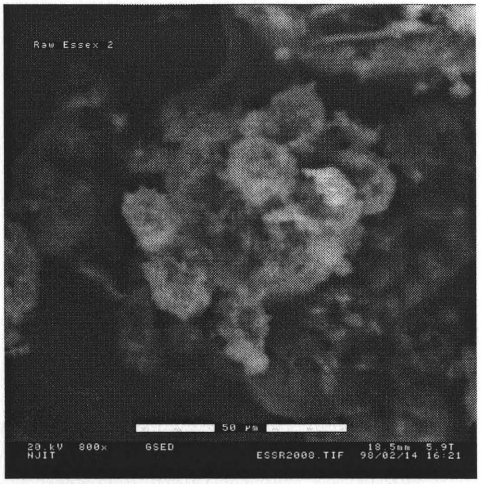

(b) Raw NJIT 2 fly ash, 800x

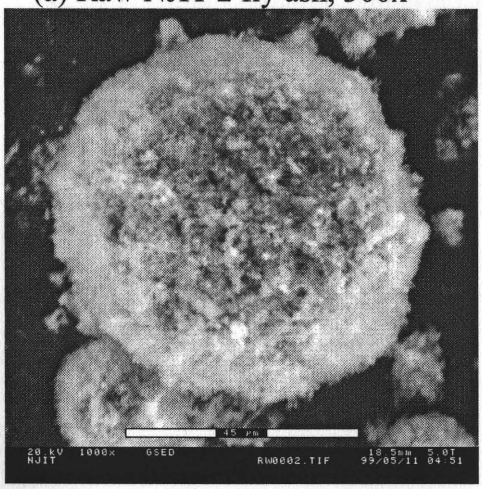

(c) Raw NJIT 2 fly ash, 1000x

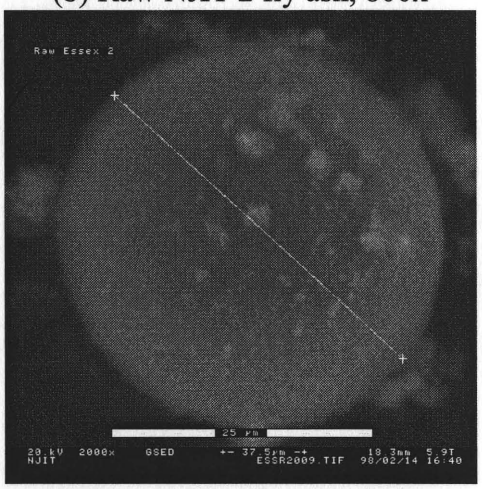

(d) Raw NJIT 2 fly ash , 2000x

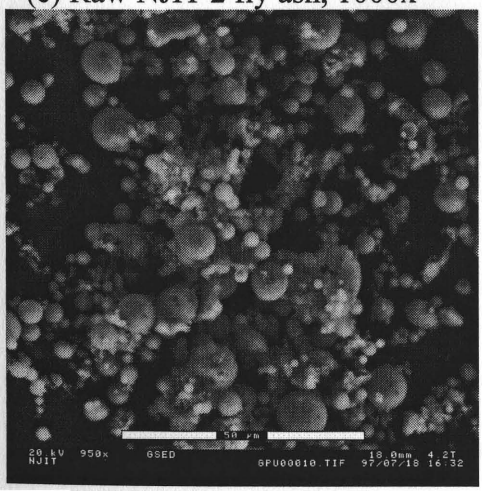

(e) Coal fly ash, 950x

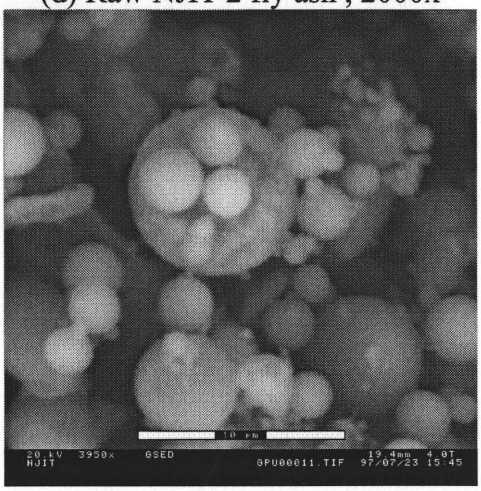

(f) Coal fly ash, 3950x

Figure 5.17 Micrographs of Raw NJIT 2 Fly Ash and Coal fly ash

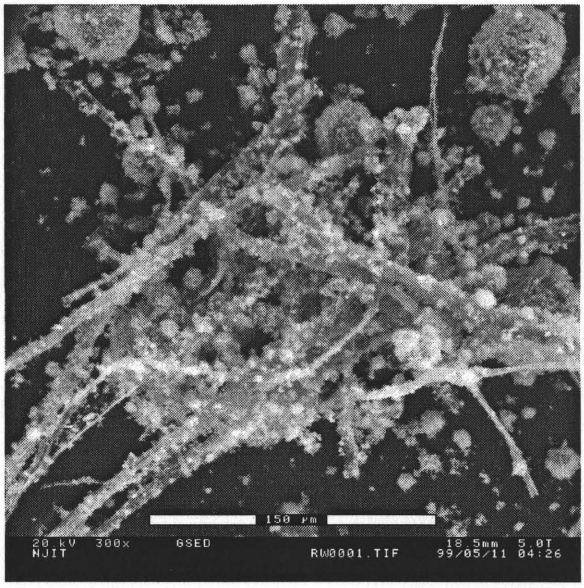

Figure 5.18 Micrographs of Fibrous Char Particles in Raw NJIT 2 Fly Ash (300x)

The EDX was employed to analyze for surface elemental compositions of acquired image of the raw fly ash and prepare maps of selected elements as shown in Figure 5.19.

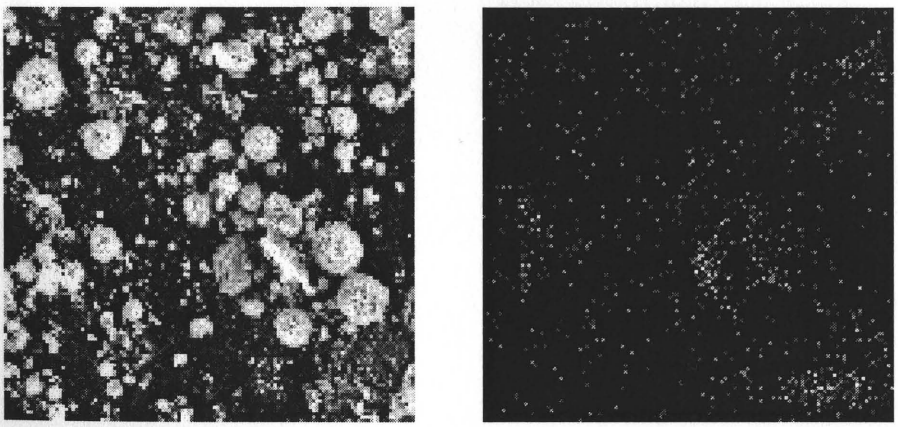

Image (300x) **Al**

Figure 5.19 Elemental Mapping of Raw MSWI Fly Ash

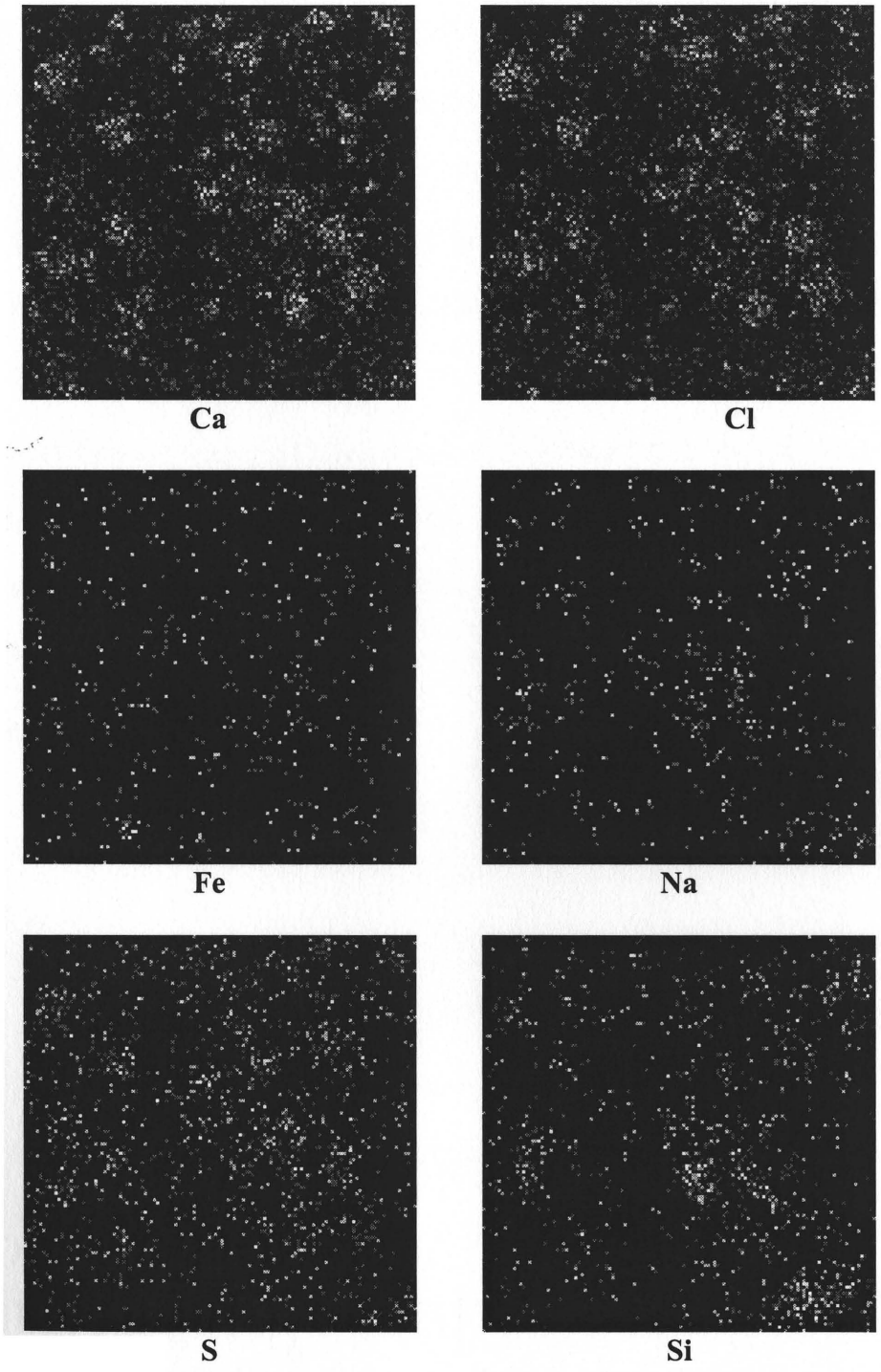

Figure 5.19 Elemental Mapping of Raw MSWI Fly Ash (Continued)

The elemental maps confirm the XRF result in Section 5.2.1 that Ca and Cl are the major constituents of the surface of the particles. Reactions between injected lime and

flue gas, e.g. HCl, are responsible for the partition of Ca and Cl onto the particle surface. Other elements, including Na, S, and Fe appear to scatter around. It is interesting to note that dark spots representing high concentrations of Al and Si were found in the kernel of the particle. This indeed agrees with the leaching study done by Cheng and Bishop (1992) who discovered that a fly ash particle basically consisted of a kernel and a surface layer. Fernández et al. (1992) and Auer et al. (1995) proposed that elements with boiling points higher than the combustion temperature, including Ca, Al, and Si, form matrix of fly ash. More volatile metals with lower boiling points, such as As, Cd, Cu, Pb, and Zn, are volatilized during combustion. Compounds of these metals then deposited on the surface of the fly ash particles when the gas stream cooled down, thus forming a layer that can be leached by acid.

Coal fly ash particles, on the other hand, are smooth glass spheres as shown in Figures 5.17 (e) and (f). In the rare event that glass spheres of MSWI fly ash did not undergo reactions on their surfaces in the APC train, its distinct feature is as shown in Figure 5.17 (d). These glass spheres are considerably more inert than typical MSWI fly ash particles which are full of reactive compounds deposited on the surface. The inert spheres do not participate in the hydration process of cement at early ages, but involve in pozzolanic reaction at later ages (Bumrongjaroen, 1999). As the results from compressive strength tests in Sections 5.10 and 5.11 will later show, the rate of strength development of the mortar pastes containing MSWI fly ash and cement is significantly faster and higher than those of control and coal fly ash mortar pastes. One possible explanation is the rough surface containing active phases, such as CaClOH and $CaCl_2.Ca(OH)_2.H_2O$.

5.6.3 Morphology and Elemental Surface Analysis of Fractionated NJIT 2 Fly Ashes

5.6.3.1 Fine NJIT 2 Fly Ash: From the particle size distribution of NJIT 2 fly ashes in Section 5.5, 90% of fine fly ash particles ($d_{90\%}$) are smaller than 65 microns compared with 133.62 microns of raw NJIT 2 fly ash. By visual inspection, most of the particles in Figure 5.20 are indeed smaller than 65 microns with the presence of sub 20-micron particles. This fraction of sub 20-micron was set as one of the criteria for determining the optimal operating condition of the air classifier in the fractionation experiments previously discussed in Section 5.4.

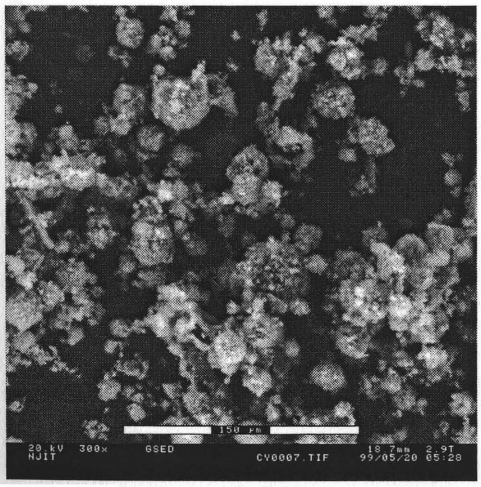

(a) 300x

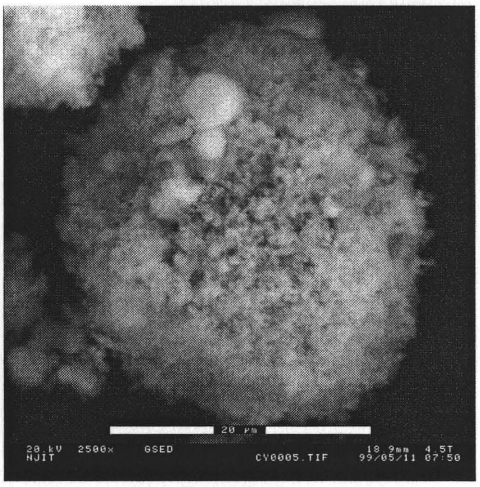

(b) 2500x

Figure 5.20 Micrographs of Fine MSWI Fly Ash

The fine fly ash particles in Figure 5.20 are very similar in appearance to the raw fly ash particles. Each particle is actually composed of tiny particulates that give a porous appearance to the particle. EDX maps of selected elements given in Figure 5.21 show that the surface chemical analysis of the particle, 25 microns in size, is enriched with Ca, Cl, and S which is also consistent with that of the raw fly ash. In Section 5.3.2, the XRD

analysis shows that $CaCO_3$, CaSO4, CaClOH, $CaCl_2.Ca(OH)_2.H_2O$ $Mg_2Al_4Si_5O_{18}$, $Ca_2Al(OH)_7.3H_2O$, $Na_2SiO_6.5H_2O$, and $ZnCl_2$ are major phases in fine NJIT 2 fly ash.

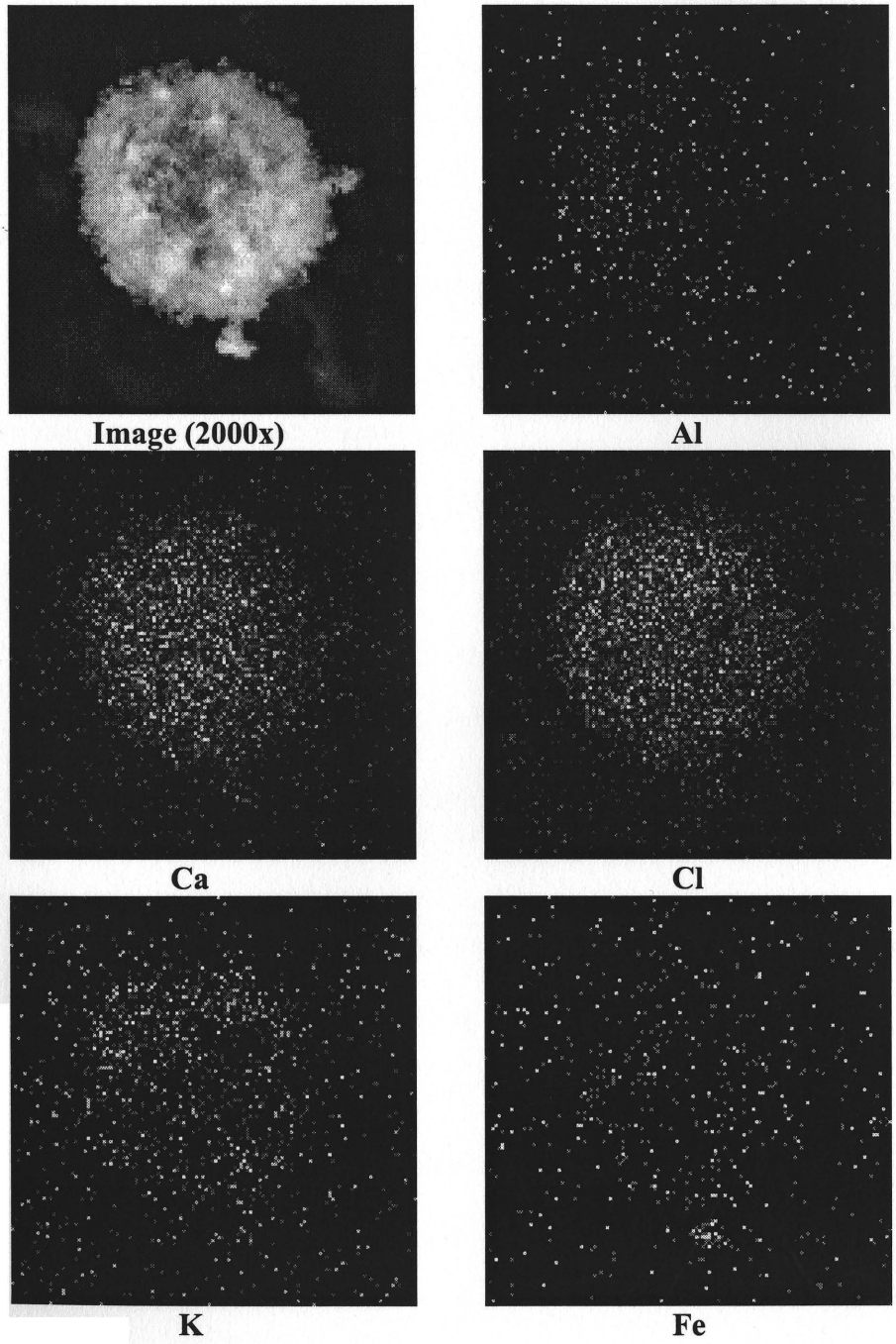

Figure 5.21 Elemental Mapping of Fine MSWI Fly Ash

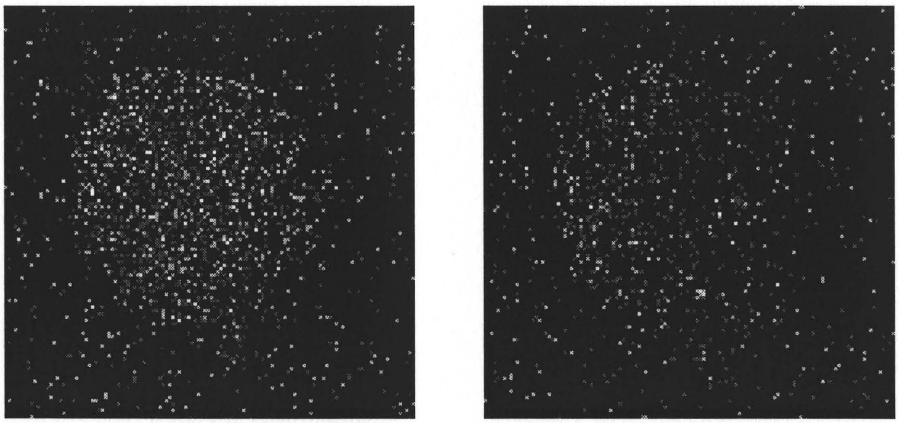

Figure 5.21 Elemental Mapping of Fine MSWI Fly Ash (Continued)

5.6.3.2 Coarse NJIT 2 Fly Ash: Micrographs of the coarse fly ash fraction indicated that an observable quantity of sub 20-micron particles were present in this larger fraction. These may be charged particles electrostatically attached to the larger particulate, or agglomerates formed during separation. Visual examination of the particles in Figure 5.22 shows features very similar to those of raw and fine fly ashes. That is, the large particles are porous structured agglomerates encrusted by fine particulates (0.1 to 1.0 microns).

As with raw and fine fly ashes, the surface of coarse fly ash is enriched with Ca and Cl. High concentrations of Na, S, and Si were also detected while Al and Fe were found to scatter on the surface of the particles as shown in Figure 5.23. This is directly in agreement with the XRF result listed in Section 5.2.2. The XRD analysis result given in Section 5.3.2 shows that coarse fly ash has the highest concentrations of CaClOH and $CaCl_2.Ca(OH)_2.H_2O$ which explains the Ca and Cl enrichment. The compressive strength test results of MSWI fly ash-cement mortars in Sections 5.10 and 5.11 shows that the

mortars incorporating 15% coarse fly ash have the highest strengths when the water-to-binder ratio (w/(c+Fa)) was maintained at 0.50.

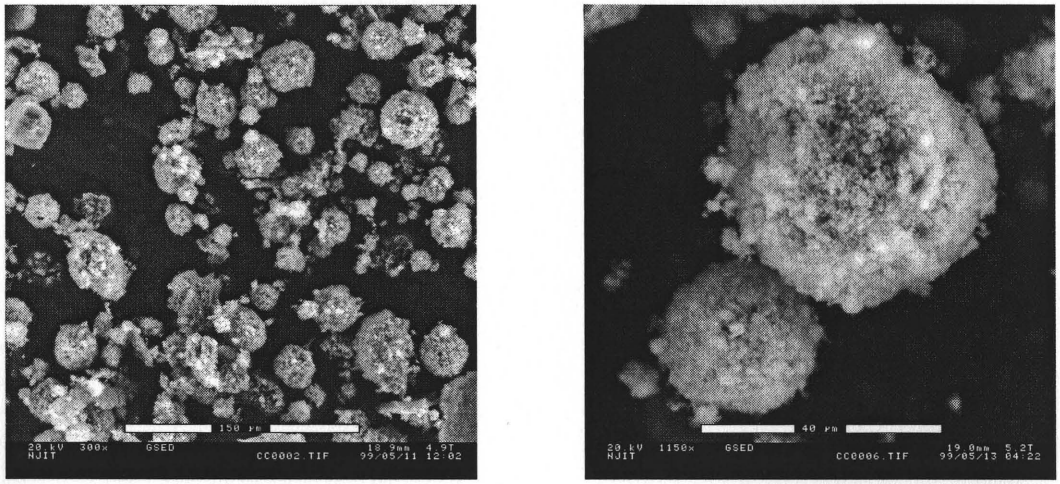

(a) 300x (b) 1150x

Figure 5.22 Micrographs of Coarse MSWI Fly Ash

It is interesting to note that at the same magnification (300x), visual observation of fine and coarse fly ash particles in Figure 5.20 (a) and Figure 5.22 (a) did not show a significant difference in particle size. This is in contrast to the particle size analysis results in Section 5.5 which show that coarse fly ash particles ($d_{90\%}$=89.65 microns and $d_{50\%}$=29.67 microns) are significantly larger than fine fly ash particles ($d_{90\%}$=64.37 microns and $d_{50\%}$=20.67 microns). The reason for this is that the particle agglomerates did not disintegrate during separation of raw fly ash by air classification. However, the use of dispersant and rigorous water recirculation broke up the agglomerates and freed finer particles during the determination of particle size distributions.

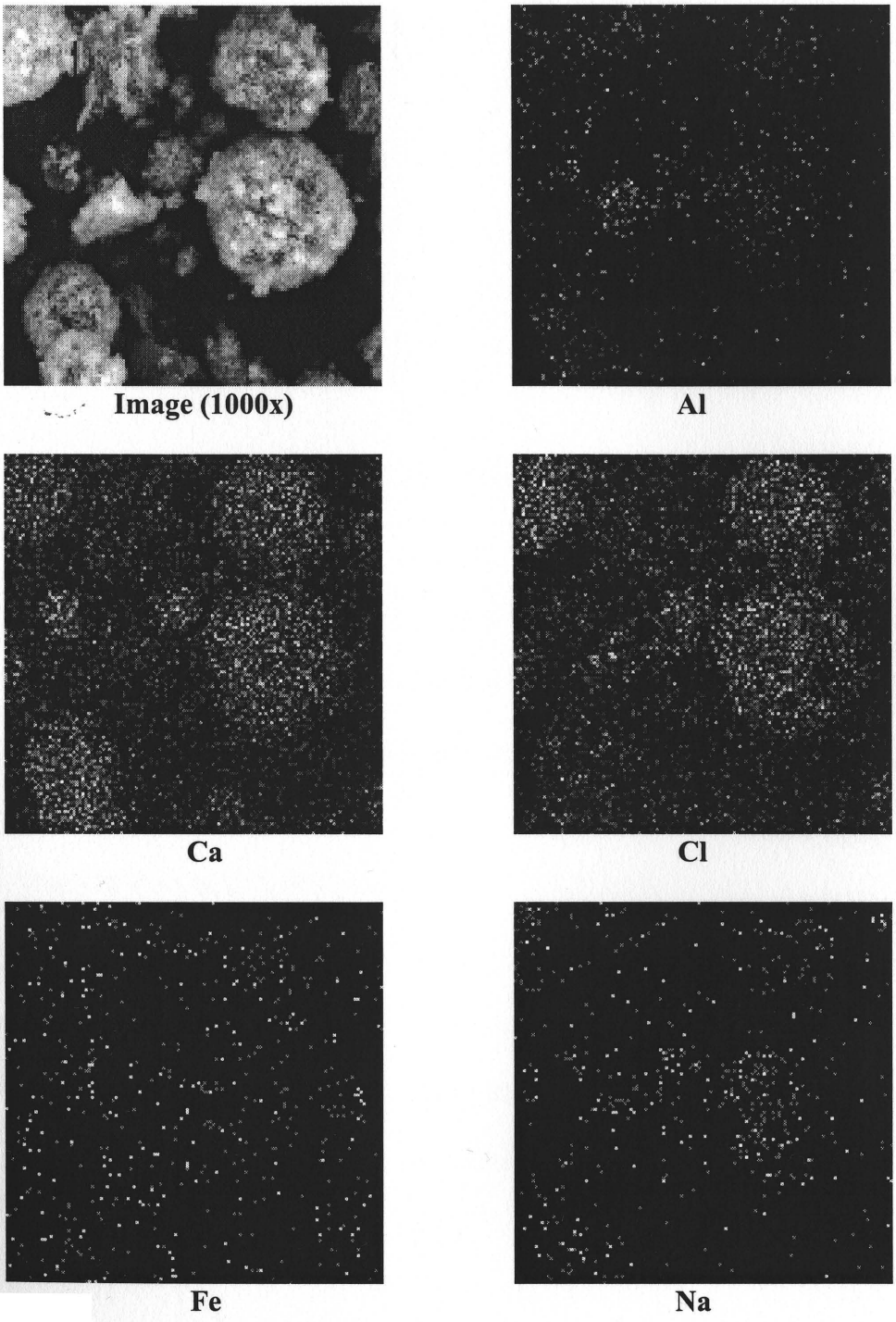

Figure 5.23 Elemental Mapping of Coarse MSWI Fly Ash

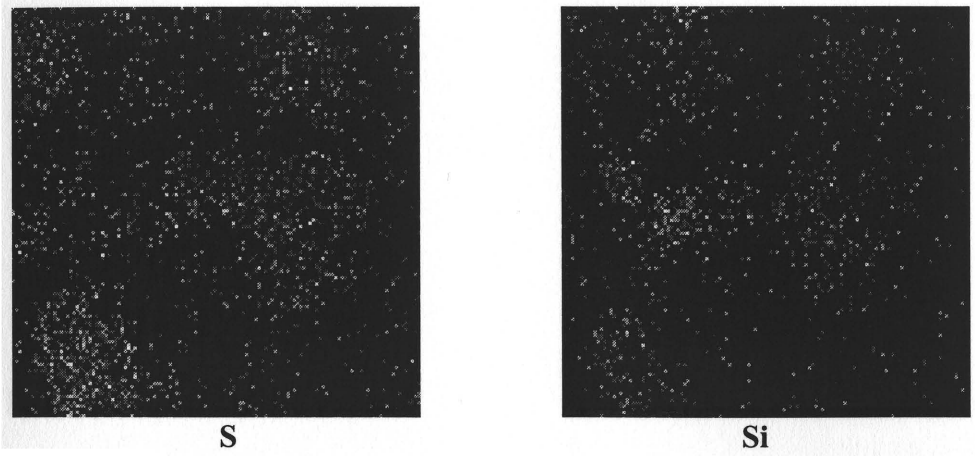

Figure 5.23 Elemental Mapping of Coarse MSWI Fly Ash (Continued)

Although not shown, some small charred particles were encountered in coarse fly ash. The amount of these particles was less than those in NJIT 1 fly ash and raw NJIT 2 fly ash since the large particles were separated from the fly ash prior to fractionation.

5.6.4 Washed Fine NJIT 2 Fly Ash

The major differences caused by washing are apparent in the chemical analysis results presented in Section 5.2.3. On a particle-to-particle basis, though, the samples appear to be about the same. As depicted in Figure 5.24, at lower magnification (300x), most of the particles show the characteristic porous agglomeration typical of MSWI fly ash.

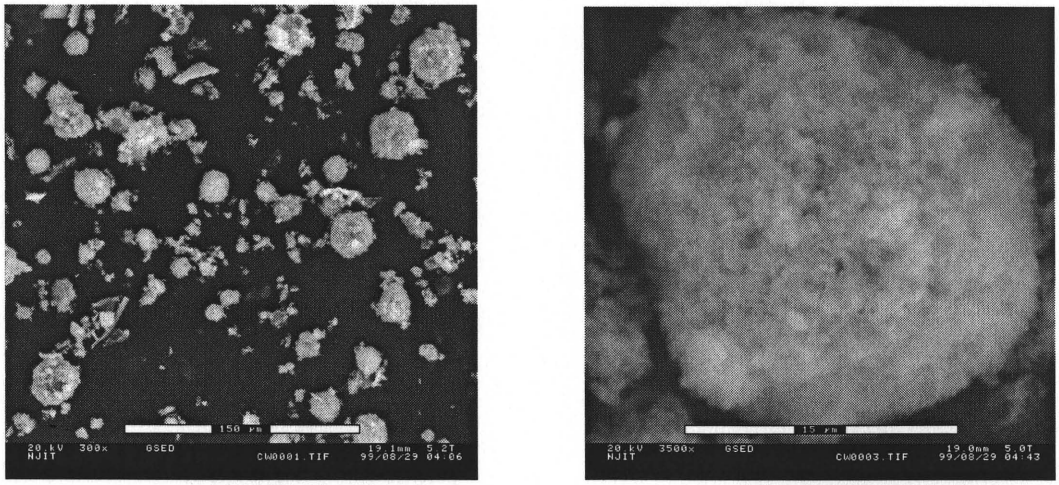

(a) 300x (b) 3500x

Figure 5.24 Micrographs of Washed Fine MSWI Fly Ash

Upon closer examination (Figure 5.24 (b)), the washed fly ash particle seems to be similar to those of raw and fractionated fly ashes. Nevertheless, the particle appears to be less porous than the raw and fractionated fly ashes. Clearly, washing removed most of the soluble phases, e.g. NaCl, from the surface of the particle and left the less soluble phases, such as CaClOH and $CaSO_4$. In the washing process, hydrated phases produced, such as $CaCl_2.Ca(OH)_2.H_2O$ bridged voids on the surface, thus making the particle less porous.

Side-by-side comparison of microstructures of the raw and processed fly ash particles are provided in Figure 5.25. It can be seen that the raw, fine, and coarse fly ash particles are very similar in nature. Their puffiness appearance came from minute particulates that attached to surface of the particles.

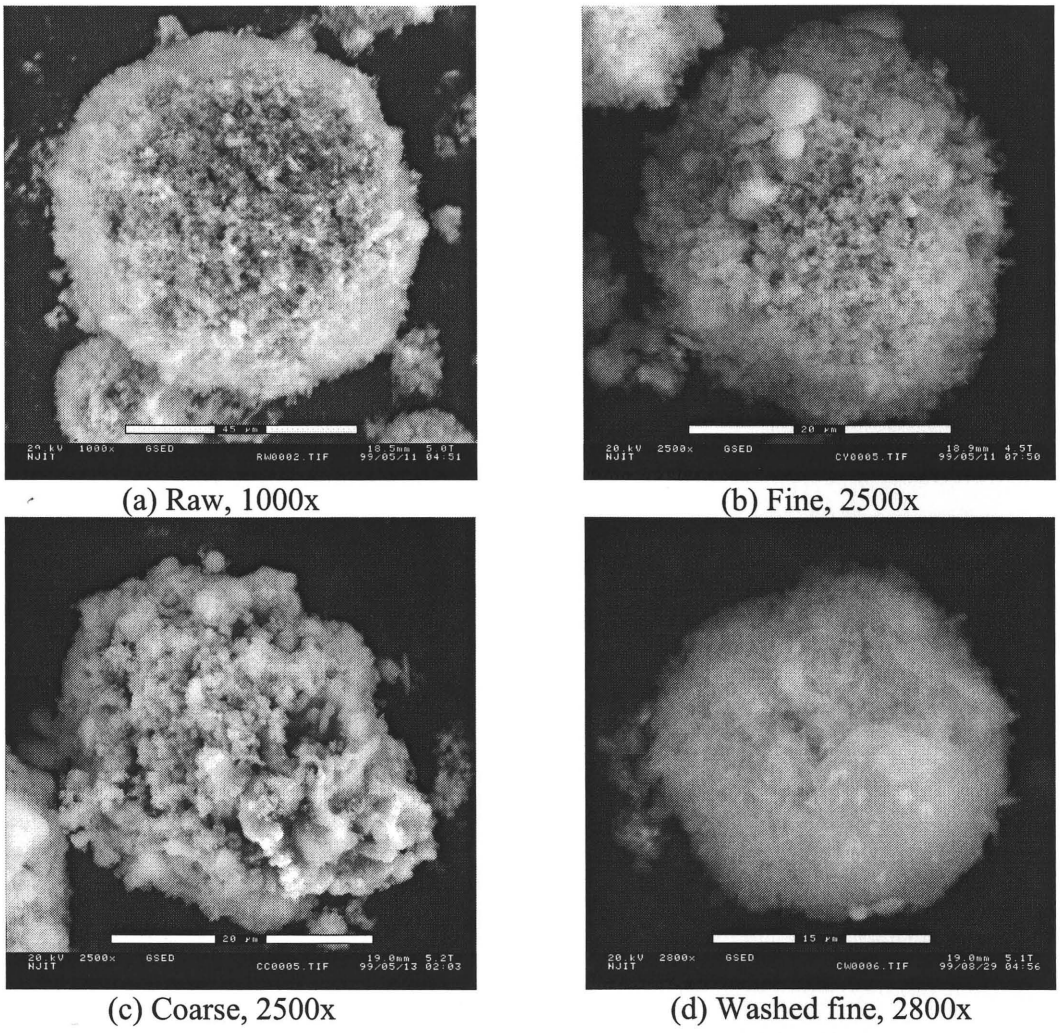

(a) Raw, 1000x (b) Fine, 2500x

(c) Coarse, 2500x (d) Washed fine, 2800x

Figure 5.25 Comparison of Raw and Processed MSWI Fly Ash particles

Surface elemental analysis results in Table 5.12 show comparable levels of the major elements, Na, Al, Si, S, Cl, and Ca, of raw, fine, and coarse fly ashes. The washed fine fly ash particle, on the other hand, has elemental compositions that are drastically different. Reduction in the soluble compounds was found to be as much as 86% (Cl) in major elements (Na, S, Ca) and as much as 100% in trace elements (Mg, Cr, Mn, As). Nonetheless, the matrix elements, Al and Si, that formed kernel of fly ash particles were

unaffected by washing. This may be beneficial to applications since Al and Si are important elements in hardening of cement.

Once fine fly ash was in contact with water, some of the compounds on particle surface, such as NaCl, were washed away in the supernatant while others formed hydration products, e.g. $Ca(OH)_2$ and $CaCl_2.Ca(OH)_2.H_2O$, as evident in the substantial increase in O content (from 27.93 to 74.33 % atom). A large piece of hydrated phase was found to be attached to the lower part of the washed fine fly ash particle shown in Figure 5.25 (d).

Table 5.12 Semi-quantitative Surface Compositions of Raw and Processed MSWI Fly Ash Particles Shown in Figure 5.25

Ele.	(a) Raw		(b) Fine		(c) Coarse		(d) Washed	
	Wt%	At%	Wt%	At%	Wt%	At%	Wt%	At%
O	19.85	37.34	12.52	27.93	14.88	31.81	51.22	74.33
Na	4.08	5.34	2.23	3.44	5.15	7.66	1.34	1.35
Mg	0.00	0.00	0.32	0.47	0.66	0.92	0.00	0.00
Al	1.21	1.34	1.74	2.30	1.51	1.91	2.77	2.38
Si	1.64	1.76	1.70	2.17	1.88	2.29	2.49	2.06
P	0.36	0.35	1.66	1.91	1.56	1.72	0.26	0.20
S	3.65	3.43	2.78	3.10	4.14	4.42	1.23	0.89
Cl	21.05	17.87	19.96	20.09	14.25	13.75	4.10	2.68
K	1.81	1.39	1.51	1.37	1.25	1.09	0.55	0.33
Ca	37.06	27.83	29.64	26.39	25.80	22.01	22.51	13.04
Ti	0.55	0.35	1.11	0.82	1.11	0.79	0.32	0.15
Cr	0.00	0.00	1.12	0.77	1.13	0.75	0.00	0.00
Mn	0.00	0.00	0.90	0.59	1.13	0.71	0.00	0.00
Fe	0.72	0.39	1.20	0.77	3.73	2.28	0.45	0.19
Cu	1.32	0.63	2.54	1.43	3.57	1.92	1.14	0.42
Zn	2.33	1.07	3.32	1.81	4.14	2.16	1.42	0.50
As	0.00	0.00	1.61	0.77	1.11	0.51	0.00	0.00
Cd	0.00	0.00	2.17	0.69	1.76	0.54	0.51	0.11
Sn	0.62	0.16	1.69	0.51	1.64	0.47	0.71	0.14
Sb	2.07	0.51	7.47	2.19	6.14	1.72	2.96	0.56
Pb	1.68	0.24	2.81	0.48	3.46	0.57	6.02	0.67
Total	100.00	100.00	100.00	100.00	100.00	100.00	100.00	100.00

As discussed previously, the surface elemental concentrations of the particles did not reflect the total elemental concentrations observed in Section 5.2.3. The XRF analysis result shows higher concentrations of the matrix elements, Al and Si. This by no means implies that washing increased the Al and Si contents, but rather it reflects the reduction in concentrations of other elements in the surface layer.

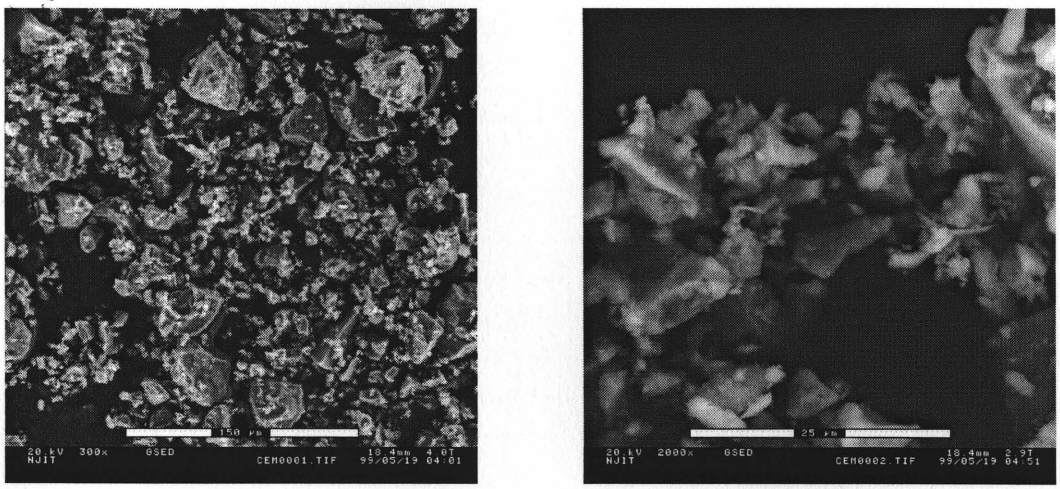

(a) 300x (b) 2000x

Figure 5.26 Micrographs of Dry Portland Type I Cement Grains

For comparison, micrographs of portland Type I cement grains are given in Figure 5.26. The XRD analysis result in Section 5.3 shows that the major phases detected are C_3S, $CaSO_4.2H_2O$, and MgO. Indeed, Table 5.13 shows high levels of Ca, Si, and S on the surfaces of the particles in Figures 5.26 (a) and (b). Other elements present in major amounts are Al, K, Fe, Cu, Zn, and Sb. Possible explanations why phases of these elements were not detected by the XRD are crystallinity and orientation. Phases with higher degree of crystallinity are readily detectable while those with lower degree of

crystallinity may not be detected at all, i.e., amorphous phases. Orientation of crystals in one way or another also determines how well they can be detected as well.

The principal component, tricalcium silicate or C_3S, reacts with water during hydration of cement to produce calcium silicate hydrate [C-S-H]. Gypsum [$CaSO_4.2H_2O$] also forms a strength-providing phase, ettringite.

Table 5.13 Semi-quantitative Surface Compositions of Portland Type I Cement Particles Shown in Figure 5.26

Ele.	(a)		(b)	
	Wt%	At%	Wt%	At%
O	16.13	32.96	14.62	32.37
Na	0.00	0.00	1.46	2.26
Mg	1.13	1.52	0.79	1.15
Al	1.69	2.05	2.75	3.61
Si	6.77	7.88	6.25	7.88
P	0.28	0.30	1.40	1.60
S	1.92	1.96	2.54	2.81
Cl	0.28	0.26	0.99	0.99
K	1.33	1.12	2.06	1.87
Ca	57.99	47.30	36.66	32.41
Ti	0.00	0.00	1.05	0.77
Cr	0.00	0.00	1.34	0.91
Mn	0.00	0.00	1.30	0.84
Fe	2.87	1.68	2.49	1.58
Cu	2.02	1.04	3.52	1.96
Zn	0.00	0.00	2.93	1.59
As	0.00	0.00	1.75	0.83
Cd	0.54	0.16	2.21	0.70
Sn	0.58	0.16	1.59	0.47
Sb	5.52	1.46	10.83	3.15
Pb	0.95	0.15	1.47	0.25
Total	100.00	100.00	100.00	100.00
Ca:Si	6.00:1.00		4.11:1.00	

The surface elemental compositions in Table 5.13 show high ratios of percent atom calcium to that of silicon (Ca:Si) of 6.00:1.00 and 4.11:1.00 for the cement particles in Figures 5.26 (a) and (b), respectively. Obviously, these ratios are much more than that of C_3S [$3CaO.SiO_2$] which is 3:1. The ratios indeed reflect the existence of other calcium compounds, such as gypsum [$CaSO_4$].

In summary, there are two major types of particles in the raw MSWI fly ash samples: chars and agglomerated spheres. Charred particles appeared mostly in NJIT 1 fly ash and raw NJIT 2 fly ash. Fewer charred particles were found in coarse NJIT 2 fly ash due to sifting of raw fly ash prior to air classification. These porous and fibrous particles have high surface areas, thus enabling them to absorb water. The agglomerated fly ash particles themselves also have high surface areas. This results in as much as 170% absorption capacity of NJIT 1, raw and coarse NJIT 2 fly ashes.

Fractionation reduced the particle size of NJIT 2 fly ash, as detected by the particle size analyzer, although the sizes appeared to be the same under visual microscopic observation. All but washed fine fly ash had high concentrations of Ca, Na, Cl, and, S on the surfaces of particles. High surface areas and high concentrations of reactive phases, such as $CaSO_4$, should enable the NJIT 2 fly ash particles to be more reactive than smooth particles of coal fly ash. In fact, the results from the compressive strength test of MSWI fly ash-cement mortars in Sections 5.10 to 5.12 show superior strength properties of all mortars containing MSWI fly ashes. How chemical compositions of MSWI fly ashes affects reactions taking place in cement at various stages of cement hydration will be discussed in the next Section.

5.7 Investigation on Hydration and Pozzolanic Reactions in MSWI Fly Ash- Cement Pastes by X-ray Diffraction Method

The chemical reactions describing the hydration of MSWI fly ash-cement pastes can be understood through the study of hydration of pure cement paste. It is usually assumed that hydration of each compound takes place independently of the others that are present in portland cement. Although this assumption neglects interactions between hydrating compounds, it reasonably simplifies the complex reactions.

Hydration of tricalcium silicates [C_3S] and dicalcium silicates [C_2S], which are key components in cement, produces calcium silicate hydrate and calcium hydroxide [$Ca(OH)_2$]. The formula for calcium silicate hydrate [$C_3S_2H_3$] or C-S-H gel is only approximate since the composition of this compound is variable over a wide range. This poorly crystalline material is responsible for the strength of concrete. The equation describing hydration of these two compounds are as follow.

$$2C_3S + 6H \rightarrow C_3S_2H_3 + 3CH$$

$$2C_2S + 4H \rightarrow C_3S_2H_3 + CH,$$

where C : CaO, S : SiO_2, H : H_2O, and CH : $Ca(OH)_2$.

Pozzolanic reactions in coal fly ash involve depolymerization of the glass matrix of the fly ash particles initiated or catalyzed by alkali ions at high pH. At the early stages, most of the hydrolyzed products remain attached to the matrix. As more bonds are hydrolyzed, low molecular weight polymer fragments and oligomers will cause the increase in aluminate, silicate, and aluminosilicate oligomers and monomers to enter the pore fluid. $Ca(OH)_2$ is consumed by the reactions that result in precipitation of various

calcium silicates, aluminates, and aluminosilicates. Silica and alumina from fly ash react with alkalis produced during cement hydration to form cementitious compounds as shown below (Plowman, 1984).

$$Ca^{2+} + SiO_2 + H_2O \rightarrow xCaO.ySiO_2.zH_2O$$

$$Ca^{2+} + Al_2O_3 + H_2O \rightarrow xCaO.yAl_2O_3.zH_2O$$

$$Ca^{2+} + SO_4^{2-} + Al_2O_3 + H_2O \rightarrow xCaO.yAl_2O_3.zCaSO_4.wH_2O$$

$$SiO_2 + 2Na^+ (or\ 2K^+) + 2OH^- \rightarrow Na_2\ (K_2)\ SiO_3H_2O$$

It can be seen from the first three pozzolanic equations that these reactions involve not only alkali (Ca^{2+}) and silica, but alumina and sulfate as well. Products of the first two equations are C-S-H and calcium aluminate hydrate [C-A-H] which give strength and density to hardened concrete. When supply of sulfate becomes abundant a calcium sulfoaluminate hydrate compound, ettringite [$C_3A.3CaSO_4.32H_2O$] may form. However, monosulfoaluminate [$C_3A.CaSO_4.12H_2O$] may form as a result of sulfate ion deficiency. From the last equation, alkali ions (Na^+ or K^+) participate in a similar reaction with silica and forms silicates. This reaction is typical of alkali-aggregate reaction that occurs in concrete structures. In a reaction that destroys the integrity of aggregate particles, amorphous silica from aggregates is attacked by alkali hydrolysis to further form alkali-silica gel with Na^+ or K^+.

5.7.1 Influence of Hydration on Tricalcium Silicate

Hydration process of MSWI fly ash-cement pastes can be evaluated by the amount of reduction in the starting materials and the increase in the hydration products. The former can be estimated by measuring the characteristic peak intensities of C_3S. Tricalcium silicate, C_3S or $3CaO.SiO_2$, which is the major and most important compound in cement that produces strength upon hydration, presents well-defined characteristic peaks at 51.83°2θ. Although the relative intensity of C_3S at this 2-theta angle is only 55% (PDF-1 database from ICDD), the peak has relatively no interference, unlike the peak representing 100% relative intensity at 34.44°2θ. The relationship between intensity value and the curing age is as shown in Figure 5.27.

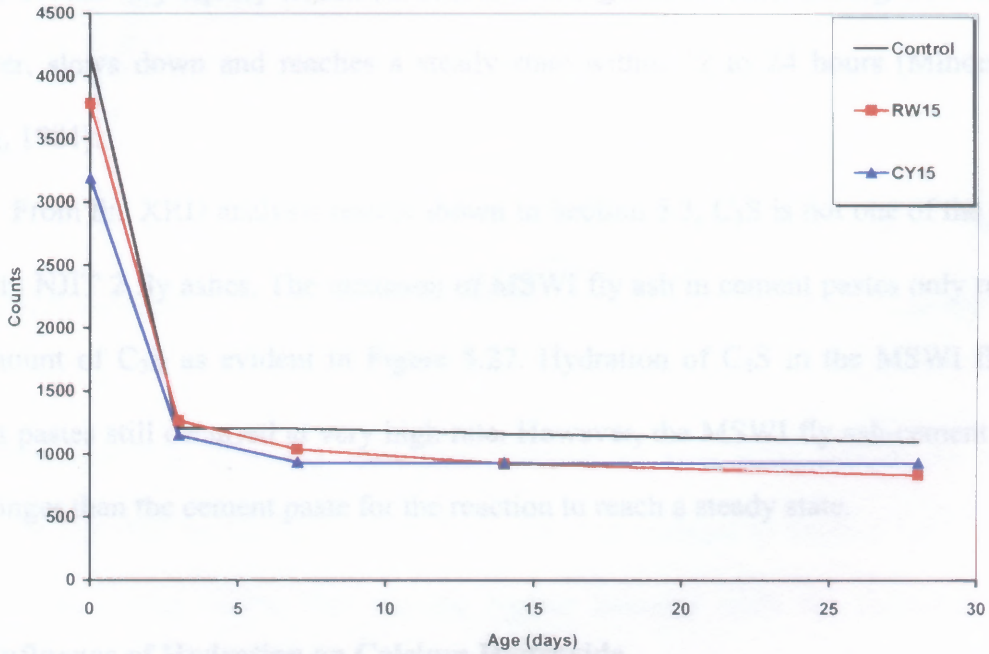

Figure 5.27 Intensities of C_3S at 51.83°2θ in 15% MSWI Fly Ash-Cement Mortar Pastes

It is clear that C_3S was consumed at a very high rate during the first three days of curing. The rate of reduction in C_3S was consistent with the rate of the strength gain as will be discussed later in Section 5.10. The consumption rate was more pronounced in the control mortar paste although those of the pastes containing 15% raw fly ash (RW15) and 15% fine fly ash (CY15) were not significantly lower. In fact, the amount of C_3S was reduced to the same level for all of the samples despite the fact that the initial amounts of C_3S in the fly ash-cement mixes were lower than that of the control. It seems that the fly ashes did not hinder the hydration process at any point. After three days, the consumption rates of all of the samples slowed down and it seemed that the reactions involving C_3S had stopped. This agrees well with the characteristic of the rapid reaction of C_3S to form calcium silicate hydrate [C-S-H] and calcium hydroxide [$Ca(OH)_2$ or CH]. The hydration process occurs very rapidly within the first four to eight hours after mixing. The reaction, however, slows down and reaches a steady state within 12 to 24 hours (Mindess and Young, 1981).

From the XRD analysis results shown in Section 5.3, C_3S is not one of the phases found in NJIT 2 fly ashes. The inclusion of MSWI fly ash in cement pastes only reduced the amount of C_3S as evident in Figure 5.27. Hydration of C_3S in the MSWI fly ash-cement pastes still occurred at very high rate. However, the MSWI fly ash-cement pastes took longer than the cement paste for the reaction to reach a steady state.

5.7.2 Influence of Hydration on Calcium Hydroxide

Figure 5.28 illustrates the production of $Ca(OH)_2$ in the MSWI fly ash-cement pastes. It was determined from the experiment that the peak intensity of $Ca(OH)_2$ at 34.11°2θ was

the strongest (100%) and free of overlapping peaks from other crystalline phases, such as CaClOH. It was, therefore, used to make the measurements. The control and fly ash-cement pastes show elevated intensities of $Ca(OH)_2$ within the first three days. This corresponds very well with the significant decrease in C_3S due to rapid hydration as shown in Figure 5.27.

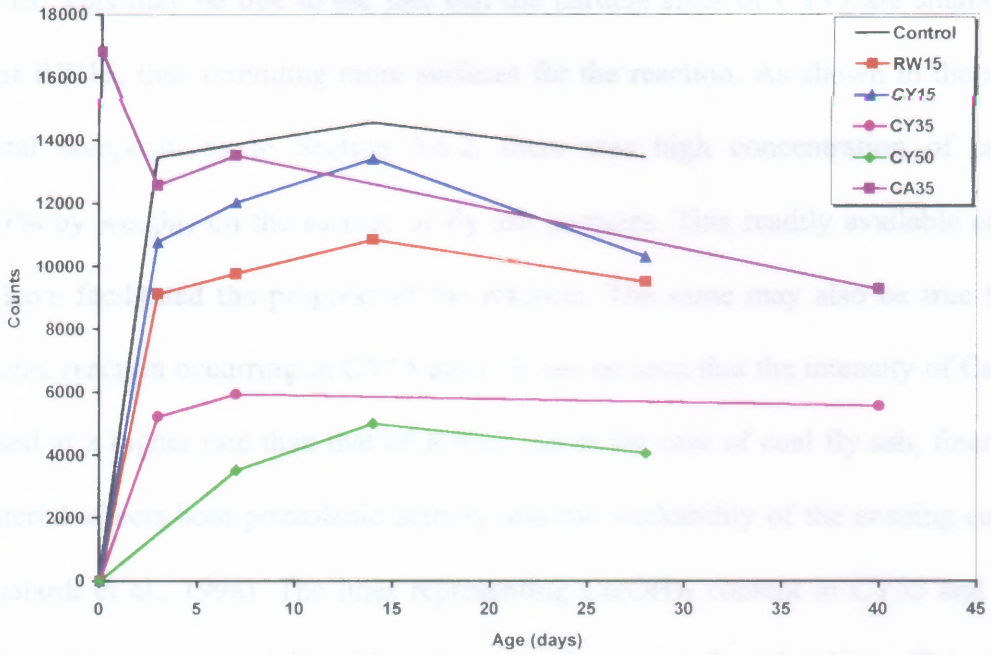

Figure 5.28 Intensities of $Ca(OH)_2$ at 34.12 °2θ in MSWI Fly Ash-Cement Mortar Pastes

As should be expected, the initial intensity of each paste reflects its calcium content as reported by the XRF in the bulk chemical analyses in Section 5.2. The pure cement paste having 64.3% CaO has the highest intensity while the degree to which cement was replaced corresponds to how low the level of the intensity was in the fly ash-cement pastes. After the period of rapid hydration, the production of $Ca(OH)_2$ slowed down until the maximum intensity was reached at day 14. Then, the intensities started to

decreased gradually. One possible explanation is that reactions involving $Ca(OH)_2$ became significant and thus resulted in the decrease. Pozzolanic activity is the likely candidate since it involves formation of C-S-H at the expense of $Ca(OH)_2$ and amorphous SiO_2. Direct XRD examination of the product, C-S-H, is very difficult since it has a poor crystalline non-stoichiometric structure.

As shown in Figure 5.28, the intensity line of CY15 is somewhat higher than that of RW15. This may be due to the fact that the particle sizes of CY15 are smaller than those of RW15, thus providing more surfaces for the reaction. As shown in the surface elemental compositions in Section 5.6.2, there was high concentration of calcium (CaO37% by weight) on the surface of fly ash particles. This readily available calcium might have facilitated the progress of the reaction. The same may also be true for the pozzolanic reaction occurring in CY15 paste. It can be seen that the intensity of $Ca(OH)_2$ decreased at a higher rate than that of RW15. As in the case of coal fly ash, fineness of the material affects both pozzolanic activity and the workability of the ensuing concrete (Mangialardi et al., 1998). The lines representing $Ca(OH)_2$ content in CY35 and CY50 also showed the rises and falls, although not as obvious as the other lines. This may be because there was less C_3S and silica in the pastes as cement was replaced by fly ash.

The lower $Ca(OH)_2$ contents in the cement pastes incorporating 15% of raw and fine fly ashes may be beneficial to concrete. Studies have shown that alkali-aggregate reactions are reduced substantially due to low levels of $Ca(OH)_2$ used by pozzolanic fly ash (Shashiprakash et al., 1994).

CA35 paste which was composed of 35% CaO and 65% fine MSWI fly ash did not solidify throughout the entire experiment. Its intensity line shows high $Ca(OH)_2$

content (17000 counts) brought about by hydration of CaO at mixing. The $Ca(OH)_2$ content dropped sharply (12600 counts) at day 3 and rose slightly at day 7 (13500 counts). Then, the line assumed a decreasing trend as evident at day 40. Obviously, the fluctuation was caused by chemical reactions which can be explained by a XRD pattern as will be discussed later in this section.

Summarized diffraction patterns of pure cement paste and MSWI fly ash-cement pastes are given in Figures 5.29 to 5.31. Although it is apparent in the XRD patterns that the characteristic peak of $Ca(OH)_2$ at 18.10°2θ shows highest intensity, the peak at 34.11°2θ was used for measurement as stated above. This is because there are peaks of other phases that occurred in the same vicinity. The overlapping phases were identified as calcium chloride hydroxide [CaClOH] and calcium chloride hydroxide hydrate [$CaCl_2.Ca(OH)_2.H_2O$] which appeared at 17.98 and 18.03°2θ, respectively.

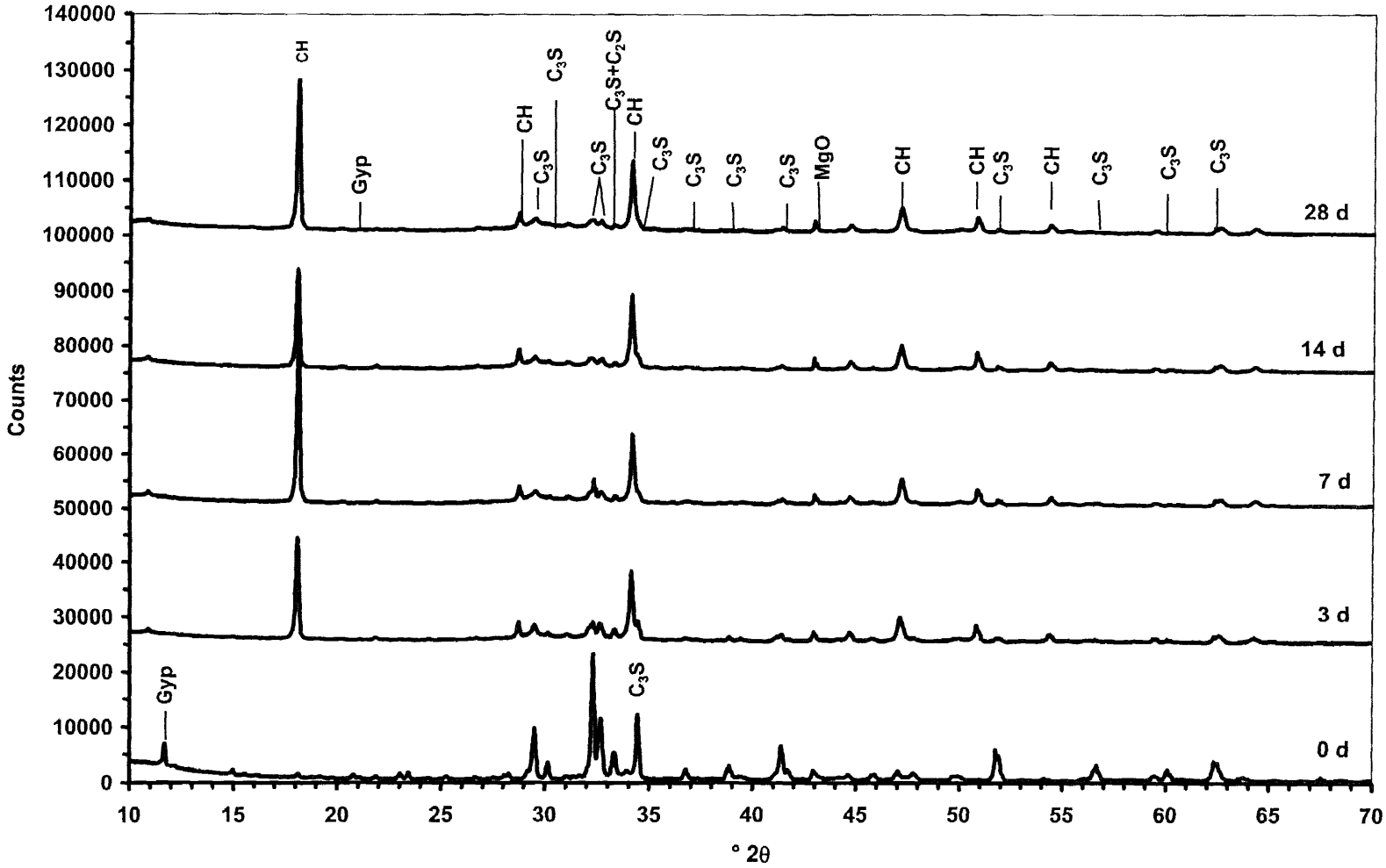

Figure 5.29 XRD Patterns of Cement Paste at Different Ages

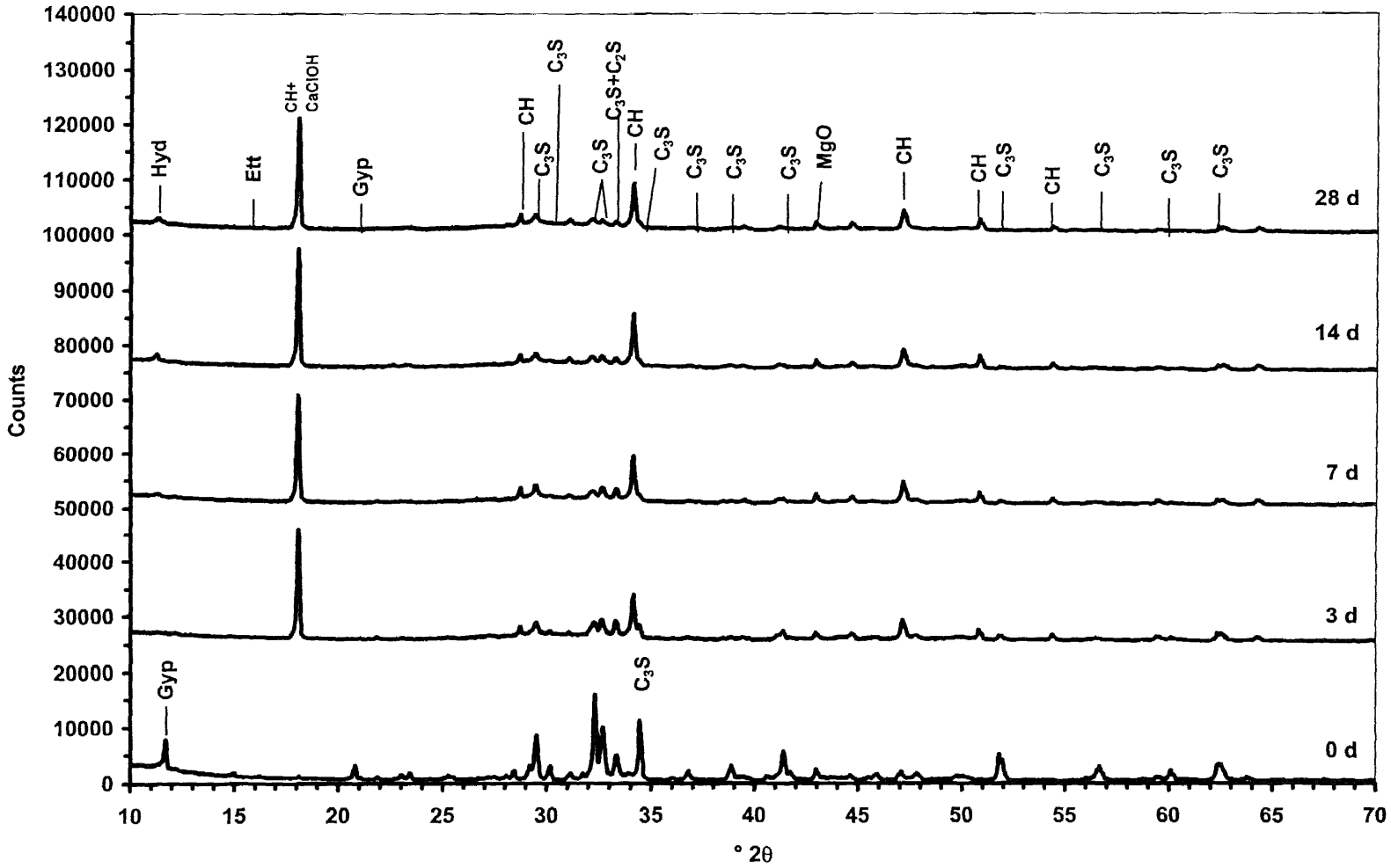

Figure 5.30 XRD Patterns of Cement Paste with 15% Raw MSWI Fly Ash (RW15) at Different Ages

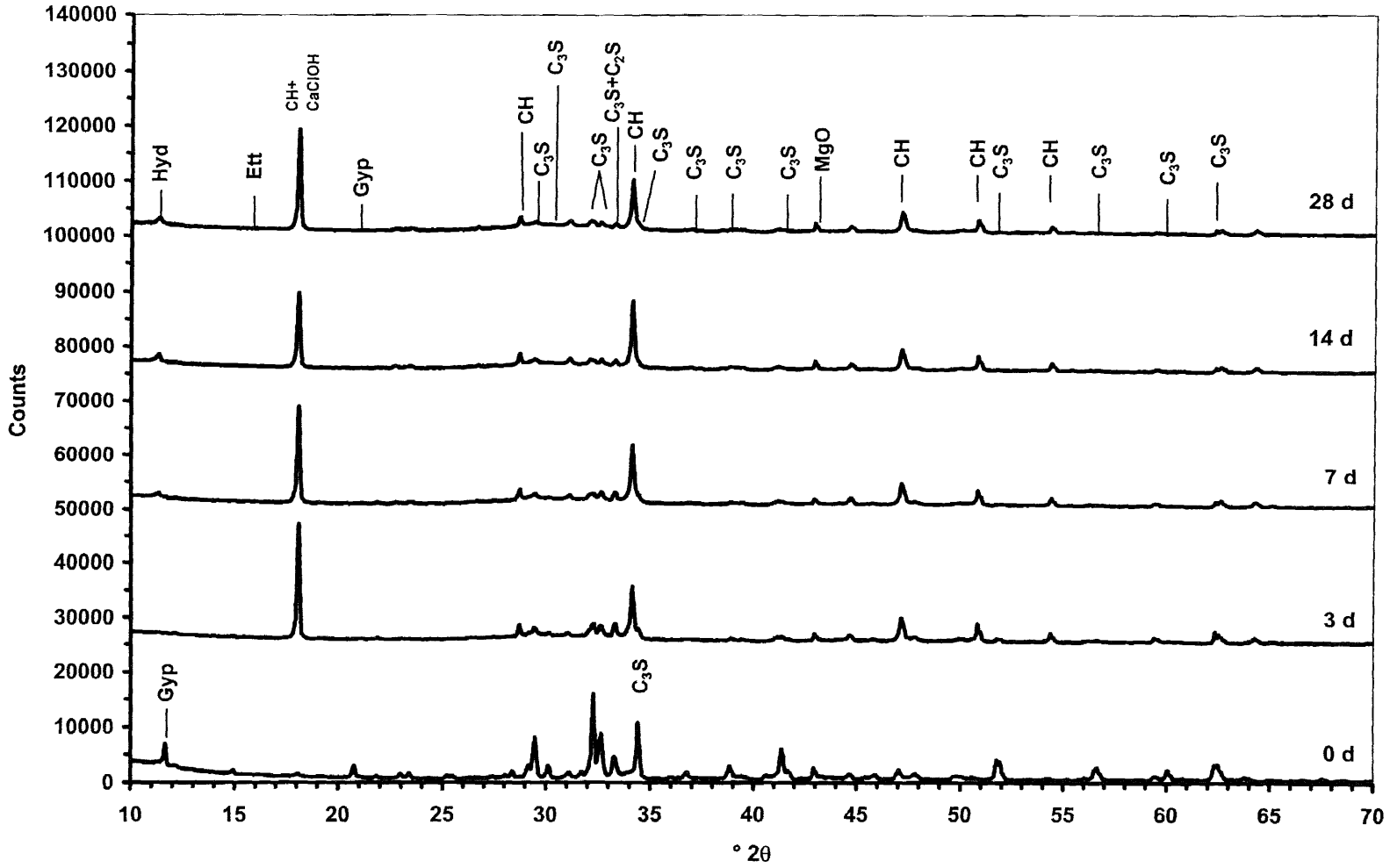

Figure 5.31 XRD Patterns of Cement Paste with 15% Fine MSWI Fly Ash (CY15) at Different Ages

Major phases identified in the diffractograms of cement and MSWI fly ash-cement pastes are C_3S, C_2S, $Ca(OH)_2$, periclase [MgO], and gypsum (Gyp or $CaSO_4.2H_2O$). Additional phases that appeared in the diffractograms of MSWI fly ash-cement pastes are halite [NaCl], sylvite [KCl], hydrocalumite [$C_3A.CaCl_2.10H_2O$], calcium chloride hydroxide [CaClOH], and calcium chloride hydroxide hydrate [$CaCl_2.Ca(OH)_2.H_2O$]. Apparently, these additional phases are major phases identified in the fine NJIT 2 MSWI fly ash in Section 5.3.1.

Figures 5.29 through 5.31 depict XRD patterns of cement paste, cement paste incorporating 15% raw MSWI fly ash (RW15), and cement paste incorporating 15% fine MSWI fly ash (CY15), respectively. Generally, at day 0, the XRD patterns of fly ash-cement pastes resemble that of cement paste although the characteristic peaks of cement component, i.e., C_3S are relatively smaller. This is true since 15% of cement was replaced by fly ashes. However, peaks that represent gypsum in both fly ash-cement pastes seem to be higher than that of pure cement. The additional gypsum was clearly from the MSWI fly ashes as reported by the XRD results in section 5.3.1. Interestingly, the patterns of both raw and fine fly ash pastes appear to be very similar. The reason for this is that the chemical compositions of raw and fine fly ashes are relatively identical (Sections 5.2 and 5.3) and that they were present in small quantities compared with those of cement. Therefore, their XRD patterns were inevitably dominated by characteristic peaks of cement components.

It is obvious in Figures 5.30 and 5.31 that the hydrocalumite peaks, marked by "hyd", increase in height as the pastes age. It was first detected on day 7 of raw and fine fly ash-cement pastes. Its development coincides with the compressive strength

development of MSWI fly-ash mortars. The role that hydrocalumite plays will be discussed in details in Section 5.10. Another change in the diffractograms is that of gypsum peaks which disappeared after day 0. Microscopic investigation in Section 5.8 shows evidence of ettringite [$C_3A.3CaSO_4.32H_2O$] in the pastes. It is very likely that gypsum reacted with tricalcium aluminate [C_3A] and water to form ettringite.

The whole scanned spectrums of diffractograms of cement paste and MSWI fly ash-cement pastes presented earlier were narrowed down to a specific range of angle, from 25 to 40 °2θ, for closer inspection in Figure 5.32 through 5.34.

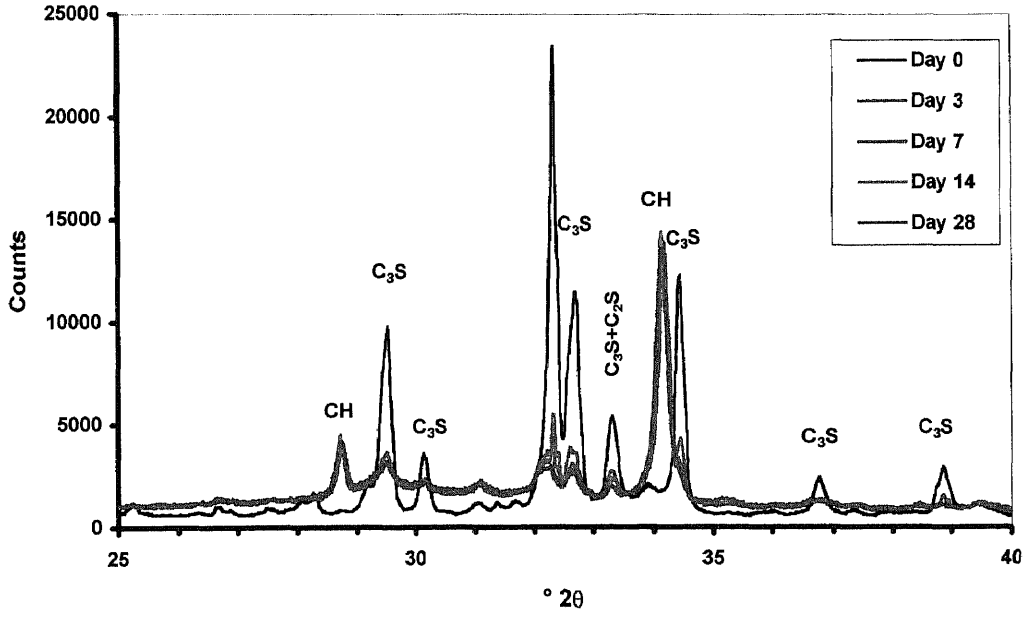

Figure 5.32 XRD Patterns of Cement Paste at 25-40°2θ

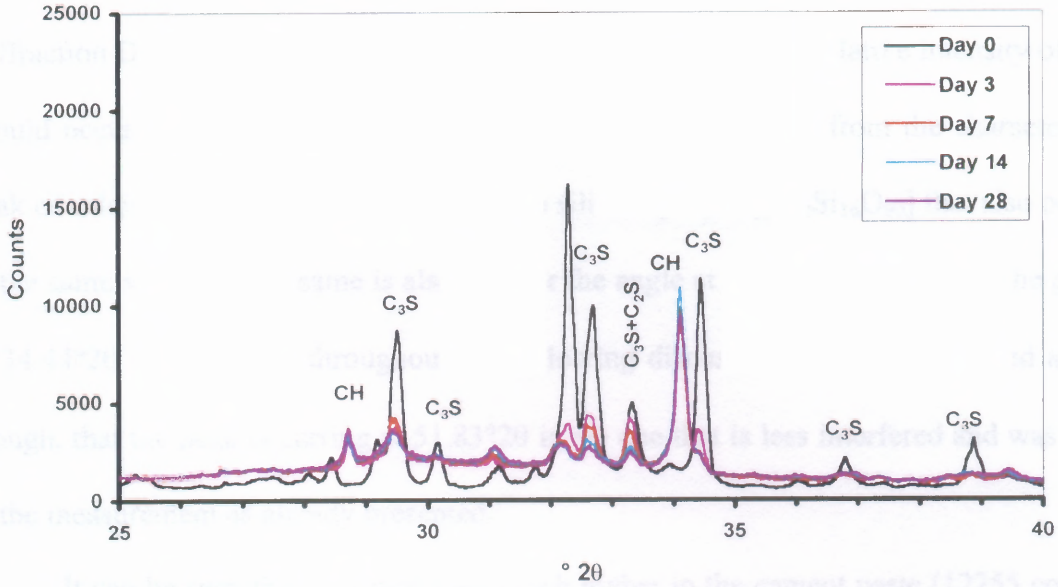

Figure 5.33 XRD Patterns of Cement Paste with 15% Raw Fly Ash (RW15) at 25-40°2θ

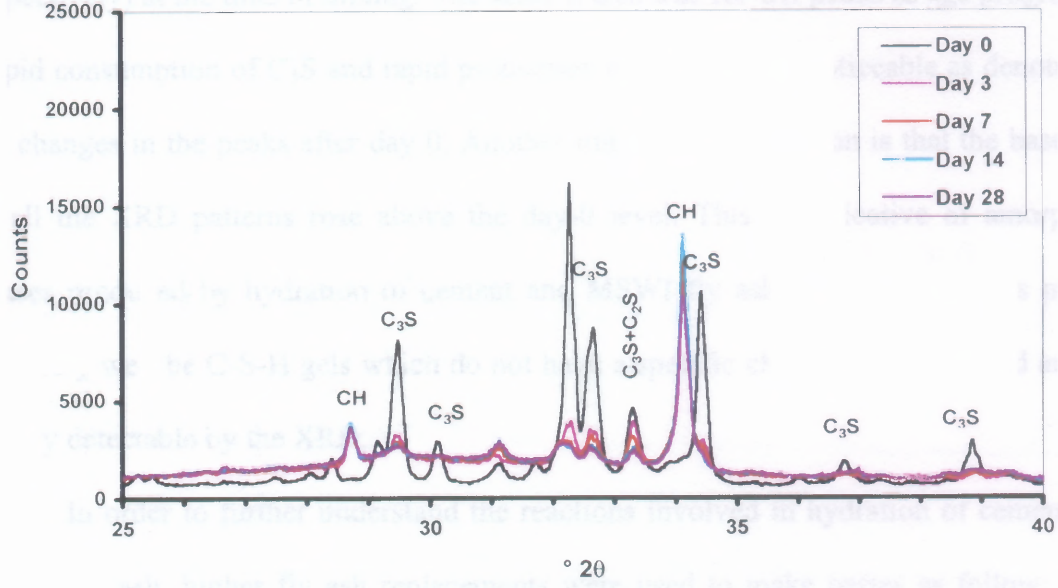

Figure 5.34 XRD Patterns of Cement Paste with 15% Fine Fly Ash (CY15) at 25-40°2θ

As seen in Figures 5.32 through 5.34, the diffractograms of the cement paste and the MSWI fly ash-cement pastes at day 0 show the highest peaks of C_3S at 32.28°2θ.

Nevertheless, according to the PDF-1 database from ICDD (International Centre for Diffraction Data), the characteristic peak corresponding to 100% relative intensity of C_3S should occur at 34.44°2θ. This is indeed due to the interference from the characteristic peak of calcium magnesium aluminum oxide silicate [$Ca_{54}MgAl_2Si_{16}O_{90}$] that also occurs in the same vicinity. The same is also true for the angle at 29.53°2θ. Therefore, the peaks at 34.44°2θ will be used throughout the following discussions. It must be noted again, though, that the peak occurring at 51.83°2θ is the one that is less interfered and was used in the measurement as already presented.

It can be seen that C_3S peaks are much higher in the cement paste (12255 counts) than in the raw and fine MSWI fly ash-cement pastes (11321 and 10588 counts, respectively) at the time of mixing. The same is also true for CH peaks as age progressed. Rapid consumption of C_3S and rapid production of CH are also noticeable as denoted by the changes in the peaks after day 0. Another important observation is that the baselines of all the XRD patterns rose above the day-0 level. This is indicative of amorphous phases produced by hydration of cement and MSWI fly ash. These amorphous phases may very well be C-S-H gels which do not have a specific chemical formula and are not readily detectable by the XRD.

In order to further understand the reactions involved in hydration of cement and MSWI fly ash, higher fly ash replacements were used to make pastes as follow: 35%, 50%, and 100%. Their diffractograms are shown in Figures 5.35 through 5.37.

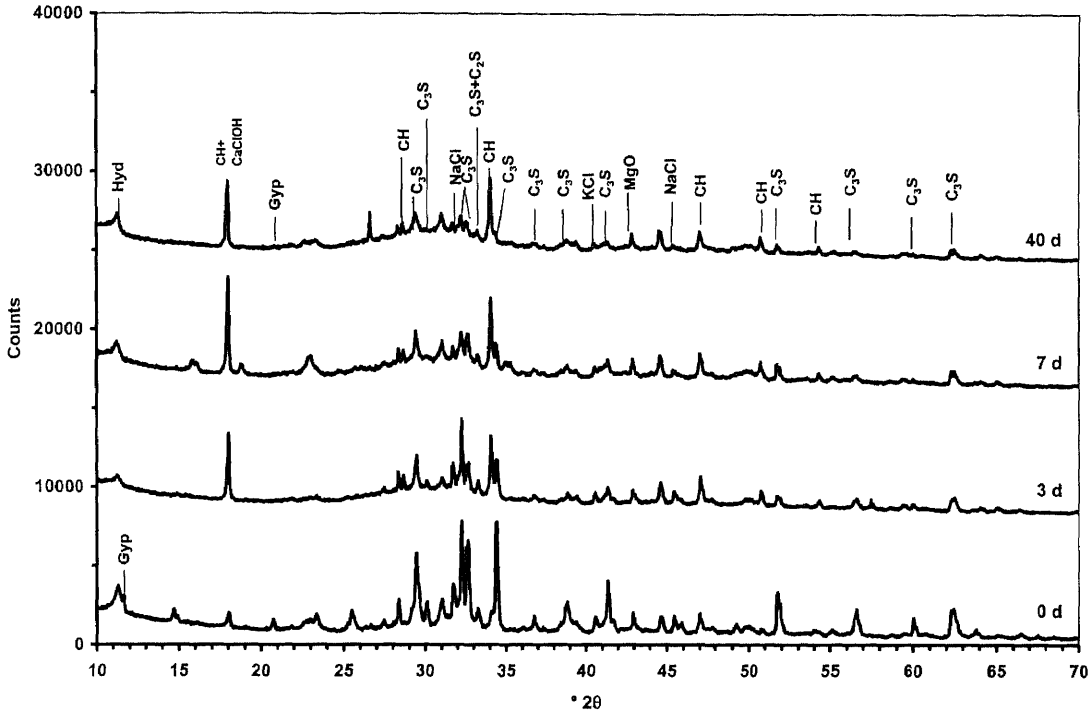

Figure 5.35 XRD Patterns of Cement Paste with 35% Fine MSWI Fly Ash (CY35) at Different Ages

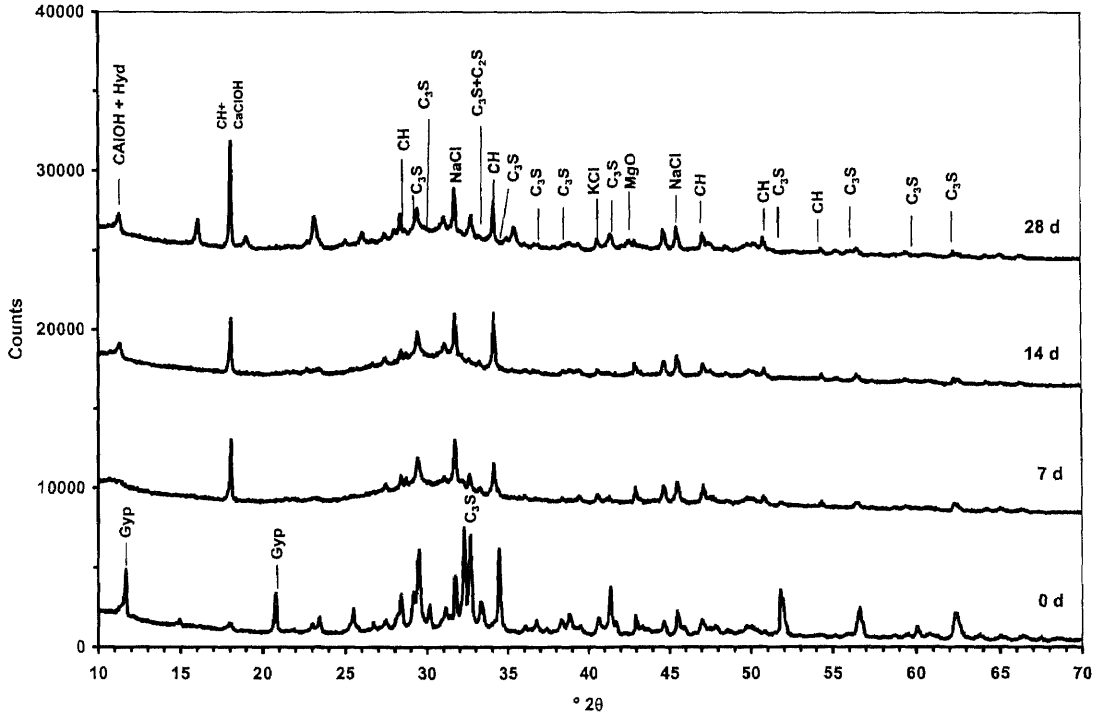

Figure 5.36 XRD Patterns of Cement Paste with 50% Fine MSWI Fly Ash (CY50) at Different Ages

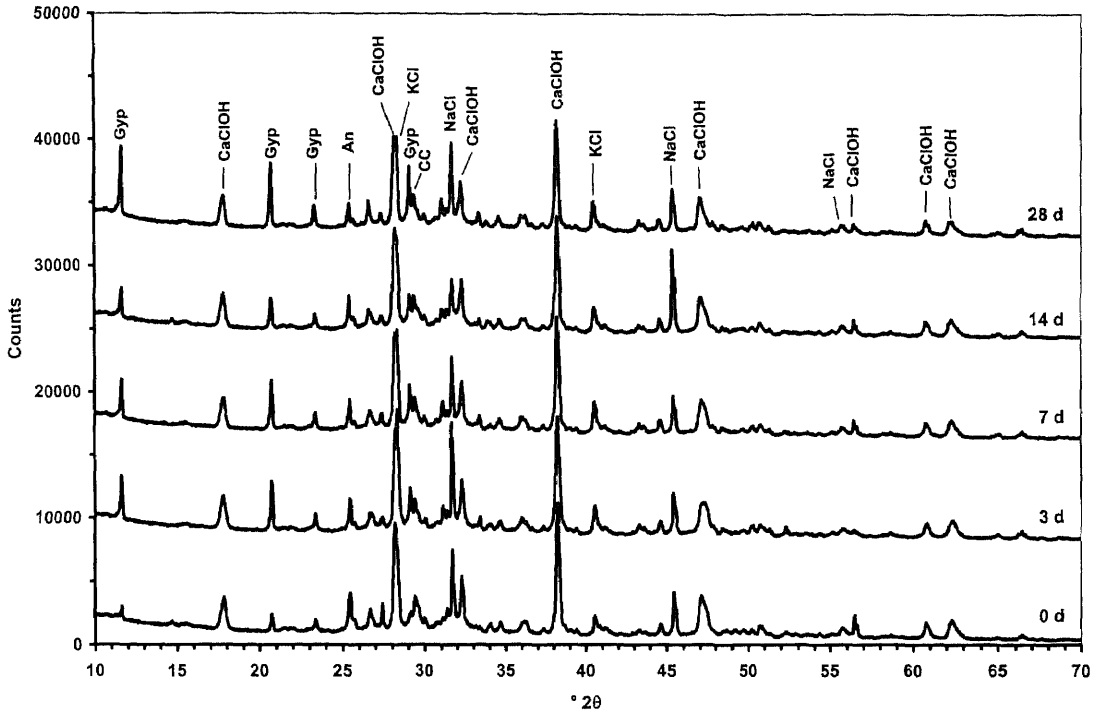

Figure 5.37 XRD Patterns of Fine MSWI Fly Ash Paste (CY100) at Different Ages

Diffraction patterns of cement paste with its content partially replaced by MSWI fly ash show higher peaks for NaCl in 50% fly ash-cement paste (CY50), 4343 counts at day 0 (31.78°2θ), than in 35% fly ash-cement paste (CY35), 3588 counts at day 0 (31.78°2θ). It is interesting to see that the peak heights of NaCl at 31.78°2θ of CY35 slightly decreased from 3588 to 2540 counts as the paste was maturing, while those of CY50 stayed the same at approximately 4000 counts. The absence of NaCl peaks is observed in RW15 as well as in CY15 pastes. The presence of small amounts of NaCl in those pastes may be involved in reactions that produced phases that are not detectable by the XRD. As more cement was replaced, C_3S peaks seem to be reduced in height. Most of C_3S was consumed during the first 3 days shown by rapid reduction of C_3S peaks. The hydration product, $Ca(OH)_2$, in turn, increased as C_3S decreased.

Pure MSWI fly ash paste (CY100) did not solidify throughout the experiment. Its XRD patterns are virtually unchanged although increase in gypsum [$CaSO_4.2H_2O$] was detected as the paste matured. This can be explained by the reduction in anhydrite [$CaSO_4$] peaks as it was being hydrated. High contents of CaClOH, $CaCl_2.Ca(OH)_2.H_2O$, and NaCl are consistent with those of dry fine MSWI fly ash in Section 5.3.2.

One important observation is the hydrocalumite [$C_3A.CaCl_2.10H_2O$] peak. It was not detected in the XRD patterns of RW15 and CY15 until day 7. On the contrary, it was detected as early as day 0 in the XRD pattern of CY35 although it took as many as 14 days to appear in the pattern of CY50. It was not at all detected in that of pure fine fly ash paste (CY100). The reason for this may be due to the fact that the formation of $C_3A.CaCl_2.10H_2O$ requires both C_3A from cement and $CaCl_2$ from the fly ash. It took longer to form if one component was not enough. In the case of 15% MSWI fly ash pastes, the amount of $CaCl_2$ from fly ash might be not be enough and C_3A reacted with available gypsum [$CaSO_4.2H_2O$] to form calcium aluminosilicates, such as ettringite. However, when there was more $CaCl_2$ and gypsum in the paste in CY50, C_3A might preferably form ettringite instead of $C_3A.CaCl_2.10H_2O$ as seen in the disappearance of gypsum after day 0 (Figure 5.36).

Closer inspection on the XRD patterns of CY35 and CY50 can be done by focusing on a specific range of the angle as shown in Figures 5.38 and 5.39. This selected spectrum shows noticeable rise in intensity baseline. Moreover, amorphous C-S-H gels show strong peaks within this range of angle.

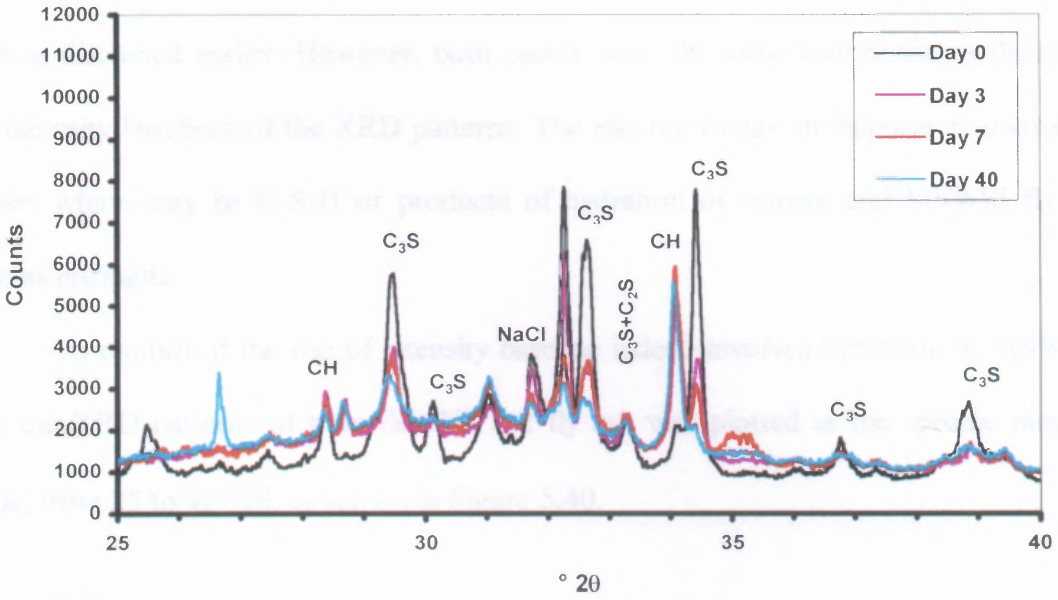

Figure 5.38 XRD Patterns of Cement Paste with 35% Fine Fly Ash (CY35) at 25-40°2θ

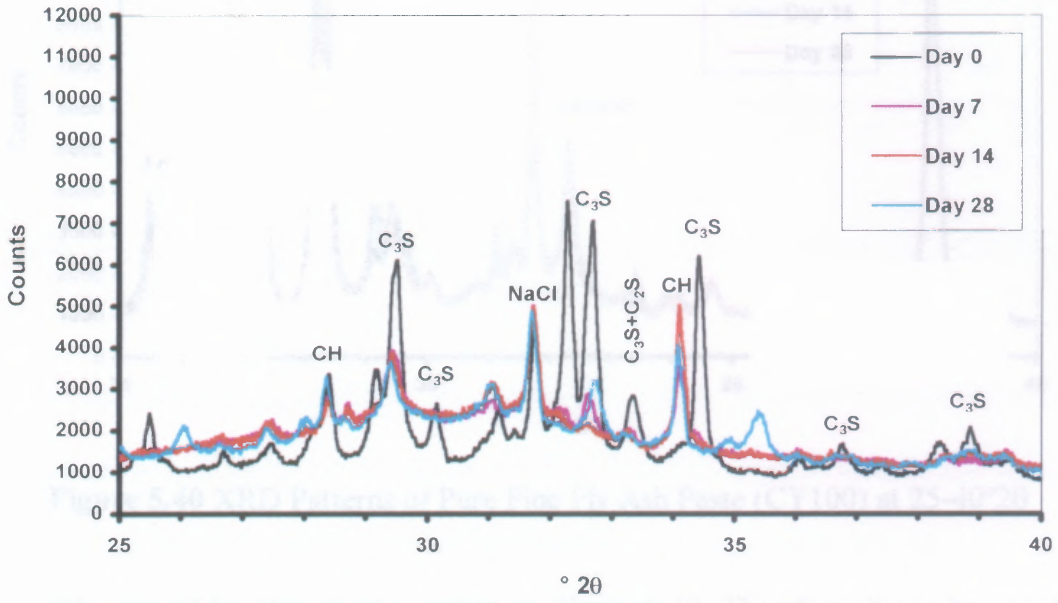

Figure 5.39 XRD Patterns of Cement Paste with 50% Fine Fly Ash (CY50) at 25-40°2θ

Figure 5.38 shows slightly higher C_3S peaks (7779 counts) than in Figure 5.39 (6194 counts) at day 0 since the CY35 paste incorporated 15% more cement. The same

explanation applies to NaCl peak that is noticeably higher in Figure 5.39 than in Figure 5.38 as discussed earlier. However, both pastes share the same feature that is the rise in the intensity baselines of the XRD patterns. The rise represents an increase in amorphous phases which may be C-S-H or products of hydration of cement and MSWSI fly ash, such as ettringite.

To confirm if the rise of intensity baseline indeed involves hydration of MSWI fly ash, the XRD patterns of pure fine NJIT 2 fly ash was plotted at the specific range of angle, from 25 to 40 °2θ, as shown in Figure 5.40.

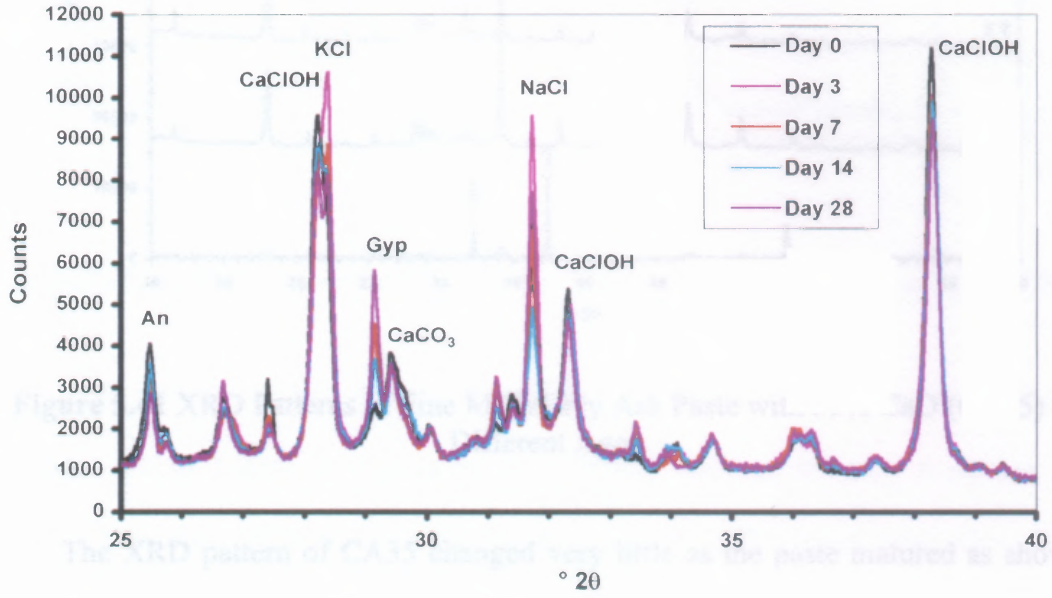

Figure 5.40 XRD Patterns of Pure Fine Fly Ash Paste (CY100) at 25-40°2θ

The rise of baseline is not evident in Figure 5.40. Therefore, it can be concluded that the increase in amorphous phases in MSWI fly ash-cement paste is caused by hydration of the cement components. Reactions between cement and MSWI fly ash components may not be totally ruled out although less contribution is expected.

The role of MSWI fly ash on hydration of fly ash-cement paste was explored further when a paste was prepared from 35% CaO and 65% fine fly ash. Its diffractograms is illustrated in Figures 5.41 and 5.42.

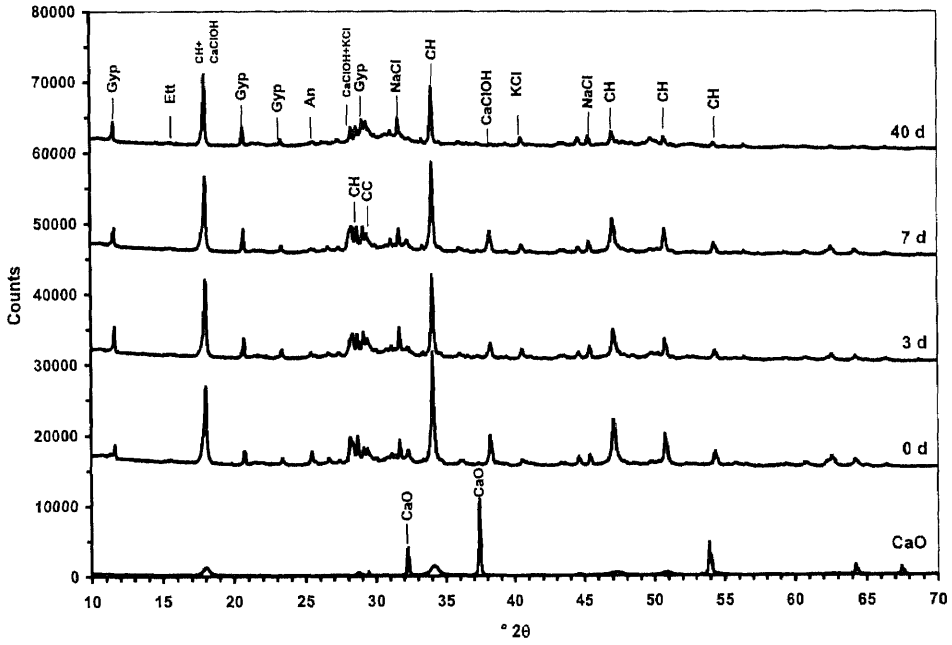

Figure 5.41 XRD Patterns of Fine MSWI Fly Ash Paste with 35% CaO (CA35) at Different Ages

The XRD pattern of CA35 changed very little as the paste matured as shown in Figure 5.41. It appears that CaO was hydrated to $Ca(OH)_2$ as soon as the paste was being prepared. Anhydrite [$CaSO_4$] was also converted to gypsum [$CaSO_4.2H_2O$].

Closer examination of Figure 5.42 reveals decreasing $Ca(OH)_2$ and CaClOH contents but increasing $CaSO_4.2H_2O$, and $CaCO_3$ contents. The disappearance of $Ca(OH)_2$ may be indicative of pozzolanic reaction that involves the production of C-S-H from alkali, amorphous silica, and/or alumina in the fly ash (Al_2O_3, 3.4%; CaO, 40.18%;

SiO_2, 4.54%). The rise of intensity baseline also supports that the amorphous content had indeed increased.

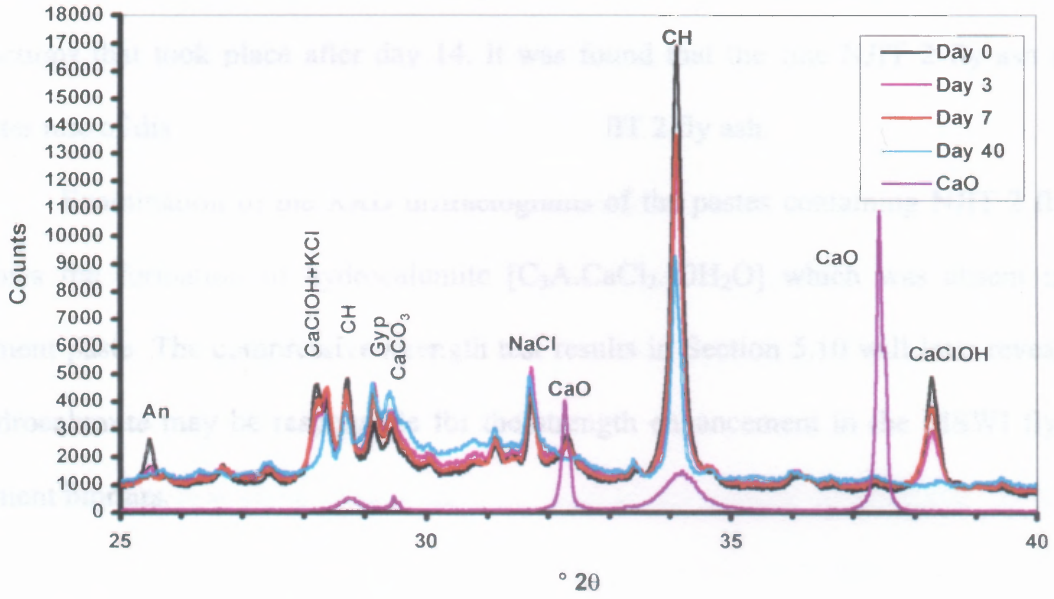

Figure 5.42 XRD Patterns of Cement Paste with 35% CaO (CA35) at 25-40 °2θ

After a rapid reaction starting from day 0, hydration of anhydrite ($CaSO_4$) seems to be over within 3 days as evident by its relatively constant intensity from day 3 and beyond. This also corresponds with the decrease in $CaSO_4$ peak intensities. On the contrary, the increase in $CaCO_3$ that was caused by carbonation of CaO and $Ca(OH)_2$ still proceeded even till later age of 40 days.

In summary, it is evident from the experiments that NJIT 2 fly ash is not a self-cementitious material. Its inclusion in cement paste retarded the hydration process during the initial period of 7 days. However, after that, the pastes containing 15% NJIT fly ashes continued to be hydrated and reached the steady state as the cement paste did.

Monitoring of CH changes in NJIT 2 fly ash-cement pastes by means of XRD analysis reveals that CH was produced rapidly by hydration during the same period as cement although the level of CH was reflected by the amount of Ca in the pastes. The initial production of CH was followed by consumption of CH, probably by the pozzolanic reactions that took place after day 14. It was found that the fine NJIT 2 fly ash had a faster rate of disappearance of CH than the raw NJIT 2 fly ash.

Examination of the XRD diffractograms of the pastes containing NJIT 2 fly ash shows the formation of hydrocalumite [$C_3A.CaCl_2.10H_2O$] which was absent in the cement paste. The compressive strength test results in Section 5.10 will later reveal that hydrocalumite may be responsible for the strength enhancement in the MSWI fly ash-cement mortars.

5.8 Examination on MSWI Fly Ash-Cement Paste Microstructures

Hardened cement paste is the result of hydration reactions that start as soon as dry portland cement is mixed with water. Microstructure of hardened cement paste is controlled by various parameters: particle size distribution, composition of cement, morphology of individual hydration products, and age of the paste (Ahmed and Struble, 1995). The microstructure, in turn, determines mechanical properties, such as strength.

At the microstructure level, hardened cement paste is an inhomogeneous mixture of a variety of crystalline and quasi-crystalline phases and pores of different sizes and shapes. Two principal hydration products are calcium silicate hydrate [C-S-H] and calcium hydroxide [$Ca(OH)_2$ or CH]. C-S-H, a highly disordered quasi-crystalline material of variable composition, takes up most of the volume in the paste. Its layered molecular structure has high internal porosity. In contrast to C-S-H, CH has a fixed composition and a highly crystalline structure. The CH crystals can grow from thin hexagonal layered platelets to massive blocks as the paste becomes mature. Although the paste is well hydrated, unhydrated cement grains should still be visible.

In MSWI fly ash-cement systems, more complex microstructures consisting of those of cement hydration products, fly ash hydration products, and, possibly, reaction products between cement and fly ash are to be expected. The results from XRD analyses in Section 5.3 will be used to identify most of the distinct structures, such as CaClOH (calcium chloride hydroxide), $CaCl_2.Ca(OH)_2.H_2O$ (calcium chloride hydroxide hydrate), and hydrocalumite, $C_3A.CaCl_2.10H_2O$ (where C=CaO and $A=Al_2O_3$).

5.8.1 24 to 72 Hours

Two major components of ordinary portland Type I cement are tricalcium silicate [C_3S] and dicalcium silicate [C_2S], which represent approximately 55% and 20% of cement, respectively. Hydration of both components, as previously discussed in Section 5.7, yields the same products, C-S-H and CH, as those of C_3S. However, the number of mole of CH produced and the reaction rate are much lower in the C_2S hydration. It is, therefore, valid to describe the reaction process of cement hydration based on that of the principal component, [C_3S].

Normally, the hydration of C_3S takes place in five distinct stages. When first mixed with water, a period of rapid evolution of heat occurs in stage 1 and stops within about 15 minutes. Stage 2 is marked by a period of inactivity which is the reason why portland cement concrete remains in plastic state for 2 to 4 hours. At the end of the dormant period, initial set occurs because of the rapid hydration of C_3S. The reaction reaches the maximum rate at the end of the acceleration period within 4 to 8 hours (stage 3). By this time final set has been passed and early hardening has begun. Then, in stage 4, the rate of reaction slows down until it reaches a steady state (stage 5) within 24 hours (Mindess and Young, 1981).

Another reaction occurring during hydration of cement is the hydration of C_3A (where A is Al_2O_3) in the presence of gypsum. Although it is usually present at lower quantity in Type I cement (approximately 7-10%), the reaction rate is the highest associated with the highest heat evolution. Ettringite [$C_3A.3CaSO_4.32H_2O$] is produced during the first 24 hours or as long as there is an ample supply of sulfate available. If the

entire sulfate is consumed before C_3A has completely hydrated, ettringite is then converted to monosulfoaluminate [$C_3A.CaSO_4.12H_2O$] (Mindess and Young, 1981).

Apparently, rapid formation of the hydration products, C-S-H, CH and ettringite, stops within one day. The reactions, however, still evolves at a much lower rate for as long as one year. As for MSWI fly ash-cement pastes, once the reactive cement components are replaced by MSWI fly ash, the hydration reactions may be retarded by some of several chemical compounds, such as $ZnCl_2$, in the fly ash. Thus, fewer hydration products should be observed in the pastes containing MSWI fly ash.

5.8.1.1 Pure Cement Paste: Crystallization of the hydration products, C-S-H and CH, begins after the dormant period that is caused by the need to achieve certain concentration of ions. C-S-H develops at the surface of cement grains and forms a coating covering the cement grains while CH develops in vacant space in the pores. Ettringite is also formed from the hydration of tricalcium aluminate [C_3A] and gypsun [$CaSO_4.2H_2O$]. A summary of properties of the hydration products is provided in Table 5.14.

Table 5.14 Properties of Hydration Products of Portland Cement

Compound	Crystallinity	Morphology in Pastes	Typical Crystal Dimensions in Pastes
C-S-H	Very poor	Spines; unresolved morphology	1 x 0.1 μm x less than 0.01 μm
CH	Very good	Nonporous striated material	0.01 to 0.1 mm
Ettringite	Good	Long slender prismatic needles	10 x 0.5 μm
Monosulfo-aluminate	Fair-good	Thin hexagonal plates; irregular rosettes	1 x 1x 0.1 μm

Note: From Mindess and Young (1981)

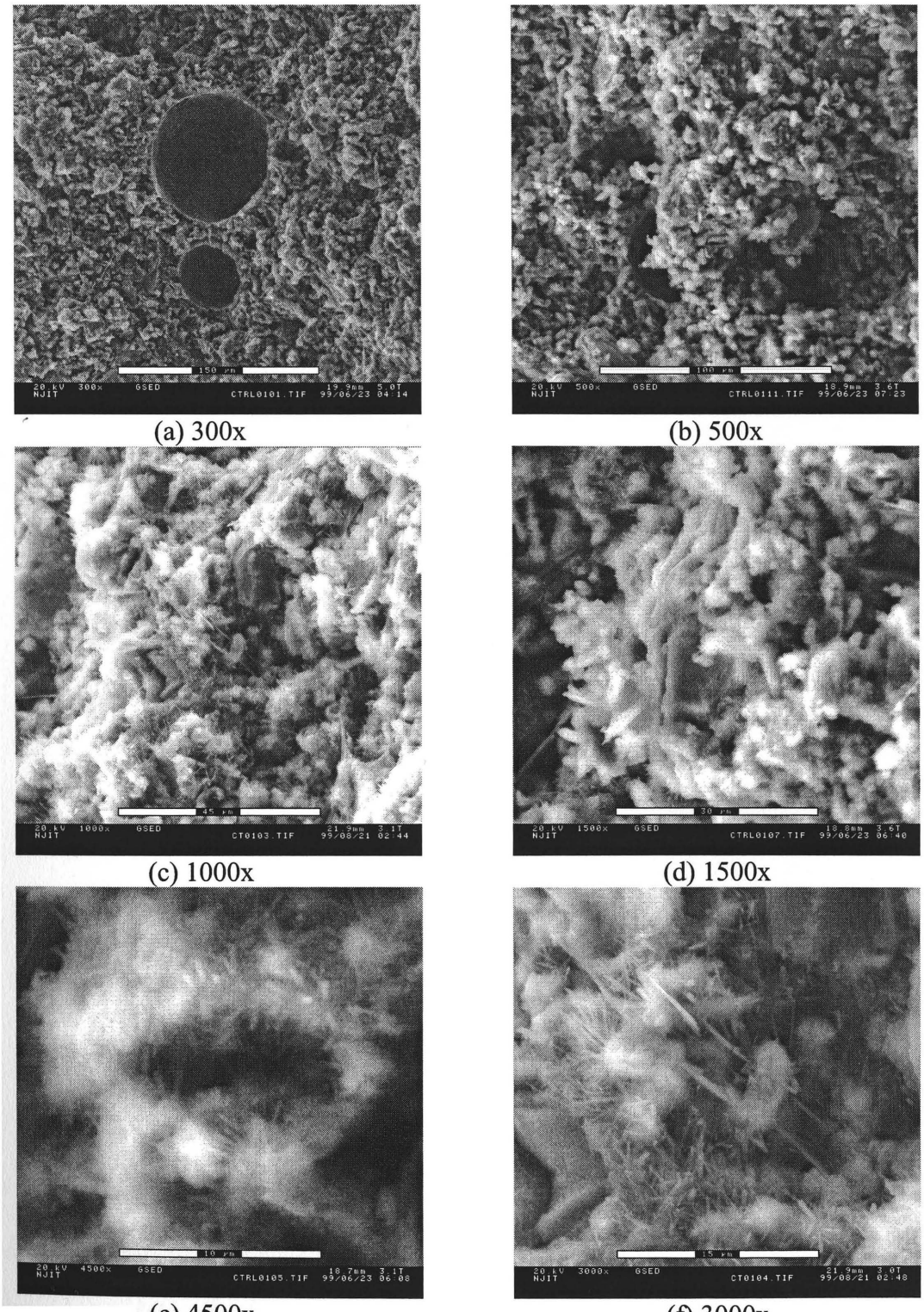

(a) 300x (b) 500x

(c) 1000x (d) 1500x

(e) 4500x (f) 3000x

Figure 5.43 Micrographs of Cement Paste after 24 and 72 Hours

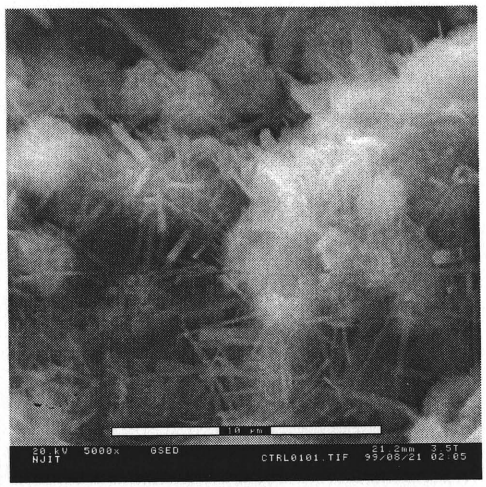

(g) 5000x

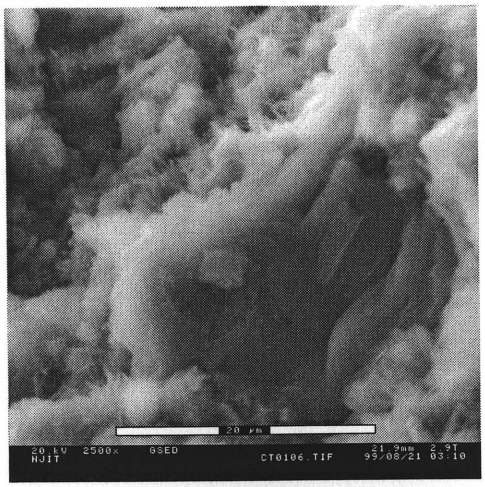

(h) 2500x

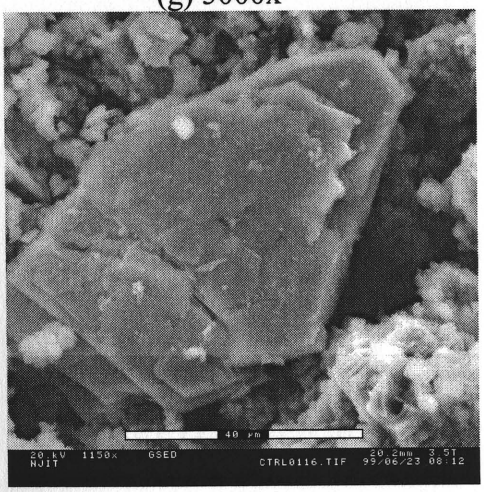

(i) 1150x

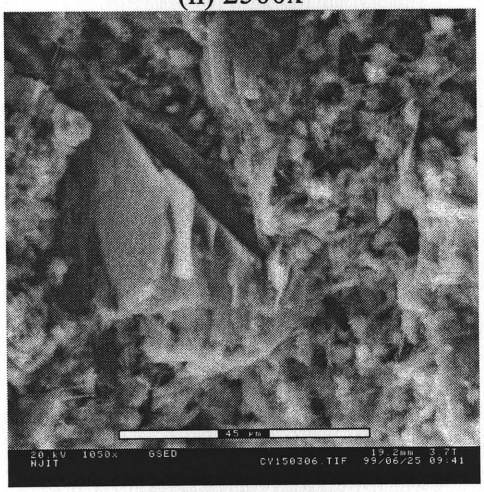

(j) Day 3, 1050x

Figure 5.43 Micrographs of Cement Paste after 24 and 72 Hours (Continued)

Figures 5.43 (a) through (j) illustrate the microstructures of hydrated cement paste at the early ages of 24 to 72 hours. At the time of mixing, water dispersed cement grains apart and remained in the capillary pores until solid hydration products form a continuous matrix and bind the residual cement grains together. However, large air voids are still present as shown in Figures 5.43 (a) and (b). Using Table 5.14 as a reference, four types of morphology stand out. First, irregularly shaped unhydrated cement grains, as those shown in Section 5.6, can be seen in Figures 5.43 (a) through (c). Second, hydration

product identified as C-S-H appears as a spiny coating that covers the cement grains. The spines are seen as pointed, flat, blunt, long, and thin since they do not have a unique morphology. Third, another hydration product, $Ca(OH)_2$, appears as dense blocks in Figures 5.43 (i) and (j). CH crystals can occupy about 20 to 25% of the paste volume. The crystals often engulf cement grains, thereby increasing their effective volume in the paste. Lastly, another long needle-like structures seen in Figures 5.43 (c) and (f) are ettringite [$Ca_6Al_2(SO_4)_3(OH)_{12}.26H_2O$], a calcium sulfoaluminate hydrate compound that crystallized as long slender needle-like hexagonal prisms. Ettringite is a stable hydration product only while there is an ample supply of sulfate available. That is why there was no monosulfoaluminate observed in the young paste.

Table 5.15 Semi-quantitative Surface Compositions of Objects in Selected Acquired Images in Figure 5.43

Element	(b)		(d)		(e)		(i)	
	Wt%	At%	Wt%	At%	Wt%	At%	Wt%	At%
O	28.31	51.33	32.67	55.04	31.69	54.26	54.25	74.12
Na	1.91	2.41	2.38	2.79	2.18	2.59	4.26	4.05
Mg	1.22	1.46	1.57	1.75	1.37	1.54	0.73	0.66
Al	2.44	2.62	2.48	2.48	2.57	2.61	3.68	2.98
Si	6.80	7.02	7.83	7.51	7.87	7.68	4.95	3.85
P	1.26	1.18	1.28	1.11	1.16	1.03	2.40	1.69
S	3.14	2.84	3.30	2.77	2.72	2.32	1.06	0.72
Cl	0.84	0.69	0.81	0.62	0.97	0.75	1.02	0.63
K	5.93	4.40	5.26	3.63	4.84	3.39	0.70	0.39
Ca	25.90	18.75	25.26	16.99	26.11	17.85	14.80	8.07
Ti	0.00	0.00	0.00	0.00	0.00	0.00	0.00	0.00
Cr	1.01	0.56	0.87	0.45	0.93	0.49	0.13	0.06
Mn	0.78	0.41	0.83	0.41	0.86	0.43	0.12	0.05
Fe	1.75	0.91	1.40	0.68	1.66	0.82	0.09	0.03
Cu	2.16	0.98	1.42	0.60	1.87	0.81	0.06	0.02
Zn	1.85	0.82	1.51	0.62	1.76	0.74	0.03	0.01
As	1.48	0.57	1.28	0.46	1.37	0.50	5.99	1.75
Cd	1.84	0.48	2.08	0.50	1.85	0.45	0.95	0.18

Table 5.15 Semi-quantitative Surface Compositions of Objects in Selected Acquired Images in Figure 5.43 (Continued)

Element	(b)		(d)		(e)		(i)	
	Wt%	At%	Wt%	At%	Wt%	At%	Wt%	At%
Sn	1.84	0.45	1.28	0.29	1.48	0.34	0.38	0.07
Sb	7.97	1.90	5.06	1.12	5.41	1.22	2.88	0.52
Pb	1.57	0.22	1.43	0.18	1.33	0.18	1.52	0.15
Total	100.00	100.00	100.00	100.00	100.00	100.00	100.00	100.00
Ca:Si	2.67:1.00		2.26:1.00		2.32:1.00		2.10:1.00	

The EDX was used exclusively to analyze for the elemental compositions of the microstructures in fracture surfaces of the cement paste in selected images. Table 5.15 lists the Semi-quantitative surface elemental compositions of the microstructures in Figures 5.43 (b), (d), (e), and (i). It should be noted that the results are provided in both weight percent (Wt%) as well as atomic percent (At%) which is the normalized ratio of weight percent of a particular element to its atomic weight. The atomic percentage can be used to empirically identify a microstructure by comparing a ratio of elements to the chemical formula of the phase of interest. For instance, $Ca(OH)_2$ is expected to have an atomic ratio between Ca and O of 1 to 2.

Evidently, the compositions of the microstructures in Figures 5.43 (b), (d), and (e) are quite similar, with Ca being the most abundant element, besides O which should be in the majority of the compounds. As previously discussed in Section 5.3, major phases identified by the XRD in the cement paste are $Ca(OH)_2$ and C_3S [$3CaO.SiO_2$] which has an atomic ratio of Ca:Si of 3 to 1. A poorly crystalline C-S-H [$3CaO.2SiO_2.3H_2O$] has variable compositions which are estimated to have an atomic ratio of Ca to Si of 0.8 to 2.0 (Lea, 1971). The reported atomic percentages and the distinct morphologies of these

phases seem to confirm their presence. However, in Figure 5.43 (i), the platy block and the overwhelming amount of O indicate that the block is indeed $Ca(OH)_2$.

In Section 5.6, EDX results for dry grains of portland cement Type I show high Ca-to-Si ratios of more than 4.11:1.00 which reflect other calcium compounds beside C_3S. One of such compounds is $CaSO_4.2H_2O$.

5.8.1.2 Raw MSWI Fly Ash-Cement Paste: The cement paste containing 15% raw MSWI fly ash shares common major phases, $Ca(OH)_2$ and C_3S, as the pure cement paste. Another major phase that is also present in the paste is CaClOH as indicated by the XRD analysis result in Section 5.3.1. Large spherical MSWI fly ash particles can be seen in Figures 5.44 (a) and (b) while objects with indeterminate structure are present in Figures 5.44 (c) (as indicated by an arrow) and (d). According to the semi-quantitative EDX result, these objects have very high concentrations of Na, K, Ca, and Cl. The phase identification of this structure may not be possible due to its poorly crystalline form.

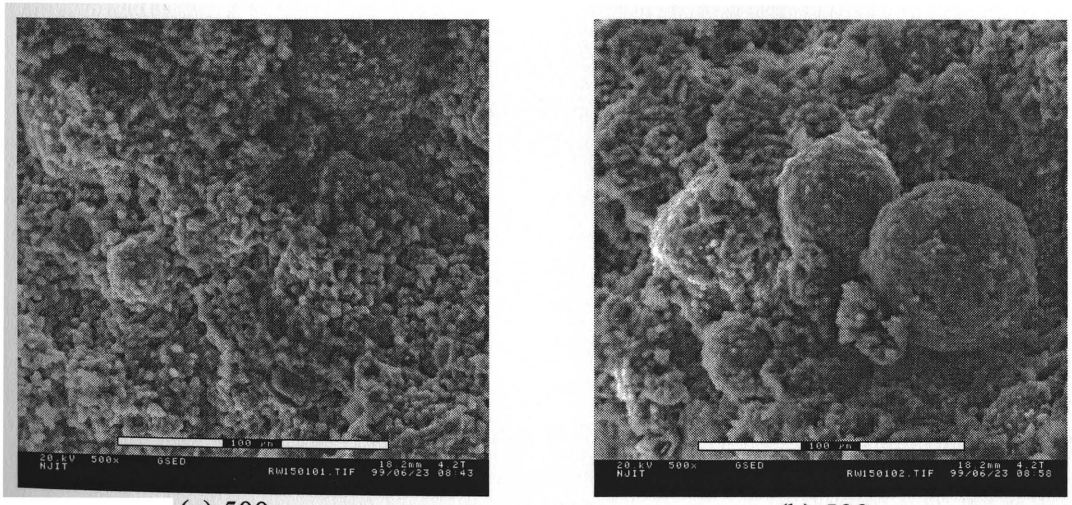

(a) 500x (b) 500x

Figure 5.44 Micrographs of 15% Raw MSWI Fly Ash Paste after 24 Hours

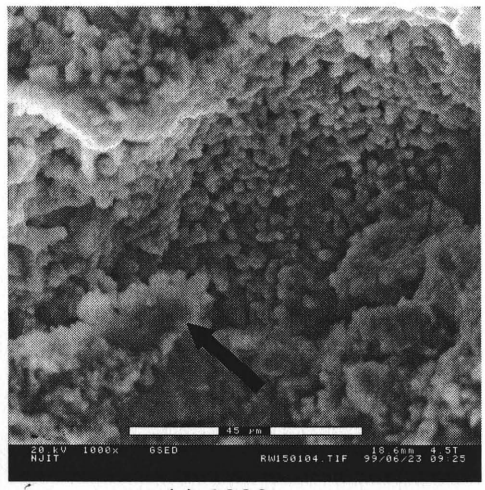

(c) 1000x

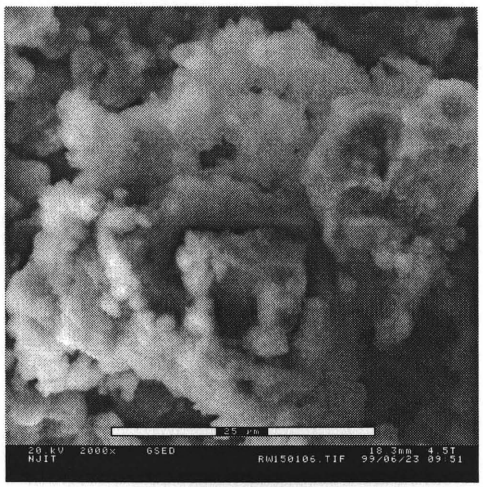

(d) 2000x

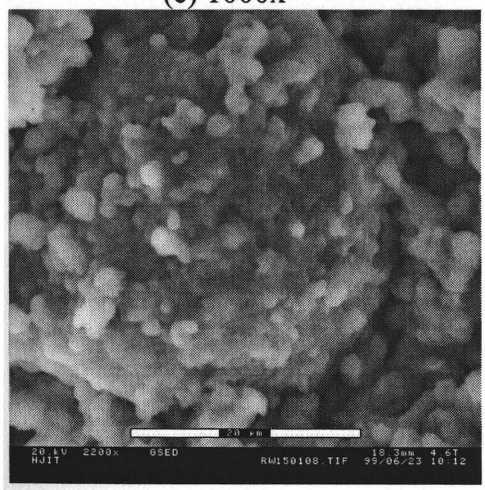

(e) 2200x

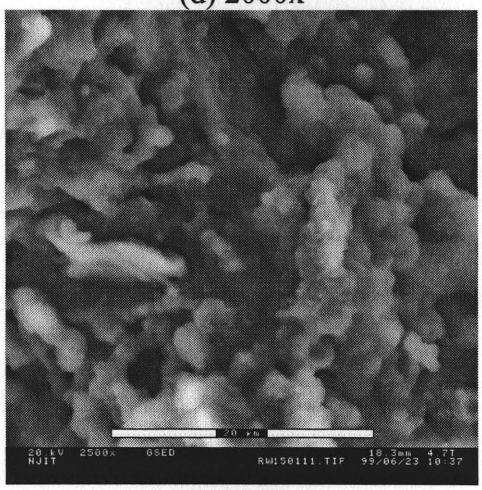

(f) 2500x

Figure 5.44 Micrographs of 15% Raw MSWI Fly Ash Paste after 24 Hours (Continued)

Table 5.16 Semi-quantitative Surface Compositions of Objects in Selected Acquired Images in Figure 5.44

Element	(a)		(b)		(d)		(e)	
	Wt%	At%	Wt%	At%	Wt%	At%	Wt%	At%
O	14.93	31.23	21.01	41.02	22.05	42.87	8.57	20.56
Na	2.61	3.79	3.31	4.49	1.85	2.51	1.57	2.62
Mg	1.17	1.62	0.63	0.81	0.90	1.15	0.89	1.41
Al	1.84	2.28	2.11	2.44	1.91	2.20	1.60	2.28
Si	4.45	5.30	4.51	5.01	5.64	6.24	2.70	3.69
P	1.33	1.44	1.25	1.26	1.47	1.48	1.03	1.28
S	1.64	1.71	1.65	1.61	1.36	1.32	0.96	1.15
Cl	16.13	15.23	13.34	11.75	9.20	8.07	20.76	22.50
K	14.25	12.20	8.93	7.13	6.89	5.48	16.95	16.63

Table 5.16 Semi-quantitative Surface Compositions of Objects in Selected Acquired Images in Figure 5.44 (Continued)

Element	(a)		(b)		(d)		(e)	
	Wt%	At%	Wt%	At%	Wt%	At%	Wt%	At%
Ca	19.63	16.39	20.95	16.33	26.83	20.82	13.44	12.88
Ti	0.00	0.00	0.00	0.00	0.00	0.00	0.00	0.00
Cr	0.97	0.62	0.89	0.54	1.02	0.61	1.23	0.91
Mn	1.15	0.70	0.96	0.55	1.13	0.64	1.59	1.11
Fe	2.47	1.48	2.18	1.22	1.85	1.03	2.67	1.84
Cu	2.79	1.47	2.17	1.06	1.63	0.80	5.49	3.32
Zn	2.33	1.19	2.06	0.98	2.40	1.14	5.59	3.29
As	1.22	0.55	2.23	0.93	2.01	0.83	0.81	0.42
Cd	1.74	0.52	2.47	0.68	1.93	0.54	2.32	0.79
Sn	1.15	0.33	1.42	0.37	1.10	0.29	2.13	0.69
Sb	5.68	1.56	5.88	1.51	6.37	1.63	6.37	2.01
Pb	2.52	0.38	2.05	0.31	2.46	0.35	3.33	0.62
Total	100.00	100.00	100.00	100.00	100.00	100.00	100.00	100.00
Ca:Si	3.09:1.00		3.26:1.00		3.34:1.00		3.49:1.00	
Ca:Cl	1.08:1.00		1.39:1.00		2.58:1.00		0.57:1.00	

Generally, as illustrated in Table 5.16, concentrations of heavy metals, such as Cr, Mn, Fe, Cu, Zn, and Pb appear to increase as a result of the addition of raw MSWI fly ash.

Upon comparing the microstructures of the raw fly ash-cement paste and those of the pure cement paste, one should notice that, unlike the pure cement paste, the hydration products of cement are not present. It seems that MSWI fly ash somehow retarded the hydration process of the cement compounds. Salt crystals can be seen more clearly at higher magnifications in Figures 5.44 (e) and (f). The surface elemental composition of the object in Figure 5.44 (e) shows high concentrations of Cl and Ca as indicated by the low Ca:Cl ratios (0.57:1.00). The salts may very well be chloride salts, CaClOH and $CaCl_2.Ca(OH)_2.H_2O$, as reported by the XRD.

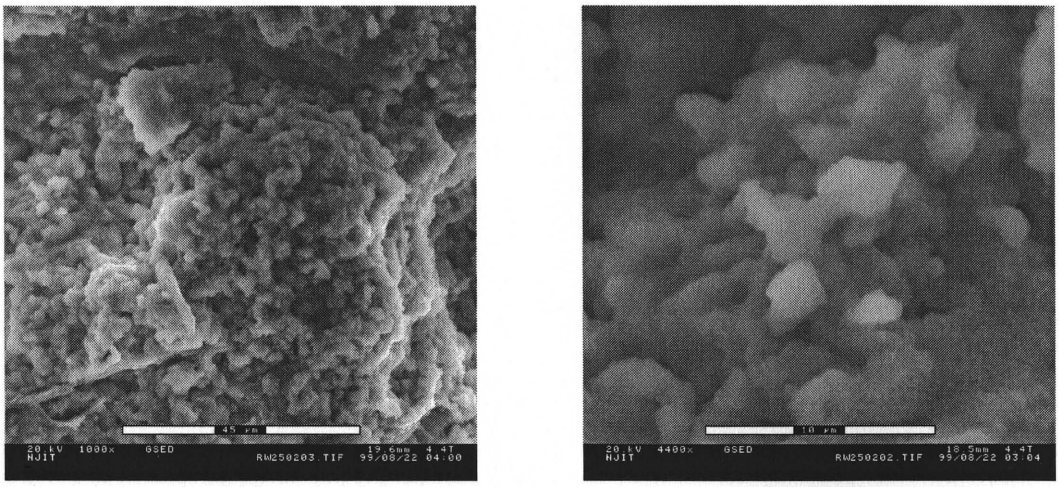

(a) 1000x (b) 4400x

Figure 5.45 Micrographs of 25% Raw MSWI Fly Ash Paste after 24 Hours

Figure 5.45 shows microstructures of fracture surface of a paste containing 25% raw NJIT 2 fly ash. It is apparent that there are more crystals of salt on the surface of particles. In fact, the EDX analysis results in Table 5.17 show high levels of Na, Cl, and Ca. The ratios of Ca to Cl are as low as 0.50:1.00, reflecting Cl content of as high as 17.66%. However, unlike the 15% raw fly ash paste, high Na content of more than 13% was also detected. Therefore, it is very likely that the salts of Ca, Na, and Cl, such as NaCl and CaClOH or $CaCl_2.Ca(OH)_2.H_2O$ were the dominant phases on the particle surfaces.

Table 5.17 Semi-quantitative Surface Compositions of Objects in Selected Acquired Images in Figure 5.45

Element	(a)		(b)	
	Wt%	At%	Wt%	At%
O	32.39	52.05	26.35	42.37
Na	12.14	13.57	16.66	18.65
Mg	0.00	0.00	0.50	0.53
Al	0.99	0.94	0.77	0.73
Si	2.81	2.57	3.40	3.11

Table 5.17 Semi-quantitative Surface Compositions of Objects in Selected Acquired Images in Figure 5.45 (Continued)

Element	(a)		(b)	
	Wt%	At%	Wt%	At%
P	0.00	0.00	0.27	0.22
S	1.20	0.97	0.95	0.76
Cl	20.51	14.87	24.34	17.66
K	5.65	3.71	8.40	5.53
Ca	14.29	9.16	13.88	8.91
Ti	0.33	0.18	0.18	0.10
Cr	0.24	0.12	0.00	0.00
Mn	0.00	0.00	0.26	0.14
Fe	0.50	0.23	0.50	0.23
Cu	0.46	0.19	0.00	0.00
Zn	0.74	0.29	0.70	0.27
As	0.00	0.00	1.43	0.49
Cd	0.35	0.08	0.24	0.05
Sn	0.46	0.10	0.41	0.09
Sb	1.18	0.25	0.76	0.16
Pb	5.76	0.72	0.00	0.00
Total	100.00	100.00	100.00	100.00
Ca:Si	3.56:1.00		2.86:1.00	
Ca:Cl	0.62:1.00		0.50:1.00	

5.8.1.3 Fine MSWI Fly Ash-Cement Paste: The microstructures of the objects in Figures 5.46 (a) through (d) are indeed similar to those in Figure 5.45. MSWI fly ash particles can obviously be seen to have salt crystals grow on their surfaces as shown in Figure 5.46 (c). The salt crystals may be NaCl since the contents of Na and Cl are high, 3.31 and 5.71, respectively.

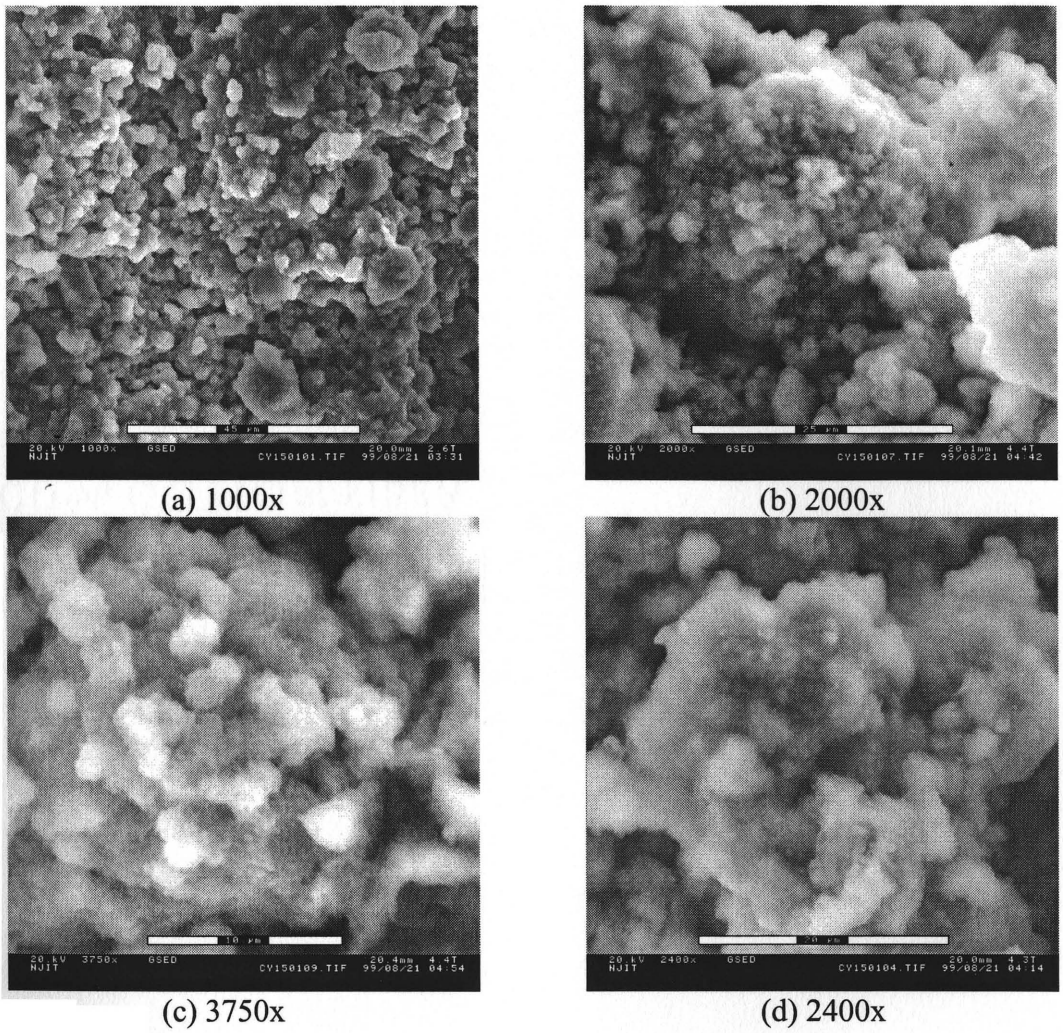

(a) 1000x (b) 2000x

(c) 3750x (d) 2400x

Figure 5.46 Micrographs of 15% Fine MSWI Fly Ash Paste after 24 Hours

Table 5.18 Semi-quantitative Surface Compositions of Objects in Selected Acquired Images in Figure 5.46

Element	(a)		(b)		(c)		(d)	
	Wt%	At%	Wt%	At%	Wt%	At%	Wt%	At%
O	30.79	44.68	44.68	68.27	32.60	61.76	50.42	72.48
Na	3.13	2.57	2.57	2.74	2.51	3.31	2.36	2.36
Mg	0.70	1.21	1.21	1.22	0.82	1.02	1.05	0.99
Al	1.29	2.15	2.15	1.95	1.30	1.46	2.01	1.72
Si	3.39	4.70	4.70	4.09	2.64	2.85	4.53	3.71
P	0.85	1.05	1.05	0.83	0.74	0.73	0.90	0.67
S	1.08	1.40	1.40	1.07	0.82	0.78	1.78	1.28
Cl	10.26	6.06	6.06	4.18	6.68	5.71	4.54	2.94
K	4.18	2.35	2.35	1.47	2.58	2.00	1.68	0.99

Table 5.18 Semi-quantitative Surface Compositions of Objects in Selected Acquired Images in Figure 5.46 (Continued)

Element	(a)		(b)		(c)		(d)	
	Wt%	At%	Wt%	At%	Wt%	At%	Wt%	At%
Ca	17.17	17.23	17.23	10.51	16.66	12.60	16.76	9.62
Ti	0.47	0.46	0.46	0.24	0.40	0.25	0.51	0.24
Cr	0.50	0.48	0.48	0.22	0.48	0.28	0.44	0.20
Mn	0.76	0.42	0.42	0.19	0.61	0.34	0.47	0.19
Fe	1.25	0.69	0.69	0.30	1.05	0.57	0.85	0.35
Cu	1.56	0.90	0.90	0.35	1.64	0.78	0.86	0.31
Zn	2.42	0.96	0.96	0.36	2.09	0.97	1.11	0.39
As	0.00	0.00	0.00	0.00	0.00	0.00	0.00	0.00
Cd	2.24	1.37	1.37	0.30	1.73	0.47	1.18	0.24
Sn	0.70	1.02	1.02	0.21	1.16	0.30	0.86	0.17
Sb	3.38	3.63	3.63	0.73	3.98	0.99	3.60	0.68
Pb	13.88	6.67	6.67	0.77	19.51	2.83	4.09	0.47
Total	100.00	100.00	100.00	100.00	100.00	100.00	100.00	100.00
Ca:Si	3.67:1.00		2.57:1.00		4.42:1.00		2.59:1.00	
Ca:Cl	2.84:1.00		2.51:1.00		2.21:1.00		3.27:1.00	

In Figure 5.46 (d), the indeterminate structure has a Ca:Si ratio of 2.59:1 and Ca:Cl ratio of 3.27:1. It is very important to note that these ratios can only serve as an estimation tool since they were determined from semi-quantitative compositions measured from surfaces of the objects of interest. Nonetheless, these ratios may give an idea as to what the objects might be. Typically, C-S-H has a Ca:Si ratio of 0.8 to 2.0 depending on water content, temperature and other environmental conditions (Lea, 1971). The presence of foreign ions such as Na^+ and Cl^- may affect the morphology of C-S-H as well (Scriverner, 1989). One possible reason why the determined Ca:Si ratio is quite high may be due to the fact that there are other calcium compounds, such as CaClOH, $CaCl_2$, or $Ca(OH)_2$ in the acquired image.

5.8.1.4 Coarse MSWI Fly Ash-Cement Paste: The salt crystals on the surface of particles in Figures 5.47 (a) and (b) can obviously be seen as in the fine MSWI fly ash-cement pastes. Close investigation at higher magnifications reveals characteristics of microstructure typical of C-S-H as depicted in Figures 5.47 (c) and (d). It can be seen that the degree of hydration is far less than that of the pure cement paste.

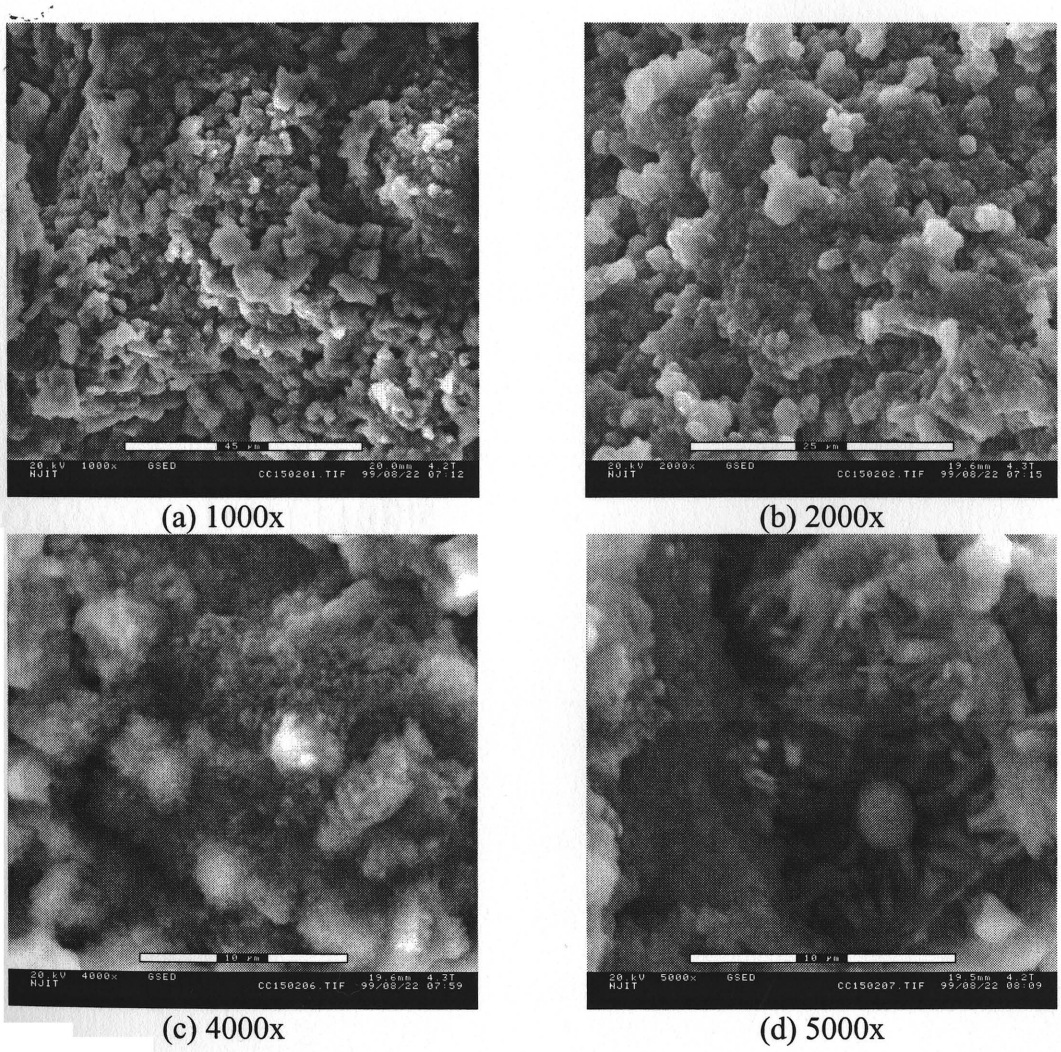

Figure 5.47 Micrographs of 15% Coarse MSWI Fly Ash Paste at day 2

Table 5.19 Semi-quantitative Surface Compositions of Objects in Selected Acquired Images in Figure 5.47

Element	(a)		(b)		(c)		(d)	
	Wt%	At%	Wt%	At%	Wt%	At%	Wt%	At%
O	36.90	59.65	30.29	50.54	31.64	55.19	35.78	59.18
Na	6.68	7.52	10.82	12.57	4.75	5.76	5.13	5.90
Mg	0.66	0.71	0.74	0.81	0.47	0.54	1.02	1.11
Al	1.77	1.69	2.18	2.15	1.78	1.84	1.62	1.59
Si	3.64	3.35	3.87	3.68	5.07	5.04	3.65	3.44
P	0.96	0.80	1.29	1.11	1.06	0.95	0.82	0.70
S	0.72	0.58	0.89	0.74	0.77	0.67	0.96	0.79
Cl	11.23	8.19	15.84	11.93	10.51	8.28	10.78	8.05
K	5.38	3.56	6.84	4.67	6.05	4.32	6.34	4.29
Ca	15.70	10.13	11.93	7.95	17.66	12.30	16.02	10.58
Ti	0.51	0.28	0.65	0.36	0.59	0.34	0.57	0.32
Cr	0.49	0.24	0.51	0.26	0.53	0.28	0.58	0.30
Mn	0.51	0.24	0.51	0.25	0.40	0.21	0.50	0.24
Fe	0.63	0.29	0.63	0.30	0.83	0.42	0.73	0.34
Cu	1.01	0.41	0.73	0.31	1.29	0.57	0.93	0.39
Zn	0.82	0.32	1.04	0.42	1.30	0.55	1.06	0.43
As	0.00	0.00	0.00	0.00	0.00	0.00	0.00	0.00
Cd	1.42	0.33	1.97	0.47	1.69	0.42	1.36	0.32
Sn	0.53	0.12	0.72	0.16	0.91	0.21	0.60	0.13
Sb	3.33	0.71	2.29	0.50	4.24	0.97	4.84	1.05
Pb	7.11	0.88	6.26	0.82	8.46	1.14	6.71	0.85
Total	100.00	100.00	100.00	100.00	100.00	100.00	100.00	100.00
Ca:Si	3.02:1.00		2.16:1.00		2.44:1.00		3.08:1.00	
Ca:Cl	1.24:1.00		0.67:1.00		1.49:1.00		1.31:1.00	

The Ca:Si ratios of objects in Figures 5.47 (a) through (d) were determined using the compositional data in Table 5.19 and were found to be 3.02, 2.16, 2.44, and 3.08, respectively. The obtained ratios are somewhat higher than that of C-S-H, which ranges from 0.8 to 2.0, suggesting that Ca was involved in the formation other phases., such as CaClOH. Moreover, the elevated amounts of Na, K, and Cl, especially in Figure 5.47 (b), are evident in Table 5.19 implying that chloride salts, such as CaClOH, NaCl, and KCl may be present in the paste.

5.8.1.5 Washed Fine MSWI Fly Ash-Cement Paste: Hydration of the paste containing 15% washed fine NJIT 2 fly ash and cement produced more products, such as CH and C-S-H as shown in Figures 5.48 (a) through (d). Large blocks of $Ca(OH)_2$ are conspicuous in the lower part of Figure 5.48 (a) while its platy structure is obvious in Figure 5.48 (d). The atomic ratio between Ca and Si calculated using the compositional data in Table 5.20 is 6.44 which reflects the abundance of Ca over Si. As for the Ca:Cl ratios, it is apparent that Ca was present in the quantity as high as 39 times of that of Cl. This is in fact due to the presence of the CH crystals. The Ca:Si ratios of the microstructures in Figures 5.48 (a), (b), and (c) are 2.90, 4.44, and 6.69, respectively. The absence of the slender needle-like structure, ettringite, is due to the low concentration of sulfate in the paste as determined by the XRF.

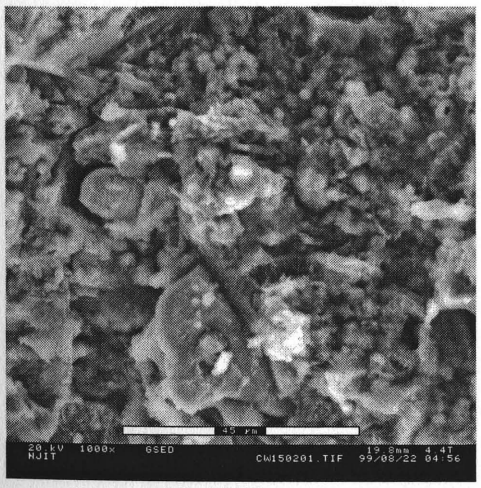

(a) 1000x

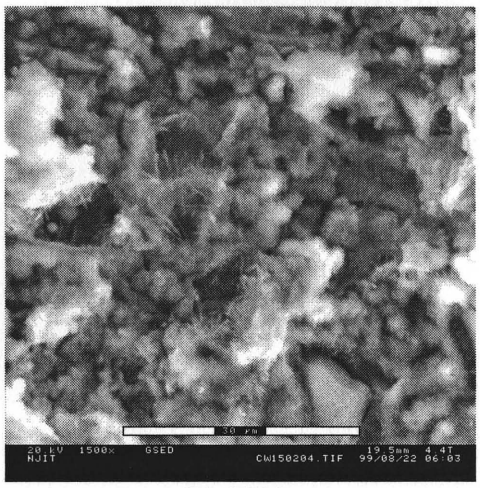

(b) 1500x

Figure 5.48 Micrographs of 15% Washed Fine MSWI Fly Ash Paste after 48 Hours

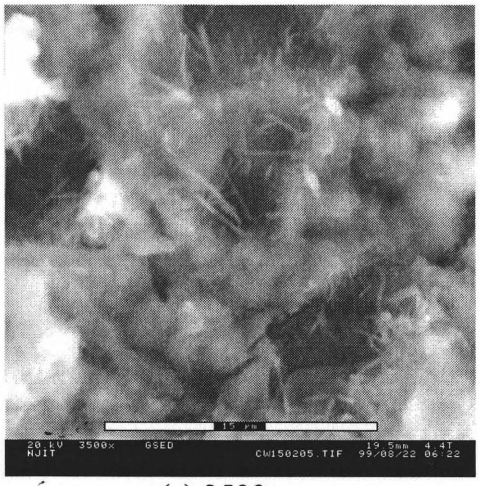

(c) 3500x

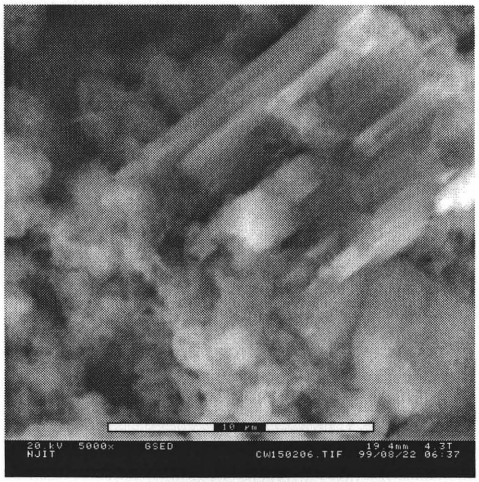

(d) 5000x

Figure 5.48 Micrographs of 15% Washed Fine MSWI Fly Ash Paste after 48 Hours (Continued)

Table 5.20 lists very low concentrations of Na and Cl for all of the microstructures which agree well with the XRF analysis result for the washed fine fly ash in Section 5.2.3. Washing was found to considerably reduce levels of Na and Cl in the fine MSWI fly ash, especially Cl from more than 3% down to approximately 1%. The presence of the hydration products in the washed fly ash-cement paste shows that washed fine fly ash had less adverse effect on hydration of the cement paste.

Table 5.20 Semi-quantitative Surface Compositions of Objects in Selected Acquired Images in Figure 5.48

Element	(a)		(b)		(c)		(d)	
	Wt%	At%	Wt%	At%	Wt%	At%	Wt%	At%
O	40.09	67.49	45.70	70.60	43.14	68.48	34.60	61.20
Na	2.24	2.62	0.00	0.00	0.00	0.00	1.86	2.29
Mg	0.00	0.00	0.00	0.00	0.65	0.68	0.75	0.87
Al	1.80	1.80	1.22	1.12	1.44	1.36	1.38	1.45
Si	4.67	4.48	4.48	3.95	3.21	2.90	3.18	3.20
P	0.90	0.78	0.00	0.00	0.00	0.00	1.03	0.94
S	1.42	1.19	0.78	0.60	0.82	0.65	0.89	0.78
Cl	1.45	1.10	0.65	0.45	0.70	0.50	1.14	0.91

Table 5.20 Semi-quantitative Surface Compositions of Objects in Selected Acquired Images in Figure 5.48 (Continued)

Element	(a)		(b)		(c)		(d)	
	Wt%	At%	Wt%	At%	Wt%	At%	Wt%	At%
K	2.12	1.46	3.73	2.36	4.12	2.68	2.27	1.64
Ca	19.33	12.99	28.46	17.55	30.64	19.41	29.18	20.60
Ti	0.57	0.32	0.13	0.07	0.28	0.15	0.56	0.33
Cr	0.61	0.31	0.40	0.19	0.26	0.13	0.62	0.34
Mn	0.50	0.24	0.23	0.10	0.00	0.00	0.59	0.30
Fe	0.97	0.47	1.09	0.48	1.07	0.49	0.86	0.44
Cu	1.49	0.63	0.29	0.11	0.80	0.32	1.12	0.50
Zn	1.71	0.71	1.95	0.74	1.25	0.49	1.68	0.73
As	0.00	0.00	0.00	0.00	0.00	0.00	0.00	0.00
Cd	1.43	0.34	0.00	0.00	0.00	0.00	1.63	0.41
Sn	1.02	0.23	0.98	0.20	0.87	0.19	1.09	0.26
Sb	5.86	1.30	3.40	0.69	3.13	0.65	7.13	1.66
Pb	11.82	1.54	6.51	0.79	7.62	0.92	8.44	1.15
Total	100.00	100.00	100.00	100.00	100.00	100.00	100.00	100.00
Ca:Si	2.90:1.00		4.44:1.00		6.69:1.00		6.44:1.00	
Ca:Cl	11.81:1.00		39.00:1.00		38.82:1.00		22.64:1.00	

5.8.1.6 CaO-Enhanced Cement Paste: Calcium oxide (98%) was used to replace 15% of cement in the paste mixture in order to study the effect of available CaO on hydration of cement paste. Upon comparing the micrographs of the CaO-enhanced cement paste and that of the pure cement paste, one can see that the microstructures of the fracture surface of the two pastes are very similar. Indeed, a large piece of $Ca(OH)_2$ is noticeable in Figure 5.49 (a) while small elongated prisms are present in Figure 5.49 (b).

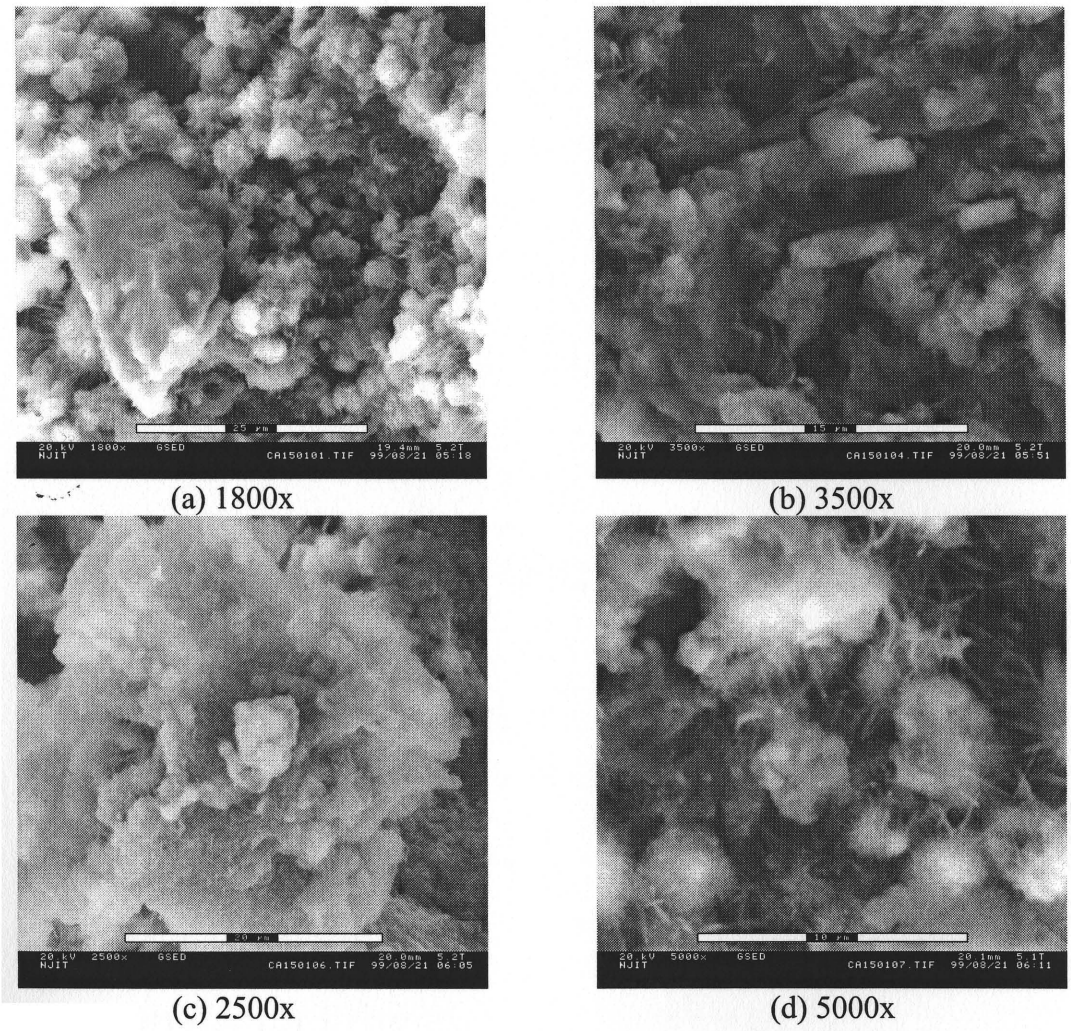

Figure 5.49 Micrographs of 15% CaO-Cement Paste at day 1

Figure 5.50 which shows the microstructures of hydrated CaO powder is given as a reference and so is its elemental composition in Table 5.21. It can be seen that the Ca:Si ratio of the hydrated CaO powder (22.54:1.00) is much higher than those of the objects in Figures 5.49 (a) and (c) (2.13 and 2.49). The Ca:Cl ratios are also high indicating that Cl was present in insignificant amount compared with Ca.

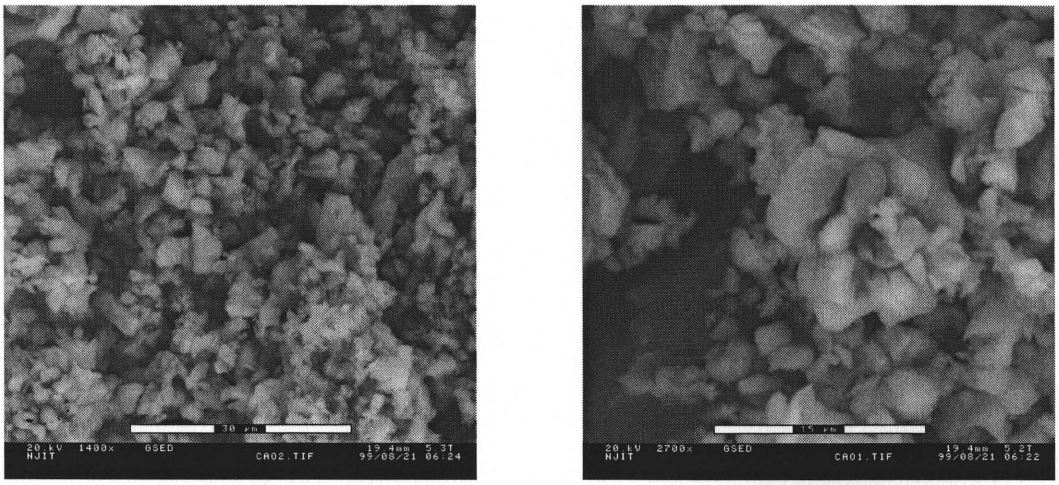

(a) 1400x (b) 2700x

Figure 5.50 Micrographs CaO Paste at 15 minutes

Table 5.21 Semi-quantitative Surface Compositions of Objects in Selected Acquired Images in Figures 5.49 and 5.50

Element	Figure 5.49 (a)		Figure 5.49 (c)		Figure 5.50 (b)	
	Wt%	At%	Wt%	At%	Wt%	At%
O	53.12	75.30	51.90	74.00	42.21	68.79
Na	1.96	1.93	2.06	2.04	1.26	1.43
Mg	1.08	1.01	1.46	1.37	0.75	0.80
Al	1.81	1.52	1.97	1.67	1.06	1.03
Si	5.60	4.52	5.04	4.09	0.99	0.92
P	0.85	0.62	0.99	0.73	0.96	0.81
S	0.95	0.67	1.14	0.81	0.15	0.12
Cl	0.57	0.36	0.52	0.33	0.81	0.59
K	2.21	1.28	2.51	1.47	0.12	0.08
Ca	16.98	9.61	17.93	10.20	31.88	20.74
Ti	0.51	0.24	0.53	0.25	0.49	0.26
Cr	0.43	0.19	0.56	0.25	0.47	0.23
Mn	0.49	0.20	0.53	0.22	0.53	0.25
Fe	0.68	0.28	0.88	0.36	0.47	0.22
Cu	0.76	0.27	0.73	0.26	1.09	0.45
Zn	0.75	0.26	0.87	0.30	0.96	0.38
As	0.00	0.00	0.00	0.00	0.00	0.00
Cd	1.13	0.23	1.25	0.25	1.64	0.38
Sn	0.80	0.15	1.07	0.21	1.08	0.24
Sb	4.27	0.80	3.85	0.72	7.03	1.51
Pb	5.05	0.56	4.21	0.47	6.05	0.77

Table 5.21 Semi-quantitative Surface Compositions of Objects in Selected Acquired Images in Figures 5.49 and 5.50 (Continued)

Total	100.00	100.00	100.00	100.00	100.00	100.00
Ca:Si	2.13:1.00		2.49:1.00		22.54:1.00	
Ca:Cl	26.69:1.00		30.91:1.00		35.15:1.00	

In summary, the inclusion of MSWI fly ashes in cement pastes retards the hydration of cement to some degree since the hydration products, C-S-H and CH, were less visible than the control paste at the same age. Salt crystals, such as that of NaCl, were observed on the surfaces. However, washing of fine fly ash significantly reduced the amount of Na and Cl as evident by the low surface compositions as well as the disappearance of salt crystals. Washed fine fly ash-cement paste seemed to be in a more advanced hydration stage than raw, fine, and coarse NJIT 2 fly ash-cement pastes since more hydration products, $Ca(OH)_2$ and C-S-H, were observed in the washed fine fly ash paste.

5.8.2 Day 7

Hardening of cement is a continuing process even after one year. According to Lea (1971), the rate of hydration of C_3S, the major component in portland cement, detected by XRD method varies from 15 to 55% at one day, 35 to 60% at 3 days, and 40 to 70% at 7 days. As for C_2S, which presents as a minor component, is hydrated at a lower rate varying from 20% at 3 days, 8 to 25% at 7 days, and 20 to 75% at three months. Most of the hardened pastes should show more advanced stage of hydration.

5.8.2.1 Pure Cement Paste: Figure 5.51 (a) shows a remnant of a volume previously occupied by air. Air pockets in hardened cement mortar paste or concrete are typical. In fact, air entrainment admixture is normally added to achieve about 4 to 8% by volume in concrete intended to withstand frost attack (Mindess and Young, 1981).

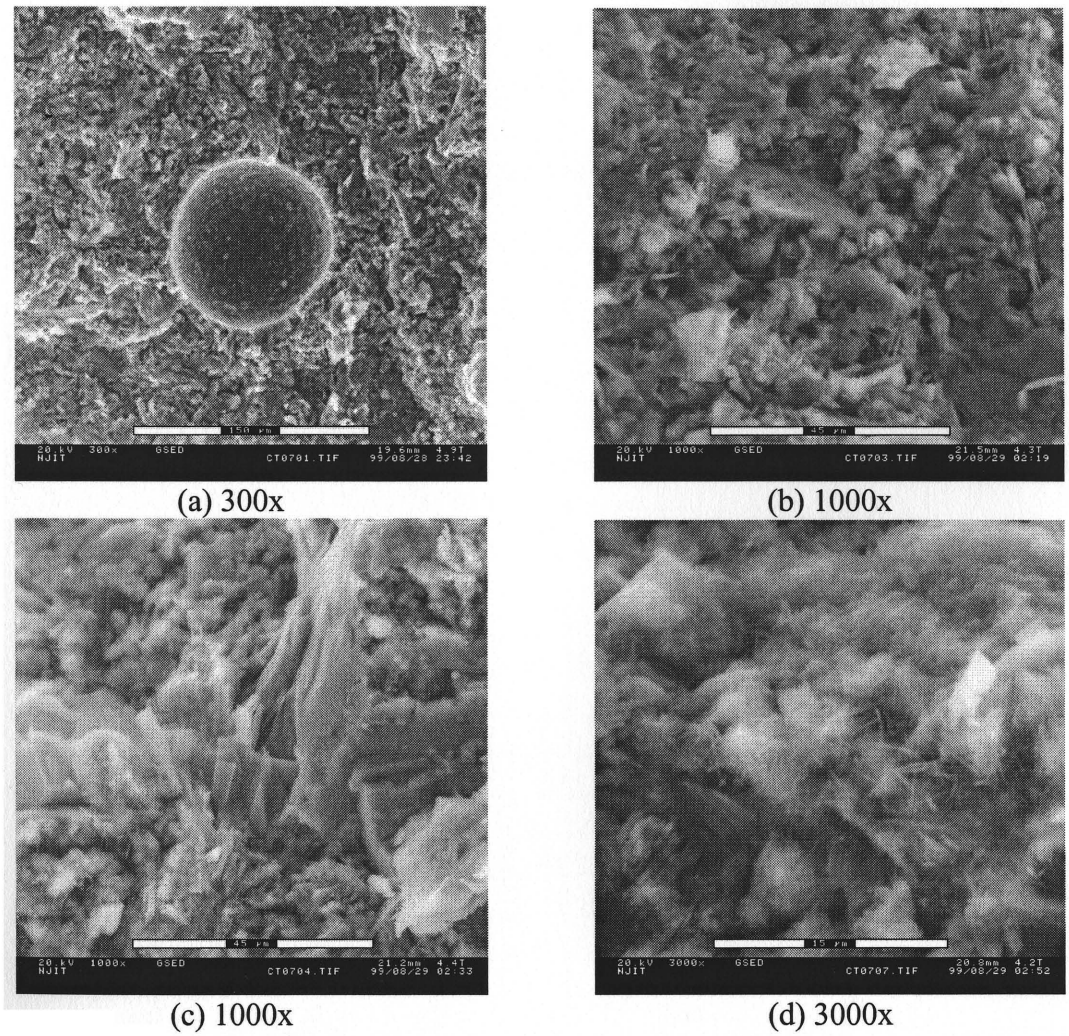

(a) 300x (b) 1000x

(c) 1000x (d) 3000x

Figure 5.51 Micrographs of Cement Paste at day 7

System of air voids in concrete acts as a buffer area where freezing water can escape from capillary pores. This relieves the pressure building up in the capillary that

would have caused concrete to crack. However, concrete with excessive air content may compromise the strengths of concrete.

Hydration products are evident in Figures 5.51 (a) through (d). Large CH crystals are observed to occupy more space at 7 days as shown in Figures 5.51 (b) and (c) than at 1 day. The crystals can gradually spread throughout the paste and take up 20 to 25% of the volume of the paste (Mindess and Young, 1981). Advanced stage of hydration is also evident by different morphology of C-S-H in Figure 5.51 (d) at higher magnification (3000x). As hydration proceeds, the underlying C-S-H grows in thickness and becomes the dominant form of C-S-H in mature pastes. The spines of C-S-H begin to intermesh as depicted.

Table 5.22 Semi-quantitative Surface Compositions of Objects in Selected Acquired Images in Figure 5.51

Element	(a)		(b)		(c)		(d)	
	Wt%	At%	Wt%	At%	Wt%	At%	Wt%	At%
O	55.41	76.21	52.27	74.29	60.25	80.32	58.36	77.20
Na	0.00	0.00	0.00	0.00	0.00	0.00	0.62	0.57
Mg	0.85	0.77	0.90	0.84	0.89	0.78	1.93	1.68
Al	1.46	1.19	1.58	1.33	0.84	0.67	1.97	1.54
Si	5.57	4.37	6.29	5.09	3.52	2.67	7.24	5.45
P	0.00	0.00	0.00	0.00	0.00	0.00	0.14	0.09
S	1.03	0.71	0.91	0.65	0.55	0.37	1.28	0.85
Cl	0.15	0.09	0.15	0.10	0.13	0.08	0.00	0.00
K	1.07	0.6	1.32	0.77	0.52	0.28	1.19	0.64
Ca	26.15	14.35	26.63	15.11	24.98	13.29	19.94	10.53
Ti	0.14	0.07	0.19	0.09	0.24	0.11	0.26	0.12
Cr	0.12	0.05	0.00	0.00	0.18	0.07	0.17	0.07
Mn	0.00	0.00	0.00	0.00	0.15	0.06	0.13	0.05
Fe	1.05	0.41	0.61	0.25	0.43	0.17	0.72	0.27
Cu	0.49	0.17	0.43	0.15	0.33	0.11	0.19	0.06
Zn	0.26	0.09	0.38	0.13	0.33	0.11	0.22	0.07
As	0.00	0.00	0.00	0.00	0.00	0.00	0.00	0.00
Cd	0.00	0.00	0.34	0.07	0.00	0.00	0.23	0.04

Table 5.22 Semi-quantitative Surface Compositions of Objects in Selected Acquired Images in Figure 5.51 (Continued)

Element	(a)		(b)		(c)		(d)	
	Wt%	At%	Wt%	At%	Wt%	At%	Wt%	At%
Sn	0.23	0.04	0.55	0.11	0.31	0.06	0.39	0.07
Sb	3.21	0.58	2.77	0.52	2.85	0.50	2.56	0.45
Pb	2.81	0.30	4.68	0.50	3.50	0.35	2.46	0.25
Total	100.00	100.00	100.00	100.00	100.00	100.00	100.00	100.00
Ca:Si	3.28:1.00		2.97:1.00		4.98:1.00		1.93:1.00	
Ca:Cl	159.44:1.00		151.10:1.00		166.13:1.00		-	

Table 5.22 shows that the Ca:Si ratios of the acquired images in Figures 5.51 (a) and (b) are quite high at 3.28 and 2.97. This is because the compositions were taken for the objects at low magnification, thus giving overall surface elemental contents of the objects with different morphologies. Upon closer inspection, the platy crystals in the center of Figure 5.51 (c) possesses a Ca:Si ratio of 4.98. That high ratio reflects the high Ca content in the platy CH crystals. Microstructures in Figure 5.51 (d) consist mainly of C-S-H with a Ca:Si ratio of 1.93 which is well within the range of 0.8 to 2.0 as previously discussed.

The high Ca:Cl ratios of more than 150:1 indicate that Cl was not present in a significant amount in the paste. This is confirmed by the bulk chemical analysis result of cement in Section 5.2.1 that shows only 0.01% of Cl in cement.

5.8.2.2 Raw MSWI Fly Ash-Cement Paste: Figures 5.52 (a) through (d) show the microstructures of a fracture surface of 15% raw NJIT 2 fly ash-cement paste at the age of 7 days. It is apparent that the hydration products had developed and covered the fly ash

particles previously visible at the age of 1 day. Platy crystals of CH, which are a major product of hydration of cement, are visible in all of the pictures.

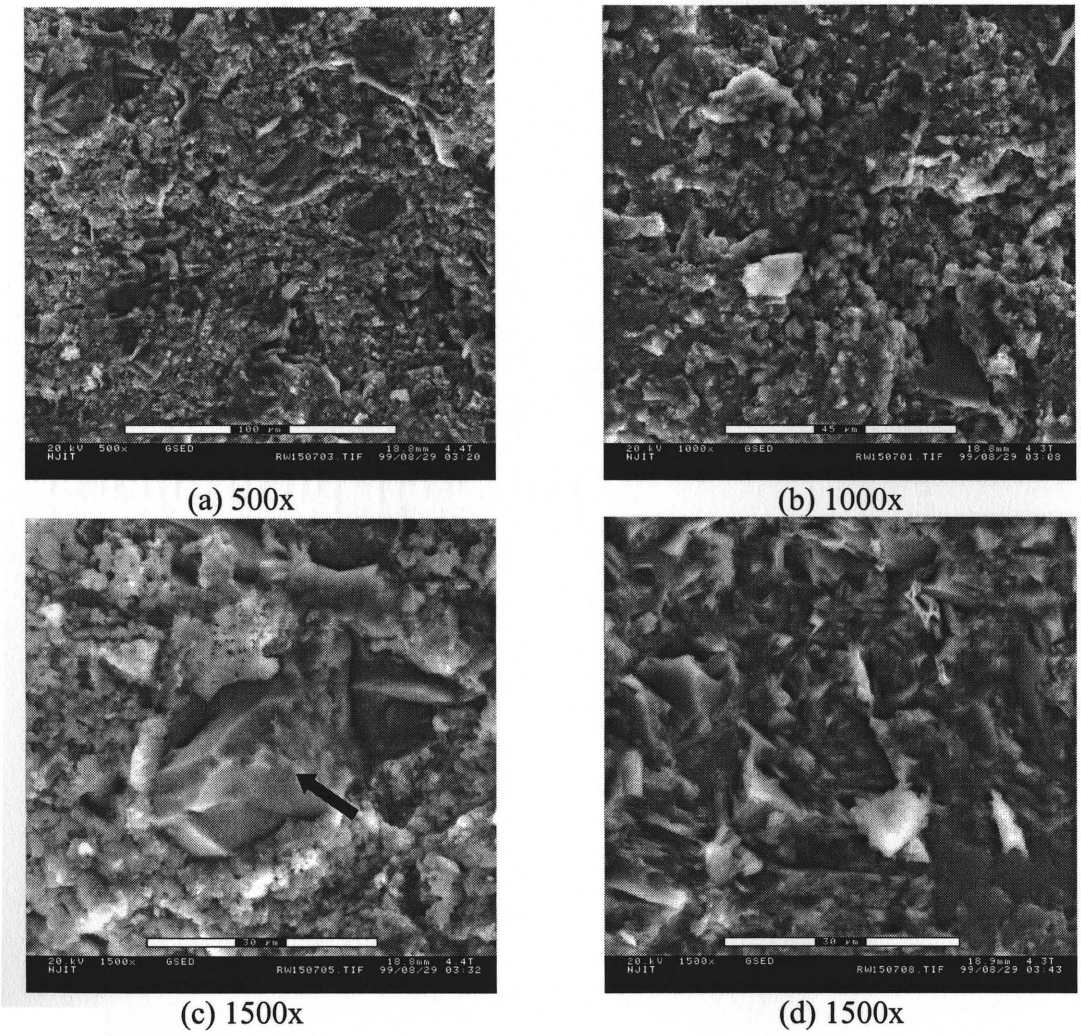

(a) 500x (b) 1000x

(c) 1500x (d) 1500x

Figure 5.52 Micrographs of 15% Raw MSWI Fly Ash Paste at day 7

Table 5.23 Semi-quantitative Surface Compositions of Objects in Selected Acquired Images in Figure 5.52

Element	(a)		(b)		(c)		(d)	
	Wt%	At%	Wt%	At%	Wt%	At%	Wt%	At%
O	26.28	47.10	29.24	50.88	32.06	54.09	20.40	43.99
Na	2.22	2.76	1.99	2.42	0.93	1.09	0.00	0.00
Mg	0.00	0.00	0.66	0.76	1.22	1.35	0.00	0.00

Table 5.23 Semi-quantitative Surface Compositions of Objects in Selected Acquired Images in Figure 5.52 (Continued)

Element	(a)		(b)		(c)		(d)	
	Wt%	At%	Wt%	At%	Wt%	At%	Wt%	At%
Al	0.66	0.71	0.89	0.92	1.10	1.10	0.30	0.38
Si	3.85	3.93	4.64	4.60	8.28	7.96	1.60	1.97
P	0.00	0.00	0.17	0.15	0.22	0.19	0.16	0.18
S	0.91	0.81	0.83	0.72	0.38	0.32	0.35	0.38
Cl	17.52	14.16	14.42	11.33	4.85	3.69	5.34	5.20
K	14.94	10.96	11.78	8.39	3.78	2.61	4.61	4.07
Ca	24.44	17.48	25.14	17.46	36.61	24.66	43.80	37.70
Ti	0.25	0.15	0.27	0.16	0.23	0.13	0.50	0.36
Cr	0.00	0.00	0.00	0.00	0.00	0.00	0.22	0.15
Mn	0.00	0.00	0.00	0.00	0.25	0.12	0.00	0.00
Fe	1.36	0.70	0.86	0.43	1.59	0.77	0.68	0.42
Cu	0.46	0.21	0.22	0.10	0.76	0.32	1.00	0.54
Zn	0.00	0.00	0.53	0.23	0.42	0.17	0.90	0.47
As	0.00	0.00	0.00	0.00	0.00	0.00	0.00	0.00
Cd	0.00	0.00	0.45	0.11	0.00	0.00	0.00	0.00
Sn	0.48	0.12	1.09	0.26	1.13	0.26	1.23	0.36
Sb	0.00	0.00	1.91	0.44	3.89	0.86	5.84	1.66
Pb	6.63	0.91	4.91	0.64	2.30	0.31	13.07	2.17
Total	100.00	100.00	100.00	100.00	100.00	100.00	100.00	100.00
Ca:Si	4.48:1.00		3.80:1.00		3.10:1.00		19.14:1.00	
Ca:Cl	1.23:1.00		1.54:1.00		6.68:1.00		7.25:1.00	

Compositional data listed in Table 5.23 were used to determine the Ca:Si and Ca:Cl ratios of the large block in the middle of Figure 5.52 (c), as indicated by the arrow, which were found to be 3.10 and 6.68, respectively. It means that the Ca can be found in other phases that did not involve Si and Cl. This confirms the observation that the crystals are indeed $Ca(OH)_2$. With an aid from Ca:Si and Ca:Cl determination, most objects in the fracture surface in Figure 5.52 (d) should very well be CH crystals.

An object with indeterminate structure is given in Figure 5.53. Its surface is composed of high concentrations of Ca, Cl, and K.

5.8.2.3 Fine MSWI Fly Ash-Cement Paste: The nature of the fracture surface microstructures is similar to that of the raw MSWI fly ash-cement paste in that there are very few visible fly ash particles. The products of hydration seemed to bridge between particles and grow to cover them. C-S-H is also visible at higher magnification in Figure 5.53 (c). However, the development of C-S-H seems to be in an early stage compared with that in the pure cement paste at the same age. The delayed hydration caused by MSWI fly ash addition was also found by Ubbriaco (1996) who showed that hydration of lime-pozzolan paste was slowed down by the addition of MSWI fly ash by 3 days. However, after the initial delay, the hydration process accelerated. The Ca:Si and Ca:Cl ratios were found to be 1.83 and 0.56, respectively. The Ca:Si ratio is well within the range that is the characteristic of C-S-H. As seen in Table 5.24, the Cl and Na contents are really high, implying that NaCl may be present.

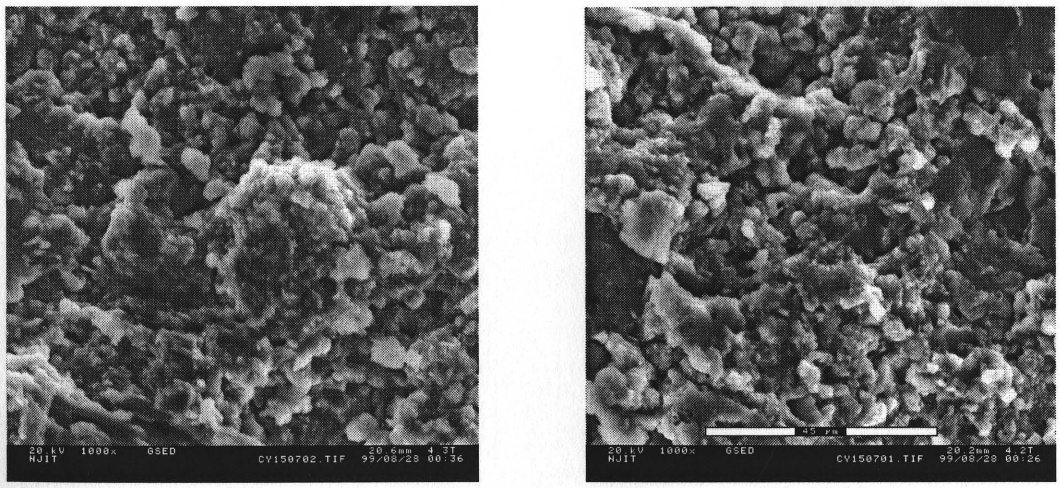

(a) 1000x (b) 1000x

Figure 5.53 Micrographs of 15% Fine MSWI Fly Ash Paste at day 7

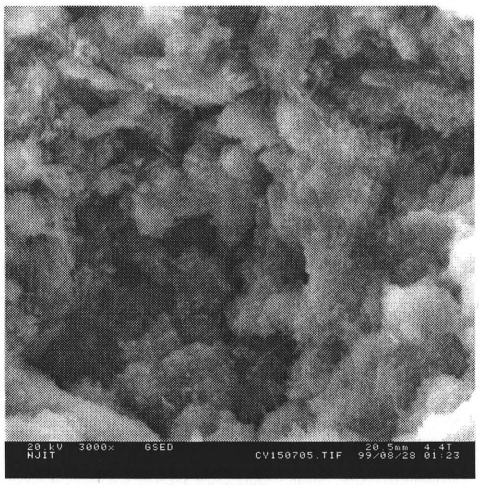

(c) 3000x

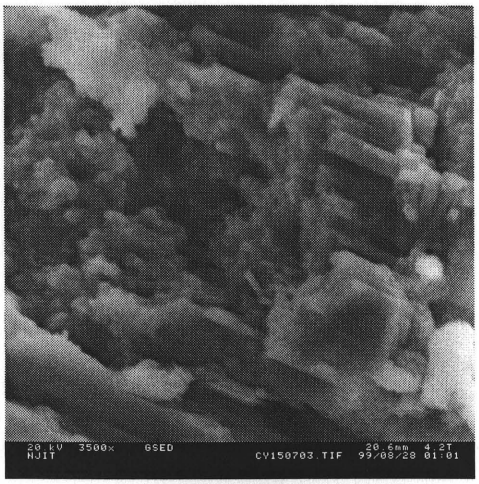

(d) 3500x

Figure 5.53 Micrographs of 15% Fine MSWI Fly Ash Paste at day 7 (Continued)

Figure 5.53 (d) shows the characteristic striated appearance of $Ca(OH)_2$ crystals which is a consequence of the way the crystal fractures within the paste. The calculated Ca:Si and Ca:Cl ratios are fairly high at 4.91 and 1.57. Assuming that C-S-H, CaClOH, NaCl, and $Ca(OH)_2$ are the only major products of concern, which is particularly true according to the XRD result in Section 5.3, high Ca content may be indicative of the presence of $Ca(OH)_2$.

Table 5.24 Semi-quantitative Surface Compositions of Objects in Selected Acquired Images in Figure 5.53

Element	(a)		(c)		(d)	
	Wt%	At%	Wt%	At%	Wt%	At%
O	25.58	46.98	31.91	53.89	33.81	58.08
Na	4.42	5.65	6.34	7.45	3.92	4.69
Mg	0.54	0.65	0.44	0.49	0.68	0.77
Al	0.79	0.86	2.36	2.36	1.64	1.67
Si	3.09	3.24	3.82	3.67	2.68	2.62
P	0.00	0.00	1.04	0.91	1.03	0.91
S	0.77	0.70	0.95	0.80	0.76	0.65
Cl	18.10	15.00	15.61	11.89	10.54	8.17
K	13.69	10.29	11.11	7.68	7.07	4.97

Table 5.24 Semi-quantitative Surface Compositions of Objects in Selected Acquired Images in Figure 5.53 (Continued)

Element	(a)		(c)		(d)	
	Wt%	At%	Wt%	At%	Wt%	At%
Ca	17.58	12.89	9.94	6.70	18.76	12.86
Ti	0.29	0.18	0.58	0.33	0.49	0.28
Cr	0.40	0.23	0.57	0.30	0.42	0.22
Mn	0.28	0.15	0.47	0.23	0.48	0.24
Fe	0.92	0.49	0.68	0.33	0.60	0.29
Cu	0.33	0.15	0.90	0.38	1.11	0.48
Zn	1.23	0.55	1.32	0.54	1.23	0.52
As	0.00	0.00	0.00	0.00	0.00	0.00
Cd	0.61	0.16	1.66	0.40	1.28	0.31
Sn	1.20	0.30	1.33	0.30	0.89	0.21
Sb	0.96	0.23	1.81	0.40	4.08	0.92
Pb	9.22	1.30	7.16	0.95	8.53	1.14
Total	100.00	100.00	100.00	100.00	100.00	100.00
Ca:Si	3.98:1.00		1.83:1.00		4.91:1.00	
Ca:Cl	0.85:1.00		0.56:1.00		1.57:1.00	

Table 5.24 also shows significant concentrations of Al in Figures 5.53 (c) and (d) at high magnification of 3000x and 3500x. Since ettringite is not visible, there might be other phases that contain Al, such as hydrocalumite [$C_3A.CaCl_2.10H_2O$]. In fact, the XRD result in Section 5.7 shows that hydrocalumite was first detected at the age of 7 days.

5.8.2.4 Coarse MSWI Fly Ash-Cement Paste: As was the case with the raw and fine fly ash-cement pastes, the 15% coarse fly ash and cement paste shows advanced degree of hydration. Figure 5.54 (a) shows hydrated cement grains covered with C-S-H while big CH crystals are present in Figure 5.54 (b). It is interesting to note in Table 5.25 that the Cl content on the fracture surface is considerable lower than those of the raw and fine fly ash-cement pastes. This may be because the chloride salts were covered by layers of the

hydration products, C-S-H and $Ca(OH)_2$, thereby preventing them from being detected by the EDX. Another possible explanation is that the chloride salts involved in a chemical reaction and formed another phase.

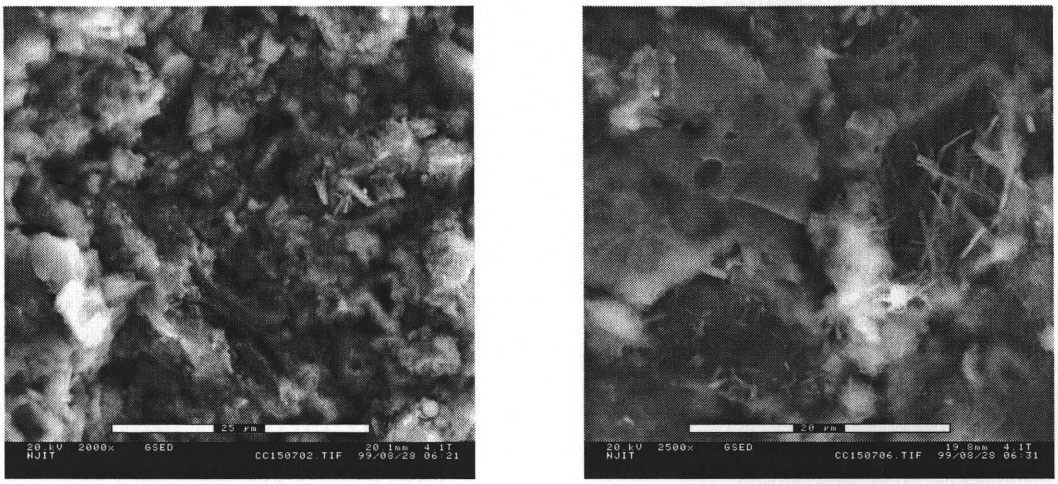

(a) 2000x (b) 2500x

Figure 5.54 Micrographs of 15% Coarse MSWI Fly Ash Paste at day 7

Table 5.25 Semi-quantitative Surface Compositions of Objects in Selected Acquired Images in Figure 5.54

Element	(a)		(b)	
	Wt%	At%	Wt%	At%
O	36.30	63.65	35.45	61.60
Na	1.82	2.22	2.30	2.78
Mg	0.67	0.77	0.59	0.67
Al	1.35	1.40	1.85	1.90
Si	5.05	5.04	5.31	5.25
P	0.71	0.64	1.07	0.96
S	0.97	0.85	1.23	1.07
Cl	2.42	1.92	3.22	2.52
K	1.82	1.31	3.36	2.39
Ca	22.55	15.78	21.34	14.80
Ti	0.46	0.27	0.52	0.30
Cr	0.44	0.24	0.49	0.26
Mn	0.64	0.33	0.74	0.38

Table 5.25 Semi-quantitative Surface Compositions of Objects in Selected Acquired Images in Figure 5.54 (Continued)

Element	(a)		(b)	
	Wt%	At%	Wt%	At%
Fe	1.20	0.60	1.10	0.55
Cu	1.39	0.61	1.26	0.55
Zn	1.92	0.82	1.45	0.62
As	0.00	0.00	0.00	0.00
Cd	1.59	0.40	1.45	0.36
Sn	1.21	0.29	1.11	0.26
Sb	5.26	1.21	6.31	1.44
Pb	12.23	1.65	9.85	1.34
Total	100.00	100.00	100.00	100.00
Ca:Si	3.13:1.00		2.82:1.00	
Ca:Cl	8.22:1.00		5.87:1.00	

From the elemental data in Table 5.25, the Ca:Si ratios of Figures 5.54 (a) and (b) were determined to be 3.13 and 2.82, respectively. These numbers reflect the presence of C-S-H and $Ca(OH)_2$ on the fracture surface of the paste. The Ca:Cl ratios were very high, 8.22 and 5.87, since there are no visible salt crystals on the surface as there were at the age of 1 day. It may be possible that the salt containing chloride, $CaCl_2.Ca(OH)_2.H_2O$, formed $C_3A.CaCl_2.10H_2O$.

5.8.2.5 Washed Fine MSWI Fly Ash-Cement Paste: As seen in Figures 5.55 (a) through (d), the cement paste incorporating 15% washed fine fly ash shows advanced stage of hydration. Apparently, almost all of the cement grains had undergone hydration reaction. Individual particles were bridged by hydration products. There is no visible fly ash particle on the fracture surface.

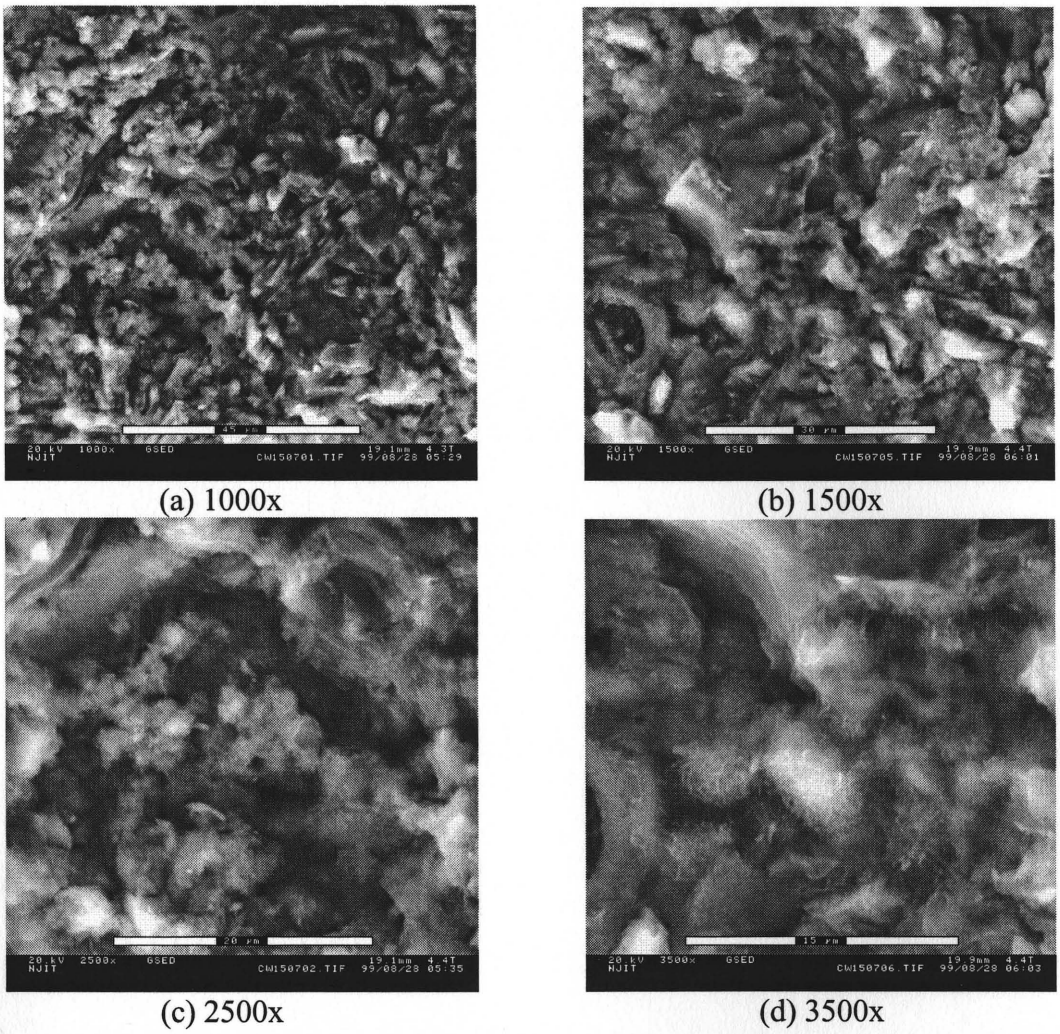

Figure 5.55 Micrographs of 15% Washed Fine MSWI Fly Ash Paste at day 7

Figures 5.55 (c) and (d) show the intermeshed spines of C-S-H and no visible CH crystals. The paste seems denser with all the hydration products forming a rigid network. The Ca:Si ratios of the microstructures in Figures 5.55 (a), (b), and (c) are 3.51, 5.18, and 2.25, respectively. This overabundance of Ca in the paste implies that Ca had participated in reactions that yielded products other than C-S-H.

Table 5.26 Semi-quantitative Surface Compositions of Objects in Selected Acquired Images in Figure 5.55

Element	(a)		(b)		(c)	
	Wt%	At%	Wt%	At%	Wt%	At%
O	40.39	66.64	44.71	69.53	33.53	61.52
Na	2.04	2.34	3.00	3.25	2.17	2.77
Mg	0.00	0.00	0.61	0.63	0.94	1.14
Al	1.80	1.77	2.14	1.98	1.48	1.61
Si	4.58	4.31	5.54	4.91	3.22	3.37
P	0.83	0.71	0.90	0.72	0.65	0.61
S	0.93	0.76	1.12	0.87	0.70	0.64
Cl	1.23	0.92	1.12	0.78	0.90	0.75
K	2.79	1.88	2.53	1.61	2.55	1.91
Ca	22.95	15.12	17.78	11.04	23.81	17.44
Ti	0.63	0.35	0.60	0.31	0.53	0.32
Cr	0.58	0.30	0.62	0.30	0.72	0.40
Mn	0.70	0.33	0.50	0.23	0.89	0.47
Fe	1.07	0.51	0.97	0.43	2.40	1.26
Cu	1.12	0.47	0.84	0.33	1.77	0.82
Zn	1.81	0.73	1.48	0.56	2.18	0.98
As	0.00	0.00	0.00	0.00	0.00	0.00
Cd	1.48	0.35	1.14	0.25	1.40	0.37
Sn	0.86	0.19	1.06	0.22	1.05	0.26
Sb	5.79	1.26	5.27	1.08	6.50	1.57
Pb	8.42	1.06	8.07	0.97	12.61	1.79
Total	100.00	100.00	100.00	100.00	100.00	100.00
Ca:Si	3.51:1.00		2.25:1.00		5.18:1.00	
Ca:Cl	16.43:1.00		14.15:1.00		23.25:1.00	

In summary, MSWI fly ash-cement pastes at the age of 7 days reached a more advanced stage of hydration, as more hydration products were observed. However, hydration process in these pastes still lagged behind that of the control paste. XRD and EDX results revealed possible formation of the new phase, $C_3A.CaCl_2.10H_2O$, which might be responsible for the disappearance of chloride salt crystals. Washed fine fly ash-cement paste might not have this new phase due to low Cl content. Nevertheless, the washed fine fly ash paste was in a more advanced hydration stage than the others.

5.8.3 Day 18 Onwards

5.8.3.1 Pure Cement Paste: As age progressed, microstructures of fracture surface cement paste shows advanced degree of hydration. Intermeshed C-S-H spines are noticeable in Figure 5.56 (a). However, less hydrated cement grains are still visible.

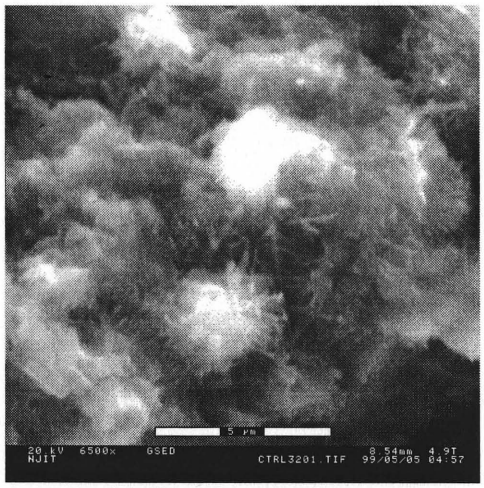

(a) Day 32, 6500x

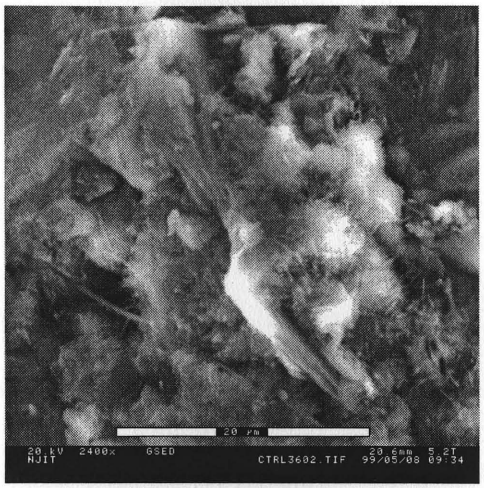

(b) Day 36, 2400x

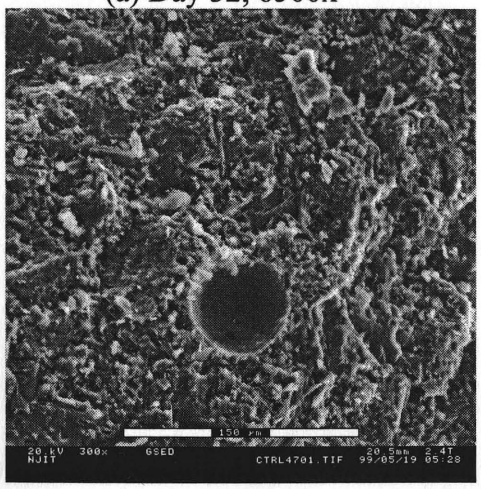

(c) Day 47, 300x

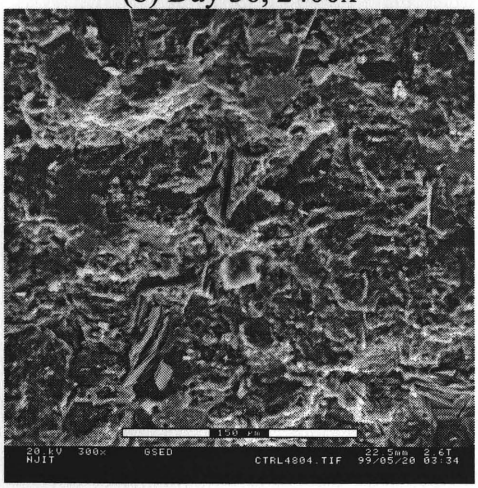

(d) Day 48, 300x

Figure 5.56 Micrographs of Cement Paste

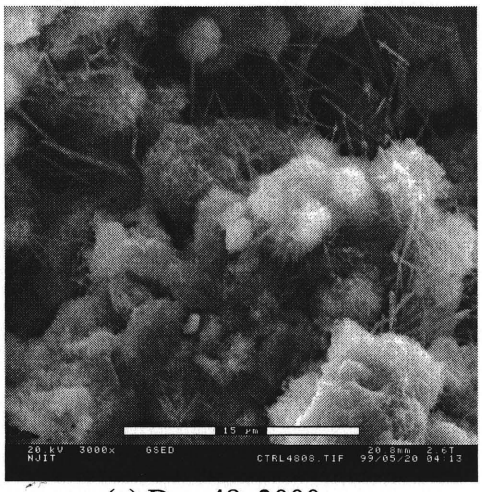

(e) Day 48, 3000x

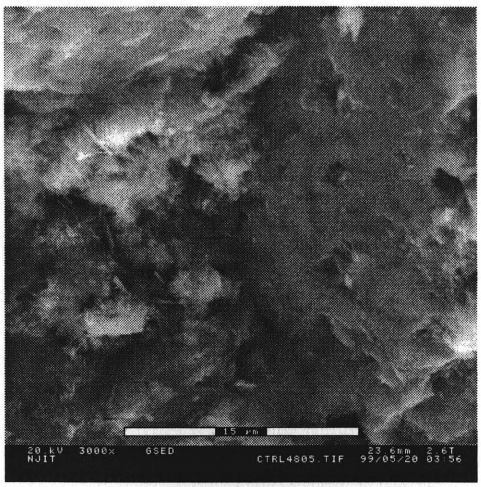

(f) Day 48, 3000x

Figure 5.56 Micrographs of Cement Paste (Continued)

The clusters of acicular C-S-H became denser and larger as time progressed. These silicate phases are present as either masses of plates or of splines (Lea, 1971). Figure 5.56 (b) clearly shows these morphologies of silicates. The hardened paste became denser and less permeable (Figures 5.56 (c) and (d)).

Even at the age of 48 days, morphologies typical of early-stage hydration products are still present as shown in Figure 5.56 (e). Ettringite which is usually encountered in young cement paste was found to grow into the capillary pores between cement grains. This may be because the cement grains were too distant from one another for C-S-H to develop intermeshed network across the capillary channels that once held water. In contrast, Figure 5.56 (f) shows cement grains in close contact forming a solid mass of rigid gel.

5.8.3.2 Raw MSWI Fly Ash-Cement Paste: The micrographs of the fracture surface of 15% raw fly ash-cement paste show less degree of hydration of the paste. Rigid mass seen in the pure cement paste is not present. Partially hydrated cement particles are seen to cover fly ash particles in Figures 5.57 (a) and (b). Small air pocket is also present in Figure 5.57 (c).

Short C-S-H spines (1 x 0.1 microns) and slender ettringite crystals (10 x 0.5 microns) are ubiquitous in Figures 5.58 (a) through (d). At very high magnification, a distinct structure can be seen to connect hydrated particles together forming a complex network (Figure 5.58 (c)). This honeycomb morphology is found in cement paste containing calcium chloride (Mindess and Young, 1981) which are major constituents in the paste.

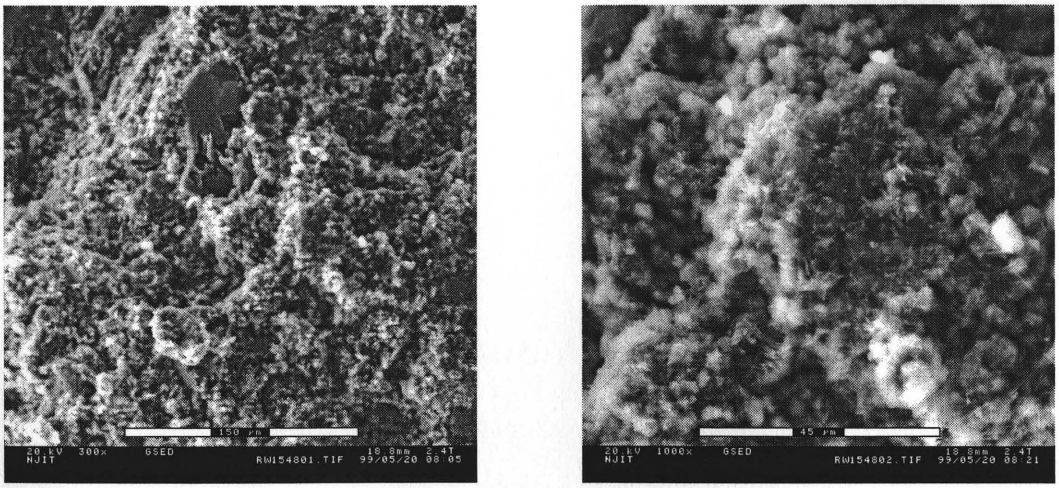

(a) 300x (b) 1000x

Figure 5.57 Micrographs of 15% Raw MSWI Fly Ash Paste at day 48

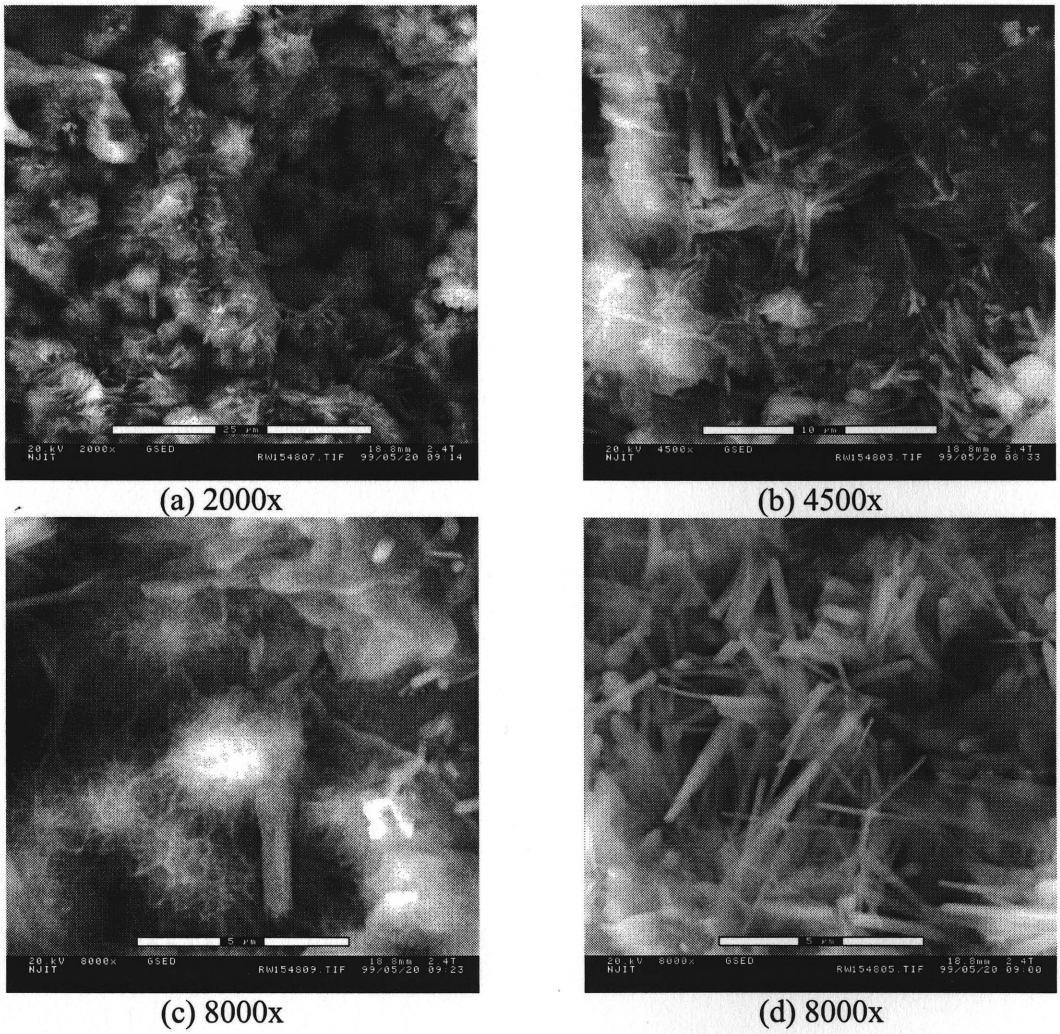

(a) 2000x (b) 4500x

(c) 8000x (d) 8000x

Figure 5.58 Micrographs of 15% Raw MSWI Fly Ash Paste at day 48

5.8.3.3 Fine MSWI Fly Ash-Cement Paste: Figures 5.59 (a) and (b) show micrographs of fracture surface of the pure fine fly ash paste at 42nd day. The paste did not solidify even after 42 days. Microscopic investigation was done by freezing the paste in liquid nitrogen and placing the specimen in a temperature-regulated environment of the ESEM with the help from a cold stage attachment. Fly ash particles and some hydration products are visible in Figure 5.59 (a) while cubic salt crystals are very noticeable at higher magnification in Figure 5.59 (b).

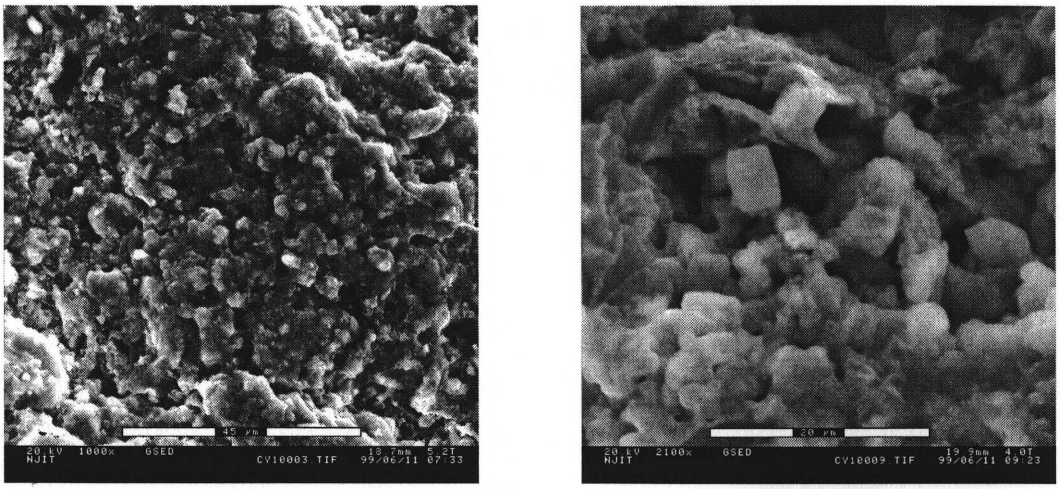

(a) 1000x (b) 2100x

Figure 5.59 Micrographs of 100% Fine MSWI Fly Ash Paste at day 42

Unlike the pure fly ash paste, the 15% fine fly ash-cement paste does not have visible salt crystals. This is confirmed by the XRD result in Section 5.3 as well. Its fracture surface shows the microstructures that are characteristics of cement hydration products. Mass of solid gel is shown in Figures 5.60 (a) and (e) while honeycombed C-S-H is shown in Figures 5.60 (d) and (e). C-S-H with short spikes is also present in pore. Ruptured platy CH crystals are also observed to be surrounded by C-S-H gel. $Ca(OH)_2$ only grows where free space is available. If it is impeded by another CH crystal, it may grow in another direction or stop growing. If its growth is obstructed by hydrating cement grains, it may grow around them (Mindess and Young, 1981).

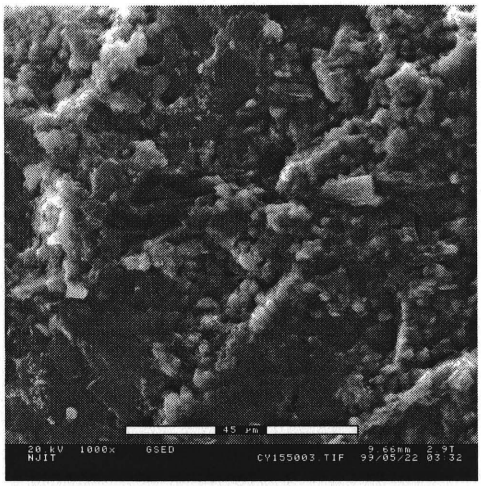

(a) 1000x

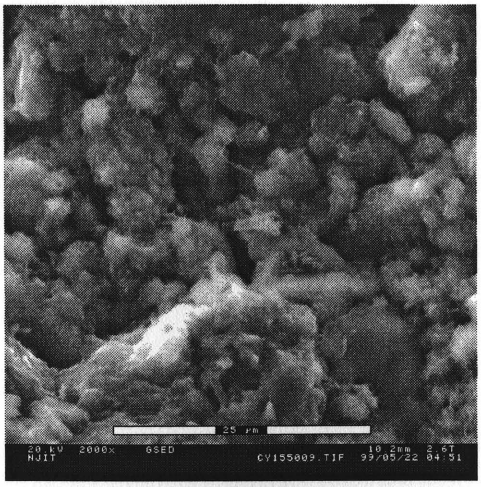

(b) 2000x

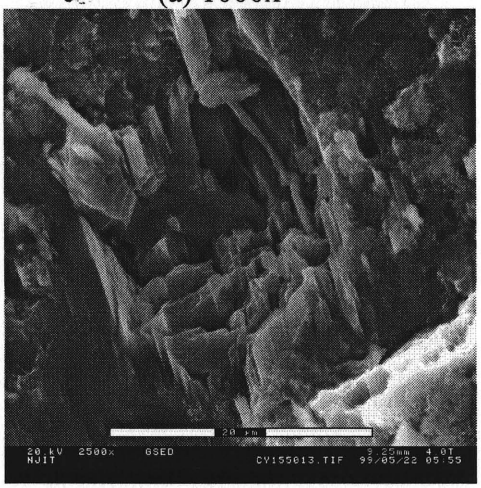

(c) 2500x

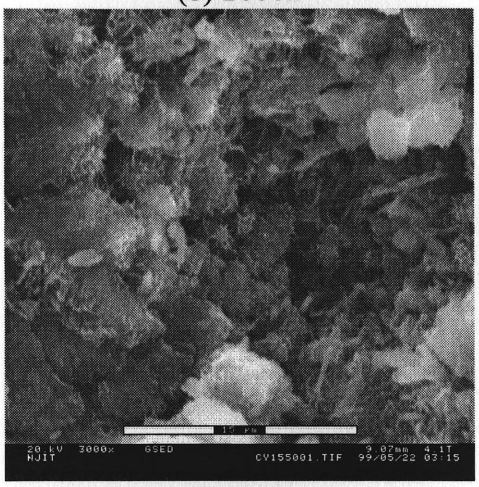

(d) 3000x

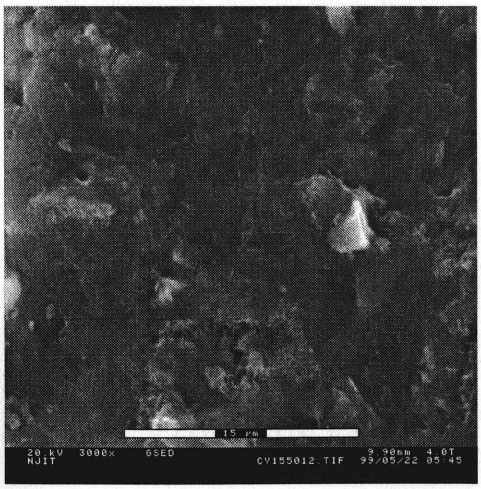

(d) 3000x

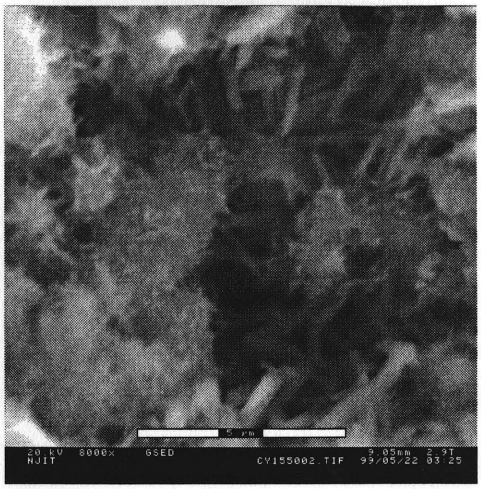

(e) 8000x

Figure 5.60 Micrographs of 15% Fine MSWI Fly Ash Paste at day 50

As with the pure MSWI fly ash paste, the cement paste incorporating 35% fine fly ash does not show distinct feature of hydration product. However, a small striated crystal can be seen in the middle of Figure 5.61 (a). From its morphology, it is very likely that it is a CH crystal.

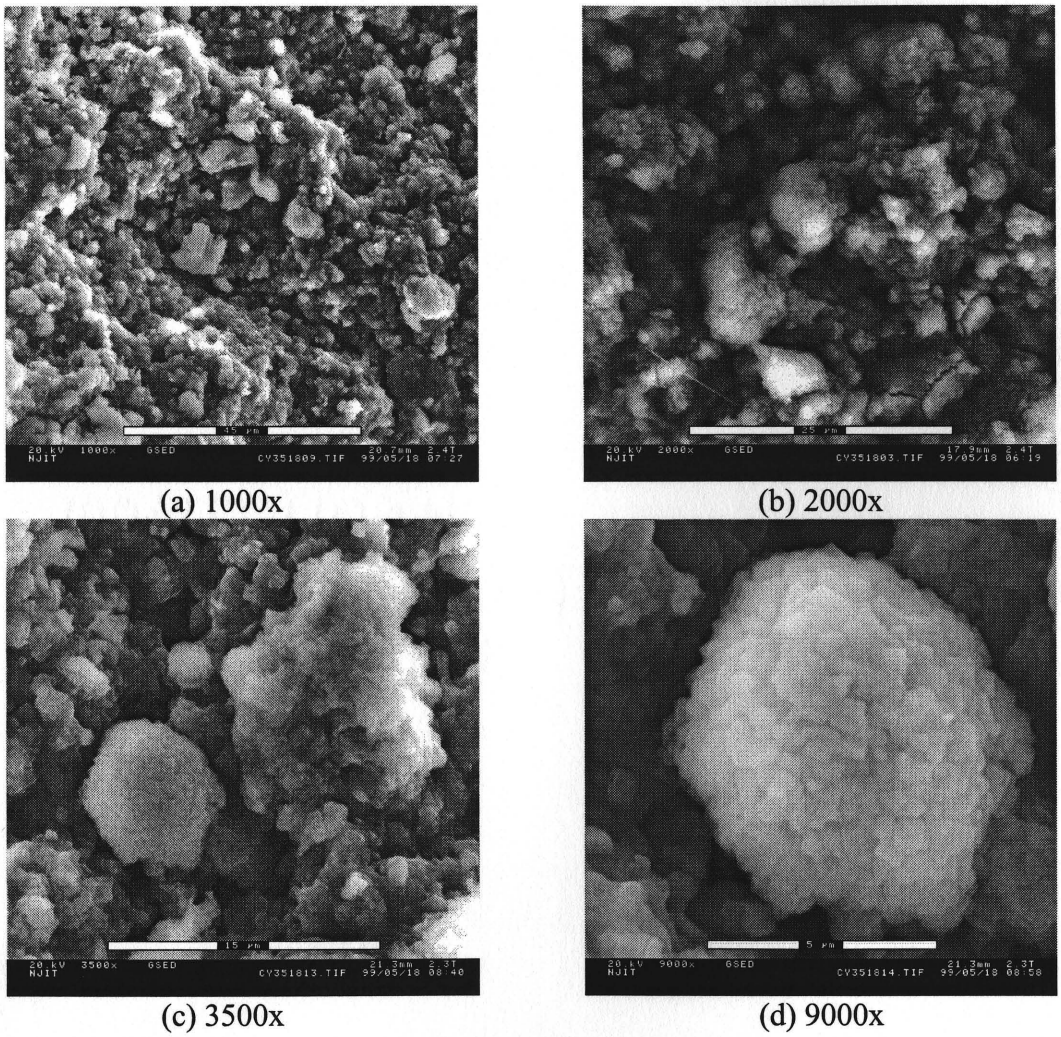

(a) 1000x (b) 2000x

(c) 3500x (d) 9000x

Figure 5.61 Micrographs of 35% Fine MSWI Fly Ash Paste at day 18

The fly ash particles appear to be covered by some salt crystals and hydration products not typical of cement. Figure 5.61 (d) shows rough surface of a particle covered by small crystals. The surface compositional information listed in Table 5.27 shows that

this crystal-covered particle has very high concentrations of Cl and Na. This is also true for the objects captured in Figures 5.61 (a) and (c).

Table 5.27 Semi-quantitative Surface Compositions of Objects in Selected Acquired Images in Figure 5.61

Ele.	(a)		(c)		(d)	
	Wt%	At%	Wt%	At%	Wt%	At%
O	9.35	20.61	10.23	21.34	9.08	20.02
Na	9.87	15.14	10.35	15.02	7.30	11.21
Mg	0.00	0.00	0.47	0.64	0.40	0.57
Al	1.47	1.93	2.59	3.20	1.51	1.97
Si	1.46	1.84	2.88	3.42	1.89	2.37
P	1.55	1.77	1.35	1.45	1.22	1.39
S	0.67	0.74	1.17	1.22	0.35	0.39
Cl	29.05	28.91	30.34	28.55	34.81	34.65
K	6.19	5.58	7.17	6.11	7.63	6.88
Ca	9.94	8.75	11.59	9.65	10.91	9.61
Ti	1.29	0.95	0.93	0.65	1.07	0.78
Cr	1.22	0.83	1.26	0.81	1.12	0.76
Mn	2.02	1.30	1.33	0.81	1.45	0.93
Fe	2.86	1.81	1.83	1.10	1.70	1.08
Cu	5.73	3.18	3.01	1.58	3.24	1.80
Zn	5.23	2.82	3.31	1.69	4.33	2.34
As	3.21	1.51	1.29	0.58	1.06	0.50
Cd	3.27	1.03	1.61	0.48	3.56	1.12
Sn	1.39	0.41	0.75	0.21	1.77	0.53
Sb	1.50	0.43	3.89	1.07	1.34	0.39
Pb	2.70	0.46	2.64	0.43	4.29	0.73
Total	99.97	100.00	99.99	100.01	100.03	100.02

5.9 Treated MSWI Fly Ash as a Fine Aggregate

MSWI fly ash from a proprietary treatment process (NJIT 1) was used to directly replace sand in mortar mixes at water-to-cement ratios of 0.45, 0.50, and 0.55. However, due to large quantity of NJIT 1 fly ash used (cement:fly ash = 1:2.75) and its high water absorption capacity as discussed in Section 5.1.6, water was adsorbed onto fly ash surfaces, leaving none to fluidize the mixes. Consequently, all of the mortar mixes at different water-to-cement ratios were very dry, making it impossible to cast into molds. Indeed, all of the mixes had to be rejected.

Obviously, NJIT 1 fly ash is not suitable for use as a total fine aggregate replacement, although partial replacement of fine aggregate may be worth investigating. Having realized this problem, one should shift his further interest in fly ash utilization toward NJIT 2 fly ash, which was acquired from a conventional APC system, as will be discussed in the following sections.

5.10 Effect of Fractionated MSWI Fly Ash on Strength Development of Mortars

Jaturapitakkul (1993) among other researchers found that performance of cement mortars with up to 15% replacement of cement by fine coal fly ash was equal to or better than that of control. Despite the fact that MSWI fly ash has somewhat different physical, chemical, and morphological properties from coal fly ash, fractionation may improve its strength properties and make it more useful in civil engineering applications. Similar principles of utilizing fine pozzolanic particles to enhance concrete strength exist in MSWI fly ash.

In this section, an attempt was made to investigate the influence of particle size of MSWI fly ash on the strength of mortars. As discussed earlier, the raw NJIT 2 fly ash was fractionated using an air classifier into two fractions; namely, fine and coarse. The raw (RW), fine (CY), and coarse (CC) fly ashes were used to replace 15%, 25%, and 35% of cement in mortar mixes while the water-to-binder ratio (w/(c+fa)) was maintained at 0.50. Strength development data of raw coal fly ash-cement mortars (MO) at the same replacement and water-to-binder ratio were given for comparison (Bumrongjaroen, 1999). Sample identification for the reference coal fly ash-cement mortars is of the form, MOxx, where xx represents the replacement percentage. For example, MO00 is a control mortar series that did not incorporate coal fly ash while MO15 is a mortar series that had 15% of its cement content replaced by coal fly ash. Tabulated strength results are provided in Appendix A.

It is understood from this experiment and other prior investigations that strength properties of fly ash-cement concrete and mortars may be negatively affected by inclusion of fly ash above certain levels of cement replacement. This occurs due to net reduction in the amount of reactive cementitious components of the mixtures. These

components are responsible for forming strength-providing hydration products, especially calcium silicate hydrates [C-S-H].

5.10.1 Compressive Strength of Fractionated MSWI Fly Ash Mortar with 15% Replacement

As seen in Figure 5.62, the compressive strengths of mortars incorporating 15% raw (RW115) and fractionated MSWI fly ashes (CY115 and CC115) outperformed control mortars (C50 and MO00) and 15% coal fly ash-cement mortars (MO15) at the age of as early as 3 days.

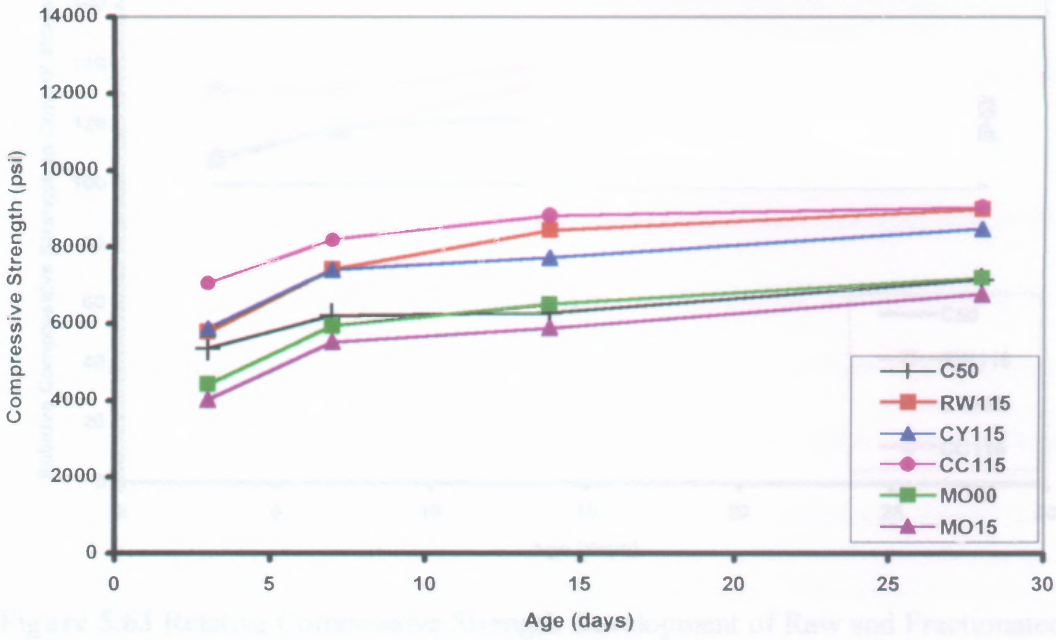

Figure 5.62 Compressive Strength Development of Raw and Fractionated MSWI Fly Ash-Cement Mortars with 15% Replacement

In fact, Figure 5.63 shows that the 28-day compressive strength of coarse fly ash mortars (CC115) exceeded that of control (C50) by as much as 40% (8810 psi) at day 14 and 27% (9028 psi) at day 28. All other MSWI fly ash-cement mortars also exhibited

superior strength development than the control, with more than 8472 psi or 119% of the control at the age of 28 days (CY115). Raw fly ash mortars (RW115) had lower early strength than coarse fly ash mortars (5772 psi vs. 7044 psi at day 3, but the 28-day compressive strength was comparable to that of coarse fly ash mortars (8976 psi vs. 9028 psi). Fine fly ash mortars had the lowest strength of all with 8472 psi or 119% at day 28 although that was still significantly higher than those of control (7134 psi) and coal fly ash mortars (6744 psi).

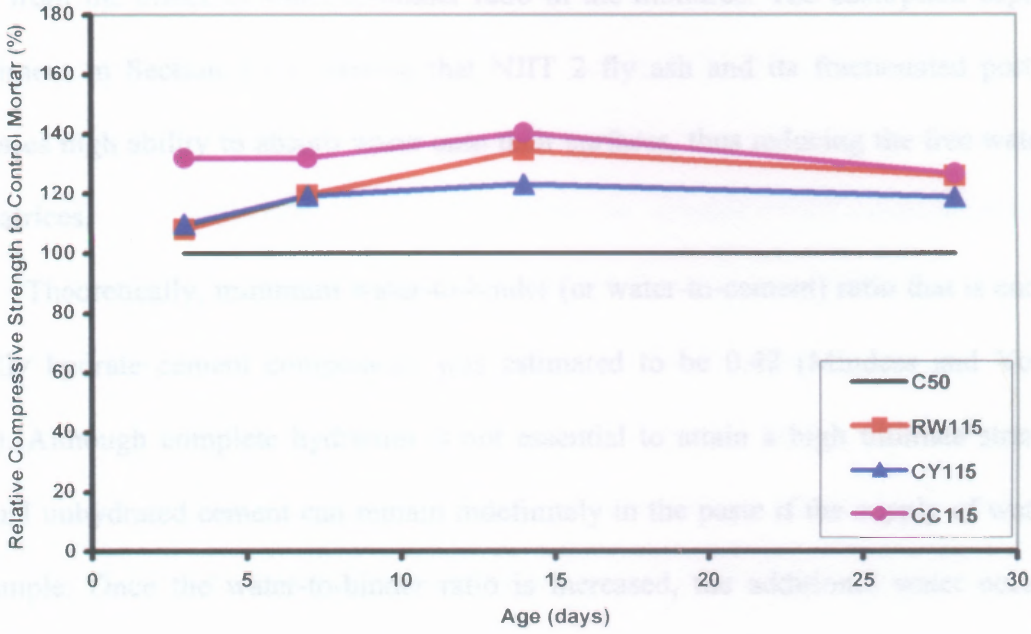

Figure 5.63 Relative Compressive Strength Development of Raw and Fractionated MSWI Fly Ash-Cement Mortars with 15% Replacement

The observed superior strength performance of MSWI fly ash-cement mortars was unexpected since MSWI fly ash mortars had less reactive cement components than control. MSWI fly ash did not demonstrate self-cementitious characteristic due to the fact that the paste did not solidify throughout the course of the study. Investigation on

hydration of fine fly ash (CY100) paste in Section 5.7 showed that fly ash by itself did not produce any hydration product that is similar to those of cement. Therefore, the additional strength must have come from other mechanisms.

Normally, hydration of cement components is dominated by rapid hydration of C_3S, the most abundant component, to produce C-S-H gel. The facts that the MSWI fly ash-cement mortars had less reactive components due to cement replacement and that MSWI fly ash is not self-cementitious point to another mechanism that may not involve chemical reactions. High early compressive strengths of the fly ash mixtures may have come from the effect of water-to-binder ratio in the mixtures. The absorption capacity experiment in Section 5.1.6 showed that NJIT 2 fly ash and its fractionated portions possesses high ability to absorb water onto their surfaces, thus reducing the free water in the matrices.

Theoretically, minimum water-to-binder (or water-to-cement) ratio that is enough to fully hydrate cement components was estimated to be 0.42 (Mindess and Young, 1981). Although complete hydration is not essential to attain a high ultimate strength, residual unhydrated cement can remain indefinitely in the paste if the supply of water is not ample. Once the water-to-binder ratio is increased, the additional water occupies space that later turns into capillary pores when it evaporates. These newly created pores negatively affect the compressive strength property of concrete. Therefore, it may be concluded that the MSWI fly ash absorbed water, thereby reducing the effective water-to-binder ratio. Available water might still be enough for hydration of cement since a portion of cement was replaced by fly ash. Since there was less free water occupying the

capillary pores, porosity caused by evaporation of water might be reduced. This could thus be responsible for high early strength.

As previously discussed in Section 5.8, semi-quantitative analyses of fracture surfaces of MSWI fly ash-cement pastes showed very high calcium and chloride contents. The XRD analyses in Sections 5.3 and 5.7 confirmed the presence of calcium chloride hydroxide [CaClOH] and calcium chloride hydroxide hydrate [$CaCl_2.Ca(OH)_2.H_2O$] in MSWI fly ashes and pastes.

Calcium chloride is an accelerating admixture. An optimal dose (Type I calcium chloride, 77% pure) of 2-4% by weight of cement will approximately double the 1-day compressive strength of concrete (Mindess and Young, 1981; Lea, 1971). However, the increase diminishes with time. Moreover, high contents of calcium chloride and excess lime in NJIT 2 fly ashes may form hydrated calcium chloride which could solidify and fill pores, thus providing some mechanical strength to the specimens (Chandler, 1997).

Shi (1996, 1998) showed that addition of $CaCl_2$ (4% by weight) induced consumption of $Ca(OH)_2$ in class F (low calcium) coal fly ash-lime pastes and that $C_3A.CaCl_2.10H_2O$ (hydrocalumite) was produced in significant amount by that reaction. $C_3A.CaCl_2.10H_2O$ was found to provide better strength in $CaCl_2$ activated lime-fly ash paste than in control. Investigation on hydrolysis of MSWI fly ash-cement pastes in Section 5.7 revealed that significant formation of $C_3A.CaCl_2.10H_2O$ was detected in addition to C-S-H in MSWI fly ash-cement pastes. This may explain the superior strength properties of maturing MSWI fly ash-cement mortar specimens since mortars containing coarse fly ash, which is enriched with CaClOH and $CaCl_2.Ca(OH)_2.H_2O$, exhibited the highest strength.

In contrast to coal fly ash (Jaturapitakkul, 1993), particle size does not seem to have a significant influence on the strength of the MSWI fly ash-cement mortars. Rather, water absorption capacity and chemical reactions involving calcium chloride, can greatly affect the strength of MSWI fly ash-cement mortars. This is evident in Figures 5.62 and 5.63 that show higher 28-day compressive strength of raw fly ash mortars (RW115, 8976 psi) than in fine fly ash mortars (CY115, 8472 psi). This behavior may be due to the fact that fine fly ash contains the lowest amount of CaClOH and $CaCl_2.Ca(OH)_2.H_2O$ as shown in the XRD results in Section 5.3.2.

However, it remains to be seen if the very fine particles of MSWI fly ash, e.g. smaller than 10 microns, can affect the strength properties of MSWI fly ash-cement pastes in the future work.

5.10.2 Compressive Strength of Fractionated MSWI Fly Ash Mortar with 25% Replacement

Once cement replacement percentage was increased from 15% to 25%, compressive strengths of all MSWI fly ash-cement mortars decreased. In fact, Figure 5.64 shows that the strengths of raw and fine MSWI fly ash-cement mortars were lower than those of coal fly ash and controls. With 25% replacement, the strengths of raw (RW125) and fine (CY125) MSWI fly ash mortars were roughly 65% of that of control at day 1. After 28 days of curing, the strengths increased to only as high as 88% (CY125). Unlike raw and fine MSWI fly ash mortars, coarse fly ash mortar (CC125) exhibited higher early strength of 88% of the control at day 1 and 99% at day 28.

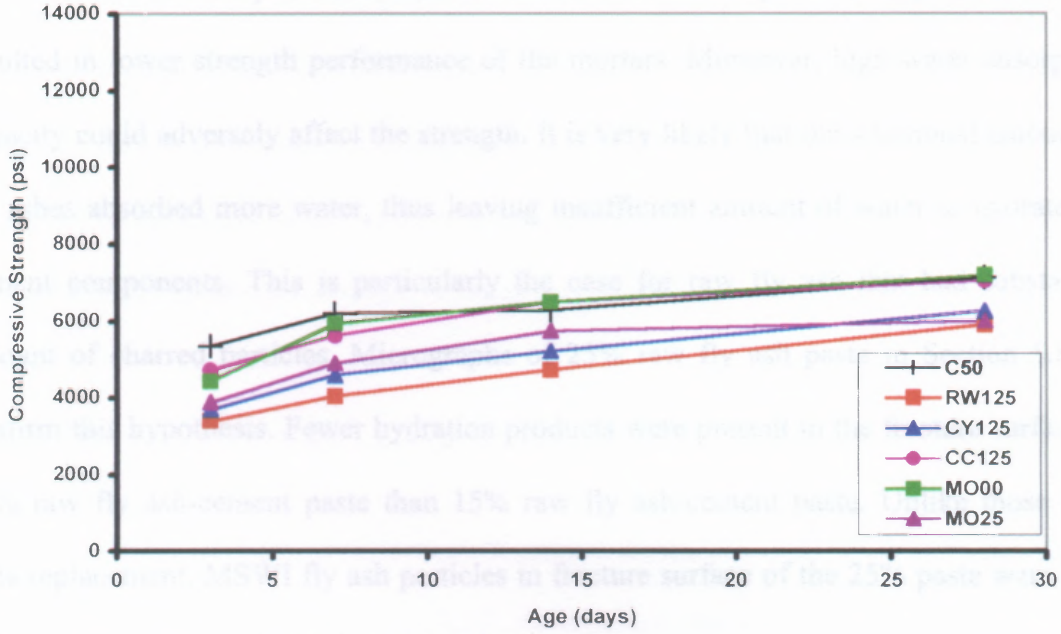

Figure 5.64 Compressive Strength Development of Raw and Fractionated MSWI Fly Ash-Cement Mortars with 25% Replacement

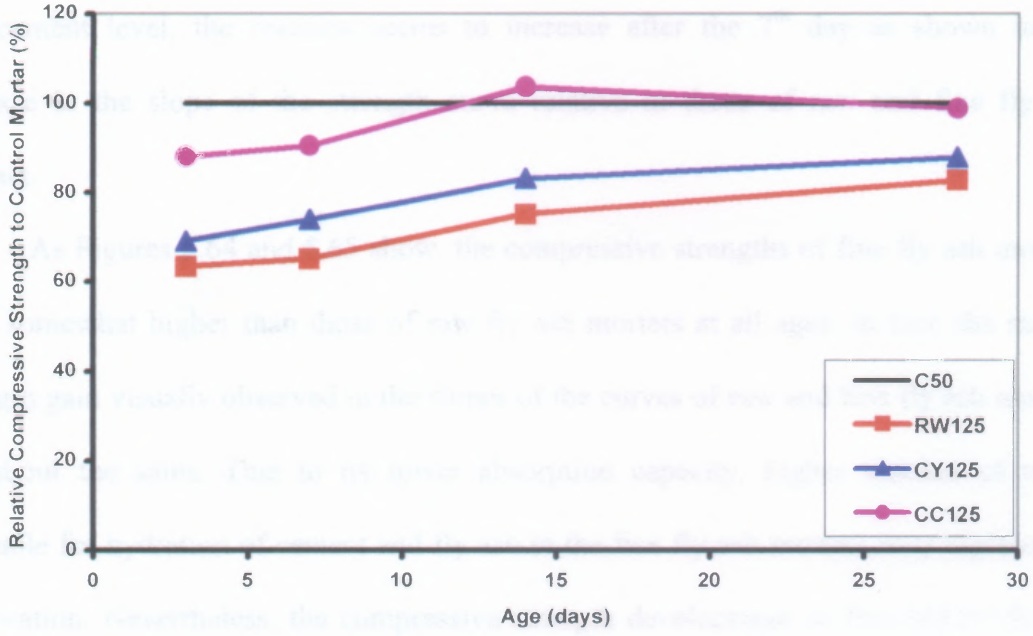

Figure 5.65 Relative Compressive Strength Development of Raw and Fractionated MSWI Fly Ash-Cement Mortars with 25% Replacement

Since MSWI fly ashes are not self-cementitious, their presence in place of cement resulted in lower strength performance of the mortars. Moreover, high water absorption capacity could adversely affect the strength. It is very likely that the additional amount of fly ashes absorbed more water, thus leaving insufficient amount of water to hydrate the cement components. This is particularly the case for raw fly ash that had substantial amount of charred particles. Micrographs of 25% raw fly ash paste in Section 5.8.1.2 confirm this hypothesis. Fewer hydration products were present in the fracture surface of 25% raw fly ash-cement paste than 15% raw fly ash-cement paste. Unlike those with 15% replacement, MSWI fly ash particles in fracture surface of the 25% paste were seen without being covered by hydration products.

The highest strength found in mortars containing coarse MSWI fly ash (CC125) might be attributable to the formation of additional $C_3A.CaCl_2.10H_2O$ which was induced by high concentration of calcium chloride in the coarse fly ash. Similar to that of the 15% replacement level, the reaction seems to increase after the 7^{th} day as shown in the increase in the slope of the strength curve relative to those of raw and fine fly ash mortars.

As Figures 5.64 and 5.65 show, the compressive strengths of fine fly ash mortars were somewhat higher than those of raw fly ash mortars at all ages. In fact, the rate of strength gain visually observed in the slopes of the curves of raw and fine fly ash mortars are about the same. Due to its lower absorption capacity, higher amount of water available for hydration of cement and fly ash in the fine fly ash mortars may explain this observation. Nevertheless, the compressive strength development of fine MSWI fly ash was quite low. It was the lowest at the replacement percentage of 15%. In fact, it would

have been the lowest if the strength of raw fly ash mortar had not suffered from the effect of high absorption. As the diffractogram of fine fly ash in Section 5.3.2 shows, unlike coarse fly ash, it contained low concentration of CaClOH and $CaCl_2.Ca(OH)_2.H_2O$. As a result, chemical reactions involving calcium chloride might be minimized. This might be responsible for the inferior strength development at different replacement levels.

5.10.3 Compressive Strength of Fractionated MSWI Fly Ash Mortar with 35% Replacement

The compressive strength development of cement mortars incorporating 35% fine MSWI fly ash is shown in Figures 5.66 and 5.67. As expected, the strength was much lower than those of control and reference coal fly ash.

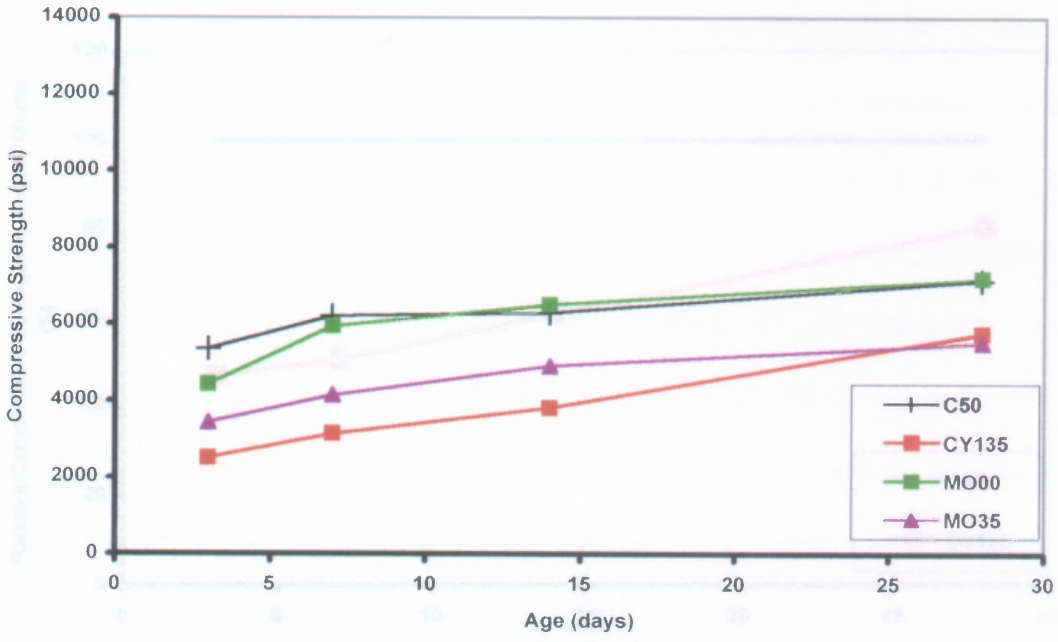

Figure 5.66 Compressive Strength Development of Fractionated MSWI Fly Ash-Cement Mortars with 35% Replacement

The net reduction in active cementitious components due to replacement by less reactive fine MSWI and coal fly ashes is responsible for the low strengths of both fine MSWI fly ash (CY135) and coal fly ash (MO35) mortars. The higher water absorption capacity of fine fly ash may also cause its early strength to be much lower than control (40% of the control strength) and coal fly ash. The relative compressive strengths of fine MSWI fly ash and coal fly ash mortars gradually increased with age. However, as reflected by the change in the slope from day 14 to day 28, fine fly ash mortars seemed to have gained more strength than the coal fly ash mortars. The average 28-day compressive strength of the fine fly ash mortars was slightly higher than that of the coal fly ash mortars (5741 psi vs. 5500 psi). This may be due to the pozzolanic reaction of the fine MSWI fly ash that was in effect at later ages.

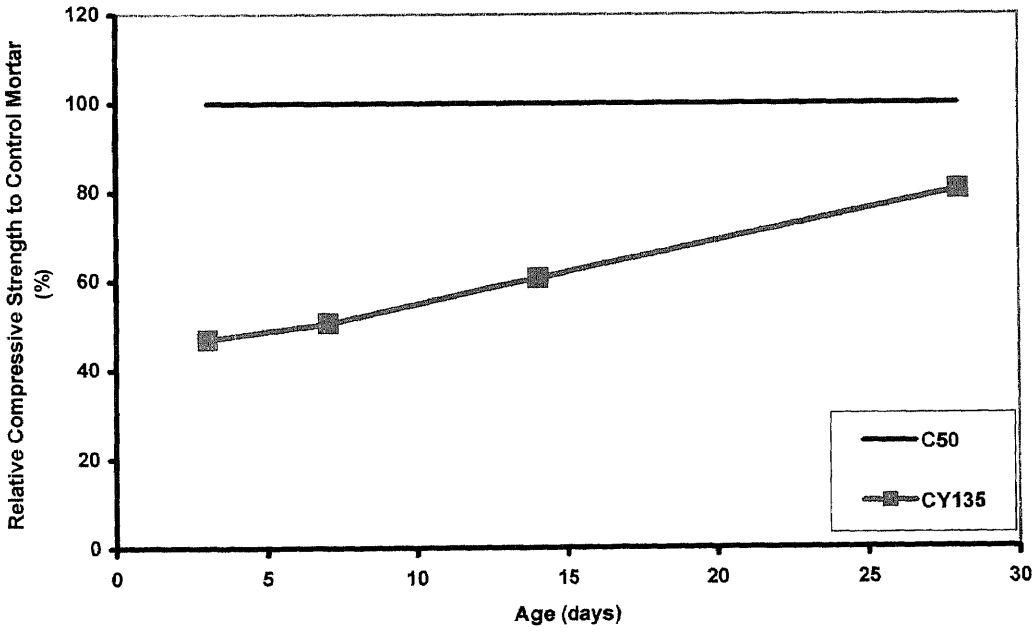

Figure 5.67 Relative Compressive Strength Development of Fractionated MSWI Fly Ash-Cement Mortars with 35% Replacement

It is important to note that due to high water absorption capacities of raw and coarse MSWI fly ash, preparation of mortars containing 35% of both materials was unsuccessful. The lower absorption capacity of fine NJIT 2 fly ash (Section 5.1.6) enabled it to be cast successfully although the mortar specimens were full of large voids as a result of inadequate compaction.

5.11 Effect of Water-to-Binder Ratio (w/(c+fa)) on the Strength of Mortars

The primary factor that governs the strength of brittle materials, particularly concrete, is capillary porosity. Difficulty involved in measurement or prediction of this quantity makes it inappropriate to be used in mix design of concrete. Water-to-cement ratio (w/c) or water-to-binder ratio (w/(c+fa)) directly influences the porosity and thus it can be used as a simplified specification in the design of properly compacted concrete.

At each cement replacement levels of 15%, 25%, and 35%, raw (RW), fine (CY), and coarse (CC) MSWI fly ashes were used to prepare 2"x2"x2" mortar cubes at the water-to-binder ratios of 0.45, 0.50, and 0.55. Sample identification is in the form of ABwxx, where AB represents the type of MSWI fly ash; w the water-to-binder ratio with 1 being 0.50, 2 being 0.45, and 3 being 0.55; xx the replacement percentage. For instance, CC225 refers to a mortar series prepared with 25% coarse MSWI fly ash at the water-to-binder ratio of 0.45. Control mortars that did not incorporate any fly ash were also prepared for each water-to-binder ratio: C45, C50, and C55. Compressive strengths of the mortars were measured at the age of 3, 7, 14, and 28 days. The tabulated compressive strength results of all mortar samples are provided in Appendix A.

5.11.1 Compressive Strengths of Fractionated MSWI Fly Ash Mortars with 15% Replacement

The compressive strengths of cement mortars with 15% replacement by raw and fractionated (fine and coarse) NJIT 2 fly ashes at different water-to-binder ratios are graphically illustrated in Figure 5.68.

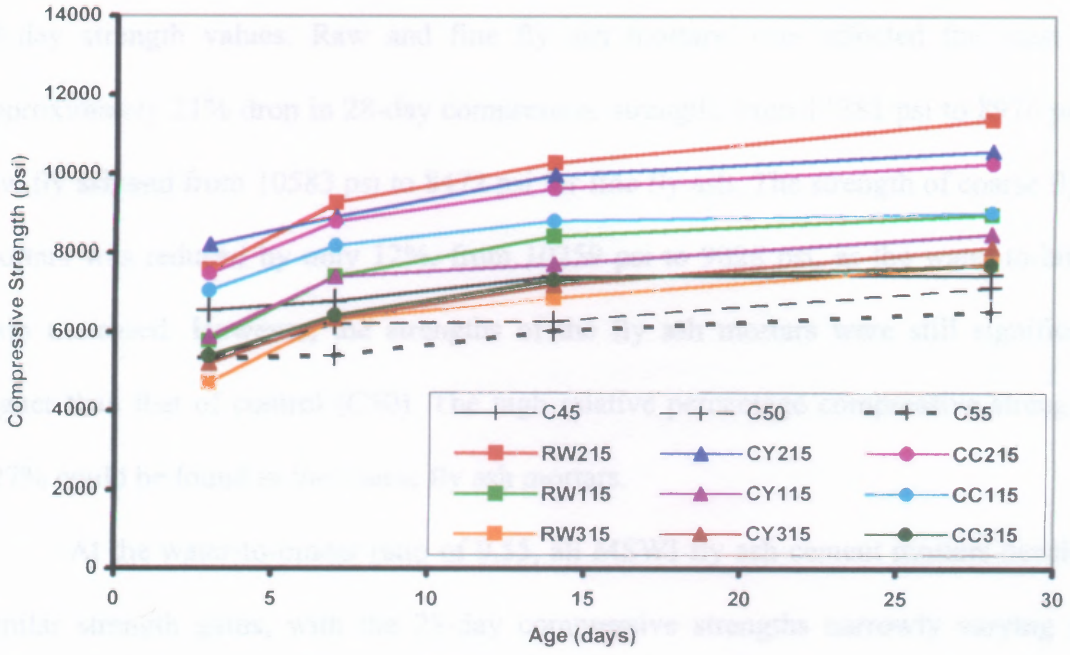

Figure 5.68 Compressive Strength Development of Raw and Fractionated MSWI Fly Ash-Cement Mortars with 15% Replacement at different w/(c+fa) ratios

As anticipated, the compressive strengths of control mortars increased as the water-to-binder ratio was lowered. At the water-to-binder ratio of 0.45, all MSWI fly ash mortars (RW215, CY215, and CC215) exhibited high compressive strengths. In fact, the 28-day strengths of these mortars exceeded 10,000 psi, or more than 138% (CC215) of the control mortar (C45). The raw MSWI fly ash mortars (RW215) went as high as 11,381 psi (153%) in compressive strength at 28 days. The superior performance of these

MSWI fly ash mortars might have come from the combined effects of high water absorption capacity and chemical reactions involving calcium chloride. The high surface areas of MSWI fly ash particles observed in Section 5.6 might also facilitate the chemical reactions by providing reaction sites for the calcium phases.

With increased amount of water (w/(c+fa)=0.50), the compressive strengths of MSWI fly ash mortars dropped, ranging from 8472 psi (CY115) to 9028 psi (CC115) in 28-day strength values. Raw and fine fly ash mortars were affected the most with approximately 21% drop in 28-day compressive strength, from 11381 psi to 8976 psi for raw fly ash and from 10583 psi to 8472 psi for fine fly ash. The strength of coarse fly ash mortars was reduced by only 12%, from 10259 psi to 9028 psi, as the water-to-binder-ratio increased. However, the strengths of the fly ash mortars were still significantly higher than that of control (C50). The high relative percentage compressive strength of 127% could be found in the coarse fly ash mortars.

At the water-to-binder ratio of 0.55, all MSWI fly ash-cement mortars developed similar strength gains, with the 28-day compressive strengths narrowly varying from 7703 psi (CC315) to 8142 psi (CY315). The strengths were still higher than that of control by as much as 125% (CY315). Reduction in 28-day compressive strength, which was caused by the increase in water-to-binder ratio from 0.50 to 0.55, by as much as 15% was found in raw fly ash mortars, from 8976 psi to 7726 psi, and coarse fly ash mortars, from 9028 psi to 7703 psi. The 28-day strength of fine fly ash mortars decreased by only 4%, from 8472 psi down to 8142 psi.

5.11.2 Compressive Strengths of Fractionated MSWI Fly Ash Mortars with 25% Replacement

As more cement was replaced by MSWI fly ashes, the compressive strengths of MSWI fly ash mortars fell to below those of the controls at each water-to-binder ratio. Reduction in active cement components caused the mixtures to develop weaker matrices, resulting in inferior strength performance.

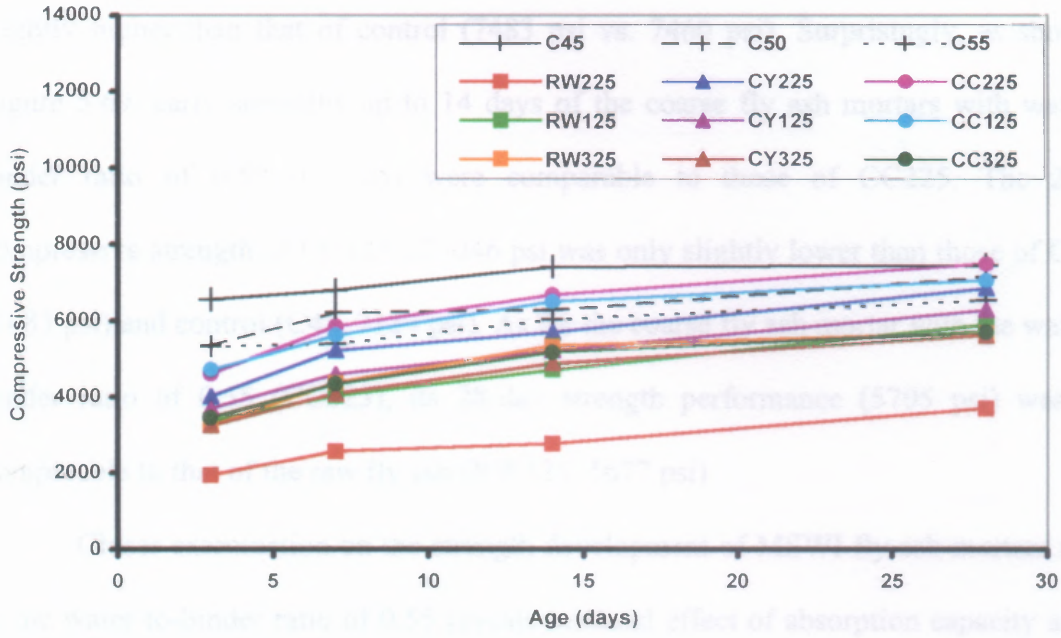

Figure 5.69 Compressive Strength Development of Raw and Fractionated MSWI Fly Ash-Cement Mortars with 25% Replacement at different w/(c+fa) ratios

Upon first notice, it is apparent in Figure 5.69 that, unlike the 15% replacement, the compressive strength developments of cement mortars with 25% replacement by MSWI fly ashes cannot be categorized into three groups according to their water-to-binder ratios. Absorption capacities of the fly ashes seemed to have the biggest influence on the strengths. Evidently, the raw fly ash mortars with the water-to-binder ratio of 0.45 (RW225) had the worst strength performance. Its highest ability to absorb water actually

caused the mix to be dry, resulting in large voids in the specimens. That, in turn, caused the specimens to fail at very low compression loads. Once the amount of water in the mixes was increased, the strengths of raw fly ash mortars increased, 7046 psi for RW125 and 5677 psi for RW325.

Coarse MSWI fly ash-cement mortars performed better than raw and fine fly ash-cement mortars at the same water-to-binder ratio. Indeed, the 28-day compressive strength of the coarse fly ash mortars with the water-to-binder ratio of 0.45 (CC225) was slightly higher than that of control (7483 psi vs. 7460 psi). Surprisingly, as shown in Figure 5.69, early strengths up to 14 days of the coarse fly ash mortars with water-to-binder ratio of 0.50 (CC125) were comparable to those of CC225. The 28-day compressive strength of CC125 of 7046 psi was only slightly lower than those of CC225 (7483 psi) and control (C45, 7134 psi). As for the coarse fly ash mortar with the water-to-binder ratio of 0.55 (CC325), its 28-day strength performance (5705 psi) was only comparable to that of the raw fly ash (RW325, 5677 psi)

Closer examination on the strength development of MSWI fly ash mortars mixed at the water-to-binder ratio of 0.55 reveals minimal effect of absorption capacity as well as chemical reactions. This is evident by very similar strength development of the fly ash mortars. At day 28, all of them performed only 87% of the control (C55).

5.11.3 Compressive Strength of Fractionated MSWI Fly Ash Mortar with 35% Replacement

Figure 5.70 shows compressive strengths of fine fly ash mortars mixed at the water-to-binder ratios of 0.50 and 0.55. Due to inadequate amount of water available for mixing, the workability of the fine fly ash mortar paste mixed at 0.45 was so low that casting was

impossible. Even at higher water-to-binder ratios, hardened mortar specimens were full of large voids, thereby resulting in low strengths.

Early strengths up to 14 days of CY135 and CY335 were almost equal. However, CY135 was able to develop better strength at 28 days possibly due to the chemical reactions involving calcium chloride and the pozzolanic reactions. The same was not true for CY335 of which the 28-day strength was largely influenced by the porosity of the mortars.

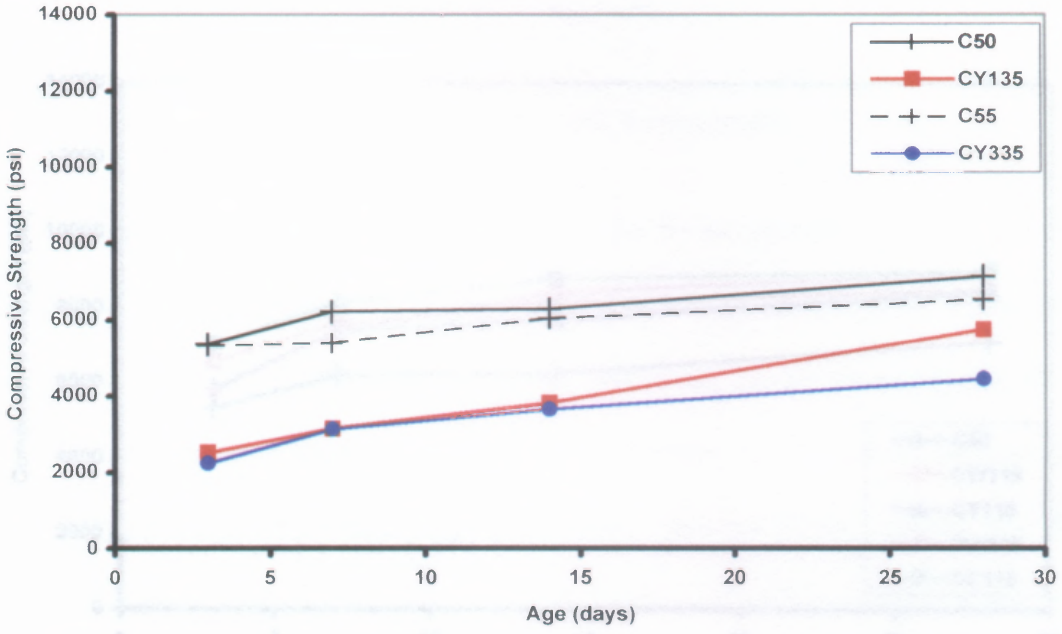

Figure 5.70 Compressive Strength Development of Raw and Fractionated MSWI Fly Ash-Cement Mortars with 35% Replacement at different w/(c+fa) ratios

5.12 Effect of MSWI Fly Ash Washing on the Strength Mortars

As discussed earlier in Sections 5.2.3 and 5.3.3, washing of fine MSWI fly ash reduced significant amounts of soluble phases containing Na by as much as 85.5% and Cl by

72.9%. However, the dilution effect made less soluble phases more concentrated as evident by the increases in Al by as much as 49.1% and Ca by 13.2%. Both the XRF and the EDX results of the fracture surfaces of washed fine fly ash-cement pastes showed very low concentration of Cl (as low as 0.5% by weight). It appears that the formation of hydrocalumite [$C_3A.CaCl_2.10H_2O$] was insignificant. Diffractogram of washed fine fly ash showed more anhydrite [$CaSO_4$], which was used in the production of ettringite, which contributes to early strength, shown in the micrographs in Sections 5.8.1.5 and 5.8.2.5.

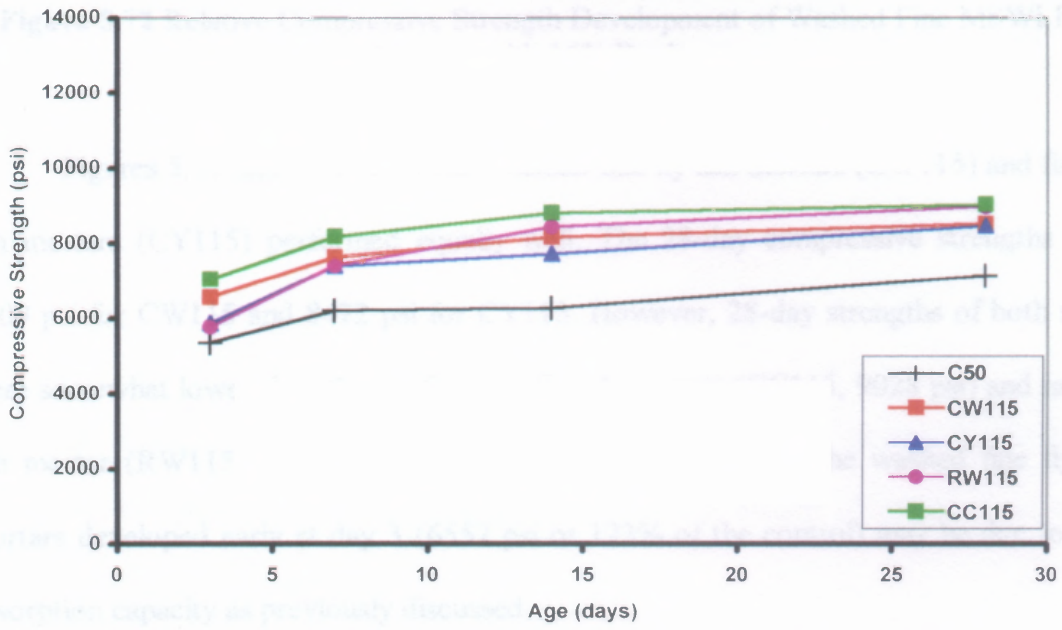

Figure 5.71 Compressive Strength Development of Washed Fine MSWI Fly Ash Mortars with 15% Replacement

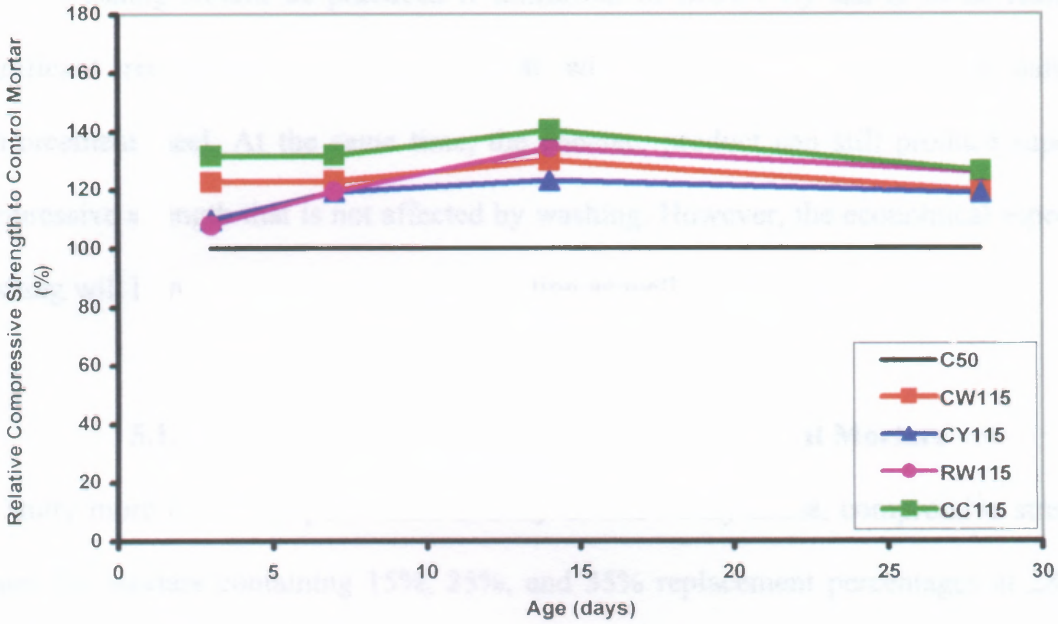

Figure 5.72 Relative Compressive Strength Development of Washed Fine MSWI Fly Ash Mortars with 15% Replacement

Figures 5.71 and 5.72 show that washed fine fly ash mortars (CW115) and fine fly ash mortars (CY115) performed equally well. The 28-day compressive strengths were 8509 psi for CW115 and 8472 psi for CY115. However, 28-day strengths of both series were somewhat lower than those of coarse fly ash mortars (CC115, 9028 psi) and raw fly ash mortar (RW115, 8976 psi). High compressive strength of the washed fine fly ash mortars developed early at day 3 (6557 psi or 123% of the control) may be due to high absorption capacity as previously discussed.

As discussed in Section 5.8, hydration of washed fine fly ash-cement mortar paste was in more advanced hydration stages, showing more C-S-H and ettringite productions, than other fly ash mortars at the same age. This is probably why its strengths at later ages were comparable to others although hydrocalumite was not produced as much.

Washing should be practiced if utilization of MSWI fly ash is to be realized. Significant reduction in chloride content will produce concrete that is safe to reinforcement steel. At the same time, the concrete product can still produce superior compressive strength that is not affected by washing. However, the economical aspect of washing will have to be taken into consideration as well.

5.13 Pozzolanic Activity of MSWI Fly Ash-Cement Mortars

To study more about the pozzolanic activity of MSWI fly ashes, compressive strength values for mortars containing 15%, 25%, and 35% replacement percentages at 28-day curing time and at the water-to-binder ratios of 0.45, 0.50, and 0.55 were measured. Strength gains for each mix series can then be calculated from the following formula (Payá et al., 1996).

$$SG_i = R_i - \left(R_c \times \frac{w_c}{w_c + w_f} \right),$$

where R_i is the 28-day compressive strength of fly ash-cement mortar, R_c the 28-day compressive strength of control cement mortar, w_c the weight of cement, and w_f the weight of fly ash in the mix.

The formula is based on the assumption that strength of MSWI fly ash-cement mortar comes from two separate sources. First, the strength contributed by cement hydration that is directly proportion to its content in the mix. Typically, hydration of cement is rapid during the first 12 to 24 hours and reaches steady state thereafter. Second, the additional strength that comes from pozzolanic reactions brought about by MSWI fly

ash. Pozzolanic reactions involve first alkali dissolution of amorphous silica in fly ash particles. The processes are usually slow, thereby providing strength at later ages. More discussions regarding pozzolanic process are provided in Section 5.7. The calculated strength gains for MSWI fly ash-cement mortars mixed at each water-to-binder ratio are provided in Table 5.28 through 5.30.

It should be noted here, though, that the given formula could be used only for the sake of comparison since it does not take into account reactions and interactions between cement and MSWI fly ash, nor does it address the physical properties of the fly ash, e.g. water absorption capacity. MSWI fly ash may either aid or retard in the reactions, or form totally new strength-giving compounds with cement.

Table 5.28 28-day Compressive Strength Values and Calculated Strength Gains for Cement Mortars Incorporating NJIT 2 Fly Ashes with w/(c+fa) = 0.45

Fly ash	28-day Strength (psi)		Strength Gain (psi)	
	15%	25%	15%	25%
Raw (RW)	11381	3695	5040	-1900
Fine (CY)	10583	6840	4242	1245
Coarse (CC)	10259	7483	3918	1888

Table 5.28 and Figure 5.73 reveal that raw and fractionated NJIT 2 fly ashes presented high strength gain in excess of 3900 psi. at 15% replacement, especially the raw fly ash (5040 psi). As discussed in Section 5.7, $Ca(OH)_2$ contents of MSWI fly ash-cement pastes decreased sharply after 14 days of curing. The disappearance of $Ca(OH)_2$ at later age is indeed indicative of pozzolanic reactions which produce C-S-H gel at the expense of $Ca(OH)_2$. Microstructure examinations of the MSWI fly ash-containing

pastes in Section 5.8.3 showed evidence of extensive development of C-S-H and $Ca(OH)_2$.

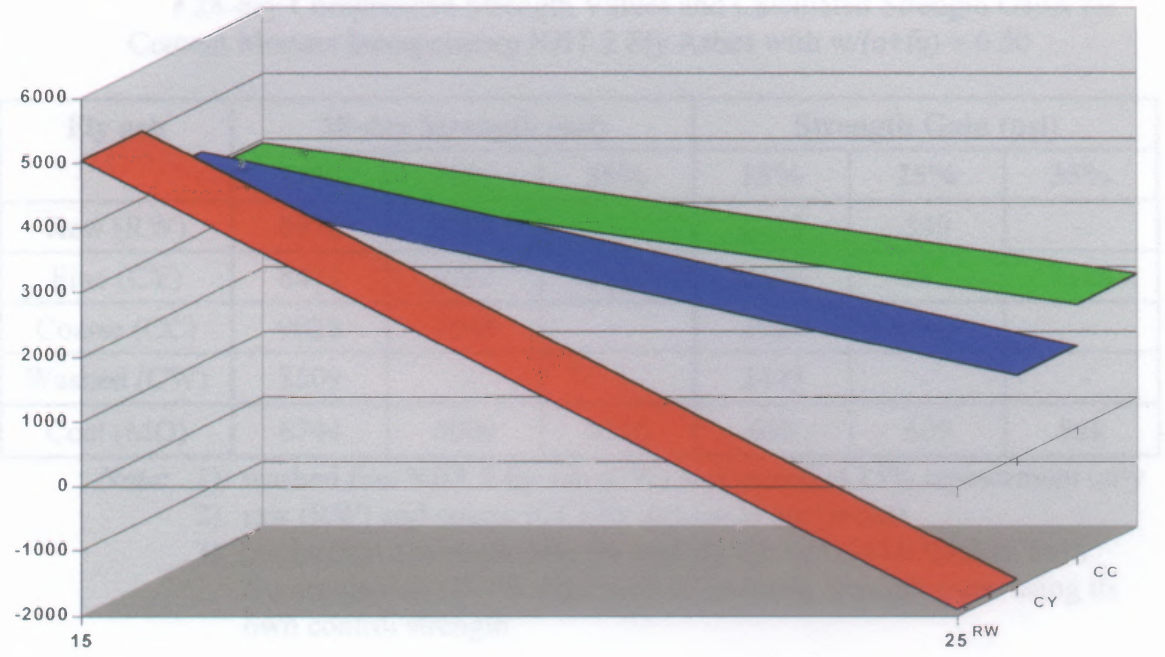

Figure 5.73 Compressive Strength Gains for MSWI Fly Ash-Cement mortars with w/(c+fa) = 0.45

The strength gains decreased as the replacement percentage increased from 15% to 25%, especially for the raw fly ash. This is because replacement of cement by fly ash, which is not self-cementitious, actually reduced the amount of active cement components responsible for forming strength-providing products, C-S-H. Also reduced was the key compound in pozzolanic reactions, $Ca(OH)_2$, which was not produced by hydration of MSWI fly ash alone. The strength gain of raw MSWI fly ash-cement mortar reached a negative value when the replacement was 25%. This is because the charred particles found in the raw fly ash absorbed water, thus leaving inadequate amount of water for the

mix. In fact, the mixture was so dry and sticky that it was not properly compacted. As a result, the cured mortars were full of large voids, which contribute to high porosity.

Table 5.29 28-day Compressive Strength Values and Calculated Strength Gains for Cement Mortars Incorporating NJIT 2 Fly Ashes with w/(c+fa) = 0.50

Fly ash	28-day Strength (psi)			Strength Gain (psi)		
	15%	25%	35%	15%	25%	35%
Raw (RW)	8976	5899	-	2912	549	-
Fine (CY)	8472	6263	5741	2408	913	1104
Coarse (CC)	9028	7046	-	2964	1696	-
Washed (CW)	8509	-	-	2445	-	-
Coal (MO)	6744	6000	5500	635	609	828

Note: 1) washed fine NJIT 2 fly ash (CW) was mixed at 15% replacement only
2) raw (RW) and coarse (CC) fly ash could not be cast
3) compressive strength data for coal fly ash series (MO) taken from Bumronjaroen (1999) were used to calculate strength gains using its own control strength

Table 5.29 lists the strength gains of MSWI fly ash-cement mortars mixed at the water-to-binder ratio of 0.50. Apparently, the strength gains at the replacement percentage of 15% for all mortars were as high as 2964 psi (CC). The raw fly ash mortar also had a very high strength gain of 2912 psi. Fine and washed fly ash had comparable strength gains of 2408 and 2445 psi, respectively. However, once the replacement increased from 15 to 25%, the strength gains dropped by as much as 81% (RW). At 35% replacement, only mortars incorporating fine NJIT 2 (CY) could be cast. The strength gain of 1104 psi reflects that pozzolanic reactions were at work. Figure 5.74 illustrates the above discussion graphically. Coal fly ash (MO), given for comparison, had lower strength gains that are indicative of lower pozzolanic activity. Its strength gain slightly

increased as the replacement percentage increased. Its maximum strength gain appeared for 35% replacement percentage of coal fly ash.

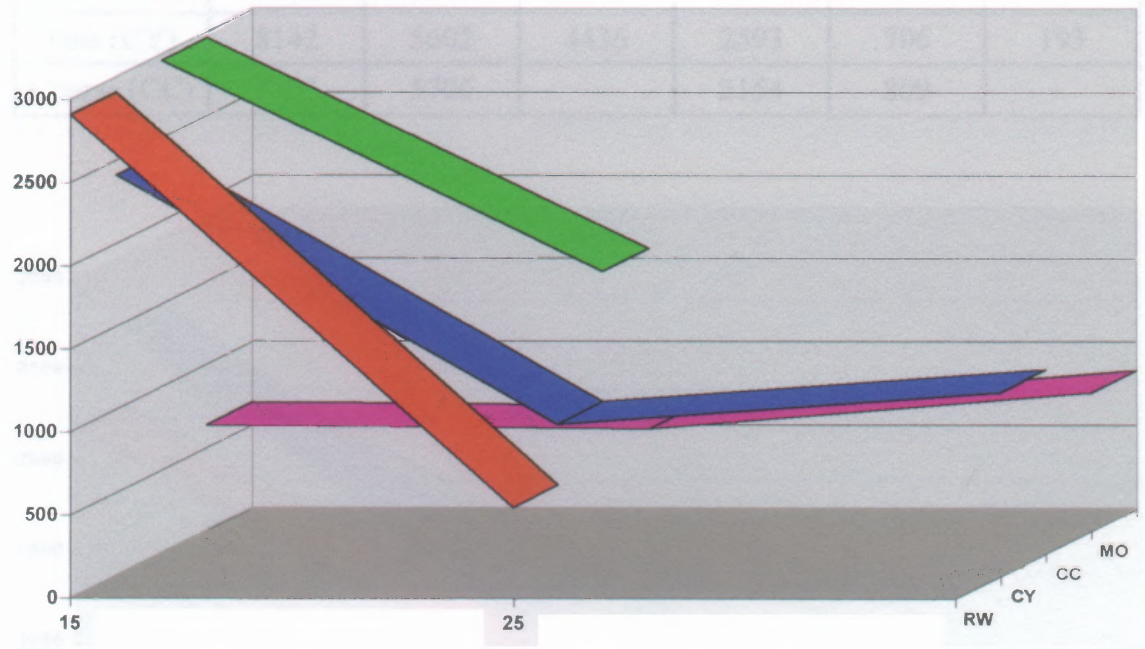

Figure 5.74 Compressive Strength Gains for MSWI Fly Ash-Cement mortars with w/(c+fa) = 0.50

It should be noted that, although the water-to-binder ratio was increased from 0.45 to 0.50 and 0.55, raw (RW) and coarse (CC) NJIT 2 fly ash could not be cast, still, due to their high water absorption. Only fine NJIT 2 fly ash (CY), with significantly slower adsorption capacity discussed in Section 5.1.6, could be cast.

At the water-to-binder ratio of 0.55, the strength gains of MSWI fly ash-cement mortars were smaller than those with lower water-to-binder ratios, as shown in Table 5.30 and Figure 5.75. This is typical in mixing of concrete since space previously occupied by excess water becomes capillary pores once the concrete hardens. These additional pores make concrete porous, thus reducing its compressive strength properties.

Table 5.30 28-day Compressive Strength Values and Calculated Strength Gains for Cement Mortars Incorporating NJIT 2 Fly Ashes with w/(c+fa) = 0.55

Fly ash	28-day Strength (psi)			Strength Gain (psi)		
	15%	25%	35%	15%	25%	35%
Raw (RW)	7726	5677	-	2177	781	-
Fine (CY)	8142	5602	4436	2593	706	193
Coarse (CC)	7703	5705	-	2154	809	-

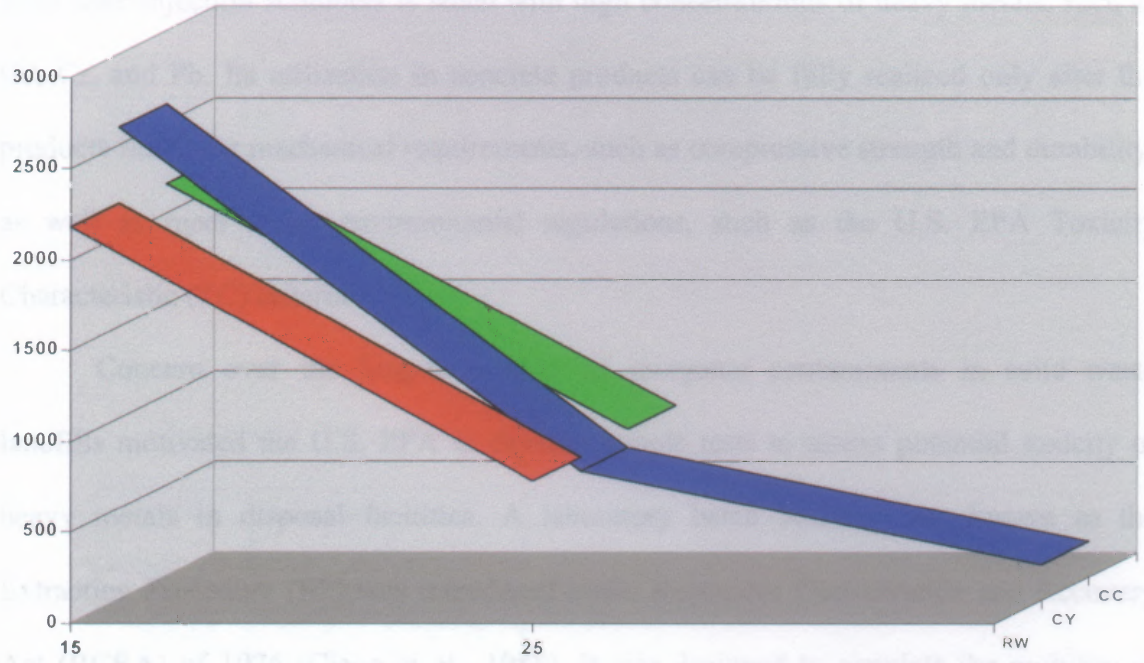

Figure 5.75 Compressive Strength Gains for MSWI Fly Ash-Cement mortars with w/(c+fa) = 0.55

Again, the strength gains dropped as sharply as 31% for fine fly ash mortars (CY) as the replacement increased from 15% to 25%. This is likely to be the results of reduction in reactive components. At 25% replacement, difference in the strength gains of all MSWI fly ash was minimal because the strengths were influenced more by the amount of water than by absorption capacity and chemical reactions.

In summary, the optimal replacement percentage was found to be 15% where compressive strength gains due to pozzolanic reactions, absorption, and chemical reactions involving hydrocalumite formation were the highest.

5.14 Leachate Characteristics

As previously discussed in Section 5.2, MSWI fly ash sampled from ESPs downstream from lime-injection scrubbers is laden with high concentrations of heavy metals, such as Cd, Cr, and Pb. Its utilization in concrete products can be fully realized only after the products fulfill the mechanical requirements, such as compressive strength and durability, as well as meet tough environmental regulations, such as the U.S. EPA Toxicity Characteristic (TC) criteria.

Concern over the long-term fates of inorganic contaminants in solid waste landfills motivated the U.S. EPA to develop simple tests to assess potential toxicity of heavy metals in disposal facilities. A laboratory batch leaching test known as the Extraction Procedure (EP) was introduced under Resources Conservation and Recovery Act (RCRA) of 1976 (Clapp et al., 1988). It was designed to simulate the mobility of inorganic contaminants from wastes. However, after much controversy regarding its applicability, a new test was adopted in 1980. The Toxicity Characteristic Leaching Procedure (TCLP) differs from the EP in that the extractant is chosen based upon the initial pH of slurried solid and that the pH is no longer maintained externally. The TCLP is currently used to determine whether a waste is hazardous based on the EPA toxicity characteristic (TC) criteria. The TCLP regular limits for selected metals are given in Table 5.31.

Table 5.31 Health-Based Heavy Metal Limits for Exclusions of Waste-Derived Residues and Their 20-time Concentrations

Element	Oxide	Conversion Factor	Element			Oxide
			Limit mg/kg	20x mg/kg	20x %	20x %
Ag	Ag_2O	1.0742	5	100	1.0E-2	1.1E-2
As	As_2O_3	1.3203	5	100	1.0E-2	1.3E-2
Ba	*BaO*	1.1165	100	2000	2.0E-1	2.2E-1
Be	*BeO*	2.7754	0.007	0.14	1.4E-5	3.9E-5
Cd	*CdO*	1.1423	1	20	2.0E-3	2.4E-3
Cr	Cr_2O_3	1.4615	5	100	1.0E-2	1.5E-2
Hg	*HgO*	1.0798	0.2	4	4.0E-4	4.3E-4
Ni	*NiO*	1.2725	7	140	1.4E-2	1.8E-2
Pb	*PbO*	1.0772	5	100	1.0E-2	1.1E-2
Sb	Sb_2O_3	1.1971	1	20	2.0E-3	2.4E-3
Se	*SeO*	1.2026	1	20	2.0E-3	2.4E-3
Tl	Tl_2O_3	1.1174	7	140	1.4E-2	1.6E-2

Note: Adapted from Appendix VII of 40 CFR 266

Table 5.32 Selected Chemical Compositions of MSWI Fly Ashes

Oxide	Cement	NJIT 1	NJIT 2			
			Raw	Fine	Coarse	Washed
Ag_2O	0.00	0.00	0.00	0.00	0.00	0.00
As_2O_3	0.00	0.00	0.00	0.00	0.00	0.00
BaO	0.02	0.09	0.00	0.02	0.02	0.03
BeO	0.00	0.00	0.00	0.00	0.00	0.00
CdO	0.00	**0.01**	**0.02**	**0.02**	**0.02**	**0.04**
Cr_2O_3	0.00	**0.06**	**0.03**	**0.03**	**0.03**	**0.05**
HgO	0.00	0.00	0.00	0.00	0.00	0.00
NiO	0.00	0.01	0.01	0.01	0.01	0.01
PbO	0.00	**0.37**	**0.32**	**0.37**	**0.32**	**0.55**
Sb_2O_3	0.00	**0.04**	**0.11**	**0.12**	**0.08**	**0.21**
SeO	0.00	0.00	0.00	0.00	0.00	0.00
Tl_2O_3	0.00	0.00	0.00	0.00	0.00	0.00

According to Method 1311 of U.S. EPA Test Methods for Evaluating Solid Waste, Physical/Chemical Methods (SW-846, 1992), if total analysis of a bulk fly ash demonstrates that individual heavy metal concentration is less than or equal to 20 times of the TCLP limits, TCLP may not be necessary for that individual metal. In order to determine if TCLP analysis was required for each metal, Table 5.32 was given to show the TCLP elemental concentrations in percent and their respective oxide concentrations using the calculated factors.

Table 5.33 TCLP Results for MSWI Fly Ashes and MSWI Fly Ash-Cement Mortar Specimens

Element	Limit mg/kg	TCLP Leachate Concentration (mg/kg)						
		NJIT 1	NJIT 2					
			Raw	RW115	RW125	CY115	CY125	CY135
Ag	5	ND	ND	ND	ND	ND	ND	ND
As	5	ND	ND	ND	ND	ND	ND	ND
Ba	100	ND	3.8	1.3	1.3	0.99	1.2	1.3
Cd	1	ND	ND	ND	ND	ND	ND	ND
Cr	5	ND	ND	0.08	0.04	0.08	0.03	0.05
Hg	0.2	ND	ND	ND	ND	ND	ND	ND
Pb	5	ND	**33.1**	ND	ND	ND	ND	ND
Se	1	ND	ND	ND	ND	ND	ND	ND

Note: ND means Not Detected

Total elemental analysis results of MSWI fly ash samples shown in Section 5.2 were provided in Table 5.32 for the TCLP metals. NJIT 1 fly ash and NJIT 2 fly ash and its processed ashes had their concentrations of Cd, Cr, Pb, and Sb in excess of 20 times of the concentration limits in Table 5.31, so TCLP was required for them. Cement undoubtedly met all the limits since it is not a significant source for any heavy metals.

It is important to note that there are only eight regulated metals as listed in 40 CFR 261.24 which are used to determine if a waste is hazardous. These metals are shown in Table 5.33 along with the analysis results of the samples. The full TCLP analysis results show that NJIT 1 fly ash did indeed pass the TCLP as intended. The proprietary phosphoric acid solution used in the treatment of the fly ash was designed to stabilize heavy metals in the fly ash, especially lead since lead usually exceeds the limit. This is evident in the results for NJIT 2 fly ash which actually failed the test for lead. Both raw fly ashes met the limits for Cd, Cr, and Sb. This is due to the fact that the total analysis reflects total concentrations of metal elements, not what is available for leaching.

All solidified MSWI fly ash-cement mortars incorporating 15% to 35% of raw and fine MSWI fly ash passed the limits. It is obvious that cement can stabilize heavy metals in the fly ash, thereby preventing them from leaching. Although the solidified MSWI fly ash-cement products passed the TCLP test, it by no means guarantees that they will not pose a threat to human health and the environment during their lifetime. The TCLP test is controversial in that concentrations of heavy metals in the leachate are governed by the pH of the leachate (Webster and Loehr, 1996; Buchholz and Landsberger, 1995). At high leachate pH values, metals of concern in most concrete systems are relatively insoluble. Moreover, sample preparation, which involves crushing of sample to below a certain size, does not reflect real condition of sample, in this case solidified cement structures. Therefore, the test may not reflect what really happens in the field. Moreover, it is very likely that the alkalinity content of solidified products may be leached away over time, thereby leading to lower leachate pH levels. The metals bound in the concrete matrix may become more soluble. The matrix which consists mostly of

calcium may be physically broken down as the calcium content is removed through the leaching of alkalinity. Therefore, it is more appropriate to use other leaching methods, such as sequential extractions which utilize different extractants to evaluate the long-term stability of the intact solidified MSWI fly ash-cement products.

CHAPTER 6

CONCLUSIONS AND SUGGESTIONS FOR FUTURE RESEARCH

This research is aimed at evaluating the potential of different types of MSWI fly ash from an incineration facility to be used in portland cement concrete by using existing standard test methods for cement and coal fly ash. The chemical and physical properties of the raw fly ashes as well as processed fly ashes were carefully tested. Microscopic examination coupled with X-ray analysis was performed on all MSWI fly-cement pastes in order to understand more clearly how the inclusion of MSWI fly ash would affect hardening of cement. To complete the evaluation process, the impact of the MSWI fly ash-cement products on the environment according to the regulatory procedure, TCLP, was also carried out. Until there are specific standards designed for the evaluation of MSWI fly ash in concrete application, this research work should be able to provide some insights into the potential of utilization of MSWI fly ash. The following conclusions from the research can be drawn:

6.1 Chemical and Physical Characterization of MSWI Fly Ashes

1. Raw NJIT 1 fly ash has a gradation that was close to the limits required by ASTM C330/331 for lightweight fine aggregates for structures and masonry units.
2. Fineness values of raw and coarse NJIT 2 fly ashes determined by wet sieving through a standard sieve #325 (45-micron openings) were comparable to that of coal fly ash. The fineness values of fine and washed fly ashes were similar to that of cement.

3. LOI values of the NJIT 2 MSWI fly ashes, including fractionated portions, are high, ranging from 12.63% for fine fly ash to 19.56% for washed fine fly ash. These fly ashes did not meet the limits required by ASTM C618 for both class C and F fly ash.
4. The bulk specific gravity of NJIT 1 fly ash is lower than those of NJIT 2 fly ashes (raw, fine, coarse, and washed fine). As for NJIT 2 fly ashes, the finer the fly ash was, the higher its bulk specific gravity was.
5. In general, the bulk specific gravity values of MSWI fly ash samples were found to be 20-35% lower than that of cement.
6. pH values of the MSWI fly ashes are above pH 11 which is the characteristic of APC fly ash that has been treated with lime to neutralize acid gases.
7. Conductivity values of NJIT 2 fly ashes are above 24 mmoh/cm with an exception of washed fine fly ash which has the lowest value. This is due to the removal of soluble phases by washing. NJIT1 fly ash that passed through an ash treatment process with a proprietary phosphoric acid solution also has lower conductivity value.
8. Generally, absorption capacity values of MSWI fly ash samples are more than twice as much as that of cement (72%) and ten times as much as that of coal fly ash (12%). The high absorption capacity value reflects the high water demand of the fly ashes in the mixes.
9. The presence of charred particles was responsible for high absorption capacity values of NJIT 1 fly ash (142%) as well as raw (170%) and coarse (148%) NJIT 2 fly ashes. Fine NJIT 2 fly ash has a lower value (131%) while washed fine NJIT 2

fly ash has a higher value (164%) due to high affinity for water of dried hydrated compounds.

10. The MSWI fly ashes contain higher CaO contents than coal fly ash (37% vs. 6%).

11. The SiO_2+Fe_2O_3+Al_2O_3 limit of 50% set by ASTM C618 class C fly ash is not satisfied by all of the fly ashes.

12. Bulk chemical data reveal that major constituents (>1%) in raw NJIT 1 and 2 fly ashes are Al, Ca, Fe, K, Na, Si, S, and Cl. High concentrations of Cl may cause corrosion in concrete reinforced with steel. High Na content may promote alkali-aggregate reaction which causes cracks in concrete structure.

13. Fractionation does not significantly change the bulk chemical compositions of NJIT fly ash. Washing of fine fly ash, on the other hand, removed Na by as much as 85% and Cl by as much as 73%.

14. Mineralogical data show that all of the MSWI fly ashes have high NaCl content and that washing effectively removed most of NaCl from fine NJIT 2 fly ash.

15. The presence of alkali and earth alkali metal salts, such as NaCl and $CaCl_2$, may contribute to high alkalinity in leachate from MSWI fly ash.

16. MSWI fly ash samples have high contents of CaClOH and $CaCl_2.Ca(OH)_2.H_2O$, especially coarse NJIT 2 fly ash.

17. Phases detected in the XRD analyses of NJIT 1 fly ash, $Ca_2Al(OH)_7.3H_2O$ and $Ca_2Al(OH)_6Cl_2.H_2O$, were also present in washed fly ash. Another calcium salt, $Ca_4Al_2O_6Cl_2.10H_2O$, was exclusively present in washed fine fly ash.

18. It is clear that NJIT 1 and 2 fly ashes do not have cementitious components, such as C_3S that is the principal component of cement. In fact, the paste made of NJIT fine fly ash did not solidify throughout the entire course of this study.

6.2 Fractionation of MSWI Fly Ashes

1. Humidity has a great influence on fractionation using an air classifier since MSWI fly ashes have high content of calcium chloride which is hygroscopic. Relative humidity of below 60% was found to have the least effect on air classification.
2. Criteria were set for the determination of optimal operating parameters; namely, rotor speed, fan speed, and run time. Operating condition that gave the highest yield (percent of fly ash captured in the fine particle reservoir to total feed) as well as the median particle size of below 20 micron would be chosen.
3. Rotor speed was found to have the greatest influence on the yield and the particle size. As the rotor speed increases, the yield decreases, and so does the median size ($d_{50\%}$). Median particle size of below 15 microns can be achieved at the expense of the yield (20%).
4. At the rotor speed of 3000 rpm, an increase in run time resulted in somewhat smaller particle size although at lower yield. The effect was less pronounced as the rotor speed was set at 4000, 5000, and 6000 rpm.
5. The operating condition optimized for highest yield (70%) as well as median particle size ($d_{50\%}$) of 17.77 microns was as follows: rotor speed, 3000 rpm; fan speed, 100%; and run time, 20 minutes.

6. Re-classification of fractionated fine fly ash did not show a significant improvement in $d_{50\%}$. Therefore, fine fly ash stock used throughout this study was prepared by air classifying once the pre-sieved fly ash (<850 microns).
7. Fractionation of pre-sieved NJIT 2 fly ash at the determined operating condition resulted in two streams of fly ash: fine fly ash ($d_{50\%}$=20.67 microns, $d_{90\%}$=64.37 microns) and coarse fly ash ($d_{50\%}$=29.67 microns, $d_{90\%}$=89.65 microns)

6.3 Morphology and Elemental Surface Analyses of MSWI Fly Ashes

1. There are two major types of particles in the raw NJIT 1 and 2 fly ash samples: chars and agglomerated spheres. Charred particles appeared mostly in NJIT 1 fly ash and raw NJIT 2 fly ash. These porous and fibrous charred particles have high surface areas, thus enabling them to absorb water. The agglomerated fly ash particles themselves also have high surface areas. This results in as much as 170% absorption capacity of NJIT 1, raw and coarse NJIT 2 fly ashes.
2. On a particle-to-particle basis, particle morphology of all of the NJIT 2 fly ash samples; namely, raw, fine, and coarse fly ashes, appeared to be the same. The particles appeared to be spherical, porous, structured agglomerates. Average size by visual estimation is approximately 30 to 40 microns with the presence of sub 20-micron particles. The washed fine fly ash particles also looked similar although there were hydrated phases, such as $Ca(OH)_2$ present on the surface.
3. High contents of reactive phases, such as CaO, and rough surfaces make MSWI fly ash particles more reactive than smooth glassy coal fly ash particles.

4. Washing of MSWI fly ash was found to effectively remove most of the soluble phases, including NaCl, which causes unfavorable effects in concrete. However, the essential elements, Si, Al, and Ca, were less impacted by washing and they should be beneficial in the utilization of washed fly ash in concrete.

6.4 Effect of MSWI Fly Ash on Hydration of Fly Ash-Cement Pastes

1. Aside from reducing the amount of C_3S in the fly ash-cement paste, both raw and fine fly ash appeared to slightly retard the hydration process.
2. The majority of $Ca(OH)_2$ produced during hydration of cement paste was consumed starting as early as day 14. This may very well be the result of the pozzolanic reaction that took place in the pastes.
3. The fine NJIT 2 fly ash showed better rate of pozzolanic activity than the raw NJIT 2 fly ash.
4. Examination of the XRD diffractograms of the pastes containing NJIT 2 fly ash shows the formation of hydrocalumite [$C_3A.CaCl_2.10H_2O$] which was absent in the cement paste. The compressive strength test results later reveal that hydrocalumite may be responsible for the strength enhancement in the MSWI fly ash-cement mortars.

6.5 Examination of MSWI Fly Ash-Cement Paste Microstructures

1. MSWI fly ash is not self-cementitious since its paste did not solidify.
2. MSWI fly ashes seemed to retard hydration of cement since fewer hydration products, C-S-H and CH, were observed at the same age as the cement paste.

3. More hydration products were found in MSWI fly ash pastes at later date.
4. After the age of 7 days, the XRD and EDX results showed possible formation of a new phase, hydrocalumite [$C_3A.CaCl_2.10H_2O$]. As the new phase formed, chloride concentrations decreased implying that chloride might be involved in the formation.
5. The washed fine fly ash paste might not have hydrocalumite formed since the chloride content in the paste was low. However, the paste was in a more advanced stage of hydration than other fly ash pastes.

6.6 Utilization of MSWI Fly Ashes in Mortars

1. Although raw NJIT 1 fly ash has a gradation that is close to the limits required by ASTM C330/331, it is not suitable for use as an aggregate replacement because of its high water absorption capacity (142%).
2. At the replacement percentage of 15% and the water-to-binder ratio (w/(c+fa)) of 0.50, the compressive strengths of the cement mortars incorporating raw (RW115), fine (CY115), and coarse NJIT 2 fly ashes outperformed the control mortars at all ages. The coarse fly ash-cement (CC115) mortars have the highest strengths that outperform those of the control mortars by as much as 40% (8810 psi) at day 14 and 27% (9028 psi) at day 28.
3. Raw, fine, and coarse fractions of NJIT 2 fly ash performed equally well on compressive strength tests. That is, the effect of fine particles was not significant.

4. At the replacement percentage of 15% and the water-to-binder ratios of 0.45, 0.50, and 0.55, all NJIT 2 fly ash-cement mortars produced better compressive strength results than the controls at the respective water-to-binder ratios.
5. The better strength development starting as early as three days of the NJIT 2 fly ash-cement mortars was found to be the combined results of high water absorption capacity of the fly ashes as well as formation of the new phase, $C_3A.CaCl_2.10H_2O$.
6. As the amount of fly ash was increased beyond 15%, the compressive strengths decreased due to the net reduction in active cementitious components.

6.7 Leachate Characteristics of MSWI Fly Ash-Cement Products

1. The total amounts of cadmium, chromium, lead, and antimony present in the MSWI fly ashes were more than 20 times of the health-based heavy metal limits (Appendix VII, 40 CFR 266); therefore, TCLP tests of these metals were required.
2. Raw NJIT 2 fly ash did not pass the TCLP. Indeed, its lead concentration was 33.1 mg/kg, thus exceeding the TCLP limit of 5 mg/kg.
3. Once the raw and fine NJIT 2 fly ashes were incorporated in cement mortars, their leachate met all of the limits for TCLP metals.

It was found in this research that MSWI fly ash from ESP units (NJIT 2 fly ash) has a great potential as a cement replacement material. Replacement of 15% NJIT 2 fly ash in all forms; namely, raw, fine, coarse, and washed fine, enhanced the 28-day

compressive strengths of cement mortars by up to 150%. As the amount of replacement fly ash was increased beyond 15%, the compressive strengths decreased due to the net reduction in active cementitious components and the high absorption capacity . Major elements encountered in the fly ashes were aluminum, calcium, and silicon. These elements that are found in portland cement may contribute to strength in concrete. Other major elements also found; potassium, sodium, sulfur, and chloride, may, however, produce undesirable effects in concrete. Major compounds found in NJIT 2 fly ash were chlorides and hydroxides of sodium and calcium, such as NaCl, CaClOH, and $CaCl_2.Ca(OH)_2.H_2O$. These alkali and alkali earth compounds contributed to high pH values of the fly ashes. High level of chloride (18%) also raised concerns regarding their detrimental impacts on concrete and reinforced concrete. That is why simple washing was employed to remove these compounds.

Microscopic examination of fly ash particles revealed that small particulates, as small as one micron, attached to the surfaces of the particles. The particles have high surface areas that contain high levels of calcium, sodium, and chloride, thus making the surfaces more reactive than those of smooth glassy coal fly ash particles.

XRD analyses of NJIT 2 fly ash-cement pastes showed the formation of a new phase, $C_3A.CaCl_2.10H_2O$ (Hydrocalumite), which was detected only in the fly ash pastes. Hydrocalumite was found to contribute to the superior strength of the fly ash mortar specimens. Although the inclusion of NJIT 2 fly ashes slightly retarded hydration process of cement as reflected by the observed amount of hydration products, high absorption capacity of the fly ashes and the formation of $C_3A.CaCl_2.10H_2O$ helped to improve the compressive strengths. It was also found in the TCLP tests that the solidified matrices of

the fly ash-cement products immobilized heavy metals, thereby allowing the specimen to pass the TCLP.

However, the strength of hardened concrete is by no means its only important characteristic; slump, tensile properties, ductility, volume, impermeability, and stability both in terms of structure and environmental exposure should be of equal importance. It is unfortunate that it has become the custom to assess concrete quality only in terms of its compressive strength. The general assumption is that an improvement in strength will improve its other properties as well. Although this is often the case, there are many important exceptions. For instance, an increased in concrete strength does not guarantee its resistance to acid or sulfate attack. Therefore, in addition to concrete strength alone, other in terms of choosing an appropriate mix design for a particular job. Especially, the unwashed MSWI fly ashes, which have high chloride content, must be tested if it can be used in reinforced concrete without the deleterious effect to the steel bars.

Lastly, before utilization of MSWI fly ash can be commercialized, several issues must be addressed. Variability of the fly ash needs to be studied since chemical and physical characteristics of the fly ash change depending upon several factors including MSW feed composition, and the incinerator operating conditions, even within the same facility. A study involving utilization of MSWI fly ash in concrete mixes is also crucial since the fly ash may behave differently in concrete than in mortars due to addition of aggregates.

6.8 Suggestions for Future Work

1. Improve the air classifier efficiency or find other means to produce particles with certain cut sizes, such as 5-micron and 10-micron.
2. A detailed study on the economic requirements for air classification of MSWI fly ash should be conducted since the processing cost must be considered before the process can be commercialized.
3. Long-term compressive strength test is required
4. The strength of hardened concrete is by no means its only important characteristic; ductility, volume, stability, and impermeability should be of equal importance. It is unfortunate that it has become the custom to assess concrete quality only in terms of its compressive strength. The general assumption is that an improvement in strength will improve its other properties as well. Although this is often the case, there are many important exceptions. For instance, an increased in concrete strength does not guarantee its resistance to acid or sulfate attack. Therefore, concrete strength alone may be misleading in terms of choosing an appropriate mix design for a particular job. Especially, the unwashed MSWI fly ashes, which have high chloride content, must be tested if
5. Long-term leaching test should be conducted on the solidified MSWI fly ash products to ensure that heavy metals will not become mobile once alkalinity is leached out.

At the present time it seems that legal impediments and concerns over liability issue pose a far greater barrier to utilization of MSWI fly ash as a construction material

than any failure on the part of engineering society to devise the technologies needed to make utilization of MSWI fly ash and its products environmentally acceptable. This is a rapid evolving technology that neither the regulatory structure nor public perception has yet caught up. To a considerable degree, acceptance of this technology depends on local and national attitudes toward interest and investment in testing and development of our knowledge on ash as well as on the presence of clear federal guidance and comprehensive regulatory measures. This research merely presents a starting point in the wake of realization of the potential of MSWI fly ash in construction application. It is hoped that the research will spark interests of the research community to produce more works.

APPENDIX A

Table A 1 Compressive Strengths of NJIT 2 Fly Ash Mortars with 15% Replacement and w/(c+fa) = 0.45

Sample No.	Compressive Strengths (psi)			
	3-d	7-d	14-d	28-d
C45	6549	6781	7408	7460
RW215	7573	9271	10275	11381
CY215	8204	8905	9973	10583
CC215	7467	8788	9630	10259

Table A 2 Percentage Compressive Strengths of NJIT 2 Fly Ash Mortars with 15% Replacement and w/(c+fa) = 0.45

Sample No.	Percentage Compressive Strengths (%)			
	3-d	7-d	14-d	28-d
C45	100	100	100	100
RW215	116	137	139	153
CY215	125	131	135	142
CC215	114	130	130	138

Table A 3 Compressive Strengths of NJIT 2 Fly Ash Mortars with 25% Replacement and w/(c+fa) = 0.45

Sample No.	Compressive Strengths (psi)			
	3-d	7-d	14-d	28-d
C45	6549	6781	7408	7460
RW225	1928	2568	2771	3695
CY225	4014	5206	5690	6840
CC225	4598	5836	6657	7483

Table A 4 Percentage Compressive Strengths of NJIT 2 Fly Ash Mortars with 25% Replacement and w/(c+fa) = 0.45

Sample No.	Percentage Compressive Strengths (%)			
	3-d	7-d	14-d	28-d
C45	100	100	100	100
RW225	29	38	37	50
CY225	61	77	77	92
CC225	70	86	90	100

Table A 5 Compressive Strengths of NJIT 2 Fly Ash Mortars with 15% Replacement and w/(c+fa) = 0.50

Sample No.	Compressive Strengths (psi)			
	3-d	7-d	14-d	28-d
C50	5349	6205	6274	7134
RW115	5772	7408	8428	8976
CY115	5865	7396	7720	8472
CC115	7044	8181	8810	9028
CW115	6557	7625	8160	8509

Table A 6 Percentage Compressive Strengths of NJIT 2 Fly Ash Mortars with 15% Replacement and w/(c+fa) = 0.50

Sample No.	Percentage Compressive Strengths (%)			
	3-d	7-d	14-d	28-d
C50	100	100	100	100
RW115	108	119	134	126
CY115	110	119	123	119
CC115	132	132	140	127
CW115	123	123	130	119

Table A 7 Compressive Strengths of NJIT 2 Fly Ash Mortars with 25% Replacement and w/(c+fa) = 0.50

Sample No.	Percentage Compressive Strengths (%)			
	3-d	7-d	14-d	28-d
C50	5349	6205	6274	7134
RW125	3383	4030	4706	5899
CY125	3688	4577	5212	6263
CC125	4706	5610	6495	7046

Table A 8 Percentage Compressive Strengths of NJIT 2 Fly Ash Mortars with 25% Replacement and w/(c+fa) = 0.50

Sample No.	Percentage Compressive Strengths (%)			
	3-d	7-d	14-d	28-d
C50	100	100	100	10
RW125	63	65	75	83
CY125	69	74	83	88
CC125	88	90	104	99

Table A 9 Compressive Strengths of NJIT 2 Fly Ash Mortars with 35% Replacement and w/(c+fa) = 0.50

Sample No.	Compressive Strengths (psi)			
	3-d	7-d	14-d	28-d
C50	5349	6205	6274	7134
CY135	2508	3136	3808	5741

Table A 10 Percentage Compressive Strengths of NJIT 2 Fly Ash Mortars with 35% Replacement and w/(c+fa) = 0.50

Sample No.	Percentage Compressive Strengths (%)			
	3-d	7-d	14-d	28-d
C50	100	100	100	100
CY135	47	51	61	80

Table A 11 Compressive Strengths of Coal Fly Ash Mortars with Different Cement Replacement Percentage and w/(c+fa) = 0.50

Sample No.	Compressive Strengths (psi)			
	3-d	7-d	14-d	28-d
MO00	4425	5937	6498	7188
MO15	4009	5500	5869	6744
MO25	3873	4885	5738	6000
MO35	3429	4136	4892	5500

Note: Reported for comparison from Bumrongjaroen (1999)

Table A 12 Compressive Strengths of NJIT 2 Fly Ash Mortars with 15% Replacement and w/(c+fa) = 0.55

Sample No.	Compressive Strengths (psi)			
	3-d	7-d	14-d	28-d
C55	5319	5389	6035	6528
RW315	4706	6299	6857	7726
CY315	5189	6338	7181	8142
CC315	5381	6423	7326	7703

Table A 13 Percentage Compressive Strengths of NJIT 2 Fly Ash Mortars with 15% Replacement and w/(c+fa) = 0.55

Sample No.	Percentage Compressive Strengths (%)			
	3-d	7-d	14-d	28-d
C55	100	100	100	100
RW315	88	117	114	118
CY315	98	118	119	125
CC315	101	119	121	118

Table A 14 Compressive Strengths of NJIT 2 Fly Ash Mortars with 25% Replacement and w/(c+fa) = 0.55

Sample No.	Compressive Strengths (psi)			
	3-d	7-d	14-d	28-d
C55	5319	5389	6035	6528
RW325	3268	4360	5333	5677
CY325	3246	4076	4871	5602
CC325	3458	4334	5164	5705

Table A 15 Percentage Compressive Strengths of NJIT 2 Fly Ash Mortars with 25% Replacement and w/(c+fa) = 0.55

Sample No.	Percentage Compressive Strengths (%)			
	3-d	7-d	14-d	28-d
C55	100	100	100	10
RW325	61	81	88	87
CY325	61	76	81	86
CC325	65	80	86	87

Table A 16 Compressive Strengths of NJIT 2 Fly Ash Mortars with 35% Replacement and w/(c+fa) = 0.55

Sample No.	Compressive Strengths (psi)			
	3-d	7-d	14-d	28-d
C55	5319	5389	6035	6528
CY335	2243	3133	3648	4436

Table A 17 Percentage Compressive Strengths of NJIT 2 Fly Ash Mortars with 35% Replacement and w/(c+fa) = 0.55

Sample No.	Percentage Compressive Strengths (%)			
	3-d	7-d	14-d	28-d
C55	100	100	100	100
CY335	42	58	60	68

Table A 18 Compressive Strengths of NJIT 2 Fly Ash Mortars with 15% Replacement

Sample No.	Compressive Strengths (psi)			
	3-d	7-d	14-d	28-d
C45	6549	6781	7408	7460
RW215	7573	9271	10275	11381
CY215	8204	8905	9973	10583
CC215	7467	8788	9630	10259
C50	5349	6205	6274	7134
RW115	5772	7408	8428	8976
CY115	5865	7396	7720	8472
CC115	7044	8181	8810	9028
C55	5319	5389	6035	6528
RW315	4706	6299	6857	7726
CY315	5189	6338	7181	8142
CC315	5381	6423	7326	7703

Table A 19 Compressive Strengths of NJIT 2 Fly Ash Mortars with 25% Replacement

Sample No.	Compressive Strengths (psi)			
	3-d	7-d	14-d	28-d
C45	6549	6781	7408	7460
RW225	1928	2568	2771	3695
CY225	4014	5206	5690	6840
CC225	4598	5836	6657	7483

Table A 19 Compressive Strengths of NJIT 2 Fly Ash Mortars with 25% Replacement (Continued)

Sample No.	Compressive Strengths (psi)			
	3-d	**7-d**	**14-d**	**28-d**
C50	5349	6205	6274	7134
RW125	3383	4030	4706	5899
CY125	3688	4577	5212	6263
CC125	4706	5610	6495	7046
C55	5319	5389	6035	6528
RW325	3268	4360	5333	5677
CY325	3246	4076	4871	5602
CC325	3458	4334	5164	5705

Table A 20 Compressive Strengths of NJIT 2 Fly Ash Mortars with 35% Replacement

Sample No.	Compressive Strengths (psi)			
	3-d	**7-d**	**14-d**	**28-d**
C50	5349	6205	6274	7134
CY135	2508	3136	3808	5741
C55	5319	5389	6035	6528
CY335	2243	3133	3648	4436

APPENDIX B

Table B 1 Mortar Mix Design with w/(c+fa) = 0.45

Material	S.G.	Unit Wt. lb/ft^3	Wt. Ratio	Wt. lb	Vol. ft^3	Wt. per 1 ft^3 lb	Wt. per 1 ft^3 kg	Wt. per 0.0611 ft^3 lb	Wt. per 0.0611 ft^3 kg
Cement	3.15	196.56	1.00	196.560	1.000	34.189	15.508	2.089	**0.948**
Sand	2.60	162.24	2.75	540.540	3.332	94.020	42.647	5.746	**2.606**
Water	1.00	62.40	0.45	88.452	1.418	15.385	6.979	0.940	**0.426**
Total					5.749		65.134		**3.980**

Table B 2 Mortar Mix Design with w/(c+fa) = 0.50

Material	S.G.	Unit Wt. lb/ft^3	Wt. Ratio	Wt. Lb	Vol. ft^3	Wt. per 1 ft^3 lb	Wt. per 1 ft^3 kg	Wt. per 0.0611 ft^3 lb	Wt. per 0.0611 ft^3 kg
Cement	3.15	196.56	1.00	196.560	1.000	33.277	15.095	2.034	**0.922**
Sand	2.60	162.24	2.75	540.540	3.332	91.513	41.510	5.592	**2.537**
Water	1.00	62.40	0.50	98.280	1.575	16.639	7.547	1.017	**0.461**
Total					5.907		64.152		**3.920**

Table B 3 Mortar Mix Design with w/(c+fa) = 0.55

Material	S.G.	Unit Wt. lb/ft^3	Wt. Ratio	Wt. lb	Vol. ft^3	Wt. per 1 ft^3 lb	Wt. per 1 ft^3 kg	Wt. per 0.0611 ft^3 lb	Wt. per 0.0611 ft^3 kg
Cement	3.15	196.56	1.00	196.560	1.000	32.413	14.703	1.981	**0.898**
Sand	2.60	162.24	2.75	540.540	3.332	89.136	40.432	5.447	**2.471**
Water	1.00	62.40	0.55	108.108	1.733	17.827	8.086	1.089	**0.494**
Total					6.064		63.221		**3.863**

REFERENCES

Ahmed, A., and L. Struble. 1995. "Effects of Microstructure on Fracture Behavior of Hardened Cement Paste." *Proceedings of the Symposium on Microstructure of Cement-Based Systems/Bonding and Interfaces in Cementitious Materials.* Materials Research Society. Boston, Massachusetts. 99-106.

Aimin, X. 1991. "Microstructural Study of Gypsum Activated Fly ash Hydration in Cement Paste." *Cement & Concrete Research.* 21: 1137-1147.

Aimin, X., and S. L. Sarkar. 1994. "Microstructural Development in High-Volume Fly Ash Cement System." *J. Materials in Civil Engineering.* 6: 117-136.

Albino, V., R. Cioffi, L. Santoro, and G. L. Valenti. 1996. "Stabilization of Residue Containing Heavy Metals by Means of Matrices Generating Calcium Trisulphoaluminate and Silicate Hydrates." *Waste Management Research.* 14: 29-41.

Allen, T., and R. Davies. 1987. "Modern Aspects of Particle-Size Analysis." *Advances in Ceramics.* 21: 721-746.

Ali, M. T., and W. F. Chang. 1994. "Strength Properties of Cement-Stabilized Municipal Solid Waste Incinerator Ash Masonary Bricks." *ACI Materials J.* 91: 256-263.

Bagchi, A. 1989. "Characterization of MSW Incinerator Ash." *J. Environmental Engineering.* 115: 447-452.

Barham. D., and H. N. Tran. 1991. "The Thermal Behaviour of Chloride and Sulphate Bearing MSW Incinerator Ash." *CIM Bulletin.* 84: 151-154.

Bawkon, B. 1991. "Incineration Technologies for Managing Solid Waste." *Pollution Engineering.* 23: 96-100.

Belevi, H., D. M. Stämpfli, and P. Baccini. 1992. "Chemical Behaviour of Municipal Solid Waste Incinerator Bottom Ash in Monofills." *Waste Management Research.* 10: 153-167.

Berg, E. R. and J. A. Neal. 1998. "Municipal Solid Waste Bottom Ash as Portland Cement Concrete Ingredient." *J. of Materials in Civil Engineering.* 10: 168-173.

Berry, E. E., R. T. Hemmings, M-H Zhang, B. J. Cornelius, and D. M. Golden. 1994. "Hydration in High-Volume Fly Ash Concrete Binders." *ACI Materials J.* 91: 382-389.

Bilodeau, A., V. Sivasundaram, K. E. Painter, and V. M. Malhotra. 1994. "Durability of Concrete Incorporating High Volumes of Fly Ash from Sources in the U.S." *ACI Materials J.* 91: 3-12.

Brereton, C. 1996. "Municipal Solid Waste – Incineration, Air Pollution Control and Ash Management." *Resources, Conservation and Recycling.* 16: 227-264.

Buchholz, B. A., and S. Landsberger. 1993. "Trace Metal Analysis of Size-Fractioned Municipal Solid Waste Incinerator Fly Ash and its Leachates." *J. Environmental Science and Health.* A28: 423-441.

---. 1995. "Leaching Dynamics Studies of Municipal Solid Waste Incinerator Ash." *J. Air & Waste Management Association.* 45: 579-590.

Bumrongjaroen, W. 1999. *Utilization of Processed Coal Fly Ash in Cement Mortar.* Ph. D. Dissertation. Department of Civil and Environmental Engineering. New Jersey Institute of Technology. New Jersey.

Cahill, C. A. and L. W. Newland. 1982. "Comparative Efficiencies of Trace Metal Extraction from Municipal Incinerator Ashes." International Journal of Environmental Analytical Chemistry. 11: 227.

Chandler, A. J., T. T. Eighmy, J. Hartlén, O. Hjelmar, D. S. Kosson, S. E. Sawell, H. A. van der Sloot, and J. Vehlow. 1997. *Municipal Solid Waste Incinerator Residues.* The Netherlands: Elsevier Science B.V.

Cheng, K. Y., and P. L. Bishop. 1992a. "Metals Distribution in Solidified/Stabilized Waste Forms after Leaching." *Hazardous Waste & Hazardous Materials.* 9: 163-171.

---. 1992b. "Sorption, Important in Stabilized/Solidified Waste Forms." *Hazardous Waste & Hazardous Materials.* 9: 289-296.

Chiang, K.-Y., K.-S. Wang, F.-L. Lin, and W.-T. Chu. 1997. "Chloride Effects on the Speciation and Partitioning of Heavy Metal During the Municipal Solid Waste Incineration Process." *The Science of Total Environment.* 203: 129-140.

Clapp, T. L., J. F. Magee II, R. C. Ahlert, and D. S. Kosson. 1989. "Municipal Solid Waste Combustion and the Behavior of Metals in Incinerator Ashes." *Environmental Progress.* 7: 22-29.

Davison, R. L., D. F. S. Natusch, and J. R. Wallace. 1974. "Trace elements in Fly Ash: Dependence of Concentration on Particle Size." *Environmental Science & Technology.* 8: 1107-1113.

Denison, R. A., and J. Ruston. 1990. *Recycling & Incineration: Evaluating the Choices.* Washington, D.C.: Island Press.

Egemen, E., and C. Yurteri. 1996. "Regulatory Leaching Tests for Fly Ash: A Case Study." *Waste Management Research.*14: 43-50.

Eighmy, T. T. and D. S. Kosson. 1996. "U.S.A. National Overview on Waste Management." *Waste Management.* 16: 361-366.

Eighmy, T. T., J. D. Eusden, Jr., J. E. Krzanowski, D. S. Domingo, D. Stämpfli, J. R. Martin, and P. M. Erickson. 1995. "Comprehensive Approach toward Understanding Element Speciation and Leaching Behavior in Municipal Solid Waste Incineration Electrostatic Precipitator Ash." *Environmental Science and Technology.* 29: 629-646.

Fernández, M. A., L. Martínez, M. Segarra, J. C. Garcia, and F. Espiell. 1992. "Behavior of Heavy Metals in the Combustion Gases of Urban Waste Incinerators." *Environmental Science & Technology.* 26: 1040-1047.

Glasser, F. P. 1992. "Progress in the Immobilization of Radioactive Wastes in Cement." *Cement & Concrete Research.* 22: 201.

Goh, A. T. C., and J.-H. Tay. 1993. "Municipal Solid-Waste Incinerator Fly Ash for Geotechnical Applications." *J. Geotechnical Engineering.* 119: 811-825.

Goldin, A., C. Bigelow, and P. L. M. Veneman. 1992 "Concentrations of Metals in Ash from Municipal Solid Waste Combusters." *Chemosphere.* 24: 271-280.

Gong, Y., and D. W. Kirk. 1994. "Behaviour of Municipal Solid Waste Incinerator Flyash I: General Leaching Study." *J. Hazardous Materials.* 36: 249-264.

Gopalan, M. K. 1993. "Nucleation and Pozzolanic Factors in Strength Development of Class F Fly Ash Concrete." *ACI Materials J.* 90: 117-121.

Goumans, J. J. J. M., H. A. van der Sloot, and Th. G. Aalbers. 1991. *Waste Meterials in Construction, Proceedings of the International Conference on Environmental Implications of Construction With Waste Materials*, Maastricht, The Netherlands.

Greenberg, R. R., W. H. Zoller, and G. E. Gordon. 1978. "Composition and Size Distribution of Particles Released in Refuse Incineration." *Environmental Science & Technology.* 12: 566-573.

Ham, R. K., V. A. Hammer, and G. Boley. 1992. "Partitioning of Elements by Refuse Processing." *J. Environmental Engineering.* 118: 725-743.

Hamernik, J. D., and G. C. Frantz. 1991a. "Physical and Chemical Properties of Municipal Solid Waste." *ACI Materials J.* 88: 294-301.

---. 1991b. "Strength of Concrete Containing Municipal Solid Waste Fly Ash." *ACI Materials J.* 88: 508-517.

Hinshaw, G. D. 1994. "Behavior and Control of Metals in a Hazardous Waste Incinerator." *Hazardous Waste & Hazardous Materials.* 11: 93-109.

Hjelmar, O. 1996. "Disposal Strategies for Municipal Solid Waste Incineration Residues." *J. Hazardous Materials.* 47: 345-386.

Jakob, A., S. Stucki, and P. Kuhn. 1995. "Evaporating of Heavy Metals during the Heat Treatment of Municipal Solid Waste Incinerator Fly Ash." *Environmental Science & Technology.* 29: 2429-2436.

Jaturapitakkul, C. 1993. *Utilization of Fly Ash in Concrete.* Ph. D. Dissertation. Department of Civil and Environmental Engineering. New Jersey Institute of Technology. New Jersey.

Johnson, C. A., S. Brandenberger, and P. Baccini. 1995. "Acid Neutralizing Capacity of Municipal Waste Incinerator Bottom Ash." *Environmental Science & Technology.* 29: 142-147.

Khanbilvardi, R., and S. Afshari. 1995. "Sludge Ash as Fine Aggregate for Concrete Mix." *J. Environmental Engineering.* 121: 633-638.

Kirby, C. S., and J. D. Rimstidt. 1994a. "Interaction of Municipal Solid Waste Ash with Water." *Environmental Science & Technology.* 28: 443-451.

---. 1994b. "Mineralogy and Surface Properties of Municipal Solid Waste Ash." *Environmental Science & Technology.* 27: 652-660.

Klein, D. H., A. W. Ander, J. A. Carter, J. F. Emery, C. Feldman, W. Fulkerson, W. S. Lyon, J. C. ogle, Y. Talmi, R. I. Vann Hook, and N. Bolton. 1975. "Pathways of Thirty-seven Trace Elements Through Coal-Fired Power Plant." *Environmental Science & Technology.* 9: 973-979.

Konduri, R. and E. Altwicker. 1994. "Analysis of Time Scales Pertinent to Dioxin/Furan Formation on Fly Ash Surfaces in Municipal Solid Waste Incinerators." *Chemosphere.* 28: 23-45.

Kronlöf, A. 1994. "Effect of Very Fine Aggregate on Concrete Strength." *Materials & Structures.* 27:15-25.

Langley, W. S., G. G. Carette, and V. M. Malhotra1. 1989. "Structural Concrete Incorporating High Volumes of ASTM Class F Fly Ash." *ACI Materials J.* 86: 507-514.

Lea, F. M. 1971. *The Chemistry of Cement and Concrete.* 3rd Edition. New York: Chemical Publishing Company, Inc.

Lee, C. C., and G. L. Huffman. 1989. "Incineration of Solid Waste." *Environmental Progress.* 8: 144-151.

Legiec, I. A., C. A. Hayes, and D. S. Kosson. 1989. "Continuous Recovery of Heavy Metals from MSW Incinerator Ashes." *Environmental Progress.* 8: 212-216.

Lin, C.-F., and H.-C. His. 1995. "Resource Recovery of Waste Fly Ash: Synthesis of Zeolite-lke Materials." *Environmental Science & Technology.* 29: 1109-1117.

Lu, C. 1996. "A Model of Leaching Behaviour from MSW Incinerator Residue Landfills." *Waste Management Research.* 14: 51-70.

Macphee, D. E., C. J. Black, and A. H. Taylor. 1993. "Cements Incorporating Brown Coal Fly Ash from the Latrobe Valley Region of Victoria, Australia." *Cement & Concrete Research.* 23: 507-517.

Mangialardi, T., L. Piga, G. Schena, and P. Sirini. 1998. "Characteristics of MSW Incinerator Ash for Use in Concrete." *Environmental Engineering Science.* 15: 291-297.

Martin, J. H., A. R. Collins, and R. G. Diener. 1995. "A Sampling Protocol for Composting, Recycling, and Re-use of Municipal Solid Waste." *J. Air & Waste Management Association.* 45: 846-870.

McKinley, M. D., G. W. Warren, S. M. Lahoti, and K. Sreenivasarao. 1992. "Stabilization and Hydrometallurgical Treatment of Flyash from a Municipal Incinerator." *J. Hazardous Materials.* 29: 255-273.

Milligan, M. S., and E. Altwicker. 1993. "The Catalytic Gasification of Carbon in Incinerator Fly Ash." *Carbon.* 31: 977-986.

Mindess, S., and J. F. Young. 1981. *Concrete.* New Jersey: Prentice-Hall, Inc.

Naik, T. R., S. S. Singh, and M. M. Hossain. 1995. "Permeability of High-Strength Concrete Containing Low Cement Factor." *J. Energy Engineering.* 122: 21-39.

Oluokun, F. A. 1994. "Fly Ash Concrete Mix Design and the Water-Cement Ratio Law." *ACI Materials J.* 91: 362-371.

Ontiveros, J. L., T. L. Clapp, and D. S. Kosson. 1989. "Physical Properties and Chemical Species Distributions within Municipal Waste Combuster Ashes." *Environmental Progress*. 8: 200-206.

Payá, J., J. Monzó, M. V. Borrachero, and E. Paris-Mora. 1996. "Comparisons among Magnetic and Non-Magnetic Fly Ash Fractions: Strength Development of Cement-Fly Ash Mortars." *Waste Management*. 16: 119-124.

Plowman, C. 1984. "The Chemistry of PFA in Concrete-A Review of Current Knowledge." *Proceedings 2nd International Conference on Ash Technology and Marketting*. London. 437-443.

Plüss, A., and R. E. Ferrel, Jr. 1991. "Characterization of Lead and Other Heavy Metals in Fly Ash from Municipal Waste Incinerators." *Hazardous Waste & Hazardous Materials*. 8: 275-292.

Poran, C. J., and F. Abtchi-Ali. 1989. "Properties of Solid Waste Incinerator Fly Ash." *J. Geotechnical Engineering*. 115: 1118-1133.

Ranganath, R. V., R. C. Sharma, and S. Krishnamoorthy. 1995. "Influences of Fineness and Soluble Silica Content of Fly Ashes on Their Strength Development with Respect to Age." Proceedings of the Fifth International Conference on Fly Ash, Silica Fume, Slag, and Natural Pozzolans in Concrete. Milwaukee. Virginia. June 4-9. 355-366.

Rashed, A. I., and R. B. Williamson. 1991a. "Microstructure of Entrained Air Voids in Concrete, Part I." *J. Materials Research*. 6: 2004-2012.

---. 1991b. "Microstructure of Entrained Air Voids in Concrete, Part II." *J. Materials Research*. 6: 2474-2483.

Rashid, R. A., and G. C. Frantz. 1992. "MSW Incinerator Ash as aggregate in Concrete and Masonary." *J. Materials in Civil Engineering*. 4: 353-368.

Reardon, E. J., C. A. Czank, C. J. Warren, R. Dayal, and H. M. Johnston. 1995. "Determining Control on Element Concentrations in Fly Ash Leachate." *Waste Management Research*. 13: 435-450.

Rebeiz, K. S., and K. L. Mielich. 1995. "Construction Use of Municipal-Solid-Waste Ash." *J. Energy Engineering*. 121: 2-13.

Reddy, K. J., S. P. Gloss, and L. Wang. 1994. "Reaction of CO_2 with Alkaline Solid Wastes to Reduce Contaminant Mobility." *Water Research*. 28: 1337-1382.

Rhodes, M. J. 1990. *Principles of Particle Technology*. New York: Wiley, Inc.

Rink, K. K., J. A. Kozinski, and J. S. Lighty. 1995. "Biosludge Incineration in FBCS: Behavior of Ash Particles." *Combustion & Flame.* 100: 121-130.

Roy, W. R., I. G. Krapac, and J. D. Steele. 1993. "Sorption of Cadmium and Lead by Clays from Municipal Incinerator Ash-Water Suspension." *J. Environmental Quality.* 22: 537-543.

Sandell, J. F., G. R. Dewey, L. L. Sutter, and J. A. Willemin. 1996. "Evaluation of Lead-Bearing Phases in Municipal Waste." *J. Environmental Engineering.* 122: 34-40.

Sawell, S. E., S. Hetherington, A. J. Chandler, H. G. Rigo, and J. Fraser. 1993. "The Waste Analysis, Sampling, Testing, and Evaluation Program: Effects of Lead and Cadmium Spiking of MSW on the Characteristics of MSW Incinerator Residues." *Proceedings of Municipal Waste Combustion Conference.* Williamsburg, Virginia. March 29-April 2.

Saxena, S. C. and C. K. Jotshi. 1997. "Incineration of Solid Waste and Energy Recovery: A State-of-Art Survey." *Arabian Journal for Science and Engineering.* 22: 3-40.

Scrivener, K. L. 1989. "The Microstructure of Concrete." *Materials Science of Concrete I.* The American Ceramic Society, Inc. 127-162.

Shashiprakash, S. G., T. S. Nagaraj, S. Raviraj, and B. V. Yenagi. 1994. "Proportioning of Fly Ash Cement Concrete Mixes." *Cement, Concrete, and Aggregates.* 16: 104-109.

Shi, C. 1996. "Early Microstructure Development of Activated Lime-Fly Ash Pastes." Cement and Concrete Research. 26: 1351-1359.

---. 1998. "Pozzolanic Reaction and Microstructure of Chemical Activated Lime-Fly Ash Pastes." ACI Materials Journal. 95: 537-545.

Simpson, R. S., and D. L. Charlesworth. 1989. "Immobilization of Incinerator Ash in a Concrete Matrix." *Waste Management Research.* 9: 95-99.

Singer, A., and V. Berkgaut. 1995. "Cation Exchange Properties of Hydrothermally Treated Coal Fly Ash." *Environmental Science & Technology.* 29: 1748-1753.

Sivapullaiah, P. V., J. P. Prashanth, and A. Sridharan. 1995. "Optimization of Lime Content for Fly Ash." *J. Testing & Evaluation.* 23: 222-227.

Tilly, J., G. Dietrich, and D. Pyne. 1989. "Exposure and Risk Assessment for a Proposed Hazardous Waste Incinerator." *Environmental Progress.* 8: 207-211.

Travis, C. C., and H. A. Hattermer-Frey. 1989. "Human Exposure to Dioxin from Municipal Solid Waste Incineration." *Waste Management Research.* 9: 151-156.

Triano, J. R., and G. C. Frantz. 1992. "Durability of MSW Fly-Ash Concrete." *J. Materials in Civil Engineering.* 4: 369-384.

Ukita, K., Ishii, M., Yamamoto, K., Azuma, K., and Kohno, K. 1992. "Properties of High Strength Concrete Using "Classified Fly Ash"." *Proceedings of the International Conference on the Use of Fly Ash, Silica Fume, Slag, and Natural Pozzolans in Concrete 4th*. Istanbul, Turkey: American Concrete Institute. 37-52.

U.S. Environmental Protection Agency. 1989. *Municipal Waste Combustion Study: Assessment of Health Risks Associated with Municipal Waste Combustion Emissions*. Hemisphere Publishing Corporation.

U.S. Environmental Protection Agency. 1992. *Test Methods for Evaluating Solid Waste, Physical/Chemical Methods. SW-846.* CD-ROM. Revision 0.

U.S. Environmental Protection Agency. 1993. *Operational Parameters for Hazardous Waste Combustion Devices*. Seminar Publication, EPA625-R-93-008.

U.S. Environmental Protection Agency. 1995. *Guidance for the Sampling and Analysis of Municipal Waste Combustion Ash for the Toxicity Characteristic.* EPA530-R-95-036.

U.S. Environmental Protection Agency. Office of Solid Waste Management Programs. 1998. *Characterization of Municipal Solid Waste in the United States: 1997 Update.* Report No. EPA 530-R-98-007.

Webster, M. T., and R. C. Loehr. 1996. "Long-Term Leaching of Metals from Concrete Products." *J. Environmental Engineering.* 122: 714-721.

Wu, C-Y, P. Biswas, and N. J. Fendinger. 1994. "Model to Access Heavy Metal Emission from Municipal Solid Waste Incineration." *Hazardous Waste & Hazardous Materials.* 11: 71-92.

Yang, G. C. C., and S-Y Chen. 1994. "Statistical Analyses of Control Parameters for Physicochemical Properties of Solidified Incinerator Fly Ash of Municipal Solids Wastes." *J. Hazardous Materials.* 39: 317-333.

Zakaria, M., and J. G. Cabrera. 1996. "Performance and Durability of Concrete Made with Demolition Waste and Artificial Fly Ash-Clay Aggregates." *Waste Management.* 16: 151-158.

Zevenbergen, C., T. Vander Wood, J. P. Bradley, P. F. C. W. Van Der Broeck, A. J. Orbons, and L. P. Van Reeuwijk. 1994. "Morphological and Chemical Properties of MSWI Bottom Ash with Respect to the Glassy Constituents." *Hazardous Waste & Hazardous Materials.* 11: 371-383.